

**Republic of Iraq  
Ministry of Higher Education and  
Scientific Research  
University of Baghdad  
College of Education for Pure Science  
Ibn Al –Haitham**



# **New Analytical Methods for Drugs Analysis A Comparative Study**

*A Thesis*

*Submitted to the College of Education for Pure Science Ibn Al- Haitham  
University of Baghdad in Partial Fulfillment of the Requirements for the  
Degree of Doctor of philosophy (Ph.D.) of Science in Chemistry*

**By  
Husam Saleem Khalaf**

**B. Sc. University of Baghdad (1993)  
M. Sc. University of Baghdad (2006)**

**Supervised by**

*Prof. Dr. Abdul Mohsin A. Al Haidari*

*Prof. Dr. Sarmad B. Dikran*

*Prof. Dr. Alaa K. Mohammed*

**2014**

## ***Supervisor certification***

We certify that this thesis was prepared under supervision at University of Baghdad, College of Education for Pure Science Ibn Al Haitham, as partial requirements for the Degree of Doctor of Philosophy (Ph.D.) of Science in Chemistry.

**Professor**

**Dr. Abdul Muhsin A. Al Haideri**

**Date:    /    / 2014**

**Professor**

**Dr. Sarmad B. Dikran**

**Date:    /    / 2014**

**Professor**

**Dr. Alaa K. Mohammed**

**Date:    /    / 2014**

In view of the available recommendation, we forward this thesis for debate by the examining Committee.

**Signature:**

**Name     : Alaa K. Mohammed**

**Head of Chemistry Department**

**Date     :    /    / 2014**



# *Dedication*

*To All my family  
With love*

# *Acknowledgments*

*Thanks to Allah for all blessing during the pursuit of my academic and career goals.*

*I would like to express my sincere thanks and my appreciation to my supervisors Prof. Dr. Abdul-Muhsin Al Haideri, Prof. Dr. Sarmad Bahjat Dikran and Prof. Dr. Alaa Karem Mohammed for their kindly interest, encouragement throughout the course of this work,*

*Also my grateful thanks to the Dean of the College of Education for Pure Science (Ibn Al-Haitham) Dr. Kalid fahad Ali and sincere thanks to the Head of Chemistry Department Prof. Dr. Alaa Karem Mohammed and all staff members of Chemistry Department for all facilities that they offered to me during my research*

*Finally, I am deeply indebted to my family for their support and patience during the years of my study.*

***Husam***

## Summary

Four different spectrophotometric methods are used in this study for the determination of Sulfamethoxazole and sulfanilamide drugs in pharmaceutical compounds, synthetic samples, and in their pure forms. The work comprises four chapters which are shown in the following:

**Chapter One:** Includes a brief for Ultraviolet-Visible (UV-VIS) Absorption spectroscopy, antibacterial drugs and sulfonamides with some methods for their determination.

The chapter lists two methods for optimization; univariate method and multivariate method. The later includes different types, two of these were mentioned; simplex method and design of experiment method.

**Chapter Two:** Includes reaction of the two studied drugs with sodium nitrite and hydrochloric acid for diazotization reaction followed by coupling with diphenylamine in acidic medium to form, a blue colored azo dye compound which exhibits maximum absorption ( $\lambda_{\max}$ ) at 530 nm for sulfamethoxazole complex and 531 nm for sulfanilamide complex against the reagent blank and the concentration of these drugs were determined spectrophotometrically.

The optimum reaction conditions and other analytical parameters were evaluated. In addition to classical univariate optimization, modified simplex method has been applied in optimization of the variables affecting the color producing reaction.

The results show better optical characteristics for calibration curves and statistical data were obtained under optimum conditions obtained by multi simplex optimization, in comparison with those obtained via univariate method for two studied drugs.

Beer's law obeyed in the concentration range of 0.5-12.0  $\mu\text{g.mL}^{-1}$ , 0.5-7.0  $\mu\text{g.mL}^{-1}$  for sulfamethoxazole and sulfanilamide respectively with molar absorptivity of  $4.9617 \times 10^4 \text{ L.mol}^{-1}.\text{cm}^{-1}$  for sulfamethoxazole and  $5.9185 \times 10^4 \text{ L.mol}^{-1}.\text{cm}^{-1}$  for sulfanilamide. The detection limits were 0.036  $\mu\text{g.mL}^{-1}$  and 0.016  $\mu\text{g.mL}^{-1}$  for the two complexes respectively by simplex method.

No interferences from the studied excipients on the determination of these drugs were found therefore, the proposed methods were applied successfully

for the determination of the sulfamethoxazole and sulfanilamide in pharmaceutical compound and in synthetic samples.

**Chapter Three:** Is based on the formation of condensation complexes of each drug with sodium 1,2-naphthoquinon-4-sulfonate as a chromogenic reagent. The absorbance values, for the formed complexes were measured at 460 nm for sulfamethoxazole and 455 nm for sulfanilamide; against reagent blank.

Different variables affecting the completion of reaction have been carefully optimized following the classical univariate sequence and design of experiment (DOE) method and the results were obtained under optimum conditions by (DOE) optimization which shows better optical characteristics for calibration curves and statistical data in comparison with those obtained via univariate method for two studied drugs.

The calibration graphs are linear in the ranges of (5.0-50.0)  $\mu\text{g.mL}^{-1}$  for sulfamethoxazole and (5.0-30.0)  $\mu\text{g.mL}^{-1}$  for sulfanilamide with detection limit 0.359  $\mu\text{g.mL}^{-1}$  for sulfamethoxazole complex and 0.536  $\mu\text{g.mL}^{-1}$  for sulfanilamide complex. The molar absorptivity was found to be ( $7.0918 \times 10^4 \text{ L.mol}^{-1}.\text{cm}^{-1}$ ) for sulfamethoxazole and ( $7.0774 \times 10^4 \text{ L.mol}^{-1}.\text{cm}^{-1}$ ) for sulfanilamide by the design of experiment (DOE) method.

Finally no interferences from the studied excipients on the determination of these drugs were found. The proposed methods have been successfully applied for the determination of sulfamethoxazole and sulfanilamide in their pharmaceutical preparation and synthetic samples.

**Chapter Four:** Includes two parts; Derivative spectrophotometry and partial least-squares (PLS).

*Derivative spectrophotometry* is based on the first and second derivative spectra of absorption which has been applied for simultaneous spectrophotometric determination of sulfamethoxazole and sulfanilamide in their mixture in the ultraviolet region. The method offers an advantage of getting rid of the resulting error in the values of absorption because of the presence of each drug with the presence of interferences from the excipients.

It was found that the method is able to accurately estimate sulfamethoxazole in the range of (2.0-50.0)  $\mu\text{g.mL}^{-1}$ ; in mixtures containing

(2.0-30.0)  $\mu\text{g.mL}^{-1}$  of sulfanilamide, as (interferent). The results obtained, with the first derivative measurements, indicate that when the concentration of sulfanilamide is kept constant and the concentration of sulfamethoxazole varied, the peak amplitudes are measured at peak-to-baseline (223, 254, 287 nm), peak to peak height between (223- 254 nm), (254-287nm). Moreover, the height at the zero cross of sulfanilamide at (235.62, 258.72 nm), height-to-height of the two zero crosses between (235.62-258.72 nm) and area under peak between (241.95-267.04 nm), (267.04-330 nm) were found to be in proportion to the sulfamethoxazole concentration therefore they are used for the determination of it. The careful inspection of the second derivative spectra obtained for the mentioned mixtures of sulfamethoxazole and sulfanilamide shows that peak to baseline is at (239.5, 263.5, 267.75, 301, 215 nm) , height to baseline is at zero cross is at (245.86, 271.28 nm) , peak to peak is between (239.5-264.25 nm), (239.5-267.75 nm), (271.28-301 nm), (215-239.5 nm), height to height is at two zero cross (245.86-271.28 nm) in addition to peak area at the interval between (254.12-281 nm), (286.95-329.5 nm), (221.75-254.12 nm) measurements at specified wavelength could be used to quantify the exact concentration of sulfamethoxazole in presence of sulfanilamide.

Sulfanilamide was determined for the range of (2.0-50.0)  $\mu\text{g.mL}^{-1}$ ; in a mixture containing (2.0-50.0)  $\mu\text{g.mL}^{-1}$  of sulfamethoxazole as (interferent). The procedure gave good results over the studied range of concentration depending on peak-to-baseline at (224, 246, 271 nm), height at zero cross at (241.95, 267.04 nm), peak to peak between (224-246 nm), (246-271 nm), height to height at two zero cross (241.95-271 nm) and area under the peak at (235.62-258.72 nm) measurements were found to be used for the determination of sulfanilamide in the first derivative technique. On other situation, the wavelengths are at 218 nm, 231 nm, 260 nm and 278 nm (peak to base line measurements), and height at two zero cross at 254 nm and 281 nm, and peak to peak measurements between (218-231 nm), (231-260 nm) and (260-278 nm), and height at zero cross at (254, 281 nm), wavelengths at (210-224 nm) , (224-245.84 nm) and (271.28-330 nm) peak area at the interval measurements were used for the estimation of sulfanilamide on second derivative.

The results show the absence of interferences from the excipients on the determination of the two drugs by using this method, therefore; it was possible to be applied for the determination of these drugs in their pharmaceutical compounds and synthetic samples.

*Partial least-squares (PLS)* method was applied for simultaneous spectrophotometric assay of sulfamethoxazole and sulfanilamide in their mixture. In this study, training (calibration) set was prepared relying on rule of ten i.e. Twenty binary mixtures were selected (from the sixty five prepared mixtures basing upon linearity ranges of SMZ 2.0-50.0  $\mu\text{g.mL}^{-1}$  and 2.0-50.0  $\mu\text{g.mL}^{-1}$  for SNA) by random design.

The calibration matrix was obtained as digital data by scanning the absorption spectrum for each of the twenty selected solutions of SMZ and SNA mixtures, in the range 190–350 nm with 1nm data interval, 0.5 nm slit width, and medium scan speed. Originpro software version 9.1.0, 2013 program is used to build up PLS-1 and PLS-2 regression modes and the concentration of two drugs was predicted. The results of relative standard deviation percentage (RSD %) (0.0277- 0.8012) and relative error percentage (RE %) (-0.2151-0.5975) indicated excellent accuracy and precision of the PLS method for simultaneous prediction of the concentrations of SMZ and SNA. The method was successfully used for simultaneous determination of SMZ and SNA in their synthetic sample mixtures.

The results obtained from the derivative technique and partial least squares method for the two drugs was compared to each other and F-test values were calculated.



<i>List of Contents</i>	
<i>Subject</i>	<i>Page No.</i>
<b>Summary</b>	I
<b>List of contents</b>	V
<b>List of abbreviations</b>	XIII
<b>List of schemes</b>	XVI
<b>List of tables</b>	XVII
<b>List of figures</b>	XXI
<i>Chapter One</i>	
<b>1 Introduction</b>	1
<b>1-1 Ultraviolet-Visible (UV-VIS) absorption spectroscopy</b>	1
<b>1-2 Antibacterial drugs</b>	1
<b>1-2-1 Classification of antibacterial drugs</b>	2
<b>1-2-2 Sulfonamides (sulfa drugs)</b>	3
<b>1-2-2-1 Definition</b>	3
<b>1-2-2-2 Discovery</b>	3
<b>1-2-2-3 Mechanism of action</b>	4
<b>1-2-2-4 Sulfamethoxazole (SMZ)</b>	5
<b>1-2-2-5 General properties of sulfamethoxazole</b>	6
<b>1-2-2-6 Sulfanilamide (SNA)</b>	6
<b>1-2-2-7 General properties of sulfanilamide</b>	8
<b>1-2-2-8 Methods for the determination of sulfonamides</b>	8
<b>A- Spectrophotometric methods</b>	8
<b>B- Chromatographic methods</b>	13
<b>C- Flow injection analysis</b>	18
<b>D- Capillary electrophoresis methods</b>	20
<b>E- Voltametric methods</b>	23
<b>F- Potentiometric Methods</b>	24
<b>1-3 Optimizations</b>	25
<b>1-3-1 Univariate method</b>	25
<b>1-3-2 Multivariate methods</b>	26
<b>1-3-2-1 Simplex method</b>	26
<b>1-3-2-2 Modified simplex method</b>	28
<b>1-3-2-3 Design of experiment (DOE)</b>	29
<b>1-3-2-3-1 Response surface method (RSM)</b>	30

<i>Chapter Two</i>	
<b>2 Determination of sulfamethoxazole and sulfanilamide by diazotization reaction and coupling with diphenylamine</b>	35
<b>2-1 Introduction</b>	35
<b>2-1-1</b> Diazotization reaction	35
<b>2-1-2</b> Diazonium coupling reactions	36
<b>2-1-3</b> Diphenylamine (DPA)	36
<b>2-1-4</b> Spectrophotometric determination of some drugs in pharmaceutical preparations using diazotization reactions	37
<b>2-2 Experimental</b>	39
<b>2-2-1</b> Instruments	39
<b>2-2-2</b> Chemicals	40
<b>2-2-3</b> Materials and reagents	41
<b>2-2-4</b> Preparation of standard drugs solutions	42
<b>1-</b> Sulfamethoxazole (SMZ) stock solution (100 $\mu\text{g.mL}^{-1}$ )	42
<b>2-</b> Sulfanilamide(SNA) stock solution (100 $\mu\text{g.mL}^{-1}$ )	42
<b>3-</b> Solution for the analysis of sulfamethoxazole in pharmaceutical preparations	42
<b>i.</b> In tablets	42
<b>ii.</b> In syrup	43
<b>2-2-5</b> Preparation of synthetic sulfanilamide drug sample	43
<b>2-2-6</b> Primary experimental test	43
<b>2-2-7 Optimization of experimental variables</b>	44
<b>I- Univariate method</b>	44
<b>1-</b> Effect of diazotization reaction time	44
<b>2-</b> Effect of sodium nitrite	44
<b>3-</b> Effect of different acids	44
<b>4-</b> Effect of hydrochloric acid	45
<b>5-</b> Effect of sulfamic acid	45
<b>6-</b> Effect of diphenylamine (DPA)	45
<b>7-</b> Effect of coupling reaction time	46
<b>II- Multivariate method</b>	46
<b>2-2-8</b> General recommended procedures	48
<b>1-</b> Assay procedure for determination of sulfamethoxazole	48
<b>i-</b> Univariate method	48
<b>ii-</b> Simplex method	48
<b>2-</b> Assay procedure for determination of sulfanilamide	49

<b>i- Univariate method</b>	49
<b>ii- Simplex method</b>	49
<b>2-2-9 Procedure for synthetic sulfanilamide drugs sample</b>	49
<b>2-2-10 Determination of sulfamethoxazole in pharmaceutical preparation by standard additions method (SAM)</b>	50
<b>2-3 Results and discussions</b>	50
<b>I- The determination of sulfamethoxazole</b>	50
<b>2-3-1 Absorption spectra</b>	50
<b>2-3-2 Optimization of reaction variables</b>	52
<b>I- Univariate method</b>	52
<b>1- Effect of diazotization reaction time</b>	52
<b>2- Effect of sodium nitrite concentration</b>	52
<b>3- Effect of different acid</b>	53
<b>4- Effect of acidity on diazotization</b>	53
<b>5- Effect of sulfamic acid concentration</b>	54
<b>6- Effect of diphenylamine concentration</b>	55
<b>7- Effect of coupling reaction time</b>	55
<b>8- Effect of acidity</b>	56
<b>II- Simplex method</b>	56
<b>2-3-3 Calibration curves and analytical data</b>	58
<b>I- Univariate method</b>	58
<b>II- Simplex method</b>	59
<b>2-3-4 Precision and accuracy</b>	60
<b>2-3-5 Interference studies</b>	61
<b>2-3-6 Application in pharmaceutical preparation by standard addition method (SAM)</b>	61
<b>II- The determination of sulfanilamide (SNA)</b>	66
<b>2-3-7 Absorption spectra</b>	66
<b>2-3-8 Optimization of reaction variables</b>	68
<b>I- Univariate method</b>	68
<b>1- Effect of diazotization reaction time</b>	68
<b>2- Effect of sodium nitrite concentration</b>	68
<b>3- Effect of different acidic solutions</b>	69
<b>4- Effect of hydrochloric acid concentration</b>	69

5- Effect of sulfamic acid concentration	70
6- Effect of reagent concentration	71
7- Effect of coupling reaction time	71
8- Effect of acidity	72
II- Simplex method	72
2-3-9 Calibration curves and analytical data	74
I- Univariate method	74
II- Simplex method	75
2-3-10 Precision and accuracy	76
2-3-11 Interferences study	77
2-3-12 Application in synthetic sample by standard addition method (SAM)	77
<b><i>Chapter Three</i></b>	
<b>3 Determination of sulfamethoxazole and sulfanilamide by reaction with sodium 1,2-naphthoquinon-4-sulfonate (NQS)</b>	79
<b>3-1 Introduction</b>	79
3-1-1 Condensation reaction	79
3-1-2 Sodium 1,2-naphthoquinon-4-sulfonate (NQS)	80
3-1-3 Spectrophotometric determinations of some pharmaceutical preparations using condensation reaction	81
<b>3-2 Experimental</b>	83
3-2-1 Instruments	83
3-2-2 Chemicals	83
3-2-3 Materials and reagents	83
3-2-4 Preparation of standard drugs solutions	83
1- Sulfamethoxazole (SMZ) stock solution (1000 $\mu\text{g}\cdot\text{mL}^{-1}$ )	83
2- Sulfanilamide (SNA) stock solution (1000 $\mu\text{g}\cdot\text{mL}^{-1}$ )	84
3- Preparation solution for the analysis of sulfamethoxazole in pharmaceutical preparations	84

<b>i.</b> In tablets	84
<b>ii.</b> In syrup	84
<b>3-2-5</b> Preparation of synthetic sulfanilamide drug sample	85
<b>3-2-6</b> Primary experimental test	85
<b>3-2-7 Optimization of experimental variables</b>	85
<b>I- Univariate method</b>	85
<b>1-</b> Effect of different bases	85
<b>2-</b> Effect of borax concentration	85
<b>3-</b> Effect of NQS concentration	86
<b>4-</b> Effect of reaction time	86
<b>II- Multivariate method</b>	86
<b>3-2-8</b> General recommended procedures	89
<b>1-</b> Assay procedure for determination of sulfamethoxazole	89
<b>i-</b> Univariate method	89
<b>ii-</b> Design of experiment method	90
<b>2-</b> Assay procedure for determination of sulfanilamide	90
<b>i-</b> Univariate method	90
<b>ii-</b> Design of experiment method	90
<b>3-2-9</b> Procedure for synthetic sulfanilamide drug sample	91
<b>3-2-10</b> Determination of sulfamethoxazole drug in pharmaceutical preparation by standard additions method (SAM)	91
<b>3-3 Results and discussions</b>	91
<b>I- The determination of sulfamethoxazole</b>	91
<b>3-3-1</b> Absorption spectra	91
<b>3-3-2</b> Optimization of reaction variables	93
<b>I- Univariate method</b>	93
<b>1-</b> Effect of different bases	93
<b>2-</b> Effect of borax concentration	93
<b>3-</b> Effect of NQS concentration	94

4- Effect of reaction time	95
II- Design of experiment method	96
3-3-3 Calibration curves and analytical data	100
I- Univariate method	100
II- Design of experiment method	101
3-3-4 Precision and accuracy	103
3-3-5 Interferences studies	103
3-3-6 Application in pharmaceutical preparation by standard additions method (SAM)	104
II- The determination of sulfanilamide	109
3-3-7 Absorption spectra	109
3-3-8 Optimization of reaction variables	110
I- Univariate method	110
1- Effect of different bases	110
2- Effect of borax concentration	111
3- Effect of NQS concentration	112
4- Effect of reaction time	112
II- Design of experiment method	113
3-3-9 Calibration curves and analytical data	117
I- Univariate method	117
II- Design of experiment method	118
3-3-10 Precision and accuracy	119
3-3-11 Interferences studies	120
3-3-12 Application in synthetic sample	120
3-3-13 Application in synthetic sample by standard additions method (SAM)	121

<i>Chapter Four</i>	
<b>4 Simultaneous determination of sulfamethoxazole and sulfanilamide</b>	122
<b>4-1 Spectrophotometric simultaneous determination of sulfamethoxazole and sulfanilamide by derivative spectrophotometry</b>	122
<b>4-1-1 Introduction</b>	122
<b>4-1-2 Spectrophotometric determinations of some pharmaceutical</b>	124
<b>4-1-3 Experimental</b>	125
<b>4-1-3-1 Instrumentation</b>	125
<b>4-1-3-2 Chemicals</b>	125
<b>4-1-3-3 Pharmaceutical compounds</b>	125
<b>4-1-3-4 Reagents</b>	125
<b>4-1-3-5 General recommended procedures</b>	126
<b>1-Assay procedure for determination of sulfamethoxazole or sulfanilamide</b>	126
<b>2-Assay procedure for determination of each drug in the presence of the other</b>	126
<b>4-1-4 Results and discussion</b>	126
<b>4-1-4-1 Absorption spectra</b>	127
<b>4-1-4-2 First and second derivative modes</b>	127
<b>4-1-4-3 Calibration curves for sulfamethoxazole</b>	129
<b>4-1-4-4 Calibration curves for sulfanilamide</b>	159
<b>4-1-4-5 Accuracy and precision</b>	187
<b>4-1-4-6 Interferences study</b>	189
<b>4-2 Simultaneous spectrophotometric determination of binary mixture via partial least squares method</b>	190
<b>4-2-1 Introduction</b>	190
<b>4-2-2 spectrophotometric simultaneous determination of sulfamethoxazole and sulfanilamide by partial least squares</b>	190
<b>4-2-3 Experimental</b>	191
<b>4-2-3-1 Instrumentation</b>	191

<b>4-2-3-2</b> Chemicals	191
<b>4-2-3-3</b> Pharmaceutical compounds	191
<b>4-2-3-4</b> Standard drugs solution	191
<b>4-2-3-5</b> General recommended procedures	191
<b>1-Assay procedure for determination of sulfamethoxazole or sulfanilamide</b>	191
<b>2-Assay procedure for determination of each drug in the presence of the other</b>	191
<b>4-2-4 Results and discussion</b>	192
<b>4-2-4-1</b> Absorption spectra	192
<b>4-2-4-2</b> Individual calibration	193
<b>4-2-4-3</b> Multivariate methods	194
<b>4-2-4-4</b> Accuracy and precision	201
<b>4-2-4-5</b> Application of the method	201
<b>4-3</b> Conclusion	207
<b>References</b>	209



<i>List Of Abbreviations</i>	
<b>AAS</b>	Atomic absorption spectrometric
<b>ASE</b>	Accelerated solvent extraction
<b>BDD</b>	Boron-doped diamond
<b>BM</b>	Brotton marshall reagent
<b>BP</b>	British pharmacopoeia
<b>C.V</b>	Coefficient of variation
<b>CCC</b>	Central composite circumscribed
<b>CCD</b>	Central composite design
<b>CCF</b>	Central composite face
<b>CLS</b>	Classical least squares
<b>CNTs</b>	Carbon nanotubes
<b>D1</b>	First derivative
<b>D2</b>	Second derivative
<b>DL</b>	Detection limit
<b>DLLE</b>	Dispersive liquid-liquid micro extraction
<b>DOE</b>	Design of experiment
<b>DOP</b>	Diocetylphthalate
<b>DOS</b>	Diocetylsebacate
<b>DPA</b>	Diphenylamine
<b>DSPE</b>	Dispersive solid-phase extraction
<b>E</b>	Expand
<b>ε</b>	Molar absorptivity
<b>FI</b>	Flow injection
<b>GA</b>	Genetic algorithm
<b>GAPLS</b>	Genetic algorithm partial least squares
<b>HPLC</b>	High performance liquid chromatography
<b>HPLC-UV</b>	High performance liquid chromatography tandem ultra-violet
<b>HPSAM</b>	H-point standard addition method
<b>HT</b>	Hydrogen-terminated
<b>HT-BDD</b>	Hydrogen-terminated- boron-doped diamond

<b>ILATPS</b>	Ionic liquid aqueous two-phase system
<b>ILS</b>	Inverse least squares
<b>LC-MS</b>	Liquid chromatography tandem mass spectrometry
<b>LOD</b>	Limit of detection
<b>LOQs</b>	Method limits of quantification
<b>MBTH</b>	3-Methyl-2-Benzothiazolinone Hydrazone
<b>MDLs</b>	Method detection limits
<b>mM</b>	Mili mole
<b>m-MWCNTs</b>	Magnetic- multi-Walled carbon nanotubes
<b>MPM</b>	Matched potential method
<b>MRM</b>	Multiple reaction monitoring
<b>MSE</b>	Mean square error
<b>MWCNTs</b>	Multi-walled carbon nanotubes
<b>N.D.I.</b>	The State Company for medical appliances (ninawa-Iraq)
<b>NQS</b>	sodium 1,2-naphthoquinone-4-sulfonate
<b>NQSSA</b>	Potassium 1,2-naphthoquinone-4-(N-aminophenylen-4-sulphonate)
<b>o-NPOE</b>	o-Nitro phenyl octyl ether
<b>OT</b>	Oxygen-terminated
<b>OT-BDD</b>	Oxygen-terminated- boron-doped diamond
<b>PABA</b>	P-amino benzoic acid
<b>PDAC</b>	P-dimethyl amino cinnamaldehyde
<b>PHZ</b>	Phthalazine
<b>PLS</b>	Partial least squares
<b>PPY</b>	Polypyrrole
<b>PRESS</b>	Predicting the residual error sum of squares
<b>QOL</b>	Quantification of limit
<b>R</b>	Reflected
<b>r</b>	Correlation coefficient
<b>R.S.E%</b>	Relative standard error percentage
<b>r<sup>2</sup></b>	Correlation of linearity
<b>RE%</b>	Relative error percentage

<b>Rec.%</b>	Recovery percentage
<b>RMSE</b>	Root mean square error
<b>RMSED</b>	Root mean squares error deviation
<b>RSD</b>	Relative standard deviation
<b>RSM</b>	Response surface method
<b>S.D.I.</b>	The State Company for medical appliances (Samarra-Iraq)
<b>SAM</b>	Standard additions method
<b>SAs</b>	Sulfonamides
<b>SD</b>	Sulfadiazine
<b>SDR</b>	Sulfamethoxazole diazonium resocrinol
<b>SFA</b>	Sulfacetamide
<b>SMZ</b>	Sulfamethoxazole
<b>SNA</b>	Sulfanilamide
<b>SP</b>	Sephadex
<b>SPE</b>	Solid phase extraction
<b>SWV</b>	Square-wave voltammetry
<b>TMP</b>	Trimethoprim
<b>V</b>	Volt
<b>VA-LPME</b>	Voltage-assisted liquid phase micro extraction
<b>FASS</b>	Field-amplified sample stacking

<i>List of Schemes</i>	
<i>Title</i>	<i>Page No.</i>
<b>Scheme 1-1:</b> Structure of salvarsan.	2
<b>Scheme 1-2:</b> The structure formula of sulfamethoxazole	6
<b>Scheme 1-3:</b> The structure formula of sulfanilamide	7
<b>Scheme 2-1:</b> The synthetic origin of aryl diazonium ions and their most useful transformations.	35
<b>Scheme 2-2:</b> The structure formula of diphenylamine.	36
<b>Scheme 2-3:</b> The reaction mechanism for diazotization and reaction between SMZ and DPA.	60
<b>Scheme 2-4:</b> The reaction mechanism for diazotization and reaction between SNA and DPA.	76
<b>Scheme 3-1:</b> The formula structure of sodium 1, 2-naphthoquinone-4-sulfonate (NQS).	80
<b>Scheme 3-2:</b> The reaction mechanism for the condensation reaction between SMZ and NQS.	102
<b>Scheme 3-3:</b> The reaction mechanism for the condensation reaction between SNA and NQS.	119

<i>List of Tables</i>	
<i>Title</i>	<i>Page No.</i>
<b>Table 1-1:</b> Some general properties of sulfamethoxazole.	6
<b>Table 1-2:</b> Some general properties of sulfanilamide.	8
<b>Table 1-3:</b> Structures of quadratic designs used when investigating three factors.	33
<b>Table 1-4:</b> Un-coded and coded levels of the independent variables.	34
<b>Table 2-1:</b> Spectrophotometric determinations of some drugs in pharmaceutical compounds using diazotization reaction.	38
<b>Table 2-2:</b> The principle instruments and their models.	39
<b>Table 2-3:</b> The principle materials and their sources.	40
<b>Table 2-4:</b> The principle pharmaceutical compounds and their manufacturers.	41
<b>Table 2-5:</b> Boundary of simplex for the studied variables.	47
<b>Table 2-6:</b> The (n+1) experimental designs of studied variables.	47
<b>Table 2-7:</b> Effect of diazotization reaction time.	52
<b>Table 2-8:</b> Effect of different acids on diazotization of (5.0 $\mu\text{g.mL}^{-1}$ ) SMZ.	53
<b>Table 2-9:</b> Effect of coupling reaction time.	55
<b>Table 2-10:</b> Multivariate experiments (simplex) for the determination of (5.0 $\mu\text{g.mL}^{-1}$ ) SMZ.	57
<b>Table 2-11:</b> Optical characteristics and statistical data for the determination of (SMZ) by univariate method.	58
<b>Table 2-12:</b> Optical characteristics and statistical data for the determination of (SMZ) by simplex method.	59
<b>Table 2-13:</b> Evaluation of accuracy and precision for the determination of (SMZ) by proposed method.	60
<b>Table 2-14:</b> Percent recovery for (5.0 $\mu\text{g.mL}^{-1}$ ) of sulfamethoxazole in the presence of (1000 $\mu\text{g.mL}^{-1}$ ) of excipients.	61
<b>Table 2-15:</b> Application of the proposed method to the (SMZ) concentration measurements pharmaceutical preparations by (SAM).	61
<b>Table 2-16:</b> Effect of diazotization reaction time.	68

<b>Table 2-17:</b> Effect of different acids on diazotization of (5 $\mu\text{g.mL}^{-1}$ ) of SNA.	69
<b>Table 2-17:</b> Effect of coupling reaction time.	71
<b>Table 2-18:</b> Multivariate experiments (simplex) for the determination of (5.0 $\mu\text{g.mL}^{-1}$ ) SNA.	73
<b>Table 2-19:</b> Optical characteristics and statistical data for the determination of (SNA) by univariate method.	74
<b>Table 2-20:</b> Optical characteristics and statistical data for the determination of (SNA) by simplex method.	75
<b>Table 2-21:</b> accuracy and precision of the proposed method.	76
<b>Table 2-22:</b> Percent recovery for (5.0 $\mu\text{g.mL}^{-1}$ ) of sulfanilamide in the presence of (1000 $\mu\text{g.mL}^{-1}$ ) of excipients.	77
<b>Table 2-23:</b> Application of the simplex method to the (SNA) concentration measurements in synthetic sample by standard additions method.	77
<b>Table 3-1:</b> Spectrophotometric determinations of some pharmaceutical compounds using condensation reaction.	81
<b>Table 3-2:</b> Un coded and coded levels of the independent variables for the determination of (SMZ) and (SNA).	87
<b>Table 3-3:</b> The central composite design with three independent variables (un code variables) for (SMZ).	88
<b>Table 3-4:</b> The central composite design with three independent variables (un code variables) for (SNA).	89
<b>Table 3-5:</b> Effect of different bases on condensation reaction.	93
<b>Table 3-6:</b> Effect of coupling reaction time.	95
<b>Table 3-7:</b> The central composite design with three independent variables (un coded variables) and their experimental absorption values of (30 $\mu\text{g.mL}^{-1}$ ) SMZ-NQS complex.	97
<b>Table 3-8:</b> Regression coefficients, P (or probability for absorption of SMZ-NQS).	98
<b>Table 3-9:</b> Optical characteristics and statistical data for the determination of (SMZ) by univariate method.	100
<b>Table 3-10:</b> Optical characteristics and statistical data for the determination of (SMZ) by DOE method.	101

<b>Table3-11:</b> Evaluation of accuracy and precision for the determination of (SMZ) by proposed method.	103
<b>Table 3-12:</b> Percent recovery for (20.0 $\mu\text{g.mL}^{-1}$ ) of sulfamethoxazole in the presence of different concentration of excipients.	104
<b>Table 3-13:</b> Application of the proposed method to the (SMZ) concentration measurements in pharmaceutical preparation by (SAM).	104
<b>Table 3-14:</b> Effect of different bases on condensation reaction.	111
<b>Table3-15:</b> Effect of coupling reaction time.	113
<b>Table 3-16:</b> The central composite design with three independent variables (un coded variables) and their experimental absorption values of (20 $\mu\text{g.mL}^{-1}$ ) SNA-NQS complex.	114
<b>Table 3-17:</b> Regression coefficients, P (or probability for absorption of SNA-NQS).	115
<b>Table 3-18:</b> Optical characteristics and statistical data for the determination of (SNA) by univariate method.	117
<b>Table 3-19:</b> Optical characteristics and statistical data for the determination of (SNA) by DOE method.	118
<b>Table 3-20:</b> Evaluation of accuracy and precision for the determination of (SNA) by proposed method.	119
<b>Table 3-21:</b> Percent recovery for (20.0 $\mu\text{g.mL}^{-1}$ ) of sulfanilamide in the presence of different concentration of excipients.	120
<b>Table 3-22:</b> Application of the proposed method to the (SNA) concentration measurements in synthetic sample.	120
<b>Table 3-23:</b> Application of the proposed method to the (SNA) concentration measurements in synthetic sample (SNA) by (SAM).	121
<b>Table 4-1:</b> Analytical characteristics of derivative methods for simultaneous determination of some pharmaceutical compounds.	124

<b>Table 4-2:</b> Statistical analysis for the determination of sulfamethoxazole using first and second derivative spectrophotometric technique.	158
<b>Table 4-3:</b> Statistical analysis for the determination of sulfanilamide using first and second derivative spectrophotometric technique.	186
<b>Table 4-4:</b> Results of accuracy and precision for the determination of sulfamethoxazole by derivative technique.	187
<b>Table 4-5:</b> Results of accuracy and precision for the determination of sulfanilamide by derivative technique.	188
<b>Table 4-6:</b> Percent recovery for mixtures of sulfamethoxazole and sulfanilamide in the presence of (500 $\mu\text{g.mL}^{-1}$ ) of excipients.	189
<b>Table 4-7:</b> Composition of the training set for applying PLS-2 and PLS-1 methods.	196
<b>Table 4-8:</b> Composition of training set, their predictions by PLS-1 model.	198
<b>Table 4-9:</b> Composition of training set, their predictions by PLS-2 model.	199
<b>Table 4-10:</b> Goodness of fit statistics for training set analyses.	200
<b>Table 4-11:</b> Evaluation of accuracy and precision of the proposed method.	201
<b>Table 4-12:</b> Composition of synthetic mixture samples, their predictions by PLS-1 model and statistical parameters for the system.	202
<b>Table 4-13:</b> Composition of synthetic mixture samples, their predictions by PLS-2 model and statistical parameters for the system.	203
<b>Table 4-14:</b> Goodness of fit statistics for synthetic samples set analyses.	204
<b>Table 4-15:</b> Evaluation of accuracy and precision of the proposed method.	207
<b>Table 4-16:</b> F-Test Two-Sample (Derivative and PLS) for variances for the analysis of (SMZ).	208
<b>Table 4-17:</b> F-Test Two-Sample (Derivative and PLS) for variances for the analysis of (SNA).	208



<i>List of Figures</i>	
<i>Title</i>	<i>Page No.</i>
<b>Figure 1-1:</b> Mechanism of action of antibacterial drugs.	3
<b>Figure 1-2:</b> (A) Role of PABA in folic acid synthesis in bacteria, (B) inhibition of folic acid synthesis by sulfonamides.	5
<b>Figure 1-3:</b> Simplexes (A) one, (B) two, (C) three, (D) four, and (E) five dimensional factor spaces.	27
<b>Figure 1-4:</b> The simplex reflection move for (A) one dimensional, (B) two dimensional and (C) three dimensional factor spaces.	27
<b>Figure 1-5:</b> Possible moves in the variable-size simplex algorithm.	29
<b>Figure 1-6:</b> General central composite design for (a) two factors and (b) three factors.	32
<b>Figure 2-1:</b> Absorption spectrum of blank solution against distilled water (D.W.) under the primary test.	51
<b>Figure 2-2:</b> Absorption spectrum of (5.0 $\mu\text{g.mL}^{-1}$ ) SMZ-DPA against reagent blank under the optimum conditions.	51
<b>Figure 2-3:</b> Effect of sodium nitrite on the color development of dye on the estimation of (5 $\mu\text{g.mL}^{-1}$ ) SMZ.	53
<b>Figure 2-4:</b> Effect of acidity on diazotization on the estimation of (5.0 $\mu\text{g.mL}^{-1}$ ) SMZ.	54
<b>Figure 2-5:</b> Effect of sulfamic acid concentration on the estimation of (5.0 $\mu\text{g.mL}^{-1}$ ) SMZ.	54
<b>Figure 2-6:</b> Effect of DPA concentration on the development of dye on the estimation of (5.0 $\mu\text{g.mL}^{-1}$ ) SMZ.	55
<b>Figure 2-7:</b> Effect of acidity on color dye on the estimation of (5.0 $\mu\text{g.mL}^{-1}$ ) SMZ.	56
<b>Figure 2-8:</b> Response function progress for simplex.	57
<b>Figure 2-9:</b> Calibration curve for the determination of (SMZ) by univariate optimal condition.	58
<b>Figure 2-10:</b> Calibration curve for the determination of (SMZ) by simplex optimal condition.	59

<b>Figure 2-11:</b> Determination of (SMZ) in tablet (Bactrim) by standard additions method level one, (0.1 mL from 100 $\mu\text{g}\cdot\text{mL}^{-1}$ Bactrim tablet).	62
<b>Figure 2-12:</b> Determination of (SMZ) in tablet (Bactrim) by standard additions method level two, (0.2 mL from 100 $\mu\text{g}\cdot\text{mL}^{-1}$ Bactrim tablet).	62
<b>Figure 2-13:</b> Determination of (SMZ) in tablet (Methoprim) by standard additions method level one, (0.1 mL from 100 $\mu\text{g}\cdot\text{mL}^{-1}$ Methoprim tablet).	63
<b>Figure 2-14:</b> Determination of (SMZ) in tablet (Methoprim) by standard additions method level two, (0.2 mL from 100 $\mu\text{g}\cdot\text{mL}^{-1}$ Methoprim tablet).	63
<b>Figure 2-15:</b> Determination of (SMZ) in syrup (Bactrim) by standard additions method level one, (0.1 mL from 100 $\mu\text{g}\cdot\text{mL}^{-1}$ Bactrim syrup).	64
<b>Figure 2-16:</b> Determination of (SMZ) in syrup (Bactrim) by standard additions method level two, (0.2 mL from 100 $\mu\text{g}\cdot\text{mL}^{-1}$ Bactrim syrup).	64
<b>Figure 2-17:</b> Determination of (SMZ) in syrup (Cotrim) by standard additions method level one, (0.1 mL from 100 $\mu\text{g}\cdot\text{mL}^{-1}$ Cotrim syrup).	65
<b>Figure 2-18:</b> Determination of (SMZ) in syrup (Cotrim) by standard additions method level two, (0.2 mL from 100 $\mu\text{g}\cdot\text{mL}^{-1}$ Cotrim syrup).	65
<b>Figure 2-19:</b> Absorption spectrum of blank solution against (D.W.) under the primary test.	66
<b>Figure 2-20:</b> Absorption spectrum of (5 $\mu\text{g}\cdot\text{mL}^{-1}$ ) SNA-DPA against reagent blank under the primary test.	67
<b>Figure 2-21:</b> Absorption spectrum of (5 $\mu\text{g}\cdot\text{mL}^{-1}$ ) SNA-DPA against reagent blank under the optimum conditions, simplex method.	67
<b>Figure 2-22:</b> Effect of sodium nitrite on the color development of dye in the determination of (5.0 $\mu\text{g}\cdot\text{mL}^{-1}$ ) of SNA.	69

<b>Figure 2-23:</b> Effect of HCl concentration on the color development of dye in the determination of (5.0 $\mu\text{g.mL}^{-1}$ ) of SNA.	70
<b>Figure 2-24:</b> Effect of sulfamic acid concentration on the determination of (5.0 $\mu\text{g.mL}^{-1}$ ) of SNA.	70
<b>Figure 2-25:</b> Effect of DPA concentration on the determination of (5.0 $\mu\text{g.mL}^{-1}$ ) of SNA.	71
<b>Figure 2-26:</b> Effect of acidity on color dye on the estimation of (5.0 $\mu\text{g.mL}^{-1}$ ) SNA.	72
<b>Figure 2-27:</b> Response function progress for simplex.	73
<b>Figure 2-28:</b> Calibration curve for the determination of (SNA) by univariate optimal condition.	74
<b>Figure 2-29:</b> Calibration curve for the determination of (SNA) by simplex optimal condition.	75
<b>Figure 2-30:</b> Determination of (SNA) in synthetic sample by standard additions method. Level one (0.1 mL from 100 $\mu\text{g.mL}^{-1}$ synthetic sample)	78
<b>Figure 2-31:</b> Determination of (SNA) in synthetic sample by standard additions method. Level two (0.2 mL from 100 $\mu\text{g.mL}^{-1}$ synthetic sample).	78
<b>Figure 3-1:</b> Absorption spectrum of blank solution against (D.W.) under the primary test and optimization condition.	92
<b>Figure 3-2:</b> Absorption spectrum of (30 $\mu\text{g.mL}^{-1}$ ) SMZ against the reagent blank under the primary test and optimization condition.	92
<b>Figure 3-3:</b> Effect of 1.0 mL of borax concentration on the color development of dye on the determination of (20.0 $\mu\text{g.mL}^{-1}$ ) SMZ.	94
<b>Figure 3-4:</b> Effect of 1.0 mL of NQS concentration on the color development of dye on the determination of (20.0 $\mu\text{g.mL}^{-1}$ ) SMZ.	95
<b>Figure 3-5:</b> The response surface for the absorbance of (SMZ-NQS) complex as a function of reagent concentration and borax concentration (at constant optimum value of reaction time, 5.717 min.).	98

<b>Figure 3-6:</b> The response surface for the absorbance of (SMZ-NQS) complex as a function of reagent concentration and reaction time (at constant optimum value of borax concentration, 0.05 M).	99
<b>Figure 3-7:</b> The response surface for the absorbance of (SMZ-NQS) complex as a function of borax concentration and reaction time (at constant optimum value of reagent concentration, 0.9 % m/v).	99
<b>Figure 3-8:</b> Calibration curve for the determination of (SMZ) by univariate optimal condition.	101
<b>Figure 3-9:</b> Calibration curve for the determination of SMZ by DOE optimal condition.	102
<b>Figure 3-10:</b> Determination of SMZ in pharmaceutical preparation (Bactrim syrup) sample by standard additions method, (level one 0.1 mL from 500 $\mu\text{g.mL}^{-1}$ )	105
<b>Figure 3-11:</b> Determination of (SMZ) in pharmaceutical preparation (Bactrim syrup) sample by standard additions method, (level two 0.2 mL from 500 $\mu\text{g.mL}^{-1}$ ).	105
<b>Figure 3-12:</b> Determination of (SMZ) in pharmaceutical preparation (Bactrim tablet) sample by standard additions method, (level one 0.1 mL from 500 $\mu\text{g.mL}^{-1}$ ).	106
<b>Figure 3-13:</b> Determination of (SMZ) in pharmaceutical preparation (Bactrim tablet) sample by standard additions method, (level two 0.2 mL from 500 $\mu\text{g.mL}^{-1}$ ).	106
<b>Figure 3-14:</b> Determination of (SMZ) in pharmaceutical preparation (Cotrim syrup) sample by standard additions method, (level one 0.1 mL from 500 $\mu\text{g.mL}^{-1}$ ).	107
<b>Figure 3-15:</b> Determination of (SMZ) in pharmaceutical preparation (Cotrim syrup) sample by standard additions method, (level two 0.2 mL from 500 $\mu\text{g.mL}^{-1}$ ).	107
<b>Figure 3-16:</b> Determination of (SMZ) in pharmaceutical preparation (Methoprim tablet) sample by standard additions method, (level one 0.1 mL from 500 $\mu\text{g.mL}^{-1}$ ).	108
<b>Figure 3-17:</b> Determination of (SMZ) in pharmaceutical preparation (Methoprim tablet) sample by standard additions method, (level two 0.2 mL from 500 $\mu\text{g.mL}^{-1}$ ).	108

<b>Figure 3-18:</b> Absorption spectrum of blank solution against (D.W.) under the primary test and optimization condition.	109
<b>Figure 3-19:</b> Absorption spectrum of ( $20 \mu\text{g.mL}^{-1}$ ) SNA against the reagent blank under the primary test and optimization condition.	110
<b>Figure 3-20:</b> Effect of borax concentration on the color development of dye on the estimation of ( $20 \mu\text{g.mL}^{-1}$ ) SNA.	111
<b>Figure 3-21:</b> Effect of 1.0 mL of NQS concentration on the color development of dye on the determination of ( $20.0 \mu\text{g.mL}^{-1}$ ) SNA.	112
<b>Figure 3-22:</b> The response surface for the absorbance of (SNA-NQS) complex as a function of reagent concentration and borax concentration (At constant optimum value of reaction time, 22.0 sec.).	115
<b>Figure 3-23:</b> The response surface for the absorbance of (SNA-NQS) complex as a function of reagent concentration and reaction time (At constant optimum value of borax concentration, 0.036 M)	116
<b>Figure 3-24:</b> The response surface for the absorbance of (SNA-NQS) complex as a function of borax concentration and reaction time (At constant optimum value of reagent concentration, 0.975 % m/v).	116
<b>Figure 3-25:</b> Calibration curve for the determination of (SNA) by univariate optimal condition.	117
<b>Figure 3-26:</b> Calibration curve for the determination of (SNA) by DOE optimal condition.	118
<b>Figure 3-27:</b> Determination of (SNA) in synthetic sample by standard additions method.	121
<b>Figure 4-1:</b> Differentiation of computed Gaussian analytical bands.	123
<b>Figure 4-2:</b> Absorption spectra of: (A) $5 \mu\text{g.mL}^{-1}$ sulfamethoxazole, (B) $20 \mu\text{g.mL}^{-1}$ sulfanilamide and (C) a mixture of $5 \mu\text{g.mL}^{-1}$ sulfamethoxazole and $20 \mu\text{g.mL}^{-1}$ sulfanilamide.	127

<b>Figure 4-3:</b> First derivative spectra of (A) 5 $\mu\text{g.mL}^{-1}$ sulfamethoxazole, (B) 20 $\mu\text{g.mL}^{-1}$ sulfanilamide and (C) mixture of 5 $\mu\text{g.mL}^{-1}$ sulfamethoxazole and 20 $\mu\text{g.mL}^{-1}$ sulfanilamide.	128
<b>Figure 4-4:</b> Second derivative spectra of (A) 5 $\mu\text{g.mL}^{-1}$ sulfamethoxazole, (B) 20 $\mu\text{g.mL}^{-1}$ sulfanilamide and (C) mixture of 5 $\mu\text{g.mL}^{-1}$ sulfamethoxazole and 20 $\mu\text{g.mL}^{-1}$ sulfanilamide.	128
<b>Figure 4-5:</b> First derivative spectra of (5-50 $\mu\text{g.mL}^{-1}$ ) sulfamethoxazole.	129
<b>Figure 4-6:</b> First derivative spectra of mixture contain (2-50 $\mu\text{g.mL}^{-1}$ ) Sulfamethoxazole in the presence of (2 $\mu\text{g.mL}^{-1}$ ) Sulfanilamide.	130
<b>Figure 4-7:</b> First derivative spectra mixture contain of (2 - 50 $\mu\text{g.mL}^{-1}$ ) Sulfamethoxazole in the presence of (5 $\mu\text{g.mL}^{-1}$ ) Sulfanilamide.	130
<b>Figure 4-8:</b> First derivative spectra of mixture contain (2-50 $\mu\text{g.mL}^{-1}$ ) sulfamethoxazole in the presence of (10 $\mu\text{g.ml}^{-1}$ ) sulfanilamide.	130
<b>Figure 4-9:</b> First derivative spectra of mixture contain (2-50 $\mu\text{g.mL}^{-1}$ ) Sulfamethoxazole in the presence of (15 $\mu\text{g.mL}^{-1}$ ) Sulfanilamide.	131
<b>Figure 4-10:</b> First derivative spectra of mixture contain (2-50 $\mu\text{g.mL}^{-1}$ ) Sulfamethoxazole in the presence of (20 $\mu\text{g.mL}^{-1}$ ) Sulfanilamide.	131
<b>Figure 4-11:</b> First derivative spectra of mixture contain (2-50 $\mu\text{g.mL}^{-1}$ ) Sulfamethoxazole in the presence of (30 $\mu\text{g.mL}^{-1}$ ) Sulfanilamide.	131
<b>Figure 4-12:</b> Calibration curves obtained via first derivative spectra of Sulfamethoxazole for peak-to-baseline at (A) 254 nm, (B) 287 nm, (C) 223 nm, (D) peak to peak between (254-287 nm) and (E) peak to peak between (223-254 nm).	132
<b>Figure 4-13:</b> Calibration curves obtained via first derivative spectra of Sulfamethoxazole for height at zero cross at (F) 235.62 nm, (G) 258.72 nm and (H) height-to-height between (235.62-285.72 nm).	132

<b>Figure 4-14:</b> Calibration curves obtained via first derivative spectra of Sulfamethoxazole for peak area at the interval (I) 241.95 nm to 267.04 nm and (J) 267.04 nm to 330 nm.	133
<b>Figure 4-15:</b> Calibration curves obtained via first derivative spectra of mixture of Sulfamethoxazole (2-50 $\mu\text{g.mL}^{-1}$ ) in the presence of (2 $\mu\text{g.mL}^{-1}$ ) Sulfanilamide, for peak-to-baseline at (A) 254 nm, (B) 287 nm, (C) 223 nm, (D) peak to peak between (254-287 nm) and (E) peak to peak between (223-254 nm).	133
<b>Figure 4-16:</b> Calibration curves obtained via first derivative spectra of mixture of Sulfamethoxazole (2-50 $\mu\text{g.mL}^{-1}$ ) in the presence of (2 $\mu\text{g.mL}^{-1}$ ) Sulfanilamide, for height at zero cross at (F) 235.62 nm, (G) 258.72 nm and (H) height to height between (235.62-285.72 nm).	134
<b>Figure 4-17:</b> Calibration curves obtained via first derivative spectra of mixture of Sulfamethoxazole (2-50 $\mu\text{g.mL}^{-1}$ ) in the presence of (2 $\mu\text{g.mL}^{-1}$ ) Sulfanilamide, for peak area at the interval (I) 241.95 nm to 267.04 nm and (J) 267.04 nm to 330 nm.	134
<b>Figure 4-18:</b> Calibration curves obtained via first derivative spectra of mixture of Sulfamethoxazole (2-50 $\mu\text{g.mL}^{-1}$ ) in the presence of (5 $\mu\text{g.mL}^{-1}$ ) Sulfanilamide, for peak-to-baseline at (A) 254 nm, (B) 287 nm, (C) 223 nm, (D) peak to peak between (254-287 nm) and (E) peak to peak between (223-254 nm).	135
<b>Figure 4-19:</b> Calibration curves obtained via first derivative spectra of mixture of Sulfamethoxazole (2-50 $\mu\text{g.mL}^{-1}$ ) in the presence of (5 $\mu\text{g.mL}^{-1}$ ) Sulfanilamide, for height at zero cross at (F) 235.62 nm, (G) 258.72 nm and (H) height to height between (235.62-285.72 nm).	135
<b>Figure 4-20:</b> Calibration curves obtained via first derivative spectra of mixture of Sulfamethoxazole (2-50 $\mu\text{g.mL}^{-1}$ ) in the presence of (5 $\mu\text{g.mL}^{-1}$ ) Sulfanilamide, for peak area at the interval (I) 241.95 nm to 267.04 nm and (J) 267.04 nm to 330 nm.	135
<b>Figure 4-21:</b> Calibration curves obtained via first derivative spectra of mixture of Sulfamethoxazole (2-50 $\mu\text{g.mL}^{-1}$ ) in the presence of (10 $\mu\text{g.mL}^{-1}$ ) Sulfanilamide, for peak-to-baseline at (A) 254 nm, (B) 287 nm, (C) 223 nm, (D) peak to peak between (254-287 nm) and (E) peak to peak between (223-254 nm).	136

<p><b>Figure 4-22:</b> Calibration curves obtained via first derivative spectra of mixture of Sulfamethoxazole (2-50 <math>\mu\text{g.mL}^{-1}</math>) in the presence of (10 <math>\mu\text{g.mL}^{-1}</math>) Sulfanilamide, for height at zero cross at (F) 235.62 nm, (G) 258.72 nm and (H) height to height between (235.62-285.72 nm).</p>	136
<p><b>Figure 4-23:</b> Calibration curves obtained via first derivative spectra of mixture of Sulfamethoxazole (2-50 <math>\mu\text{g.mL}^{-1}</math>) in the presence of (10 <math>\mu\text{g.mL}^{-1}</math>) Sulfanilamide, for peak area at the interval (I) 241.95 nm to 267.04 nm and (J) 267.04 nm to 330 nm.</p>	137
<p><b>Figure 4-24:</b> Calibration curves obtained via first derivative spectra of mixture of Sulfamethoxazole (2-50 <math>\mu\text{g.mL}^{-1}</math>) in the presence of (15 <math>\mu\text{g.mL}^{-1}</math>) Sulfanilamide, for peak-to-baseline at (A) 254 nm, (B) 287 nm, (C) 223 nm, (D) peak to peak between (254-287 nm) and (E) peak to peak between (223-254 nm).</p>	137
<p><b>Figure 4-25:</b> Calibration curves obtained via first derivative spectra of mixture of Sulfamethoxazole (2-50 <math>\mu\text{g.mL}^{-1}</math>) in the presence of (15 <math>\mu\text{g.mL}^{-1}</math>) Sulfanilamide, for height at zero cross at (F) 235.62 nm, (G) 258.72 nm and (H) height to height between (235.62-285.72 nm).</p>	138
<p><b>Figure 4-26:</b> Calibration curves obtained via first derivative spectra of mixture of Sulfamethoxazole (2-50 <math>\mu\text{g.mL}^{-1}</math>) in the presence of (15 <math>\mu\text{g.mL}^{-1}</math>) Sulfanilamide, for peak area at the interval (I) 241.95 nm to 267.04 nm and (J) 267.04 nm to 330 nm.</p>	138
<p><b>Figure 4-27:</b> Calibration curves obtained via first derivative spectra of mixture of Sulfamethoxazole (2-50 <math>\mu\text{g.mL}^{-1}</math>) in the presence of (20 <math>\mu\text{g.mL}^{-1}</math>) Sulfanilamide, for peak-to-baseline at (A) 254 nm, (B) 287 nm, (C) 223 nm, (D) peak to peak between (254-287 nm) and (E) peak to peak between (223-254 nm).</p>	139
<p><b>Figure 4-28:</b> Calibration curves obtained via first derivative spectra of mixture of Sulfamethoxazole (2-50 <math>\mu\text{g.mL}^{-1}</math>) in the presence of (20 <math>\mu\text{g.mL}^{-1}</math>) Sulfanilamide, for height at zero cross at (F) 235.62 nm, (G) 258.72 nm and (H) height to height between (235.62-285.72 nm).</p>	139



<b>Figure 4-29:</b> Calibration curves obtained via first derivative spectra of mixture of Sulfamethoxazole (2-50 $\mu\text{g.mL}^{-1}$ ) in the presence of (20 $\mu\text{g.mL}^{-1}$ ) Sulfanilamide, for peak area at the interval (I) 241.95 nm to 267.04 nm and (J) 267.04 nm to 330 nm.	140
<b>Figure 4-30:</b> Calibration curves obtained via first derivative spectra of mixture of Sulfamethoxazole (2-50 $\mu\text{g.mL}^{-1}$ ) in the presence of (30 $\mu\text{g.mL}^{-1}$ ) Sulfanilamide, for peak-to-baseline at (A) 254 nm, (B) 287 nm, (C) 223 nm, (D) peak to peak between (254-287 nm) and (E) peak to peak between (223-254 nm).	140
<b>Figure 4-31:</b> Calibration curves obtained via first derivative spectra of mixture of Sulfamethoxazole (2-50 $\mu\text{g.mL}^{-1}$ ) in the presence of (30 $\mu\text{g.mL}^{-1}$ ) Sulfanilamide, for height at zero cross at (F) 235.62 nm, (G) 258.72 nm and (H) height to height between (235.62-285.72 nm).	141
<b>Figure 4-32:</b> Calibration curves obtained via first derivative spectra of mixture of Sulfamethoxazole (2-50 $\mu\text{g.mL}^{-1}$ ) in the presence of (30 $\mu\text{g.mL}^{-1}$ ) Sulfanilamide, for peak area at the interval (I) 241.95 nm to 267.04 nm and (J) 267.04 nm to 330 nm.	141
<b>Figure 4-33:</b> Second derivative spectra of (5-50 $\mu\text{g.mL}^{-1}$ ) sulfamethoxazole.	142
<b>Figure 4-34:</b> Second derivative spectra of mixture contain (2-50 $\mu\text{g.mL}^{-1}$ ) sulfamethoxazole in the presence of (2 $\mu\text{g.mL}^{-1}$ ) sulfanilamide.	142
<b>Figure 4-35:</b> Second derivative spectra of mixture contain (2-50 $\mu\text{g.mL}^{-1}$ ) sulfamethoxazole in the presence of (5 $\mu\text{g.mL}^{-1}$ ) sulfanilamide.	142
<b>Figure 4-36:</b> Second derivative spectra of mixture contain (2-50 $\mu\text{g.mL}^{-1}$ ) sulfamethoxazole in the presence of (10 $\mu\text{g.mL}^{-1}$ ) sulfanilamide.	143
<b>Figure 4-37:</b> Second derivative spectra of mixture contain (2-50 $\mu\text{g.mL}^{-1}$ ) sulfamethoxazole in the presence of (15 $\mu\text{g.mL}^{-1}$ ) sulfanilamide.	143

<b>Figure 4-38:</b> Second derivative spectra of mixture contain (2-50 $\mu\text{g.mL}^{-1}$ ) sulfamethoxazole in the presence of (20 $\mu\text{g.mL}^{-1}$ ) sulfanilamide.	143
<b>Figure 4-39:</b> Second derivative spectra of mixture contain (2-50 $\mu\text{g.mL}^{-1}$ ) sulfamethoxazole in the presence of (30 $\mu\text{g.mL}^{-1}$ ) sulfanilamide.	144
<b>Figure 4-40:</b> Calibration curves obtained via second derivative spectra of sulfamethoxazole for peak-to-baseline at (A) 215 nm, (B) 239.5 nm, (C) 264.25 nm, (D) 267.75 nm and (E) 301 nm.	144
<b>Figure 4-41:</b> Calibration curves obtained via second derivative spectra of sulfamethoxazole for height at zero cross at (F) 245.86 nm and (G) 271.28 nm.	145
<b>Figure 4-42:</b> Calibration curves obtained via second derivative spectra of sulfamethoxazole for peak to peak, between (H) (215-239.5 nm), (I) (239.5-264.25 nm), (J) (239.5-267.75 nm), (K) (271.28-301 nm) and (L) height to height at zero cross (245.86-271.28 nm).	145
<b>Figure 4-43:</b> Calibration curves obtained via second derivative spectra of sulfamethoxazole for peak area at the interval (M) 221.75 nm to 254.12 nm, (N) 254.12 nm to 281 nm and (O) 286.86 nm to 329.5 nm.	146
<b>Figure 4-44:</b> Calibration curves obtained via second derivative spectra of mixture of Sulfamethoxazole (2-50 $\mu\text{g.mL}^{-1}$ ) in the presence of (2 $\mu\text{g.mL}^{-1}$ ) Sulfanilamide, for peak-to-baseline at (A) 215 nm, (B) 239.5 nm, (C) 264.25 nm, (D) 267.75 nm and (E) 301 nm.	146
<b>Figure 4-45:</b> Calibration curves obtained via second derivative spectra of mixture of Sulfamethoxazole (2-50 $\mu\text{g.mL}^{-1}$ ) in the presence of (2 $\mu\text{g.mL}^{-1}$ ) Sulfanilamide, for height at zero cross at (F) 245.86 nm and (G) 271.28 nm.	147

<p><b>Figure 4-46:</b> Calibration curves obtained via second derivative spectra of mixture of Sulfamethoxazole (2-50 <math>\mu\text{g.mL}^{-1}</math>) in the presence of (2 <math>\mu\text{g.mL}^{-1}</math>) Sulfanilamide, for peak to peak between (H) (215-239.5 nm), (I) (239.5-264.25 nm), (J) (239.5-267.7 5 nm), (K) (271.28-301 nm) and (L) height to height at zero cross (245.86-271.28 nm).</p>	147
<p><b>Figure 4-47:</b> Calibration curves obtained via second derivative spectra of mixture of Sulfamethoxazole (2-50 <math>\mu\text{g.mL}^{-1}</math>) in the presence of (2 <math>\mu\text{g.mL}^{-1}</math>) Sulfanilamide, for peak area at the interval (M) 221.75 nm to 254.12 nm, (N) 254.12 nm to 281 nm and (O) 286.86 nm to 329.5 nm.</p>	148
<p><b>Figure 4-48:</b> Calibration curves obtained via second derivative spectra of mixture of Sulfamethoxazole (2-50 <math>\mu\text{g.mL}^{-1}</math>) in the presence of (5 <math>\mu\text{g.mL}^{-1}</math>) Sulfanilamide, for peak-to-baseline at (A) 215 nm, (B) 239.5 nm, (C) 264.25nm, (D) 267.75 nm and (E) 301 nm.</p>	148
<p><b>Figure 4-49:</b> Calibration curves obtained via second derivative spectra of mixture of Sulfamethoxazole (2-50 <math>\mu\text{g.mL}^{-1}</math>) in the presence of (5 <math>\mu\text{g.mL}^{-1}</math>) Sulfanilamide, for height at zero cross at (F) 245.86 nm and (G) 271.28 nm.</p>	149
<p><b>Figure 4-50:</b> Calibration curves obtained via second derivative spectra of mixture of sulfamethoxazole (2-50 <math>\mu\text{g.mL}^{-1}</math>) in the presence of (5 <math>\mu\text{g.mL}^{-1}</math>) sulfanilamide, for peak to peak between (H) (215-239.5 nm), (I) (239.5-264.25 nm), (J) (239.5-267.7 5 nm), (K) (271.28-301 nm) and (L) height to height at zero cross (245.86-271.28 nm).</p>	149
<p><b>Figure 4-51:</b> Calibration curves obtained via second derivative spectra of mixture of Sulfamethoxazole (2-50 <math>\mu\text{g.mL}^{-1}</math>) in the presence of (5 <math>\mu\text{g.mL}^{-1}</math>) Sulfanilamide, for peak area at the interval (M) 221.75 nm to 254.12 nm, (N) 254.12 nm to 281 nm and (O) 286.86 nm to 329.5 nm.</p>	150

<p><b>Figure 4-52:</b> Calibration curves obtained via second derivative spectra of mixture of Sulfamethoxazole (2-50 <math>\mu\text{g.mL}^{-1}</math>) in the presence of (10 <math>\mu\text{g.mL}^{-1}</math>) Sulfanilamide, for peak-to-baseline at (A) 215 nm, (B) 239.5 nm, (C) 264.25 nm, (D) 267.75 nm and (E) 301 nm.</p>	150
<p><b>Figure 4-53:</b> Calibration curves obtained via second derivative spectra of mixture of Sulfamethoxazole (2-50 <math>\mu\text{g.mL}^{-1}</math>) in the presence of (10 <math>\mu\text{g.mL}^{-1}</math>) Sulfanilamide, for height at zero cross at (F) 245.86 nm and (G) 271.28 nm.</p>	151
<p><b>Figure 4-54:</b> Calibration curves obtained via second derivative spectra of mixture of sulfamethoxazole (2-50 <math>\mu\text{g.mL}^{-1}</math>) in the presence of (10 <math>\mu\text{g.mL}^{-1}</math>) sulfanilamide, for peak to peak between (H) (215-239.5 nm), (I) (239.5-264.25 nm), (J) (239.5-267.7 5 nm), (K) (271.28-301 nm) and (L) height to height at zero cross (245.86-271.28 nm).</p>	151
<p><b>Figure 4-55:</b> Calibration curves obtained via second derivative spectra of mixture of Sulfamethoxazole (2-50 <math>\mu\text{g.mL}^{-1}</math>) in the presence of (10 <math>\mu\text{g.mL}^{-1}</math>) Sulfanilamide, for peak area at the interval (M) 221.75 nm to 254.12 nm, (N) 254.12 nm to 281 nm and (O) 286.86 nm to 329.5 nm.</p>	152
<p><b>Figure 4-56:</b> Calibration curves obtained via second derivative spectra of mixture of Sulfamethoxazole (2-50 <math>\mu\text{g.mL}^{-1}</math>) in the presence of (15 <math>\mu\text{g.mL}^{-1}</math>) Sulfanilamide, for peak-to-baseline at (A) 215 nm, (B) 239.5 nm, (C) 264.25 nm, (D) 267.75 nm and (E) 301 nm.</p>	152
<p><b>Figure 4-57:</b> Calibration curves obtained via second derivative spectra of mixture of Sulfamethoxazole (2-50 <math>\mu\text{g.mL}^{-1}</math>) in the presence of (15 <math>\mu\text{g.mL}^{-1}</math>) Sulfanilamide, for height at zero cross at (F) 245.86 nm and (G) 271.28 nm.</p>	153
<p><b>Figure 4-58:</b> Calibration curves obtained via second derivative spectra of mixture of sulfamethoxazole (2-50 <math>\mu\text{g.mL}^{-1}</math>) in the presence of (15 <math>\mu\text{g.mL}^{-1}</math>) sulfanilamide, for peak to peak between (H) (215-239.5 nm), (I) (239.5-264.25 nm), (J) (239.5-267.7 5 nm), (K) (271.28-301 nm) and (L) height to height at zero cross (245.86-271.28 nm).</p>	153

<p><b>Figure 4-59:</b> Calibration curves obtained via second derivative spectra of mixture of Sulfamethoxazole (2-50 <math>\mu\text{g.mL}^{-1}</math>) in the presence of (15 <math>\mu\text{g.mL}^{-1}</math>) Sulfanilamide, for peak area at the interval (M) 221.75 nm to 254.12 nm, (N) 254.12 nm to 281 nm and (O) 286.86 nm to 329.5 nm.</p>	154
<p><b>Figure 4-60:</b> Calibration curves obtained via second derivative spectra of mixture of Sulfamethoxazole (2-50 <math>\mu\text{g.mL}^{-1}</math>) in the presence of (20 <math>\mu\text{g.mL}^{-1}</math>) Sulfanilamide, for peak-to-baseline at (A) 215 nm, (B) 239.5 nm, (C) 264.25 nm, (D) 267.75 nm and (E) 301 nm.</p>	154
<p><b>Figure 4-61:</b> Calibration curves obtained via second derivative spectra of mixture of Sulfamethoxazole (2-50 <math>\mu\text{g.mL}^{-1}</math>) in the presence of (20 <math>\mu\text{g.mL}^{-1}</math>) Sulfanilamide, for height at zero cross at (F) 245.86 nm and (G) 271.28 nm.</p>	155
<p><b>Figure 4-62:</b> Calibration curves obtained via second derivative spectra of mixture of sulfamethoxazole (2-50 <math>\mu\text{g.mL}^{-1}</math>) in the presence of (20 <math>\mu\text{g.mL}^{-1}</math>) sulfanilamide, for peak to peak between (H) (215-239.5 nm), (I) (239.5-264.25 nm), (J) (239.5-267.7 5 nm), (K) (271.28-301 nm) and (L) height to height at zero cross (245.86-271.28 nm).</p>	155
<p><b>Figure 4-63:</b> Calibration curves obtained via second derivative spectra of mixture of Sulfamethoxazole (2-50 <math>\mu\text{g.mL}^{-1}</math>) in the presence of (20 <math>\mu\text{g.mL}^{-1}</math>) Sulfanilamide, for peak area at the interval (M) 221.75 nm to 254.12 nm, (N) 254.12 nm to 281 nm and (O) 286.86 nm to 329.5 nm.</p>	156
<p><b>Figure 4-64:</b> Calibration curves obtained via second derivative spectra of mixture of Sulfamethoxazole (2-50 <math>\mu\text{g.mL}^{-1}</math>) in the presence of (30 <math>\mu\text{g.mL}^{-1}</math>) Sulfanilamide, for peak-to-baseline at (A) 239.5 nm, (B) 264.25 nm, (C) 267.75 nm and (D) 301 nm.</p>	156
<p><b>Figure 4-65:</b> Calibration curves obtained via second derivative spectra of mixture of Sulfamethoxazole (2-50 <math>\mu\text{g.mL}^{-1}</math>) in the presence of (30 <math>\mu\text{g.mL}^{-1}</math>) Sulfanilamide, for height at zero cross at (E) 245.86 nm and (F) 271.28 nm.</p>	157
<p><b>Figure 4-66:</b> Calibration curves obtained via second derivative spectra of mixture of sulfamethoxazole (2-50 <math>\mu\text{g.mL}^{-1}</math>) in the presence of (30 <math>\mu\text{g.mL}^{-1}</math>) sulfanilamide, for peak to peak between ((G)) (239.5-264.25 nm), (H) (239.5-267.7 5 nm), (I) (271.28-301 nm) and (J) height to height at zero cross (245.86-271.28 nm).</p>	157

<b>Figure 4-67:</b> Calibration curves obtained via second derivative spectra of mixture of Sulfamethoxazole (2-50 $\mu\text{g.mL}^{-1}$ ) in the presence of (30 $\mu\text{g.mL}^{-1}$ ) Sulfanilamide, for peak area at the interval (K) 254.12 nm to 281 nm and (L) 286.86 nm to 329.5 nm.	157
<b>Figure 4-68:</b> First derivative spectra of (5-50 $\mu\text{g.mL}^{-1}$ ) sulfanilamide.	159
<b>Figure 4-69:</b> First derivative spectra of (5-50 $\mu\text{g.mL}^{-1}$ ) sulfanilamide in the presence of (2 $\mu\text{g.mL}^{-1}$ ) sulfamethoxazole.	160
<b>Figure 4-70:</b> First derivative spectra of (5-50 $\mu\text{g.mL}^{-1}$ ) sulfanilamide in the presence of (5 $\mu\text{g.mL}^{-1}$ ) sulfamethoxazole.	160
<b>Figure 4-71:</b> First derivative spectra of (5-50 $\mu\text{g.mL}^{-1}$ ) sulfanilamide in the presence of (10 $\mu\text{g.mL}^{-1}$ ) sulfamethoxazole.	160
<b>Figure 4-72:</b> First derivative spectra of (5-50 $\mu\text{g.mL}^{-1}$ ) sulfanilamide in the presence of (15 $\mu\text{g.mL}^{-1}$ ) sulfamethoxazole.	161
<b>Figure 4-73:</b> First derivative spectra of (5-50 $\mu\text{g.mL}^{-1}$ ) sulfanilamide in the presence of (20 $\mu\text{g.mL}^{-1}$ ) sulfamethoxazole.	161
<b>Figure 4-74:</b> First derivative spectra of (5-50 $\mu\text{g.mL}^{-1}$ ) sulfanilamide in the presence of (30 $\mu\text{g.mL}^{-1}$ ) sulfamethoxazole.	161
<b>Figure 4-75:</b> Calibration curves obtained via first derivative spectra of sulfanilamide for peak-to-baseline at (A) 224 nm, (B) 246 nm, (C) 271 nm and (D) height at zero cross at 241.95 nm and (E) height at zero cross at 267.04 nm.	162
<b>Figure 4-76:</b> Calibration curves obtained via first derivative spectra of sulfanilamide for peak to peak between (F) (224-246 nm), (G) (246-271 nm) and (H) height-to-height between (241.95-271 nm).	162
<b>Figure 4-77:</b> Calibration curves obtained via first derivative spectra of sulfanilamide for peak area at the interval (I) (235.62 nm to 258.72 nm) and (J) (258.72 nm to 331 nm).	163
<b>Figure 4-78:</b> Calibration curves obtained via first derivative spectra of mixture of sulfanilamide (2-50 $\mu\text{g.mL}^{-1}$ ) in the presence of (2 $\mu\text{g.mL}^{-1}$ ) sulfamethoxazole, for peak-to-baseline at (A) 224 nm, (B) 246 nm, (C) 271 nm, (D) height at zero cross at 241.95 nm and (E) height at zero cross at 267.04 nm.	163

<p><b>Figure 4-79:</b> Calibration curves obtained via first derivative spectra of mixture of sulfanilamide (2-50 <math>\mu\text{g.mL}^{-1}</math>) in the presence of (2 <math>\mu\text{g.mL}^{-1}</math>) sulfamethoxazole, for peak to peak between (F) (224-246 nm), (G) (246-271 nm) and (H) height-to-height between (241.95-271 nm).</p>	164
<p><b>Figure 4-80:</b> Calibration curves obtained via first derivative spectra of mixture of sulfanilamide (2-50 <math>\mu\text{g.mL}^{-1}</math>) in the presence of (2 <math>\mu\text{g.mL}^{-1}</math>) sulfamethoxazole, for peak area at the interval (I) 235.62 nm to 258.72 nm and (J) 258.72 nm to 331 nm.</p>	164
<p><b>Figure 4-81:</b> Calibration curves obtained via first derivative spectra of mixture of sulfanilamide (2-50 <math>\mu\text{g.mL}^{-1}</math>) in the presence of (5 <math>\mu\text{g.mL}^{-1}</math>) sulfamethoxazole, for peak-to-baseline at (A) 224 nm, (B) 246 nm, (C) 271 nm, (D) height at zero cross at 241.95 nm, and (E) height at zero cross at 267.04 nm.</p>	165
<p><b>Figure 4-82:</b> Calibration curves obtained via first derivative spectra of mixture of sulfanilamide (2-50 <math>\mu\text{g.mL}^{-1}</math>) in the presence of (5 <math>\mu\text{g.mL}^{-1}</math>) sulfamethoxazole, for peak to peak between (F) (224-246 nm), (G) (246-271 nm) and (H) height-to-height between (241.95-271 nm).</p>	165
<p><b>Figure 4-83:</b> Calibration curves obtained via first derivative spectra of mixture of sulfanilamide (2-50 <math>\mu\text{g.mL}^{-1}</math>) in the presence of (5 <math>\mu\text{g.mL}^{-1}</math>) sulfamethoxazole, for peak area at the interval (I) 235.62 nm to 258.72 nm and (J) 258.72 nm to 331 nm.</p>	166
<p><b>Figure 4-84:</b> Calibration curves obtained via first derivative spectra of mixture of sulfanilamide(2-50 <math>\mu\text{g.mL}^{-1}</math>)in the presence of (10 <math>\mu\text{g.mL}^{-1}</math>) sulfamethoxazole, for peak-to-baseline at (A) 224 nm, (B) 246 nm, (C) 271 nm, (D) height at zero cross at 241.95 nm and (E) height at zero cross at 267.04 nm.</p>	166
<p><b>Figure 4-85:</b> Calibration curves obtained via first derivative spectra of mixture of sulfanilamide (2-50 <math>\mu\text{g.mL}^{-1}</math>)in the presence of (10 <math>\mu\text{g.mL}^{-1}</math>) sulfamethoxazole, for peak to peak between (F) (224-246 nm), (G) (246-271 nm) and (H) height-to-height between (241.95-271 nm).</p>	167

<p><b>Figure 4-86:</b> Calibration curves obtained via first derivative spectra of mixture of sulfanilamide (2-50 <math>\mu\text{g.mL}^{-1}</math>) in the presence of (10 <math>\mu\text{g.mL}^{-1}</math>) sulfamethoxazole, for peak area at the interval (I) 235.62 nm to 258.72 nm and (J) 258.72 nm to 331 nm.</p>	167
<p><b>Figure 4-87:</b> Calibration curves obtained via first derivative spectra of mixture of sulfanilamide (2-50 <math>\mu\text{g.mL}^{-1}</math>) in the presence of (15 <math>\mu\text{g.mL}^{-1}</math>) sulfamethoxazole, for peak-to-baseline at (A) 224 nm, (B) 246 nm, (C) 271 nm, (D) height at zero cross at 241.95 nm and (E) height at zero cross at 267.04 nm.</p>	168
<p><b>Figure 4-88:</b> Calibration curves obtained via first derivative spectra of mixture of sulfanilamide (2-50 <math>\mu\text{g.mL}^{-1}</math>) in the presence of (15 <math>\mu\text{g.mL}^{-1}</math>) sulfamethoxazole, for peak to peak between (F) (224-246 nm), (G) (246-271 nm) and (H) height-to-height between (241.95-271 nm).</p>	168
<p><b>Figure 4-89:</b> Calibration curves obtained via first derivative spectra of mixture of sulfanilamide (2-50 <math>\mu\text{g.mL}^{-1}</math>) in the presence of (15 <math>\mu\text{g.mL}^{-1}</math>) sulfamethoxazole, for peak area at the interval (I) 235.62 nm to 258.72 nm and (J) 258.72 nm to 331 nm.</p>	169
<p><b>Figure 4-90:</b> Calibration curves obtained via first derivative spectra of mixture of sulfanilamide (2-50 <math>\mu\text{g.mL}^{-1}</math>) in the presence of (20 <math>\mu\text{g.mL}^{-1}</math>) sulfamethoxazole, for peak-to-baseline at (A) 224 nm, (B) 246 nm, (C) 271 nm, (D) height at zero cross at 241.95 nm and (E) height at zero cross at 267.04 nm.</p>	169
<p><b>Figure 4-91:</b> Calibration curves obtained via first derivative spectra of mixture of sulfanilamide (2-50 <math>\mu\text{g.mL}^{-1}</math>) in the presence of (20 <math>\mu\text{g.mL}^{-1}</math>) sulfamethoxazole, for peak to peak between (F) (224-246 nm), (G) (246-271 nm) and (H) height-to-height between (241.95-271 nm).</p>	170
<p><b>Figure 4-92:</b> Calibration curves obtained via first derivative spectra of mixture of sulfanilamide (2-50 <math>\mu\text{g.mL}^{-1}</math>) in the presence of (20 <math>\mu\text{g.mL}^{-1}</math>) sulfamethoxazole, for peak area at the interval (I) 235.62 nm to 258.72 nm and (J) 258.72 nm to 331 nm.</p>	170



<b>Figure 4-93:</b> Calibration curves obtained via first derivative spectra of mixture of sulfanilamide(2-50 $\mu\text{g.mL}^{-1}$ )in the presence of (30 $\mu\text{g.mL}^{-1}$ ) sulfamethoxazole, for peak-to-baseline at (A) 224 nm, (B) 246 nm, (C) 271 nm and (D) height at zero cross at 241.95 nm and (E) height at zero cross at 267.04 nm.	171
<b>Figure 4-94:</b> Calibration curves obtained via first derivative spectra of mixture of sulfanilamide (2-50 $\mu\text{g.mL}^{-1}$ )in the presence of (30 $\mu\text{g.mL}^{-1}$ ) sulfamethoxazole, for peak to peak between (F) (224-246 nm), (G) (246-271 nm) and (H) height-to-height between (241.95-271 nm).	171
<b>Figure 4-95:</b> Calibration curves obtained via first derivative spectra of mixture of sulfanilamide (2-50 $\mu\text{g.mL}^{-1}$ ) in the presence of (30 $\mu\text{g.mL}^{-1}$ ) sulfamethoxazole, for peak area at the interval (I) 235.62 nm to 258.72 nm and (J) 258.72 nm to 331 nm.	172
<b>Figure 4-96:</b> Second derivative spectra of (5-50 $\mu\text{g.mL}^{-1}$ ) sulfanilamide.	172
<b>Figure 4-97:</b> Second derivative spectra of (2-50 $\mu\text{g.mL}^{-1}$ ) sulfanilamide in the presence of (2 $\mu\text{g.mL}^{-1}$ ) sulfamethoxazole.	173
<b>Figure 4-98:</b> Second derivative spectra of (2-50 $\mu\text{g.mL}^{-1}$ ) sulfanilamide in the presence of (5 $\mu\text{g.mL}^{-1}$ ) sulfamethoxazole.	173
<b>Figure 4-99:</b> Second derivative spectra of (2-50 $\mu\text{g.mL}^{-1}$ ) sulfanilamide in the presence of (10 $\mu\text{g.mL}^{-1}$ ) sulfamethoxazole.	173
<b>Figure 4-100:</b> Second derivative spectra of (2-50 $\mu\text{g.mL}^{-1}$ ) sulfanilamide in the presence of (15 $\mu\text{g.mL}^{-1}$ ) sulfamethoxazole.	174
<b>Figure 4-101:</b> Second derivative spectra of (2-50 $\mu\text{g.mL}^{-1}$ ) sulfanilamide in the presence of (20 $\mu\text{g.mL}^{-1}$ ) sulfamethoxazole.	174
<b>Figure 4-102:</b> Second derivative spectra of (2-50 $\mu\text{g.mL}^{-1}$ ) sulfanilamide in the presence of (30 $\mu\text{g.mL}^{-1}$ ) sulfamethoxazole.	174
<b>Figure 4-103:</b> Calibration curves obtained via second derivative spectra of sulfanilamide for peak-to-baseline at (A) 218 nm, (B) 231 nm, (C) 260 nm, (D) 278 nm, (E) height at zero cross at 254 nm and (F) height at zero cross at 281 nm.	175
<b>Figure 4-104:</b> Calibration curves obtained via second derivative spectra of sulfanilamide for peak to peak (G) 218-231 nm, (H) 231-260 nm, (I) 260-278 nm and (J) height to height at zero cross 254-281 nm.	175

<p><b>Figure 4-105:</b> Calibration curves obtained via second derivative spectra of sulfanilamide for peak area at the interval (K) 210 nm to 224 nm, (L) 224 nm to 245.84 nm, (M) 245.84 nm to 271.28 nm and (N) 271.28 nm to 330 nm.</p>	176
<p><b>Figure 4-106:</b> Calibration curves obtained via second derivative spectra of sulfanilamide (2-50 <math>\mu\text{g.mL}^{-1}</math>) in the presence of (2 <math>\mu\text{g.mL}^{-1}</math>) sulfamethoxazole, for peak-to-baseline at (A) 218 nm, (B) 231 nm, (C) 260 nm, (D) 278 nm, (E) height at zero cross at 254 nm and (F) height at zero cross at 281 nm.</p>	176
<p><b>Figure 4-107:</b> Calibration curves obtained via second derivative spectra of sulfanilamide (2-50 <math>\mu\text{g.mL}^{-1}</math>) in the presence of (2 <math>\mu\text{g.mL}^{-1}</math>) sulfamethoxazole, for peak to peak (G) 218-231 nm, (H) 231-260 nm, (I) 260-278 nm and (J) height to height at zero cross 254-281 nm.</p>	177
<p><b>Figure 4-108:</b> Calibration curves obtained via second derivative spectra of sulfanilamide (2-50 <math>\mu\text{g.mL}^{-1}</math>) in the presence of (2 <math>\mu\text{g.mL}^{-1}</math>) sulfamethoxazole, for peak area at the interval (K) 210 nm to 224 nm, (L) 224 nm to 245.84 nm, (M) 245.84 nm to 271.28 nm and (N) 271.28 nm to 330 nm.</p>	177
<p><b>Figure 4-109:</b> Calibration curves obtained via second derivative spectra of sulfanilamide (2-50 <math>\mu\text{g.mL}^{-1}</math>) in the presence of (5 <math>\mu\text{g.mL}^{-1}</math>) sulfamethoxazole, for peak-to-baseline at (A) 218 nm, (B) 231 nm, (C) 260 nm, (D) 278 nm, (E) height at zero cross at 254 nm and (F) height at zero cross at 281 nm.</p>	178
<p><b>Figure 4-110:</b> Calibration curves obtained via second derivative spectra of sulfanilamide (2-50 <math>\mu\text{g.mL}^{-1}</math>) in the presence of (5 <math>\mu\text{g.mL}^{-1}</math>) sulfamethoxazole, for peak to peak (G) 218-231 nm, (H) 231-260 nm, (I) 260-278 nm and (J) height to height at zero cross 254-281 nm.</p>	178
<p><b>Figure 4-111:</b> Calibration curves obtained via second derivative spectra of sulfanilamide (2-50 <math>\mu\text{g.mL}^{-1}</math>) in the presence of (5 <math>\mu\text{g.mL}^{-1}</math>) sulfamethoxazole, for peak area at the interval (K) 210 nm to 224 nm, (L) 224 nm to 245.84 nm, (M) 245.84 nm to 271.28 nm and (N) 271.28 nm to 330 nm.</p>	179

<p><b>Figure 4-112:</b> Calibration curves obtained via second derivative spectra of sulfanilamide (2-50 <math>\mu\text{g.mL}^{-1}</math>) in the presence of (10 <math>\mu\text{g.mL}^{-1}</math>) sulfamethoxazole, for peak-to-baseline at (A) 218 nm, (B) 231 nm, (C) 260 nm, (D) 278 nm, (E) height at zero cross at 254 nm and (F) height at zero cross at 281 nm.</p>	179
<p><b>Figure 4-113:</b> Calibration curves obtained via second derivative spectra of sulfanilamide (2-50 <math>\mu\text{g.mL}^{-1}</math>) in the presence of (10 <math>\mu\text{g.mL}^{-1}</math>) sulfamethoxazole, for peak to peak (G) 218-231 nm, (H) 231-260 nm, (I) 260-278 nm and (J) height to height at zero cross 254-281 nm.</p>	180
<p><b>Figure 4-114:</b> Calibration curves obtained via second derivative spectra of sulfanilamide (2-50 <math>\mu\text{g.mL}^{-1}</math>) in the presence of (10 <math>\mu\text{g.mL}^{-1}</math>) sulfamethoxazole, for peak area at the interval (K) 210 nm to 224 nm, (L) 224 nm to 245.84 nm, (M) 245.84 nm to 271.28 nm and (N) 271.28 nm to 330 nm.</p>	180
<p><b>Figure 4-115:</b> Calibration curves obtained via second derivative spectra of sulfanilamide (2-50 <math>\mu\text{g.mL}^{-1}</math>) in the presence of (15 <math>\mu\text{g.mL}^{-1}</math>) sulfamethoxazole, for peak-to-baseline at (A) 218 nm, (B) 231 nm, (C) 260 nm, (D) 278 nm, (E) height at zero cross at 254 nm and (F) height at zero cross at 281 nm.</p>	181
<p><b>Figure 4-116:</b> Calibration curves obtained via second derivative spectra of sulfanilamide (2-50 <math>\mu\text{g.mL}^{-1}</math>) in the presence of (15 <math>\mu\text{g.mL}^{-1}</math>) sulfamethoxazole, for peak to peak (G) 218-231 nm, (H) 231-260 nm, (I) 260-278 nm and (J) height to height at zero cross 254-281 nm.</p>	181
<p><b>Figure 4-117:</b> Calibration curves obtained via second derivative spectra of sulfanilamide (2-50 <math>\mu\text{g.mL}^{-1}</math>) in the presence of (15 <math>\mu\text{g.mL}^{-1}</math>) sulfamethoxazole, for peak area at the interval (K) 210 nm to 224 nm, (L) 224 nm to 245.84 nm, (M) 245.84 nm to 271.28 nm and (N) 271.28 nm to 330 nm.</p>	182
<p><b>Figure 4-118:</b> Calibration curves obtained via second derivative spectra of sulfanilamide (2-50 <math>\mu\text{g.mL}^{-1}</math>) in the presence of (20 <math>\mu\text{g.mL}^{-1}</math>) sulfamethoxazole, for peak-to-baseline at (A) 218 nm, (B) 231 nm, (C) 260 nm, (D) 278 nm, (E) height at zero cross at 254 nm and (F) height at zero cross at 281 nm.</p>	182

<b>Figure 4-119:</b> Calibration curves obtained via second derivative spectra of sulfanilamide (2-50 $\mu\text{g.mL}^{-1}$ ) in the presence of (20 $\mu\text{g.mL}^{-1}$ ) sulfamethoxazole, for peak to peak (G) 218-231 nm, (H) 231-260 nm, (I) 260-278 nm and (J) height to height at zero cross 254-281 nm.	183
<b>Figure 4-120:</b> Calibration curves obtained via second derivative spectra of sulfanilamide (2-50 $\mu\text{g.mL}^{-1}$ ) in the presence of (20 $\mu\text{g.mL}^{-1}$ ) sulfamethoxazole, for peak area at the interval (K) 224 nm to 245.84 nm, (M) 245.84 nm to 271.28 nm and (N) 271.28 nm to 330 nm.	183
<b>Figure 4-121:</b> Calibration curves obtained via second derivative spectra of sulfanilamide (2-50 $\mu\text{g.mL}^{-1}$ ) in the presence of (30 $\mu\text{g.mL}^{-1}$ ) sulfamethoxazole, for peak-to-baseline at (A) 218 nm, (B) 231 nm, (C) 260 nm, (D) 278 nm, (E) height at zero cross at 254 nm and (F) height at zero cross at 281 nm.	184
<b>Figure 4-122:</b> Calibration curves obtained via second derivative spectra of sulfanilamide (2-50 $\mu\text{g.mL}^{-1}$ ) in the presence of (30 $\mu\text{g.mL}^{-1}$ ) sulfamethoxazole, for peak to peak (G) 218-231 nm, (H) 231-260 nm, (I) 260-278 nm and (J) height to height at zero cross 254-281 nm.	184
<b>Figure 4-123:</b> Calibration curves obtained via second derivative spectra of sulfanilamide (2-50 $\mu\text{g.mL}^{-1}$ ) in the presence of (30 $\mu\text{g.mL}^{-1}$ ) sulfamethoxazole, for peak area at the interval (K) 224 nm to 245.84 nm, (M) 245.84 nm to 271.28 nm and (N) 271.28 nm to 330 nm.	185
<b>Figure 4-124:</b> Normal mode spectrum of (A) 10 $\mu\text{g.mL}^{-1}$ of sulfamethoxazole and (B) 10 $\mu\text{g.mL}^{-1}$ sulfanilamide against their blanks	192
<b>Figure 4-125:</b> Calibration curve of sulfamethoxazole constructed at 266 nm.	193
<b>Figure 4-126:</b> Calibration curve of Sulfanilamide constructed at 258 nm.	194
<b>Figure 4-127:</b> Plot of PRESS against the number of factors for SMZ and SNA mixture: (A) PLS-2 model, (B) PLS-1 model for SMZ and (C) PLS-1 model for SNA.	197

<b>Figure 4-128:</b> Plot of predicated concentrations of training sulfamethoxazole and sulfanilamide sets obtained by PLS-1 against those obtained by PLS-2 model.	200
<b>Figure 4-129:</b> Plots of predicated sulfamethoxazole and sulfanilamide concentrations in synthetic mixture samples obtained by PLS-1 against their true concentrations.	204
<b>Figure 4-130:</b> Plots of predicated sulfamethoxazole and sulfanilamide concentrations in synthetic mixture samples obtained by PLS-2 against their true concentrations.	205
<b>Figure 4-131:</b> Plots of residuals of SMZ and SNA against their actual concentrations in the synthetic mixture samples, by PLS-1 model.	206
<b>Figure 4-132:</b> Plots of residuals of SMZ and SNA against their actual concentrations in the synthetic mixture samples, by PLS-2 model.	206



# ***CHAPTER ONE***

## ***Introduction***

## Chapter One

### 1 Introduction

#### 1-1 Ultraviolet-Visible (UV-VIS) Absorption Spectroscopy

Absorption of light by solution is one of the oldest and still one of the most useful instrumental methods <sup>(1)</sup>. Ultraviolet-Visible Spectroscopy is a technique that measures the interaction of molecules with electromagnetic radiation between 190 nm to about 800 nm and is divided into the ultraviolet (UV, 190 to about 400 nm) and visible (VIS, about 400-800 nm) regions <sup>(2,3)</sup>.

The energy of this radiation is absorbed from analyte species and it is used to promote their valance electrons from the ground state to an excited state<sup>(2)</sup>. A spectrum is obtained when the absorption of light is measured as a function of its frequency or wavelength<sup>(2)</sup>. Absorbing species include organic molecules and ions as well as a number of inorganic anions <sup>(4)</sup>.

The absorption of UV or visible radiation corresponds to the three types of electronic transition <sup>(5)</sup>:

1. Transitions involving  $\pi$ ,  $\sigma$ , and  $n$  electrons.
2. Transitions involving charge-transfer electrons.
3. Transitions involving  $d$  and  $f$  electrons.

Ultraviolet-Visible Spectroscopy have somewhat limited application for qualitative analysis because the number of absorption maxima and minima are relatively few while Lambert-Beer law offers a valuable and simple method to the chemist for quantitative analysis <sup>(3,4)</sup>.

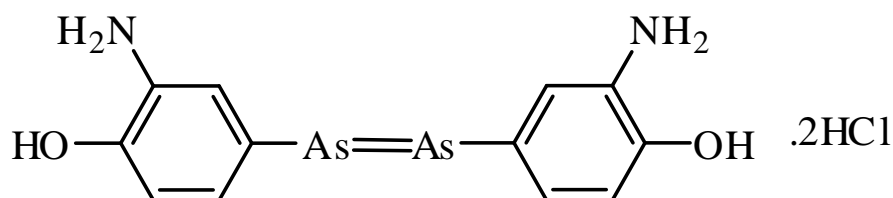
In general, spectroscopic measurements are high sensitive, nondestructive, have good accuracy, and require only small amounts of material for analysis <sup>(2,4)</sup>, thus it has innumerable applications in the drugs and pharmaceutical industry <sup>(3)</sup>.

#### 1-2 Antibacterial Drugs

Antibacterials are drugs of natural or synthetic origin that have the capacity to kill or to inhibit the growth of micro-organisms. Antibacterials that are sufficiently non-toxic to the host are used as chemotherapeutic agents in the treatment of infectious diseases amongst humans, animals and plants <sup>(6)</sup>.

The first antibacterial agent in the world was salvarsan as shown in scheme (1-1), an organoarsenic compound was found to be highly effective for the treatment of syphilis (replacing mercury which had often disastrous side effects) that was synthesized by a German medical doctor and researcher named Paul Ehrlich, who is known as the father of immunology and chemotherapy. He had won the Nobel Prize for medicine in 1908<sup>(7-9)</sup>.

Ehrlich hypothesized that certain dyes could selectively “stain” harmful bacteria cells without harming host cells. He referred to such compounds as “magic bullets” and coined the term chemotherapy as a general descriptor for chemical remedies targeted to selectively kill infectious cells<sup>(8,9)</sup>.



**Scheme 1-1:** Structure of salvarsan.

### 1-2-1 Classification of antibacterial drugs and their mechanism of action

Antibacterial drugs have selective toxicity against the infecting organisms and are usually divided into two groups<sup>(10)</sup>:

- a. Bacteriostatic, those that inhibit growth of the organism.
- b. Bactericidal, those that kill the organism.

Antibacterial agents primarily act by<sup>(11)</sup>:

1. Inhibiting cell wall synthesis e.g.; penicillin, cycloserine, vancomycin and bacitracin.
2. Damaging/inhibiting the cell membrane function e.g.; Polymixins, collistins, Polyene antibiotics and detergents.
3. Inhibition of Protein synthesis and impairment of ribosomal functions e.g.; tetracycline, erythromycin, streptomycin and chloramphenicol.
4. Inhibition of nucleotide synthesis there by interfering with the transcription and translation of genetic information e.g.; quinolones, metronidazole and rifampicin.
5. Inhibiting of folic acid synthesis e.g.; sulfonamides, trimethoprim.

Figure 1-1 refers to the mechanism of action of antibacterial drugs.



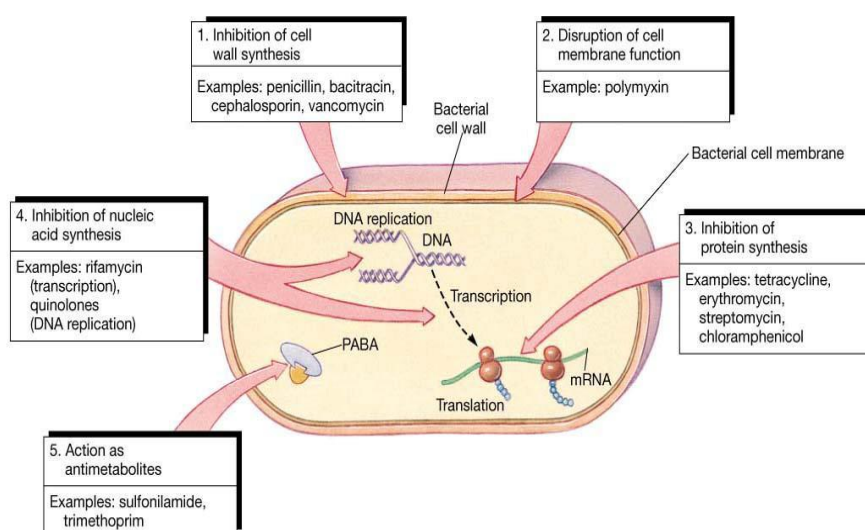


**Figure 1-1:** Mechanism of action of antibacterial drugs.

## 1-2-2 Sulfonamides

### 1-2-2-1 Definition

Sulfonamides are one of a group of drugs derived from (4-amino benzene sulfonamide) also called sulfanilamide, they were the first chemotherapeutic agents used to treat and prevent bacterial infections in humans and animals. Sulfonamides are broad spectrum bacteriostatic drugs; they work by inhibiting the growth and multiplication of bacteria without killing them<sup>(12,13)</sup>.

Sulfonamides are commonly used in the treatment of urinary tract infections, eye infections and as a prophylaxis of rheumatic fever<sup>(14)</sup>, gastrointestinal tract infections, respiratory infections<sup>(9)</sup>, Nocardia infections<sup>(15)</sup>, and veterinary medicine<sup>(8)</sup>.

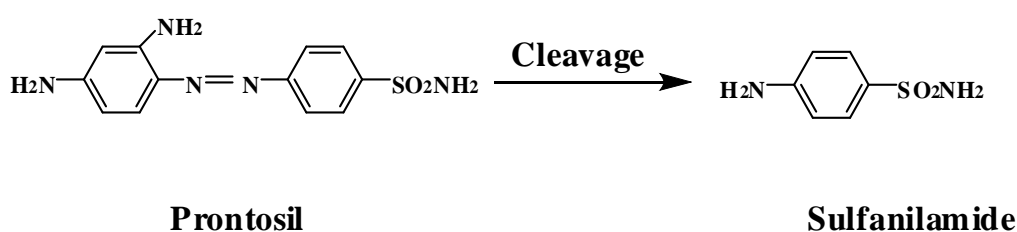
Sulfonamides have the potential to cause a variety of untoward reactions, including urinary tract disorders, haemopoietic disorders, prophyria, and hyper sensitivity reactions. When used in large doses, they may cause a strong allergic reaction<sup>(16)</sup>.

### 1-2-2-2 Discovery

The sulfonamides story was begun when doctor Gerhard Domagk and other researcher discovered a red azo dye called "Prontosil" that was inactivate in vitro but activate in vivo<sup>(12)</sup>.

In 1932 Gerhard Domagk performed a miraculous cure when he used Prontosil to treat child had 10-month old suffering from a fatal staphylococcal infection, in 1935 he cured his daughter of same infection. Systematic testing followed and Domagk had won the Nobel Prize in 1939 in medicine <sup>(8,12)</sup>.

The antibacterial properties of Prontosil had nothing at all to do with its being a dye. In the body Prontosil undergoes a reductive cleavage of its azo linkage to form sulfanilamide, which is the agent responsible for the observed biological activity as shown in below equation. This is why Prontosil is active in vivo, but not active in vitro <sup>(12)</sup>.



During the period 1935-1946, over 5000 compounds related to sulfanilamide were prepared. The sulfa drugs are used less now than they were in mid-twentieth century, not only are more active, less toxic antibiotics available, such as the penicillins and tetracyclines, but many bacteria that were once susceptible to sulfa drugs have become resistant <sup>(12)</sup>.

### 1-2-2-3 Mechanism of action

Sulfonamides called folate pathway inhibitors or anti-metabolites <sup>(17)</sup>. Sulfonamides are analogues with p-amino benzoic acid (PABA), that is part of folic acid, thus they compete with it for the enzyme dihydropteroate synthetase, and affect the synthesis of dihydrofolic acid that is required by the bacteria <sup>(18,13)</sup>. Figure 1-2 shows the mechanism of inhibition of folic acid synthesis by sulfonamides <sup>(19)</sup>.

Folic acid is essential for the synthesis of adenine and thymine, two of the four nucleic acids that make up our genes, DNA and RNA both in bacteria and in mammals. Bacteria need PABA because they are incapable of using folic acid directly, but mammals obtain their folic acid in their diet, thus a lack of PABA does not affect them <sup>(18,13)</sup>.

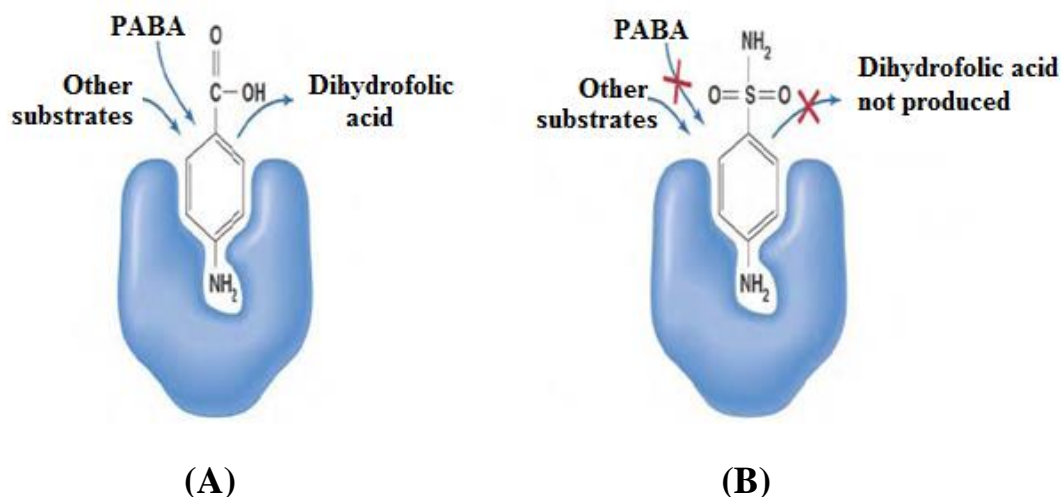


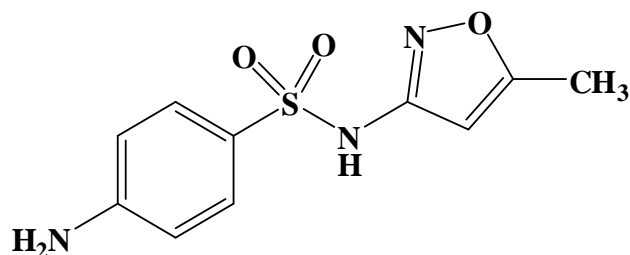
**Figure 1-2:** (A) Role of PABA in folic acid synthesis in bacteria, (B) inhibition of folic acid synthesis by sulfonamides.

Sulfonamides are rarely used alone today. The sulfonamides are used in combination with trimethoprim and other drugs; this combination blocks two distinct steps in folic acid metabolism and prevents the emergence of resistant strains. Trimethoprim is bacteriostatic drug that ties up dihydrofolate reductase enzyme and inhibit formation of tetrahydrofolic acid. Its antibacterial spectrum is similar to that of sulfonamide, but the antibacterial action is stronger<sup>(13,15)</sup>.

#### 1-2-2-4 Sulfamethoxazole (SMZ)

Sulfamethoxazole is a member of the sulfonamide family of antibacterials. Its use has been limited by the development of resistance and it is now used mainly as a mixture with trimethoprim<sup>(20)</sup>.

Mixture of sulfamethoxazole and trimethoprim which is known as co-trimoxazole is used to treat a wide variety of bacterial infections e.g.: middle ear infections, genito-urinary tract infections, respiratory-tract infections such as bronchitis, and enteric infections. Its main uses now are in *Pneumocystis carinii* pneumonia, toxoplasmosis, and nocardiosis. Gastrointestinal disturbances (mainly nausea and vomiting) and skin reactions are the most common adverse effects for this drug combination<sup>(21,22)</sup>.



**Scheme 1-2:** The structure formula of sulfamethoxazole.

### 1-2-2-5 General properties of sulfamethoxazole<sup>(23,24)</sup>

Some general properties of sulfamethoxazole are shown in Table 1-1.

**Table 1-1:** Some general properties of sulfamethoxazole.

<b>Chemical Name</b>	4-Amino-N-(5-methyl-3-isoxazolyl) benzene sulfonamide
<b>Additional Name</b>	Sulfamethoxazole (SMZ)
<b>Appearance</b>	White to slightly off-white crystalline powder
<b>Molecular Formula</b>	C <sub>10</sub> H <sub>11</sub> N <sub>3</sub> O <sub>3</sub> S
<b>Molecular Weight (g.mol<sup>-1</sup>)</b>	253.28
<b>Melting Point</b>	167 °C
<b>Solubility</b>	Slightly soluble in water, soluble in acetone, ethanol, methanol and dissolves in dilute solutions of sodium hydroxide and in dilute acids
<b>Storage</b>	Store in cool place and protected from light
<b>Therapeutic</b>	Antibacterial agent

### 1-2-2-6 Sulfanilamide (SNA)

Sulfanilamide (also spelled sulphanilamide) is a sulfonamide antibacterial. Chemically, it is a molecule containing the sulfonamide functional group attached to an aniline. As a sulfonamide antibiotic, it functions by competitively inhibiting (i.e., by acting as a substrate analogue) enzymatic reactions involving para-aminobenzoic acid (PABA).<sup>(25)</sup> PABA is needed in enzymatic reactions that produce folic acid which acts as a coenzyme in the synthesis of purine, pyrimidine and other amino acids.

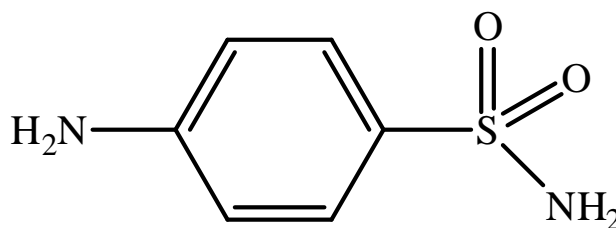
The term "sulfanilamides" is also used to describe a family of molecules containing these functional groups. Examples include:

- Furosemide, a loop diuretic
- Sulfadiazine, an antibiotic
- Sulfamethoxazole, an antibiotic

Sulfanilamide was first prepared in 1908 by Paul Gelmo as part of his dissertation for a doctoral degree from the Technische Hochschule of Vienna, Austria<sup>(26)</sup>. It was patented in 1909<sup>(27)</sup>. Gerhard Domagk, who directed the testing of the prodrug Prontosil in 1935,<sup>(28)</sup> and Jacques and Thérèse Tréfouël, who along with Federico Nitti and Daniel Bovet in the laboratory of Ernest Fourneau at the Pasteur Institute, determined sulfanilamide as the active form<sup>(29)</sup>, are generally credited with the discovery of sulfanilamide as a chemotherapeutic agent. Domagk was awarded the Nobel Prize for his work<sup>(30)</sup>.

Sulfanilamide is a medicinal compound used to guard against certain bacterial infections. It is frequently used in the form of a topical cream or powder to treat surface infections, as well as a pill for internal infections. It falls into the category of sulfonamide antibacterial drugs. Common infections treated by sulfanilamide include urinary tract infections, vaginal infections, strep throat, and some staph infections. Depending on the type of infection, either a cream or a pill will be prescribed.

Sulfanilamide works as an antibiotic by hindering bacterial growth within the body. Like other sulfonamide compounds, its mechanism involves blocking a specific chemical pathway in bacteria. It acts as a competitive inhibitor for the compound para-aminobenzoic acid (PABA), which means that it mimics the structure of PABA. Bacterial enzymes will bind to sulfanilamide instead of PABA, which stops their activity and slowly kills the cell<sup>(25)</sup>.



**Scheme 1-3:** The structure formula of sulfanilamide.

**1-2-2-7 General properties of sulfanilamide** <sup>(31,32,33)</sup>

Some general properties of sulfanilamide are shown in Table 1-2.

**Table 1-2:** Some general properties of sulfanilamide.

<b>Chemical Name</b>	4-aminobenzenesulfonamide
<b>Additional Name</b>	Sulfanilamide (SNA)
<b>Appearance</b>	White or yellowish-white crystals or fine powder
<b>Molecular Formula</b>	C <sub>6</sub> H <sub>8</sub> N <sub>2</sub> O <sub>2</sub> S
<b>Molecular Weight (g.mol<sup>-1</sup>)</b>	172.205
<b>Melting Point</b>	165.0 °C
<b>Solubility</b>	Soluble in boiling water, glycerol, hydrochloric acid, potassium hydroxide and sodium hydroxide solution.
<b>Storage</b>	Store in cool place and protected from light
<b>Therapeutic</b>	Antibacterial agent

**1-2-2-8 Methods for the determination of sulfonamides****A- Spectrophotometric methods**

Nagamalleswari et al<sup>(34)</sup> developed four simple, sensitive and reproducible spectrophotometric methods (Method A, Method B, Method C and Method D) for the determination of sulfacetamide (SFA) in pure form and its pharmaceutical formulation. Method A was developed based on diazotization of the SFA by sodium nitrite in acidic medium followed by coupling with BM reagent (N-(1-naphthyl) ethylene di-amine dihydrochloride) having absorption maximum at 530 nm. Method B was developed based on reaction of NQS with primary amine in SFA in presence of alkaline medium having maximum absorption at 466 nm. Method C was based on reaction of primary amine with MBTH in presence of FeCl<sub>3</sub> having maximum absorption at 562 nm. Method D was developed based on reduction of phosphor molybdo tungstic acid in presence of alkali medium having an absorption maximum at 760 nm. Beer's law was obeyed in the range of 1-3 µg.mL<sup>-1</sup> for Method A, 5-30 µg.mL<sup>-1</sup> for Method B, 10-50 µg.mL<sup>-1</sup> for Method C, and 100-300

$\mu\text{g.mL}^{-1}$  for Method D. These methods were successfully validated and estimated in bulk and pharmaceutical formulations.

The applicability of a novel net analyte signal standard addition method to the resolving of overlapping spectra corresponding to the sulfamethoxazole and trimethoprim was verified by UV-visible spectrophotometry. The results confirmed that the net analyte signal standard additions method with simultaneous addition of both analytes is suitable for the simultaneous determination of sulfamethoxazole and trimethoprim in aqueous media. Moreover, applying the net analyte signal standard additions method revealed that the two drugs could be determined simultaneously with the concentration ratios of sulfamethoxazole to trimethoprim varying from 1:35 to 60:1 in the mixed samples. In addition, the limits of detections were 0.26 and 0.23  $\mu\text{mol.L}^{-1}$  for sulfamethoxazole and trimethoprim, respectively. The proposed method has been effectively applied to the simultaneous determination of sulfamethoxazole and trimethoprim in some synthetic, pharmaceutical formulation and biological fluid samples<sup>(35)</sup>.

Upadhyay et al<sup>(36)</sup> study a solid phase extractive spectrophotometric method for the determination of three sulfa drugs in bulk, in pharmaceutical dosage forms and in biological fluids was developed. The method is based upon coupling of diazotized sulfa drug with phloroglucinol in an acidic medium. The resulting yellow dye has absorption maximum at 420 nm and the resulting dye is stable for several days. The Beer's law range for sulfamethoxazole, sulfacetamide and sulfadiazine in aqueous medium are 0.2-2.0, 0.2-2.0 and 0.1-1.0  $\mu\text{g.mL}^{-1}$  respectively and in extractive medium range for above drugs are 0.02-0.20, 0.02-0.20, and 0.01-0.10  $\mu\text{g.mL}^{-1}$ . The molar absorptivities for the sulfa drugs were  $9.21 \times 10^5$ ,  $7.79 \times 10^5$  and  $1.820 \times 10^6$   $\text{L.mol}^{-1}.\text{cm}^{-1}$  respectively. The developed method is free from the interference of common excipients used in pharmaceutical dosage. The method was also used for the determination of sulfa drugs in pharmaceutical dosage as well as in human serum and urine samples.

Spectrophotometric methods are proposed for assay of drugs containing a phenol group and drugs containing an aromatic amine group in pharmaceutical dosage forms. The methods are based on coupling of (N,N-diethyl-p-phenylene diamine sulfate) with the drugs in the presence of  $\text{KIO}_4$  to give a green colored product ( $\lambda$  max at 670 nm) and a red

colored product ( $\lambda$  max at 550 nm), respectively. Linear relationships with good correlation coefficients (0.9986-0.9996) were found between absorbance and the corresponding concentration of drugs in the range 1-25  $\mu\text{g.mL}^{-1}$ . Variable parameters such as temperature, reaction time and concentration of the reactants have been analyzed and optimized. The RSD of intra-day and inter-day studies was in the range of 0.2-1.0 and 0.4-1.0 %, respectively. The reliability and performance of the proposed methods were validated statistically; the percentage recovery ranged from  $99.5 \pm 0.1$  to  $99.9 \pm 0.3$  %. Limits of detection were ranged from 0.14-0.51  $\mu\text{g.mL}^{-1}$  <sup>(37)</sup>.

Sulfacetamide sodium (SFA) and sulfamethoxazole (SMZ) were determined by spectrophotometric method in pharmaceutical preparations. The method was based on the oxidative coupling organic reaction of SFA and SMZ with pyrocatechol in the presence of sodium periodate to form red water soluble product with maximum absorbance at 500 nm for both drugs. The reaction conditions were studied and optimized. The linear in the range for the determination of SFA and SMZ, and the detection limit were 2-26 and 2-26  $\mu\text{g.mL}^{-1}$ , and 0.855 and 0.764  $\mu\text{g.mL}^{-1}$ , respectively. The effect of the substrates commonly employed as excipients with SFA and SMZ have been studied <sup>(38)</sup>.

Two spectrophotometric methods (Method A and Method B) were suggested by Raja et al <sup>(39)</sup> for the determination of sulfamethoxazole in bulk and in dosage forms. Method A is based on reduction of phosphor molybdic acid present in Folin Ciocalteu reagent by the drug sulfamethoxazole in the presence of sodium carbonate to form a blue colored chromogen having maximum absorption at 760 nm. Method B is based on the diazotization of the drug by sodium nitrite in acidic medium at 5 °C followed by coupling with orcinol to form yellow colored species ( $\lambda$ max 390 nm). Beer's law is obeyed in the range of 5-25  $\mu\text{g.mL}^{-1}$  for method A and 2-10  $\mu\text{g.mL}^{-1}$  for method B. Results of analysis were validated statistically and by recovery studies. These methods are successfully employed for the determination of sulfamethoxazole in various pharmaceutical preparations and biological fluids.

Nagaraja et al <sup>(40)</sup> analyze some sulfonamide drugs spectrophotometrically. The method is based on the diazotization of sulfacetamide, sulfadiazine, sulfaguanidine, sulfamerazine, sulfamethazine, sulfamethoxazole, and their coupling with 8-hydroxyquinoline in alkaline



media to yield red colored products with absorption maxima at 500 nm. Beer's law is obeyed from 0.1-7.0  $\mu\text{g.mL}^{-1}$ . The limits of quantification and limits of detection were 0.11- 0.18  $\mu\text{g.mL}^{-1}$  and 0.03- 0.05  $\mu\text{g.mL}^{-1}$ , respectively. Intraday precision (RSD 0.1- 0.5 %) and accuracy (recovery 97.3-100.8 %) of the developed method were evaluated. No interference was observed from common adjuvants. The method has been successfully applied to the assay of sulfa drug in pharmaceutical formulations.

Hajian et al<sup>(41)</sup> study, a net analyte signal standard addition method has been used for the simultaneous determination of sulphadiazine and trimethoprim by spectrophotometry in some bovine milk and veterinary medicines. The method combines the advantages of standard addition method with the net analyte signal concept which enables the extraction of information concerning a certain analyte from spectra of multi-component mixtures. This method has some advantages such as the use of a full spectrum realisation, therefore it does not require calibration and prediction step and only a few measurements require for the determination. Cloud point extraction based on the phenomenon of solubilisation used for extraction of sulphadiazine and trimethoprim in bovine milk. It is based on the induction of micellar organised media by using Triton X-100 as an extraction solvent. At the optimum conditions, the norm of NAS vectors increased linearly with concentrations in the range of 1.0–150.0  $\mu\text{molL}^{-1}$  for both sulphadiazine and trimethoprim. The limits of detection (LOD) for sulphadiazine and trimethoprim were 0.86 and 0.92  $\mu\text{mol L}^{-1}$ , respectively.

Sulfanilic acid was determined by spectrophotometric method in the presence of sulfonamides. This method is based on measuring the intensity of the red colour that develops when sulfanilic acid is allowed to react with potassium 1,2-naphthoquinone-4-sulphonate (NQS) in a chloroaceticchloroacetate buffer at pH 3,4. Color development reaches completion after 2h, allowing sulfanilic acid to be quantified spectrophotometrically at 470 nm ( $\epsilon = 4.7 \times 10^3 \text{ L mol}^{-1} \text{ cm}^{-1}$ ). The main product causing colour formation, potassium 1,2-naphthoquinone-4-(N-aminophenyl-4-sulphonate) (NQSSA), was isolated and characterized. When samples also contain sulfonamides an extraction into chloroform must be performed. Sulfanilic acid in binary mixtures with sulfanilamide, sulfacetamide, or sulfathiazole can be determined either by direct measurement of the aqueous phase after extraction at 470 nm or by

subtracting from the absorbance of the aqueous phase before extraction the absorbance of sulfonamide as determined by measuring the extracted chloroform phase at 345 nm. Sulfadiazine, sulfamethoxypyridazine, and sulfamethoxazole interferences are prevented by their extraction into chloroform at pH 7.2; these species cannot be determined. The effects of pH, reagent concentration, time, and temperature on colour formation were investigated. In all cases the standard addition method gave more accurate results. The method was applied to several pharmaceutical samples<sup>(42)</sup>.

Betageri et al<sup>(43)</sup> applied rapid, simple and sensitive kinetic spectrophotometric methods for the determination of some sulfa drugs namely Sulfacetamide Na, sulfadimidine and Sulfanilamide. The method based on oxidation of each of studied drugs with alkaline potassium permanganate. The reaction is followed spectrophotometrically by measuring the rate of change of absorbance at 526 nm & 610nm. The rate constant and fixed time methods are utilized for construction of calibration graphs to determine the concentration of the studied drugs. The results are validated statistically and checked through recovery studies. The method has been successfully applied for the determination of the studied sulfa drugs in commercial dosage forms.

Givianrad et al<sup>(44)</sup> performed a spectrophotometric method for the determination of sulfamethoxazole (SMZ) and trimethoprim (TMP) mixtures in bovine milk by simultaneous method is, due to spectral interferences, a difficult problem in analytical chemistry. By means of multivariate calibration methods, such as partial least square (PLS) regression, it is possible to obtain a model adjusted to the concentration values of the mixtures used in the calibration range. A genetic algorithm (GA) is a suitable method for selecting the wavelengths for PLS calibration of mixtures with almost identical spectra without the loss of prediction capacity using a spectrophotometric method. In this study, a calibration model is based on the absorption spectra in the 200-400 nm range for 25 different mixtures of SMZ and TMP. Calibration matrices were formed from samples containing 0.25-20.00 and 0.3-21.0  $\mu\text{g mL}^{-1}$  for SMZ and TMP, at pH 10, respectively. The root mean squared error of deviation (RMSED) for SMZ and TMP with PLS and genetic algorithm partial least square (GAPLS) were 0.242 and 0.066  $\mu\text{g mL}^{-1}$ , and 0.074 and 0.027  $\mu\text{g mL}^{-1}$ , respectively. This procedure allowed the

simultaneous determination of SMZ and TMP in synthetic and real samples and good reliability of the determination was proved.

Givianrad et al<sup>(45)</sup> study the applicability of H-point standard additions method (HPSAM) to the resolving of overlapping spectra corresponding to the sulfamethoxazole and trimethoprim which are verified by UV-vis spectrophotometry. The results show that the H-point standard additions method with simultaneous addition of both analytes is suitable for the simultaneous determination of sulfamethoxazole and trimethoprim in aqueous media. The results of applying the H-point standard additions method showed that the two drugs could be determined simultaneously with the concentration ratios of sulfamethoxazole to trimethoprim varying from 1:18 to 16:1 in the mixed samples. Also, the limits of detections were 0.58 and 0.37  $\mu\text{mol L}^{-1}$  for sulfamethoxazole and trimethoprim, respectively. In addition, the means of the calculated RSD (%) were 1.63 and 2.01 for SMZ and TMP, respectively in synthetic mixtures.

### **B- Chromatographic methods**

The method of liquid-phase microextraction assisted with voltage was developed and applied on the determination of sulfonamides in water samples. Four analytes, sulfamethazine, sulfathiazole, sulfadimethoxine, and sulfamethoxazole were extracted from a sample solution at pH 4.5 through a polypropylene membrane of immobilized with 2-octanone, and then into 25 L of the acceptor phase of 10 mM sodium hydroxide, and applied voltage of 100 V. Subsequently, the acceptor solution was directly subjected to analysis by LC-MS or capillary zone electrophoresis. Linearity was obtained in the range of 1.0-25.0  $\text{ng.mL}^{-1}$  with  $R^2 > 0.992$  in LC-MS, and 50-1000  $\text{ng.mL}^{-1}$  with  $R^2 > 0.995$  in capillary zone electrophoresis. The development of VA-LPME was also applied in analysis of sulfonamides in water samples to evaluate its practical applicability.<sup>(46)</sup>

A new method based on the use of off-line dispersive solid-phase extraction (dSPE) combined with ultra-high performance liquid chromatography with diode-array detection was developed to determine 11 sulfonamide antibiotics (sulfanilamide, sulfacetamide, sulfadiazine, sulfathiazole, sulfamerazine, sulfadimidin, sulfamethoxy pyridazine, sulfadoxine, sulfamethoxazole, sulfisoxazole and sulfadimethoxine) in mineral waters with different mineral content. For this purpose, pristine multi-walled carbon nanotubes (MWCNTs) and magnetic-MWCNTs (m-

MWCNTs) were used as sorbents. Magnetic nanoparticles were synthesized by means of a solvothermal process, assembled onto CNTs through an "aggregation wrap" mechanism and characterized by scanning electron microscopy. Parameters affecting the extraction such as volume and pH of the sample, amount of sorbent and type and volume of eluent were optimized. Once optimum extraction conditions (250 mL of water at pH 6.0 and elution with 25 mL of MeOH) were obtained, the extraction efficiency of the different carbon nanomaterials was compared. Results demonstrated the higher extraction capacity of pristine MWCNTs with recoveries between 61 and 110% (except for sulfacetamide which ranged between 40 and 53%) and between 22 and 77% for m-MWCNTs. Limits of detection lower than 32 ng/L were achieved for all of the analyzed samples<sup>(47)</sup>.

Sulfonamides (SAs) are one of the most frequently used antibiotics. SAs have been found in various environmental compartments. If SAs are not degraded in the environment, they can affect bacteria by their antibiotic properties and contribute to bacterial antibiotic resistance. Therefore, the biodegradability of 11 SAs (sulfanilamide, sulfaguanidine monohydrate, sulfadiazine, sulfathiazole, sulfapyridine, sulfamerazine, sulfamethoxy pyridazine, sulfachloropyridazine, sulfamethazine, sulfamethoxazole, and sulfadimethoxine) was studied. For this purpose, the Closed Bottle Test (CBT, OECD 301D) was performed, which includes a toxicity control. In order to monitor the environmental fate of the parent compound and to check for transformation products, a simple, efficient, and reliable HPLC-UV method for the simultaneous determination of these SAs has been developed. Acetonitrile and water (with 0.1% formic acid) were used as mobile phase solvents for gradient elution. The method was validated in terms of precision, detection and quantitation limits, selectivity, and analytical solution stability. In the CBT, none of these SAs was readily biodegradable. The HPLC-UV analysis confirmed that no degradation of any SA took place. In the toxicity control, these SAs showed no toxic effect in the used concentration of environmental bacteria applied in the test.<sup>(48)</sup>

A robust and sensitive analytical method is developed to quantitatively determine tetracyclines and sulfonamides, two major antibiotic classes, in sewage sludge. The antibiotic agents, oxytetracycline, tetracycline, doxycycline, chlorotetracycline, sulfathiazole, sulfapyridine,

sulfamethazine and sulfamethoxazole, were extracted using pressurized liquid extraction (PLE) with citric acid at pH 3 and methanol (1:1 v/v). Clean-up of the extracts was performed by solid phase extraction (SPE) with hydrophilic-lipophilic balance cartridges. Identification and quantification of the compounds is by liquid chromatography-tandem mass spectrometry in multiple reaction monitoring (MRM) mode. High recoveries ranging from 90.4 to 99.9% for sulfonamides and 96.2 to 100.9% for the tetracyclines are obtained. Method detection limits (MDLs) range from 0.6 to 4.2 ng/g for sulfonamides and 3.2 to 13 ng/g for tetracyclines. After validation, the method is applied to the analysis of sludges collected from different WWTPs in Spain <sup>(49)</sup>.

Two multivariate calibration methods are compared for the simultaneous chromatographic determination and separation of Sulfamethoxazole (SMZ) and Phthalazine (PHZ) by High Performance Liquid Chromatography (HPLC). Multivariate calibration techniques such as Classical Least Squares (CLS) and Inverse Least Squares (ILS) were introduced into HPLC to determine the quantification by using UV detector at 235, 250, 260 and 270 nm. Sixteen binary mixtures of SMZ and PHZ as calibration set and eight binary mixtures as prediction set were used. Results show that, Relative Errors of Prediction (REP) of CLS and ILS for SMZ and PHZ were 0.17%, 0.63% and 0.15%, 0.56%, respectively. <sup>(50)</sup>

An ionic liquid aqueous two-phase system (ILATPS) of 1-butyl-3-methyl imidazolium tetrafluoroborate ([Bmim]BF<sub>4</sub>)/ammonium citrate ((NH<sub>4</sub>)<sub>3</sub>C<sub>6</sub>H<sub>5</sub>O<sub>7</sub>) coupled with high-performance liquid chromatography was developed for the separation and determination of sulfadiazine (SD) and sulfamethoxazole (SMZ) in water samples as well as aquaculture products. The effect of such parameters as the types and concentrations of salts, temperature, the concentrations of SD and SMZ and the extraction time on the partitioning behavior expressed in terms of extraction efficiency has been evaluated. Under the optimal conditions, this extraction method has been successfully applied to the analysis of SD and SMZ in water samples and aquaculture products with the recoveries of 98.29-99.55 % (SD) and 92.09-99.82 % (SMZ). The detection limits for two analytes were 0.9 ng mL<sup>-1</sup> (SD) and 1.8 ng mL<sup>-1</sup> (SMZ). In comparison with the traditional solvent extraction, ILATPS is much

simpler and more environmentally friendly for the separation and enrichment of the sulfonamides antibiotics <sup>(51)</sup>.

Ionic liquid-salt aqueous two-phase extraction coupled with high-performance liquid chromatography with ultraviolet detection was developed for the determination of sulfonamides in water and food samples. In the procedure, the analytes were extracted from the aqueous samples into the ionic liquid top phase in one step. Three sulfonamides, sulfamerazine, sulfamethoxazole, and sulfamethizole were selected here as model compounds for developing and evaluating the method. The effects of various experimental parameters in extraction step were studied using two optimization methods, one variable at a time and Box-Behnken design. The results showed that the amount of sulfonamides did not have effect on the extraction efficiency. Therefore, a three-level Box-Behnken experimental design with three factors, which combined the response surface modeling, was used to optimize sulfonamides extraction. Under the most favorable extraction parameters, the detection limits and quantification limits of the proposed method for the target compounds were achieved within the range of 0.15-0.30 ng/mL and 0.5-1.0 ng/mL from spiked samples, respectively, which are lower than or comparable with other reported approaches applied to the determination of the same compounds. Finally, the proposed method was successfully applied to the determination of sulfonamide compounds in different water and food samples and satisfactory recoveries of spiked target compounds in real samples were obtained. <sup>(52)</sup>

A fast and reliable method of liquid chromatography and ultraviolet detection of sulfaguanidine, sulfadiazine, sulfamethazine, sulfamethizole, and sulfamethoxazole in feeding stuffs was described. The method involves the procedure of preparation of spiked samples, and extraction of sulphonamides from the matrix using a mixture of methanol and acetonitrile, followed by drying the extract and dissolving it in a phosphate buffer. The analysis uses octadecyl (C18) analytical column with UV detection at  $\lambda = 260$  nm and a gradient programme of mobile phase composition. The analytical procedure has been successfully adopted and validated for quantitative determination of the sulfonamides in feeding stuff samples. Validation included sensitivity, specificity, linearity, repeatability, and intra-laboratory reproducibility. The mean recovery of sulfonamides was 84%, within the working range

of 200-2000  $\mu\text{g/g}$ . Direct, simple sample preparation and HPLC-UV analysis allow the method to be successfully included in the scope of routine analyses.<sup>(53)</sup>

A dispersive liquid-liquid micro extraction (DLLME) procedure combined with ultra-high performance liquid chromatography with diode-array detection was developed to determine 25 antibacterials in mineral and run-off waters. Optimum DLLME conditions (5 mL of water at  $\text{pH}=7.6$ , 20% (w/v) NaCl, 685  $\mu\text{L}$  of  $\text{CHCl}_3$  as extractant solvent, and 1250  $\mu\text{L}$  of ACN as disperser solvent) allowed the repeatable, accurate and selective determination of 11 sulfonamides and 14 quinolones. The method was validated by means of the obtention of calibration curves of the whole method as well as a recovery study at two levels of concentration. The D.Ls of the method were in the range 0.35-10.5  $\mu\text{g.L}^{-1}$  with recoveries between 78 % and 117 %<sup>(54)</sup>.

Shaaban and Gońrecki<sup>(55)</sup> introduce a fast analytical method based on HPLC-UV using a sub-2 mm column at elevated temperature for the simultaneous determination of nine sulfonamides. Owing to the lower viscosity of the mobile phase, the separation could be achieved in 3 min. at 60 °C for all analytes. The effect of temperature, the organic modifier percentage and the flow rate on the retention time were studied. The method developed was used for the determination of selected sulfonamides in surface and waste water samples. Sample preparation was carried out by solid phase extraction. The method developed was validated based on the linearity, precision, accuracy, detection and quantification limits. The recovery ranged from 70.6 to 96.0 % with standard deviations not higher than 4.7%, except for sulfanilamide. Limits of detection were ranged from 1 to 10  $\text{mg.L}^{-1}$  after optimization of all analytical steps.

A fast and sensitive method was developed by Liu et al<sup>(56)</sup> for the simultaneous quantitative determination of 16 sulfonamides in animal feeds using ultra-high performance liquid chromatography tandem mass spectrometry. With the developed method, a feed sample can be analyzed in less than 2 h. A solid phase extraction method using acetonitrile and basic alumina column was developed to extract and purify sulfonamides from animal feeds. The analysis time can be greatly reduced with this method compared with previous reports. A linear range of 0.2~40  $\text{ng.mL}^{-1}$  ( $R^2 > 0.996$ ) were obtained for most of the compounds. The limits of

quantification for all sulfonamides were in the range of 0.5~20  $\mu\text{g.kg}^{-1}$ . The high precision and accuracy of this method were represented by average recoveries ranging from 80% to 120% and coefficients of variation of less than 10% for spiked animal feed samples. The method is suitable for fast determination of sulfonamides in concentrates, premixes, and complete feeds.

Thin layer chromatography with fluorometric scanning densitometry were used for assay of 15 sulfonamides. After addition of an internal standard, the tissue is extracted with ethyl acetate. The sulfonamides are then partitioned into glycine buffer. After pH adjustment, the aqueous phase is extracted with methylene chloride. Separation of the drugs from co-extractives is carried out on a silica gel plate containing a pre-adsorbent spotting area. Visualization is accomplished using UV light after dipping in fluorescamine solution <sup>(57)</sup>.

A micellar electrokinetic capillary chromatography method was performed at 25 °C and 30 kV (under pressure 15 mbar) using 25  $\text{mmol.dm}^{-3}$  phosphate buffer (pH = 8.0) containing 70  $\text{mmol.dm}^{-3}$  sodium dodecyl sulfate and 10 % (volume fraction) methanol as the background electrolyte for separation and determination of SMZ, SFA and other drugs. UV detection was set at 210 nm. The method was validated and antibacterials were quantitatively determined as additives in spiked animal feedstuffs. Results were compared with a new HPLC method for the evaluation of four antibacterials in real samples. Both developed methods can be used for routine analysis of these drugs as additives in animal feedstuffs <sup>(58)</sup>.

### C- Flow injection analysis

Ozkorucuklu et al <sup>(59)</sup> used a polypyrrole (PPy) electrode as a potentiometric electrochemical detector in a flow injection system in order to determine sulfamethoxazole in pharmaceutical formulations. The PPy electrode was prepared by cyclic voltammetry in acetonitrile solution. A linear relationship was observed over the concentration range of  $2.5 \times 10^{-5}$ - $1.25 \times 10^{-3}$  M with a correlation coefficient of 0.9977 and detection limit (DL) of  $1.03 \times 10^{-6}$  M. The recoveries in tablet and syrup formulations were found as 97.4 and 90.8% with the relative standard deviations of 0.62 and 1.04 %, respectively, which closely agree with those measured by high performance liquid chromatography (HPLC) with



UV detector. Therefore, it was concluded that the PPy electrode can be used as an alternative novel potentiometric detector material for determination of sulfamethoxazole in pharmaceuticals with the advantages of easy preparation and regeneration capability of the electrode surface.

A flow injection spectrophotometric method is described for the estimation of sulfonamides in aqueous and biological samples. The method is based on the oxidative coupling reaction of 4-amino-N,N-diethylaniline with sulfonamide drugs in the presence of potassium dichromate as oxidizing agent. Intense violet, water soluble dye was obtained which has a maximum absorption at 550 nm. Linear calibration graphs were obtained for different sulfonamides with a molar absorptivity of 4200-5270 L.mol<sup>-1</sup>.cm<sup>-1</sup> and a relative standard deviation less than 0.56 %. The proposed method has proved to be highly sensitive (detection limit range 0.30-0.63 µg.mL<sup>-1</sup> sulfonamide) and accurate (recovery % was 98.2-101.2 %). The nature of the colored dye and its stability constant were determined. The method was applied successfully for the determination of sulfonamide drugs in pharmaceutical preparations, blood and urine samples <sup>(60)</sup>.

The determination is performed in a FI-assembly by using a photo reactor consisting of a 670 cm×0.5 mmi.d. long piece of PTFE tubing coiled around a 8 W low-pressure mercury lamp. Linear calibration graphs were obtained over a concentration range of 2-3 orders of magnitude, typically in the range ≈ 0.06–8 µg.mL<sup>-1</sup> (sulfamethoxazole, sulfacetamide, sulfadimidine, sulfanilamide, sulfathiazole, sulfaguanidine); and in the range ≈ 0.08-100 µg.mL<sup>-1</sup> (sulfadiazine, sulfamerazine and sulfamethoxy pyridazine). Limits of detection were between 30 µg.mL<sup>-1</sup> (for sulfanilamide) and 80 µg.mL<sup>-1</sup> (for sulfadiazine, sulfamethoxy pyridazine, sulfadimidine and sulfaguanidine). The sample throughput was 60 h<sup>-1</sup> in all cases. The assessment of the photo degradation step on the molecular structure of sulfonamides was established by recording UV and fluorimetric spectra <sup>(61)</sup>.

A flow-through sensor based on integration of spectrophotometric detection and the different kinetics of retention/elution of analytes on a solid support is proposed for the simultaneous determination of sulfamethoxazole (SMZ) and trimethoprim (TMP). The solid support (Sephadex SP C-25) fills both, a microcolumn placed on-line and the

sensing microzone. The intrinsic absorbance of both compounds is monitored directly on the solid phase at 269 nm and so, no derivatization step is required. Using two alternate solutions,  $10^{-4}$  M hydrochloric acid and 0.20 M NaAc/HAc (pH 5.0) buffer, the sensor responds linearly in the measuring range of 50–250 and 10–70  $\mu\text{g ml}^{-1}$  with detection limits of 9.5 and 0.6  $\mu\text{g ml}^{-1}$  (500  $\mu\text{l}$  of sample volume) for SMZ and TMP, respectively. The main advantages of the sensor are simplicity, rapidity and low reagents consumption. Its application to SMZ and TMP determination in synthetic samples and pharmaceutical preparations is demonstrated <sup>(62)</sup>.

#### **D- Capillary electrophoresis (CE) methods**

In the present study, a rapid method for simultaneous determination of trimethoprim and sulfamethoxazole compounds using CE with capacitively coupled contactless conductivity detection was developed. A favorable working region for both analytes was from 12.5 to 200  $\mu\text{mol/L}$  (linear responses with  $R > 0.999$  for  $N = 5$ ). Other parameters calculated were sensitivity ( $1.28 \pm 0.10/1.45 \pm 0.11$ )  $\text{min}/(\mu\text{mol L})$ , RSD (4.5% / 2.0%), and LOD (1.1/3.3)  $\mu\text{mol/L}$  for trimethoprim and sulfamethoxazole, respectively. Under this condition, the total run time was only 2.6 min. The proposed method was applied for the determination of trimethoprim and sulfamethoxazole in commercial samples and the results were compared to those obtained by using a HPLC pharmacopoeia method. This new method is advantageous for quality-control analyses of trimethoprim and sulfamethoxazole in pharmaceuticals samples, because it is rapid and precise. Moreover, it is less laborious and demands minimum amounts of reagents in comparison to the recommended method. <sup>(63)</sup>

A rapid and effective method was developed in the first time for the determination of four sulfonamides (SAs) and their  $\text{N}^4$ -acetylated metabolites in aquatic products using capillary electrophoresis with accelerated solvent extraction (ASE). The eight residues were extracted with acetonitrile at 70 °C under 10.3 MPa pressure and two static cycles with a static time of 5 min. The eight analytes can be baseline separated with 6 min. The standard curves for the determination of eight residues by the capillary electrophoretic method have good linearity ( $r^2 > 0.999$ ). The method limits of quantification (LOQs) for N-4-acetylsulfadiazine,

sulfadiazine, sulfamerazine, sulfamethoxazole, sulfamethazine, N-4-acetylsulfamethazine, N-4-acetylsulfamerazine, and N-4-acetylsulfamethoxazole in aquatic products were 26.4, 33.0, 33.0, 33.0, 39.6, 370, and 1,076  $\mu\text{g}\cdot\text{kg}^{-1}$ , respectively. Intra- and inter-day precision (RSD) were 0.4-2.2 % and 1.4-3.5 %, respectively. Their average recoveries with three spiked levels ranged from 83 % to 116 % with the RSDs less than 4 %. The proposed method provides a rapid and simple extraction procedure with high sensitivity and recoveries, and can permit routine detection of the studied SAs residues in aquatic products at the maximum residue level.<sup>(64)</sup>

A simple and sensitive microfluidic capillary electrophoresis method with laser induced fluorescence detection was developed for the analysis of sulfonamides using fluorescein isothiocyanate as derivatization reagent. The performance of the system was demonstrated through the separation and determination of sulfamethazine, sulfamerazine and sulfamethoxazole in a running buffer solution containing 20 mmol/L borax (pH 9.2) with 15 % (v/v) ethanol. The injection and separation voltages, the concentration of borax, pH of the buffer and the content of ethanol in running buffer were optimized to get great influence on the separation. This proposed method showed satisfactory sensitivity with the limits of detection of 0.01 to 0.04  $\mu\text{mol/L}$  for the sulfonamides. The method also exhibited very good reproducibility with the relative standard deviations of not more than 9.2 and 2.2 % for fluorescence intensity and migration time, respectively. The analysis was achieved within only 1.6 min.<sup>(65)</sup>

Yuqin et al <sup>(66)</sup> developed a new capillary electrophoresis method with field-amplified sample stacking (FASS) was developed for the analysis of sulfadiazine and sulfamethoxazole. After optimization of the separation and concentration conditions, the two compounds can be separated within 7 min. and quantified with high sensitivity, with detection limits of 0.48  $\text{ng}\cdot\text{mL}^{-1}$  for sulfadiazine and 0.76  $\text{ng}\cdot\text{mL}^{-1}$  for sulfamethoxazole. This resulted in a 300-1500-fold improvement in concentration sensitivity relative to conventional capillary electrophoresis methods. The method was useful for qualitative and quantitative analysis of sulfadiazine and sulfamethoxazole in their preparations with recovery of 99.0 % to 102.0 % for sulfadiazine and 99.5 % to 99.7 % for sulfamethoxazole.

A novel method for the simultaneous determination of sulfonamides (SAs) in water samples has been developed by using dispersive liquid-liquid micro extraction (DLLME) coupled with capillary electrophoresis orthogonal and Box–Behnken designs were employed together to assist the optimization of DLLME parameters, including volumes of extraction and disperser solvents, ionic strength, extraction time, and centrifugation time and speed as variable factors. Under the optimum extraction and detection conditions, successful separation of the five (SAs) was achieved within 5 min, and excellent analytical performances were attained, such as good linear relationships ( $R > 0.980$ ) between peak area and concentration for each (SAs) from  $0.5\text{--}50.0\ \mu\text{g}\cdot\text{mL}^{-1}$ , low limits of detection for the five (SAs) between  $0.020$  and  $0.570\ \mu\text{g}\cdot\text{mL}^{-1}$  and the intra-day precisions of migration time below  $0.80\%$ . The method recoveries obtained at fortified  $10\ \mu\text{g}\cdot\text{mL}^{-1}$  for three water samples ranged from  $53.6$  to  $94.0\%$  with precisions of  $1.23\text{--}5.60\%$ . The proposed method proved highly sensitive and selective, rapid, convenient and cost-effective, showing great potential for the simultaneous determination of (SAs) in water samples <sup>(67)</sup>.

Sulfadiazine (SD) and sulfamethoxazole (SMZ) were estimated by capillary electrophoresis method with field-enhanced stacking concentration. The separation was achieved with a fused-silica capillary ( $60.2\ \text{cm}\times 75\ \mu\text{m}$ , effective length was  $50\ \text{cm}$ ) and a running buffer containing  $50\ \text{mmol}\cdot\text{L}^{-1}\ \text{NaH}_2\text{PO}_4$  (pH 6.0). The UV detection wavelength was  $214\ \text{nm}$ . The applied voltage was  $27.5\ \text{kV}$ , and the cartridge temperature was  $25\ ^\circ\text{C}$ . Water plug was introduced from the anode by  $3.42\ \text{kPa}\times 12\ \text{s}$  before injection. Sample was injected by electrokinetic injection- $10\ \text{kV}\times 9\ \text{s}$ . The linear range of the calibration curve for SD was  $0.05\text{--}10.00\ \text{mg}\cdot\text{L}^{-1}$  with a correlation coefficient of  $0.9999$ , and that for SMZ was  $0.025\text{--}5.00\ \text{mg}\cdot\text{L}^{-1}$  with a correlation coefficient of  $0.9994$ . The detection limits for SD and SMZ were  $1.74\ \mu\text{g}\cdot\text{L}^{-1}$  and  $1.39\ \mu\text{g}\cdot\text{L}^{-1}$  respectively. The proposed method has been used to determine the SD and SMZ in the pharmaceutical preparations with a recovery range of  $98\% \text{--}103\%$  (SD) and  $97\% \text{--}103\%$  (SMZ) <sup>(68)</sup>.

A capillary electrophoretic method for the simultaneous determination of sulfamethoxazole and trimethoprim in plasma was studied. Sulfamethoxazole and trimethoprim extracted from human plasma with ethyl acetate were analyzed at  $20\ \text{kV}$  and  $25^\circ\text{C}$  using  $15\ \text{mm}$  phosphate

buffer (pH 6.2) as the electrolyte. The detection was by UV at 220 nm. The run time was 8.0 min and the limit of quantification was  $10 \mu\text{g}\cdot\text{mL}^{-1}$  for sulfamethoxazole and  $2 \mu\text{g}\cdot\text{mL}^{-1}$  for trimethoprim. The recovery was >99% for both compounds. This method enabled the detection of sulfamethoxazole and trimethoprim in plasma of patients after oral ingestion of their combined formulation. The present simple and rapid method is applicable to drug monitoring in immunocompromised patients who are taking the combined formulation of these compounds for the treatment or prophylaxis of *Pneumocystis carinii* pneumonia <sup>(69)</sup>.

### E- Voltametric methods

PVC-based membranes of sulfamethoxazole diazonium resorcinol (SDR) as electroactive material with dioctylphthalate (DOP), Dioctylsebacate (DOS), o- Nitrophenyloctylether (o-NPOE) as plasticizing solvent mediators have been found to act as  $\text{Ni}^{+2}$  selective sensor, the best performance was obtained with the sensor having a membrane of composition plasticizer:PVC:ionophore in the ratio 200:100:5 mg. The sensor exhibits Nernstian response in the activity range  $5.0 \times 10^{-6}$  to  $1.0 \times 10^{-1}$  M, performs satisfactorily over a wide pH range (5-9), with a fast response time (10 s). The sensor was found to work satisfactorily in partially different internal solution concentrations and could be used over a period of 2 months. Potentiometric selectivity coefficients were determined by matched potential method (MPM) indicate excellent selectivity for  $\text{Ni}^{+2}$  ions. The sensors could be used successfully in the estimation of nickel as an indicator electrode in potentiometric titration.<sup>(70)</sup>

The performance of hydrogen- terminated (HT) and oxygen-terminated (OT) boron-doped diamond (BDD) electrodes (electrochemically pretreated) on the simultaneous differential pulse voltammetric determination of sulfamethoxazole and trimethoprim in pharmaceutical products is presented. Under the optimum analytical experimental conditions, the HT-BDD electrode presented two well-defined oxidation peaks at 920 and 1100 mV vs. Ag/AgCl for sulfamethoxazole and trimethoprim, respectively. On the other hand, when the OT-BDD electrode was used, the sulfamethoxazole oxidation current peak was decreased twenty fold. The calculated D.L values for sulfamethoxazole and trimethoprim using the HT-BDD electrode were  $3.65 \mu\text{g}\cdot\text{L}^{-1}$  and  $3.92$

$\mu\text{g.L}^{-1}$ , respectively. The results obtained in the simultaneous determination of sulfamethoxazole and trimethoprim in three different commercial formulations were similar to those obtained using a standard HPLC method at 95 % confidence level <sup>(71)</sup>.

Two sulfonamides, namely sulfadiazine and sulfamethoxazole, were independently quantified in pharmaceutical products by square-wave voltammetry (SWV) using a boron-doped diamond (BDD) electrode. The electro analytical determination of sulfadiazine was carried out in ethanol plus  $0.5 \text{ mol.L}^{-1}$ ,  $\text{H}_2\text{SO}_4$  50/50 (v/v) and of sulfamethoxazole in ethanol plus pH 6.0 phosphate buffer 50/50 (v/v) solutions. Both analytes showed one well-resolved irreversible oxidation peak at around +1.1 V, which served as the analytical response. Calibration curves were obtained in the concentration ranges of  $8.01 \times 10^{-6}$ - $1.19 \times 10^{-4} \text{ mol.L}^{-1}$  ( $r = 0.9995$ ) for sulfadiazine and  $6.10 \times 10^{-6}$ - $6.01 \times 10^{-5} \text{ mol.L}^{-1}$  ( $r = 0.9995$ ) for sulfamethoxazole, with respective detection limits of  $2.19 \times 10^{-6}$  and  $1.15 \times 10^{-6} \text{ mol.L}^{-1}$ . For both sulfonamides, recovery values were in the range of 95-104 % for all samples, indicating no matrix interference effects on the analytical results. The accuracy of the electro analytical methodology reported here in was compared to the standard HPLC method, and the values for the relative error between the proposed and standard methods were -4.31 % for sulfadiazine and -0.79 % for sulfamethoxazole. The data suggest a potential and interesting alternative method for the electro analytical determination of sulfa drugs in pharmaceuticals and other products <sup>(72)</sup>.

#### **F- Potentiometric methods**

A simple and rapid indirect potentiometric titration of sulfamethoxazole in the presence of trimethoprim contained in cotrimazole tablets is described. The method is based on the formation of a complex of sulfamethoxazole with a known excess of silver ions and the titration of unreacted silver ion potentiometrically using an inexpensive lab-made copper based mercury film electrode (CBMFE). The titration conditions have been optimized for the determination of 1.0-10.0 mg of sulfamethoxazole in pure and dosage forms. The precision and accuracy of the method have been assessed by the application of lack of fit test and other statistical methods. Overall mean recovery and relative standard deviations obtained were 99.88 % and 1.32 % ( $n=7$ ) respectively. No

interference was caused by other excipients present in pharmaceutical dosage forms. The application of this method for sulfamethoxazole assay in the presence of trimethoprim in tablets was validated by the comparison of results obtained by the proposed method with that of the British Pharmacopoeia (BP) method using *F*- and *t*- statistical tests of significance <sup>(73)</sup>.

Hassan and Eldesouki <sup>(74)</sup> described potentiometric and atomic absorption spectrometric (AAS) methods for the determination of various sulfonamides in tablets, suspensions, and injections, based on reactions with silver and copper ions. The methods involve direct titration at pH 8, using either a graphite electrode in which silver and copper sulfides have been precipitated, or ion selective electrodes to monitor the potential change. (AAS) measurements of the excess metal ions after metal-sulfonamide reaction are also reported. The methods described are selective, simple and precise

### 1-3 Optimizations

Optimization was defined by Beveridge and Schechter <sup>(75)</sup> as "the collective processes of choosing a set of values of independent variable required in achieving the best results from a given experimental system".

In the quantitative spectrophotometric analysis, the aim of optimization is to maximize the response, minimize the percent error, this requires the values of all experimental parameters to be optimized to give a maximum absorbance <sup>(76)</sup>.

#### 1-3-1 Univariate method

In experimental chemistry, several important variables or factors in a procedure that affected on the response are optimized by varying its one-variable-at-a-time, while keeping the others fixed, until an optimum is reached, the strategy is known univariate method <sup>(77)</sup>. It is done by the selection of an initial value for one variable and measuring the response, then increases or decreases the value of that variable in steps, while the other variables remain constant, until the best response is obtained. The second variable is then adjusted using the best response obtained with the previous variable with each variable in turn being considered. The optimization processes could be halted after one cycle or continued by

repeating the mentioned steps until reaching a maximum acceptable response <sup>(78)</sup>.

The optimization of the influencing parameters using a “one variable-at-a-time” method requires many experiments, reagents and equipments thus its expensive and time consuming. Furthermore, there may be interactions between the investigated parameters, which cannot be easily studied by this method <sup>(79)</sup>.

### **1-3-2 Multivariate methods**

Multivariate methods overcome all the problems with univariate method because it involves simultaneous combinations of a number of parameters allowing evaluation of interdependence of variables, influence on response and optimization of these influential factors also it requires few experiments, reagents and equipments.

#### **1-3-2-1 Simplex method**

George Dantzig, a member of the U.S. Air Force, developed the simplex method of optimization in 1947 in order to provide an efficient algorithm for solving programming problems that had linear structures <sup>(80)</sup>. The application of mathematical optimization in the pharmaceutical field was first reported by Fonner et al <sup>(81)</sup>, later developments in computer science have enabled the incorporation of the optimization algorithm into the software <sup>(82)</sup>.

Simplex is iterative procedure, solving a system of linear equations in each of its steps, seeking for finding the maxima (or minima) of any n-dimensional function  $F(x_1, x_2, \dots, x_n)$  for a response surface based on the movement of a simplex over that surface and stopping when either the optimum is reached, or the solution proves infeasible <sup>(83)</sup>.

A simplex is a geometric figure that has a number of vertexes (corners) equal to one more than the number of dimensions in the factor space. For instance in two dimensions, a simplex is a triangle. Figure (1-3) shows the Simplexes in one, two, three, four, and five dimensional factor spaces.



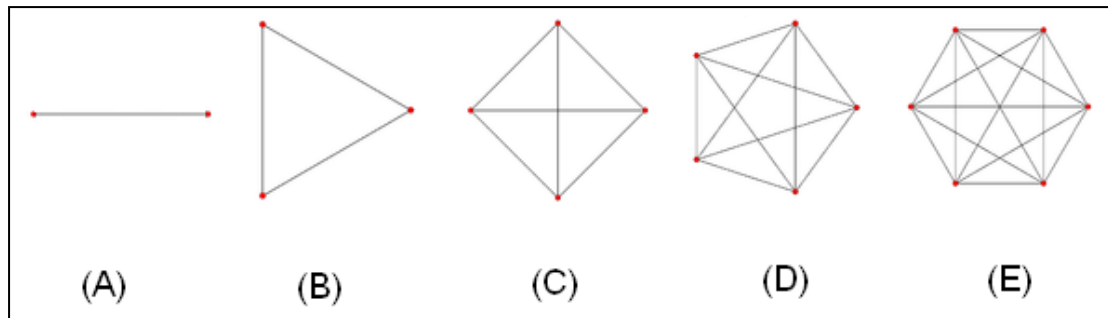


**Figure 1-3:** Simplexes (A) one, (B) two, (C) three, (D) four, and (E) five dimensional factor spaces.

When using a simplex for the optimization of experimental systems, each vertex corresponds to a set of experimental conditions. The responses obtained for each experimental condition were evaluated in such a way that the parameter setting that result might yield a better response.

Simplex can be moved into an adjacent area by rejecting one vertex (usually the vertex that gave the worst response) and projecting it through the average of the remaining vertexes to create one new vertex on the opposite side of the simplex. This new vertex corresponds to a new set of experimental conditions that can be evaluated. Figure (1-4) shows three examples of simplex movement <sup>(84)</sup>.

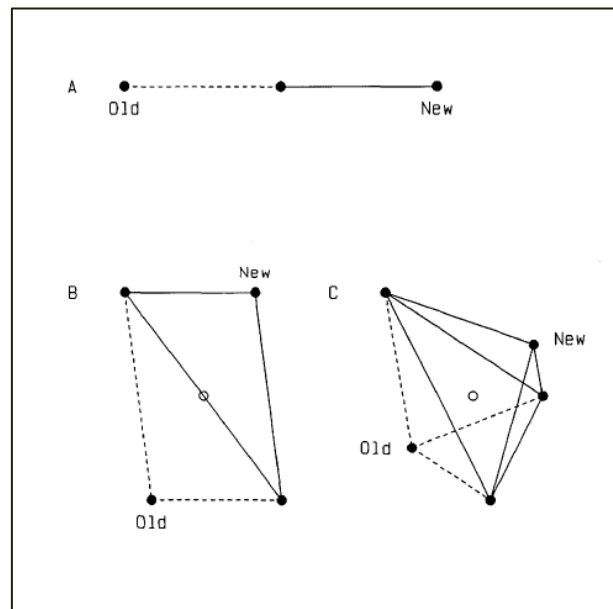


**Figure 1-4:** The simplex reflection move for (A) one dimensional, (B) two dimensional and (C) three dimensional factor spaces.

Simplex method is used by many scientists and engineers to improve the quality of products, the efficiency of processes, and the performance of analytical methods. The technique is capable to optimize several factors simultaneously and considers the interactions between these factors therefore; the method is rapid and requires a small number of experiments.

### **1-3-2-2 Modified simplex method** <sup>(85,86)</sup>

The original simplex method modified to two major modifications by Nelder and Mead. These modifications allow the simplex to expand in the direction of favorable responses and contract in the direction of unfavorable responses. The two basic modifications introduced into the basic simplex algorithm are as follows:

1. If the response of the reflected vertex (R) is better than the response at the best vertex (B) in the current simplex (i.e.  $R > B$ ), then an expansion is considered (Figure 1-5). The response at the expanded vertex is evaluated and accepted as the new vertex if the response obtained by the parameter settings is greater or equal to the response at the reflected vertex; otherwise the reflected vertex is accepted as the new vertex.
2. If the response at the reflected vertex is less than the response at the next- to worst response in the current simplex a contraction is considered. Two contractions are possible:
  - a. If the response at the reflected vertex is equal to or better than the response at the worst vertex in the current simplex ( $R \geq W$ ), then the contraction vertex will be on the reflection side  $C_r$ .
  - b. If the response at the reflected vertex is less than the response at the worst vertex in the current simplex ( $R < W$ ), then the contraction vertex will be on the worst side  $C_w$ .

In the original simplex algorithm the contraction situation is known as the reduction step and is performed by replacing all the vertexes of the current simplex by a set of new vertexes. This set of new vertexes is calculated by subtracting the coordinates of each of the vertexes of the simplex from those of vertex with the best response and then dividing by 2. In this case, the  $n + 1$  experiments should be conducted at each reduction step compared to only one experiment in the case of the modified simplex.

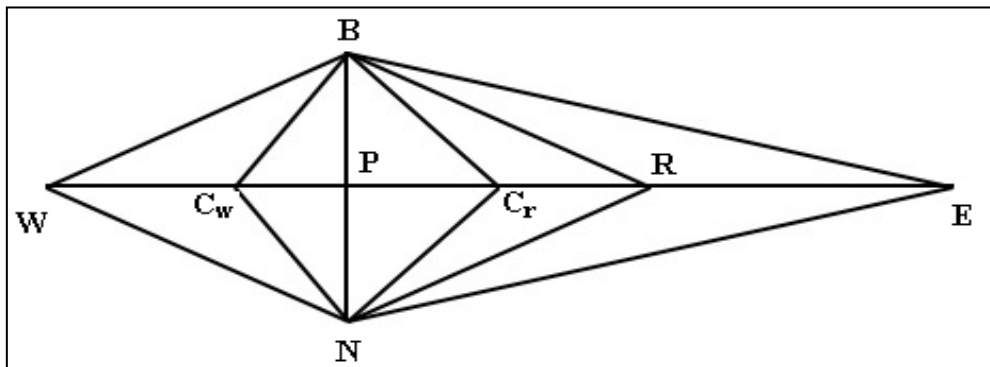


**Figure 1-5:** Possible moves in the variable-size simplex algorithm.

(P = centroid of the remaining hyperface; B = best vertex; N = next to-the-worst vertex; W = worst vertex; R = reflection vertex; E = expansion vertex;  $C_r$  = contraction vertex on the R side;  $C_w$  = contraction vertex on the W side).

### 1-3-2-3 Design of experiment (DOE)

Fisher had first developed Design of Experiment (DOE) in the 1920 s to 1930 <sup>(87)</sup>. Now a day, the methodology of the design of experiments made a special expansion in solving very complex problems in all fields of human activities because the development of electronic computers has greatly accelerated and alleviated statistical calculations <sup>(88)</sup>.

The primary goal of an experimental design is to establish a causal connection between the independent and dependent variables. A secondary goal is to extract the maximum amount of information with the minimum expenditure of resources <sup>(89)</sup>.

Design of Experiment method allows us to <sup>(88,90)</sup>:

- Build a mathematical model for a response as a function of the input variables.
- Select input variable levels that optimize the response (e.g. minimizing, maximizing, or hitting a target).
- Screen many input variables for the most important ones.
- Eliminate insignificant variables that are distracting your operators.
- Identify and manage the interactions between variables that are preventing your from optimizing your design or process or that are confusing your operators.
- Predict how manufacturing variability in the input variables induces variation in the response.

- Reduce variation in the response by identifying and controlling the input variables which are contributing the most to it.
- reduction or minimization of total number of trials.
- choice of a clear strategy that enables reliable solutions to be obtained after each sequence of experiments.

### 1-3-2-3-1 Response surface method (RSM)

Response surface map of the experimental region is one useful output of DOE. The design of experiment of RSM enables us to estimate interaction and even quadratic effects, and therefore give us an idea of the (local) shape of the response surface we are investigating. For this reason, they are termed response surface method (RSM) designs. RSM designs are used to:

- Find improved or optimal process settings.
- Trouble shoot process problems and weak points.
- Make a product or process more *robust* against external and non-controllable influences. "Robust" means relatively insensitive to these influences.

Response surface method depends on a collection of statistical and mathematical techniques useful for developing, improving, and optimizing processes by defining the effect of the independent variables, alone or in combination, on the process. In addition to analyzing the effects of the independent variables, this experimental methodology generates a mathematical model that accurately describes the overall process <sup>(91)</sup>.

There are many available standard statistical designs which could be followed to set an experimental design among them are:

- a- Full factorial design.
- b- Fractional factorial design.
- c- Box-Benhken design.
- d- Central composite design.

The number of experiments to be conducted and the information required have limited the choice of design. For simpler screening of experimental parameters (i.e. only support linear responses), low resolution designs will usually suffice. These are usually *full* or *fractional* factorial designs. Fractional factorial designs are often lower resolution than their full factorial counterparts because they require fewer

experiments and, hence, provide fewer data. Fractional factorial resolution is the most economical design, in terms of the number of experiments, but this design does not allow determination of interaction effects (interaction is a state where two or more factors are dependent on each other). For interaction models, if a non-linear response is detected or a more accurate picture of the response surface is required, a more complex design-type is necessary. Designs such as Box-Benhken or Central Composite Face (CCF) will support non-linear responses and are generally used for response-surface modeling and optimization applications<sup>(92)</sup>.

Central composite design (CCD) was introduced by Box and Wilson in (1951), it is widely used for estimating second order response surfaces. A Box-Wilson Central Composite Design contains imbedded factorial or fractional factorial designs which are frequently used together with response models of the second order. The design consists of three types of points:

- Axial points: The  $2 \cdot n$  axial points are created by a screening analysis.
- Cube points: The  $2^n$  cube points come from a full factorial design.
- Center point: A single point in the center is created by a nominal design.

The designs are described by scaled  $[-1, +1]$  as the ranges minimum and maximum values of the control parameters. A graphic of two and three dimensional (i.e. design with two and three input parameter) Central Composite Circumscribed (CCC) design are shown in Figure1-6.

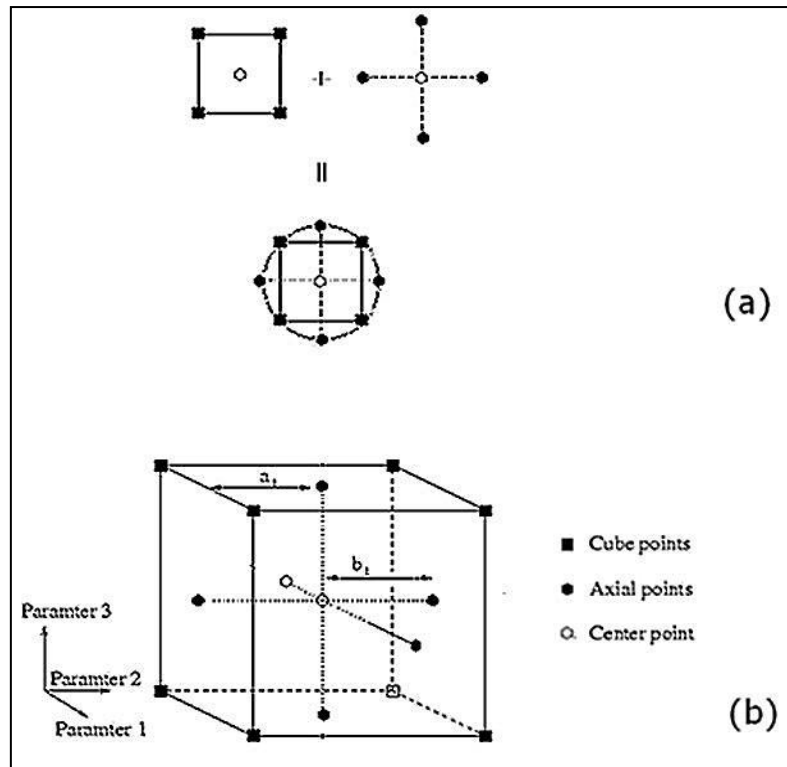


**Figure 1-6:** General Central Composite Design for (a) two factors and (b) three factors.

In the three dimensional CCD the *axial points* are located on a hyper-cube with the radius  $b_i$ . The cube was build by the cube points that has side-length of  $2.b_i$ .

When choosing three independent variables, (X1), (X2), and (X3), each variable had three levels which were  $-1$ ,  $0$  and  $+1$  (the upper, the central point and lower levels of factors respectively).

A total 20 different combinations (including six replicates of center point each had the coded value 0) is chosen in random order according to a CCD configuration for three factors <sup>(91,93)</sup>. Table (1-3) illustrates the structures of quadratic designs used when investigating three factors.

**Table 1-3:** structures of quadratic designs used when investigating three factors.

<i>Repeat</i>	<i>Variable 1 (X1)</i>	<i>Variable 2 (X2)</i>	<i>Variable 3 (X3)</i>
1	-1	-1	-1
2	+1	-1	-1
3	-1	+1	-1
4	+1	+1	-1
5	-1	-1	+1
6	+1	-1	+1
7	-1	+1	+1
8	+1	+1	+1
9	-1	0	0
10	+1	0	0
11	0	-1	0
12	0	+1	0
13	0	0	-1
14	0	0	+1
15	0	0	0
16	0	0	0
17	0	0	0
18	0	0	0
19	0	0	0
20	0	0	0

These coded values of  $x_i$  are then used to build a regression model to fit the experimental data and were found from equation <sup>(94)</sup>:

$$x_i = \frac{x_i - x_c}{\Delta x_i}$$

Where  $X_i$  is the coded unit of the studied independent variable,  $X_i$  is its upper or lower limit and  $X_c$  is its central value. The factors and levels were followed according to Table (1-4).

**Table 1-4:** Un-coded and coded levels of the independent variables.

<i>Independent variable</i>	<i>Coded unit</i>		
	-1	0	1
X1	X1 <sub>lower</sub>	X1 <sub>central</sub>	X1 <sub>upper</sub>
X2	X2 <sub>lower</sub>	X2 <sub>central</sub>	X2 <sub>upper</sub>
X3	X3 <sub>lower</sub>	X3 <sub>central</sub>	X3 <sub>upper</sub>

An empirical second-order general polynomial model that describes the mathematical relationship between the response and the factors is used to define the response surface. A general form of the model is as follows:

$$Y = \beta_0 + \beta_1 X_1 + \beta_2 X_2 + \beta_3 X_3 + \beta_4 X_1 X_2 + \beta_5 X_1 X_3 + \beta_6 X_2 X_3 + \beta_7 X_1^2 + \beta_8 X_2^2 + \beta_9 X_3^2$$

Where **Y** is the response, **X**'s are the significant effects factors, and the coefficients  **$\beta$** 's represent the magnitude of the effect of the different factors in the model. This model can be used to predict the response for any condition within the experimental space <sup>(95,96)</sup>.

The point of maximum response is calculated by taking the first derivatives of the equation of the response surface with respect to  $X_1$ ,  $X_2$ , and  $X_3$ , and equating them to zero. Then the equations with  $X_1$ ,  $X_2$ , and  $X_3$  are solved simultaneously to produce the estimated co-ordinates of the point of maximum response. The equations are <sup>(95,96)</sup>:

$$\frac{\partial y}{\partial X_1} = \beta_1 + \beta_4 X_2 + \beta_5 X_3 + 2\beta_7 X_1 = 0 \dots\dots\dots(1)$$

$$\frac{\partial y}{\partial X_2} = \beta_2 + \beta_4 X_1 + \beta_6 X_3 + 2\beta_8 X_2 = 0 \dots\dots\dots(2)$$

$$\frac{\partial y}{\partial X_3} = \beta_3 + \beta_5 X_1 + \beta_6 X_2 + 2\beta_9 X_3 = 0 \dots\dots\dots(3)$$



# ***CHAPTER TWO***

***Determination of sulfamethoxazole  
and sulfanilamide by diazotization  
reaction***

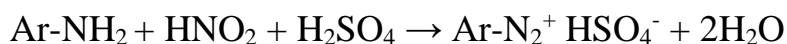
## Chapter Two

### 2 Determination of sulfamethoxazole and sulfanilamide by diazotization reaction and coupling with diphenylamine

#### 2-1 Introduction

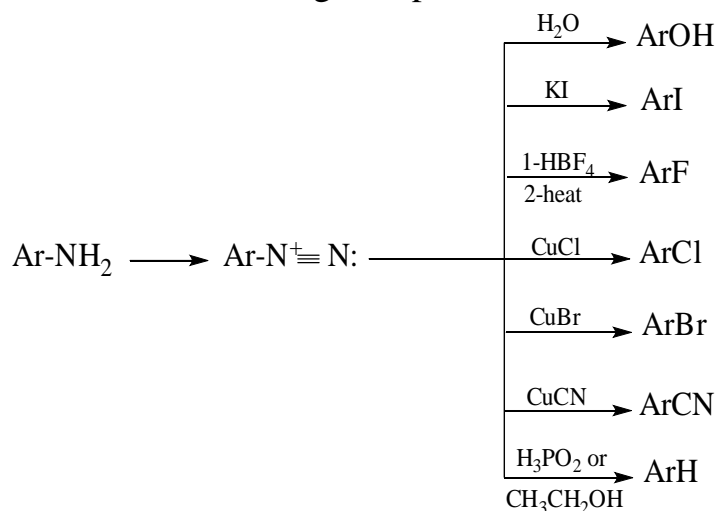
##### 2-1-1 Diazotization reaction

Primary aryl amines react with nitrous acid, ( $\text{HNO}_2$ ), to yield stable aryl diazonium salts, ( $\text{Ar-N}^+\equiv\text{NX}^-$ ). This diazotization reaction is compatible with the presence of a variety of substituents on the aromatic ring.



Alkyl amines also react with nitrous acid, but the alkyl diazonium products of these reactions are so reactive they can't be isolated. Instead, they lose nitrogen instantly to yield carbocation's. The analogous loss of  $\text{N}_2$  from an aryl diazonium ion to yield an aryl cation is disfavored by the instability of the cation<sup>(97)</sup>.

Aryl diazonium ions undergo a variety of reactions that make them versatile intermediates for preparing a host of ring substituted aromatic compounds. In these reactions, molecular nitrogen acts as a leaving group and is replaced by another atom or group as depicted in scheme (2-1). All the reactions are region specific; the entering group becomes bonded to the same carbon from which nitrogen departs<sup>(98)</sup>.



**Scheme 2-1:** The synthetic origin of aryl diazonium ions and their most useful transformations.



<b>IUPAC Name</b>	Diphenylamine
<b>Other Name</b>	DPA
<b>Appearance</b>	white to yellow crystals or powder
<b>Molecular Formula</b>	C <sub>12</sub> H <sub>11</sub> N
<b>Molecular Weight (g.mol<sup>-1</sup>)</b>	169.23
<b>Melting Point</b>	53°C (326 K)
<b>Uses</b>	Laboratory Reagent and antioxidant
<b>Solubility</b>	dissolves well in many common organic solvents (methanol)
<b>Solubility in water</b>	Slightly
<b>Handling and Storage</b>	Keep in a tightly closed container, stored in a cool, dry, ventilated area, protect from the light
<b>Stability</b>	Stable under ordinary conditions, may discolor on exposure to light. Incompatible with strong acids, strong oxidizing agents

#### 2-1-4 Spectrophotometric determination of some drugs in pharmaceutical preparations using diazotization reactions

The Primary aromatic amines are specific and sensitivity determinable by diazotization of amine group to produce diazonium compound, then coupling with activated aromatic compounds to yield an azo compounds which measured spectrophotometrically <sup>(102)</sup>.

A survey of literature reported several UV-Vis spectrophotometric methods for assay of amino drugs using diazotization reaction followed by coupling with suitable reagent. Table 2-1 list few reports on this method.

**Table 2-1:** Spectrophotometric determinations of some drugs in pharmaceutical compounds using diazotization reaction.

<b>Drug compounds (Trade Name) Chemical Nomenclature</b>	<b>Reagent</b>	<b><math>\lambda_{max}</math> (nm)</b>	<b>Linear dynamic range (<math>\mu\text{g.mL}^{-1}</math>)</b>	<b>Ref.</b>
<b>(Nifedipine)</b> dimethyl-2, 6-dimethyl-4-(2-nitrophenyl)-1, 4-dihydropyridine-3, 5-dicarboxylate	(CDNBD) 4-carboxyl-2,6-dinitrobenzene diazonium ion	470	2.9 -14.5	103
<b>(Pregabalin)</b> (S)-3-(amino methyl)-5-methyl hexanoic acid	(Ninhydrin)	402.6	50-1000	104
(Ziprasidone) 5-[2-[4-(1,2-Benzisothiazol-3-yl)piperazinyl]ethyl)-6-chloro-1,3-dihydro-2(1H)-indole-2-one	(Brotton Marshall BM) N-(1-naphthyl) ethylene diamine di hydrochloride	540	2-10	105
<b>(Lamivudine)</b> 2',3'-dideoxy-3'-thiacytidine	(Resorcinol) 3-hydroxy phenol	540	10-60	106
<b>(Metronidazole)</b> 2-methyl-5-nitroimidazole-1-ethanol, <b>(Tinidazole)</b> 1-(2-ethyl-sulphonyl ethyl)-2-methyl-5-nitroimidazole	(PDAB) (p-dimethyl amino benzaldehyde)	406, 404	4.8–76.8, 4.8–76.8	107
<b>(Alfuzosin hydrochloride)</b> N-[3-[(4- amino-6, 7-dimethoxy– quinazolin-2- yl)-methyl-amino] propyl]oxolane-2-carboxamide hydrochloride	Ethoxy ethyl enemaleic ester,  Ethyl cyano acetate and Acetyl acetone	440,  465 and 490	4-20,  4-20 and 3-15	108

<i>Drug compounds (Trade Name) Chemical Nomenclature</i>	<i>Reagent</i>	$\lambda_{max}$ (nm)	<i>Linear dynamic range (<math>\mu\text{g.mL}^{-1}</math>)</i>	<i>Ref.</i>
(Propranolol hydrochloride) (2RS)-1-[(1-Methyl ethyl)amino]-3-(naphthalen-1-yloxy) propan-2-ol hydrochloride	Bromothymol blue, Bromocresol green and Bromocresol purple	420, 420 and 425	0.4-7.0, 0.4-7.0 and 0.5-8.4	109
(Mesalamine) 5-amino-2-hydroxy benzoic acid	( $\alpha$ -naphthol) 1-hydroxy naphthalene	510	1-15	110

## 2-2 Experimental

### 2-2-1 Instruments

The instruments used in this study are presented in Table (2-2).

**Table2-2:** The principle instruments and their models.

<i>Instrument</i>	<i>Source and Model</i>
U.V.-Visible double beam spectrophotometer with 10 mm quartz cell	Shimadzu 1800, Kyoto – Japan
U.V.-Visible double beam spectrophotometer with 10 mm quartz cell	Cecil CE 7200, Cambridge-England
pH meter	HANA , pH 211,Romania
Sensitive balance $\pm 0.0001\text{g}$	Sartorius BL 210 S Scientific balance, Gottingen - Germany
Centrifuge	Hettich-EBA 20 Germany
Computer	DELL, Windows 8 China

### 2-2-2 Chemicals

Pharmaceutical grade sulfamethoxazole and sulfanilamide powders received in pure form (99.99%) were provided as a gift from the State Company for Drug Industries and Medical Appliances Samara-Iraq (SDI).

All chemicals and reagents used were of analytical grade. Table 2-3 illustrates their details.

**Table2-3:** The principle materials and their sources.

<i>No.</i>	<i>Materials</i>	<i>Purity/Assay</i>	<i>Source by</i>
1	Sulfamethoxazole	Standard powder	SDI
2	Sulfanilamide	Standard powder	SDI
3	Sodium nitrite	Pure powder	BDH
4	Sulfamic acid	99.9% w/w	BDH
5	Diphenylamine	99.9% w/w	BDH
6	Hydrochloric acid	35.0% w/w	BDH
7	Acetic acid	99.5% w/w	BDH
8	Sulfuric acid	98.0% w/w	GCC
9	Nitric acid	70.0% w/w	H&W
10	Sodium 1,2-Naphthoquinone-4-sulphonate (NQS)	99.9% w/w	BDH
11	Sodium tetraborate decahydrate (Borax)	99.9% w/w	BDH
12	Sodium hydroxide	99.9% w/w	Panreac
13	Methanol	99.8%	FLUKA
14	Glucose	Pure powder	BDH
15	Sucrose	Pure powder	BDH
16	Lactose	Pure powder	BDH
17	Vanillin	Pure powder	BDH
18	Starch soluble	Pure powder	BDH
19	Potassium hydroxide	99.9% w/w	Panreac
20	Sodium carbonate (Anhydrous)	99.9% w/w	Panreac
21	Ammonium hydroxide	32.0% w/w	Scharlau

**Table 2-4:** The principle pharmaceutical compounds and their manufacturers.

<i>Commercials drugs</i>	<i>Manufacturer</i>
<b>Bactrim</b> (sulfamethoxazole 800 mg + trimethoprim 160 mg) / tablet	Roche, France
<b>Methoprim</b> (sulfamethoxazole 400 mg + trimethoprim 80 mg) / tablet	NDI, Iraq
<b>Bactrim</b> (sulfamethoxazole 200 mg + trimethoprim 40 mg) / Syrup	Roche, France
<b>Cotrim</b> (sulfamethoxazole 200 mg + trimethoprim 40 mg) / Syrup	Asia, Syria

**2-2-3 Materials and Reagents**

\*Sodium nitrite [0.2 % (m/v)]: prepared by dissolving 0.2 g of  $\text{NaNO}_2$  in double distilled water and diluting to the mark in a 100 mL volumetric flask using distilled water.

\*Sulfamic acid [1.0 % (m/v)]: prepared by dissolving 1.0 g of  $\text{H}_3\text{NSO}_3$  in double distilled water and diluting to the mark in a 100 mL volumetric flask using distilled water.

\*Diphenylamine (DPA) [0.5 % (m/v)]: prepared by dissolving 0.5 g of DPA in 25 mL methanol and diluting to the mark in a 100 mL volumetric flask with methanol.

\*Hydrochloric acid [8M]: prepared by taking 70 mL of concentrated HCl and diluted to 100 mL with distilled water.

\*Hydrochloric acid [6 M]: prepared by taking 52.52 mL of concentrated HCl and diluted to 100 mL with distilled water.

\*Hydrochloric acid [4M]: prepared by taking 35 mL of concentrated HCl and diluted to 100 mL with distilled water.

\*Hydrochloric acid [2M]: prepared by taking 17.50 mL of concentrated HCl and diluted to 100 mL with distilled water.

\*Hydrochloric acid [1M]: prepared by taking 8.75 mL of concentrated HCl and diluted to 100 mL with distilled water.

\*Hydrochloric acid [0.4M]: prepared by taking 3.50 mL of concentrated HCl and diluted to 100 mL with distilled water.

\*Nitric acid [1 M]: prepared by taking 6.3 mL of concentrated  $\text{HNO}_3$  and diluted to 100 mL with distilled water.



\*Acetic acid [1M]: prepared by taking 5.75mL of concentrated  $\text{CH}_3\text{COOH}$  and diluted to 100 mL with distilled water.

\*Sulfuric acid [1 M]: prepared by taking 5.44 mL of concentrated  $\text{H}_2\text{SO}_4$  and diluted to 100 mL with distilled water.

\*Glucose [ $10000 \mu\text{g.mL}^{-1}$ ]: prepared by dissolving 0.25 g of glucose in 25 mL distilled water.

\* Sucrose [ $10000 \mu\text{g.mL}^{-1}$ ]: prepared by dissolving 0.25 g of lactose in 25 mL distilled water.

\* Lactose [ $10000 \mu\text{g.mL}^{-1}$ ]: prepared by dissolving 0.25 g of lactose in 25 mL distilled water.

\*Vanillin [ $10000 \mu\text{g.mL}^{-1}$ ]: prepared by dissolving 0.25 g of vanillin in 25 mL methanol.

\*Starch [ $10000 \mu\text{g.mL}^{-1}$ ]: Triturate 0.25 g of soluble starch with a little cold water into a thin paste, and add 25 mL of boiling water. Boil until a clear solution is obtained (5 minutes). This solution should be freshly prepared as required <sup>(111)</sup>.

## **2-2-4 Preparation of standard drugs solutions**

### **1- Sulfamethoxazole (SMZ) stock solution ( $100 \mu\text{g.mL}^{-1}$ )**

The standard solution of SMZ was prepared by dissolving accurate weighted 0.01 g of pure drug in 10 mL of 0.4 M HCl and completed volume to the mark in volumetric flask 100 mL with distilled water. Working solutions were freshly prepared by subsequent dilutions.

### **2- Sulfanilamide (SNA) stock solution ( $100 \mu\text{g.mL}^{-1}$ )**

The standard solution of SNA was prepared by dissolving accurate weight 0.01 g of pure drug in 10 mL of 0.4 M HCl and further diluted to the mark in volumetric flask 100 mL with distilled water. Working solutions were freshly prepared by subsequent dilutions.

### **3- Solution for the analysis of sulfamethoxazole in pharmaceutical preparations <sup>(112)</sup>**

#### **i. In Tablets**

The content of 10 tablets was grinded and mixed well. A certain amount of the fine powder was accurately weighted to give an equivalent to 800 mg for tablets and the mean value of the weight of one tablet was calculated. An amount of the powder equivalent to about 0.0126 gm. was

accurately weighted, then about 10 mL of 0.4 M HCL was added, transferred into 100 mL volumetric flask, and the solution was shaken swirled, left to stand for 5 mints and diluted to the mark in a volumetric flask 100 mL with distilled water to get 100  $\mu\text{g}\cdot\text{mL}^{-1}$ . The solution was filtered by using Whatman filter paper No.41 to avoid any suspended or un-dissolved material before use, and the first portion of the filtrate was rejected. Working solutions were freshly prepared by subsequent dilutions with distilled water, and analyzed by the recommended procedure.

## ii. In Syrup

Each 5 mL of the syrup contains (200 mg of sulfamethoxazole with 40 mg of trimethoprim). An accurately measured volume (0.25 mL) was transferred into a 100 mL volumetric flask, then added 10 mL of 0.4 M HCl swirled, left to stand for 5 mints and diluted to the mark with distilled water to get 100  $\mu\text{g}\cdot\text{mL}^{-1}$  SMZ solutions. The solution was filtered by using Whatman filter paper No.41 to avoid any suspended or un-dissolved material before use, and the first portion of the filtrate was rejected. Working solutions were freshly prepared by subsequent dilutions with distilled water, and analyzed by the recommended procedure.

### 2-2-5 Preparation of synthetic sulfanilamide drug sample

1- To 0.02 g of the bulk drug, 0.005 g of interfering substance mixture (consisting of equal weights of each substance, namely, glucose, Sucrose, lactose, soluble starch, and vanillin) was added.

2- 0.013 g of the resulted mixture was dissolved in 10 mL of 0.4 M HCl and diluted to the mark with distilled water in volumetric flask 100 mL in the same manner as used for the preparation standard drug to obtain 100  $\mu\text{g}\cdot\text{mL}^{-1}$ .

### 2-2-6 Primary experimental test

The primary test for the present method involves diazotization of 5  $\mu\text{g}\cdot\text{mL}^{-1}$  SMZ and SNA in 10 mL volumetric flasks in an ice bath followed by coupling with DPA. The test was done by adding 1.0 mL of 0.2 % (m/v) sodium nitrite to each flask followed by 1.0 mL of 1.0 M HCl. After 10 minutes, 1.0 mL of 1.0 % (m/v) sulfamic acid and 0.5 % (m/v) DPA were

added, left to stand for 10 minutes and the contents were diluted to the mark with 6 M HCl and mixed well, the absorbance of the colored azo-dye was measured for SMZ and SNA against the reagent blank after 10 minutes, and  $\lambda_{\max}$  was extracted.

## **2-2-7 Optimization of experimental variables**

### **I- Univariate method**

Various parameters were optimized to obtain maximum yield of the product dye. The optimization of the following variables was studied with ( $5.0 \mu\text{g}\cdot\text{mL}^{-1}$ ) at 530.0 and 531 nm for SMZ and SNA against the reagent blank respectively.

#### **1- Effect of diazotization reaction time**

0.5 mL of aliquots standard solution containing (50  $\mu\text{g}$ ) of SMZ and SNA were transferred in a series of 10 mL volumetric flasks. A volume of 1.0 mL of 0.2 % (m/v) sodium nitrite and 1.0 mL of 1.0 M HCl was added, after (0-20) minutes, 1.0 mL of 1.0 % (m/v) sulfamic acid and 0.5 % (m/v) DPA were added to each flask, was left to stand for 10 minutes then, the contents were diluted to the mark with 6 M HCl and mixed well. The absorbance of the colored azo-dye was measured at 530.0 and 531 nm for SMZ and SNA against the reagent blank respectively.

#### **2- Effect of sodium nitrate**

0.5 mL of aliquots standard solution containing (50  $\mu\text{g}$ ) of SMZ and SNA were transferred in a series of 10 mL volumetric flask. A volume of 1.0 mL of (0.01-0.30) % (m/v) sodium nitrite solution was added to each flask followed by 1.0 mL of 1.0 M HCl, 1.0 mL of 1.0 % (m/v) sulfamic acid was added to each flask, and then volumes of 1.0 mL of 0.5 % (m/v) DPA were added. After 10 minutes, the contents were diluted to the mark with 6.0 M HCl and mixed well; the absorbance of the colored azo-dye was measured at 530.0 and 531.0 nm for SMZ and SNA against the reagent blank respectively.

#### **3- Effect of different acids**

0.5 mL of aliquots standard solution containing (50  $\mu\text{g}$ ) of SMZ and SNA were transferred in a series of 10 mL volumetric flask. A volume of

1.0 mL of 0.02 % (m/v) and 0.14 % (m/v) sodium nitrite for SMZ and SNA was added to each flask respectively followed by 1.0 mL of 1.0 M from (HCl, H<sub>2</sub>SO<sub>4</sub>, HNO<sub>3</sub>, and CH<sub>3</sub>COOH) acid solutions, 1.0 mL of 1.0 % (m/v) sulfamic acid was added to each flask, then volumes of 1.0 mL of 0.5 % (m/v) DPA were added. After 10 minutes, the contents were diluted to the mark with 6.0 M HCl and mixed well; the absorbance of the colored azo-dye was measured at 530.0 and 531.0 nm for SMZ and SNA against the reagent blank respectively.

#### **4- Effect of hydrochloric acid**

0.5 mL of aliquots standard solution containing (50 µg), of SMZ and SNA were transferred in a series of 10 mL volumetric flask. A volume of 1.0 mL of 0.02 % and 0.14 % (m/v) sodium nitrite was added to each flask for SMZ and SNA, followed by 1.0 mL of (0.10-1.00) M HCl, 1.0 mL of 1.0 % (m/v) sulfamic acid was added, then 1.0 mL of 0.5 % (m/v) DPA were added, left to stand for 10 minutes and the contents were diluted to the mark with 6.0 M HCl, mixed well and the absorbance of the colored azo-dye was measured after 10 minutes at 530.0 and 531.0 nm for SMZ and SNA against the reagent blank respectively.

#### **5- Effect of sulfamic acid**

0.5 mL of aliquots standard solution containing (50 µg) of SMZ and SNA were transferred in a series of 10 mL volumetric flask. A volume of 1.0 mL of 0.02 % and 0.14 % (m/v) sodium nitrite were added to each flask, followed by 1.0 mL of 0.2 M and 0.8 M HCl for SMZ and SNA were added, then 1.0 mL of (0.10-1.00) % (m/v) sulfamic acid and 0.5% (m/v) DPA was added to each flask, then after 10 minutes, the contents were diluted to the mark with 6.0 M HCl, mixed well and the absorbance of the colored azo-dye was measured after 10 minutes at 530.0 and 531.0 nm for SMZ and SNA against the reagent blank respectively.

#### **6- Effect of diphenylamine (DPA)**

0.5 mL of aliquots standard solution containing (50 µg) of SMZ and SNA were transferred in a series of 10 mL volumetric flask. A volume of 1.0 mL of 0.02 % and 0.14 % (m/v) sodium nitrite was added to each flask for SMZ and SNA, followed by 1.0 mL of 0.2 M and 0.8 M HCl for SMZ and SNA were added, then 1.0 mL of 0.3 % (m/v) sulfamic acid

was added to each flask, then volumes of 1.0 mL of (0.25-1.25) % (m/v) DPA were added. After 10 minutes, the contents were diluted to the mark with 6.0 M HCl and mixed well; the absorbance of the colored azo-dye was measured at 530.0 and 531.0 nm for SMZ and SNA against the reagent blank respectively.

### **7- Effect of coupling reaction time**

0.5 mL of aliquots standard solution containing (50 µg) of SMZ and SNA were transferred in a series of 10 mL volumetric flask. A volume of 1.0 mL of 0.02 % and 0.14 % (m/v) sodium nitrite for SMZ and SNA was added to each flask, followed by 1.0 mL of 0.2 M and 0.8 M HCl was added for SMZ and SNA respectively, then 1.0 mL of 0.3 % (m/v) sulfamic acid was added to each flask, and 1.0 mL of 0.5 % and 1.0 % (m/v) DPA was added for SMZ and SNA. After (0-20) min, the contents were diluted to the mark with 6.0 M HCl and mixed well, and the absorbance of the colored azo-dye was measured at 530.0 and 531.0 nm for SMZ and SNA against the reagent blank respectively.

## **II- Multivariate method**

### **Simplex method**

A simplex method was adopted to optimize the variables. In this method, three factors were evaluated by changing their concentrations simultaneously. The concentration of sodium nitrite, diphenylamine and hydrochloric acid for SMZ and the concentration of sodium nitrite, diphenylamine and coupling reaction time for SNA were selected as independent variables. The absorbance was selected as dependent variables.

Table 2-5 shows the variables which as well as their lower and upper levels (the boundary values of the variables) and their step sizes (the physical values which correspond to a mathematical unit of each variable). The selection of the variables to be optimized, as well as their base levels and step sizes was based on our previous experience.

**Table 2-5:** Boundary of simplex for the studied variables.

<i>Drug</i>	<i>Variable</i>	<i>Minimum boundary</i>	<i>maximum boundary</i>	<i>Step size</i>
SMZ	Conc. of sodium nitrite (% m/v)	0.01	0.30	0.01
	Conc. of HCl (M)	0.10	1.00	0.10
	Conc. of DPA (% m/v)	0.25	1.25	0.25
SNA	Conc. of sodium nitrite (% m/v)	0.01	0.30	0.01
	Coupling Reaction Time (mint)	1	4	1
	Conc. of DPA (% m/v)	0.25	1.25	0.25

The initial simplex was selected by choosing four (n+1) experimental designs that covered a wide range of values in the factor space and are shown in Table (2-6). Experiments 1-4 in Table (2-6) were established within the base levels and step sizes considered for each variable according to Table (2-5) and the results were fed to the software.

Subsequently, the initial experimental design was moved in the direction given by the rules of movement of the modified simplex method as it allows operations of expansion and contraction in the searching progress and to produce new set of experimental conditions.

**Table 2-6:** The (n+1) experimental designs of studied variables.

<i>Drug</i>	<i>Exp. No.</i>	<i>Conc. of sodium nitrite (%m/v)</i>	<i>Conc. of DPA (%m/v)</i>	<i>Coupling Reaction Time (mint.)</i>	<i>Conc. of HCl (M)</i>	<i>Abs.</i>
SMZ	1	0.01	0.25	-	0.20	0.788
	2	0.02	0.40	-	0.40	0.878
	3	0.10	0.60	-	0.80	0.904
	4	0.16	0.75	-	0.50	0.918
SNA	1	0.04	0.50	4	-	1.652
	2	0.20	0.25	3	-	0.734
	3	0.08	1.00	2	-	1.642
	4	0.16	0.1	1	-	1.178

## 2-2-8 General recommended procedures

### 1- Assay procedure for the determination of sulfamethoxazole:

Two procedures were recommended for the determination of SMZ and SNA via the proposed methods. The first was carried out following the conditions obtained by univariate optimization, while the second based of those conditions was obtained by chemometric multivariate simplex optimization.

#### i. Univariate method

Aliquots of the standard solution ( $100 \mu\text{g}\cdot\text{mL}^{-1}$ ), containing (5-70)  $\mu\text{g}$  of sulfamethoxazole were transferred into a series of 10 mL volumetric flasks. After cooling in an ice bath, 1.0 mL of 0.02 % (m/v) sodium nitrite solution and 1.0 mL of 0.2 M HCl were added to each flask. The solution was shaken thoroughly; 1.0 mL of 0.3 % (m/v) sulfamic acid was added. The solutions were swirled and the resulting diazotized product was coupled with DPA by the addition of 1.0 mL of 0.5 % (m/v) and allowed to stand for 10.0 minutes. The solutions were making up to the mark with 6.0 M HCl. After mixing the solution well, the absorbance of blue colored chromogen was measured at 530.0 nm against the reagent blank.

#### ii. Simplex method

Aliquots of the standard solution ( $100 \mu\text{g}\cdot\text{mL}^{-1}$ ), containing (5-120)  $\mu\text{g}$  of sulfamethoxazole were transferred into a series of 10 mL volumetric flasks. After cooling in an ice bath, 1.0 mL of 0.2 % (m/v) sodium nitrite solution and 1.00 mL of 0.90 M HCl were added to each flask. The solution was shaken thoroughly; 1.0 mL of 0.30 % (m/v) sulfamic acid was added. The solutions were swirled and the resulting diazotized product was coupled with DPA by the addition of 1.0 mL of 1.0 % (m/v) and allowed to stand for 10.0 minutes. The solutions were making up to the mark with 6.0 M HCl. After mixing the solution well, the absorbance of blue colored chromogen was measured at 530.0 nm against the reagent blank.

## 2- Assay procedure for determination of sulfanilamide

### i. Univariate method

Aliquots of the standard solution ( $100 \mu\text{g}\cdot\text{mL}^{-1}$ ), containing (5-70)  $\mu\text{g}$  of sulfanilamide were transferred into a series of 10 mL volumetric flasks. After cooling in an ice bath, 1.0 mL of 0.14 % (m/v) sodium nitrite solution and 1.0 mL of 0.8 M HCl were added to each flask. The solution was shaken thoroughly; 1.0 mL of 0.3 % (m/v) sulfamic acid was added. The solutions were swirled and the resulting diazotized product was coupled with DPA by the addition of 1.0 mL of 1.0 % (m/v) and allowed to stand for 3.0 minutes. The solutions were making up to the mark with 6.0 M HCl. After mixing the solution well, the absorbance of blue colored chromogen was measured at 531.0 nm against the reagent blank.

### ii. Simplex method

Aliquots of the standard solution ( $100 \mu\text{g}\cdot\text{mL}^{-1}$ ), containing (5-120)  $\mu\text{g}$  of sulfanilamide were transferred into a series of 10 mL volumetric flasks. After cooling in an ice bath, 1.0 mL of 0.04 % (m/v) sodium nitrite solution and 1.0 mL of 0.8 M HCl were added to each flask. The solution was shaken thoroughly; 1.0 mL of 0.30 % (m/v) sulfamic acid was added. The solutions were swirled and the resulting diazotized product was coupled with DPA by the addition of 1.0 mL of 0.75 % (m/v) and allowed to stand for 3.0 minutes. The solutions were making up to the mark with 6.0 M HCl. After mixing the solution well, the absorbance of blue colored chromogen was measured at 531.0 nm against the reagent blank.

### 2-2-9 Procedure for synthetic sulfanilamide drug sample

Aliquots of synthetic SNA sample solutions containing (10, 30, 50  $\mu\text{g}$ ) were transferred into a series of 10 mL volumetric flasks. A volume of 1.0 mL of 0.04 % (m/v) sodium nitrite was added to each flask followed by 1.0 mL of 0.80 M HCl; 1.0 mL of 0.3 % (m/v) sulfamic acid was added to each flask. Then volumes of 1.0 mL of 0.75 % (m/v) DPA were added. After 3.0 minutes, the contents were diluted to the mark with 6.0 M HCl and mixed well; the absorbance of the colored azo-dye was measured at 531.0 nm for SNA against the reagent blank.



### **2-2-10 Determination of sulfamethoxazole in pharmaceutical preparation by standard additions method (SAM)**

- 1- Preparation of SMZ stock solution  $100 \mu\text{g.mL}^{-1}$  according to the method of preparation that previously mentioned.
- 2- Prepare solution of commercial pharmaceutical preparation (syrup or tablets) concentration of  $100 \mu\text{g.mL}^{-1}$  according to the method of preparation that previously mentioned.
- 3- Preparation of 7 solutions in 10 mL volumetric flask for measurements by adding 0.1, 0.2, 0.3 mL of solution commercial pharmaceutical preparation (syrup or tablets) from ( $100 \mu\text{g.mL}^{-1}$ ) commercial pharmaceutical preparation, and added 0, 0.05, 0.10, 0.15, 0.20, 0.25, and 0.30 mL of  $100 \mu\text{g.mL}^{-1}$  standard solution of SMZ drug. After cooling in an ice bath, 1.0 mL of 0.2 % (m/v) sodium nitrite solution and 1.0 mL of 0.9 M HCl were added to each flask. The solution was shaken thoroughly; 1.0 mL of 0.30 % (m/v) sulfamic acid was added. The solutions were swirled and the resulting diazotized product was coupled with DPA by the addition of 1.0 mL of 1.0 % (m/v) this reagent allowed to stand for 10.0 minutes. The solutions were making up to the mark with 6.0 M HCl. After mixing the solution well, the absorbance of blue colored chromogen was measured at 530.0 nm against the reagent blank. That is to level one were added 0.1 mL, the level two were added 0.2 mL and level three were added 0.3 mL from commercial product.

## **2-3 Results and discussion**

### **I- The determination of sulfamethoxazole**

#### **2-3-1 Absorption spectra**

The primary experimental test for the diazotization of SMZ and coupling with diphenylamine in acidic medium was done as described in 2-2-6. The absorption spectrum for the blue colored azo- dye was recorded and has a maximum absorption ( $\lambda_{\text{max}}$ ) at 530.0 nm. As shown blank against distilled water (D.W.) in Figure 2-1, and Absorption spectrum of  $5.0 \mu\text{g.mL}^{-1}$  SMZ-DPA against reagent blank under the primary test in figure 2-2.

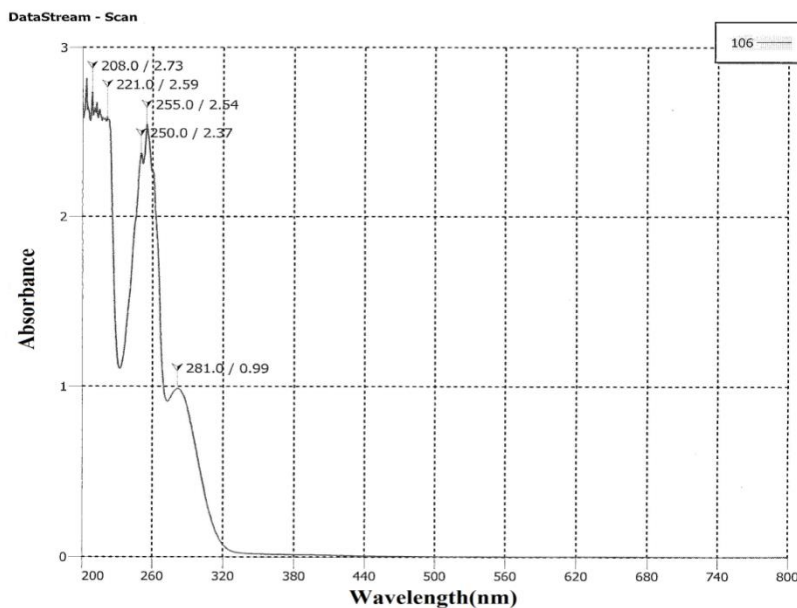


**Figure 2-1:** Absorption spectrum of blank solution against distilled water (D.W.) under the primary test.

Absorption spectrum for the reaction of diazotized sulfamethoxazole with diphenylamine in acidic medium was recorded under the optimum conditions (for univariate and simplex method) and showed the same maximum absorption at 530.0 nm for the blue chromogen against the reagent blank (Fig-2-2)

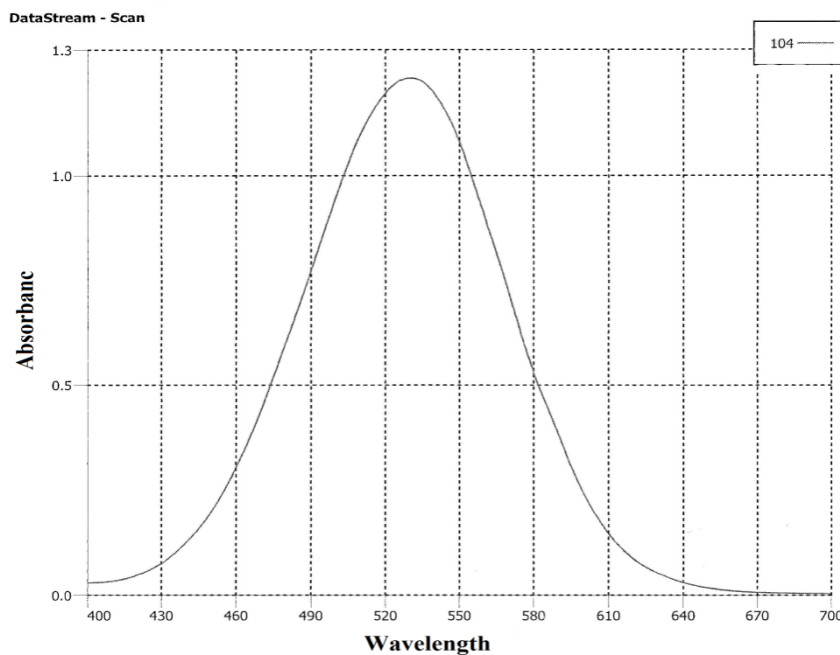


**Figure 2-2:** Absorption spectrum of  $5.0 \mu\text{g.mL}^{-1}$  SMZ-DPA against reagent blank under the optimum conditions.

## 2-3-2 Optimization of reaction variables

### I- Univariate method

A systematic study of the effects of various parameters in development of color products was taken by varying the parameters one at a time and controlling all others fixed. These variables include effects of diazotization reaction time, sodium nitrite concentration, effect of different acids, hydrochloric acid concentration, sulfamic acid concentration, diphenylamine concentration, coupling reaction time and effect of acidity.

#### 1- Effect of diazotization reaction time

The optimum diazotization reaction time was determined at ~ 0-5 °C by following the absorbance of the formed azo-dye for the period of (0-20) min. as listed in (Table 2-7). It was found that a colored product with maximum absorbance at 530.0 nm takes place instantaneous, after which no increase in absorbance values was obtained.

**Table 2-7:** Effect of diazotization reaction time.

<i>Time (min.)</i>	<i>Absorbance</i>
0	0.422
5	0.396
10	0.387
15	0.338
20	0.280

#### 2- Effect of sodium nitrite concentration

The effect of the concentration of  $\text{NaNO}_2$  was studied by measuring the absorbance of the color products at 530.0 nm as shown in (Figure 2-3); it was found that 1.0 mL of 0.02 % (m/v) solution sodium nitrite was needed for constant and maximum color intensity for azo dyes complex, low absorbance values were observed with higher concentrations. Hence 1.0 mL of 0.02 % (m/v) was used in all the subsequent experimental work.

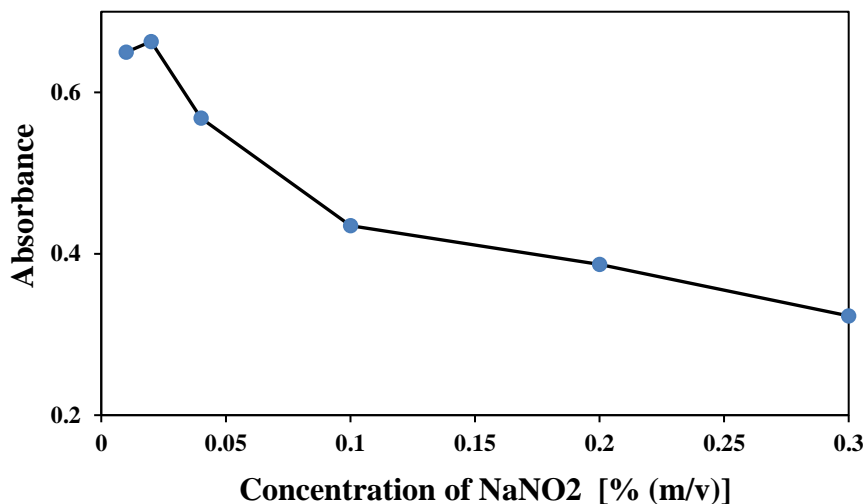


**Figure 2-3:** Effect of sodium nitrite on the color development of dye on the estimation of  $5 \mu\text{g.mL}^{-1}$  SMZ.

### 3- Effect of different acid

Various acidic solutions ( $\text{H}_2\text{SO}_4$ ,  $\text{HCl}$ ,  $\text{HNO}_3$ , and  $\text{CH}_3\text{COOH}$ ) with 1.0 M of concentration were tested for diazotization reaction. Among these,  $\text{HCl}$  was found to be the best by virtue of highest absorbance values and stability considerations for diazotization, (Table 2-8) shows the results.

**Table 2-8:** Effect of different acids on diazotization of  $5.0 \mu\text{g.mL}^{-1}$  SMZ.

<i>Acidic solution (1.0 M)</i>	<i>Absorbance</i>
$\text{H}_2\text{SO}_4$	0.575
$\text{HCl}$	0.663
$\text{HNO}_3$	0.508
$\text{CH}_3\text{COOH}$	0.290

### 4- Effect of acidity on diazotization

The influence of hydrochloric acid concentration on the diazotization reaction was studied over the range (0.1-1.0) M. Maximum and constant absorption intensities were achieved at addition of 1.0 mL of 0.2 M  $\text{HCl}$ , after which the absorbance of the reaction product began to decrease, therefore; 1.0 mL of 0.2 M was chosen as the optimum value, Figure 2-4 shows this effect.

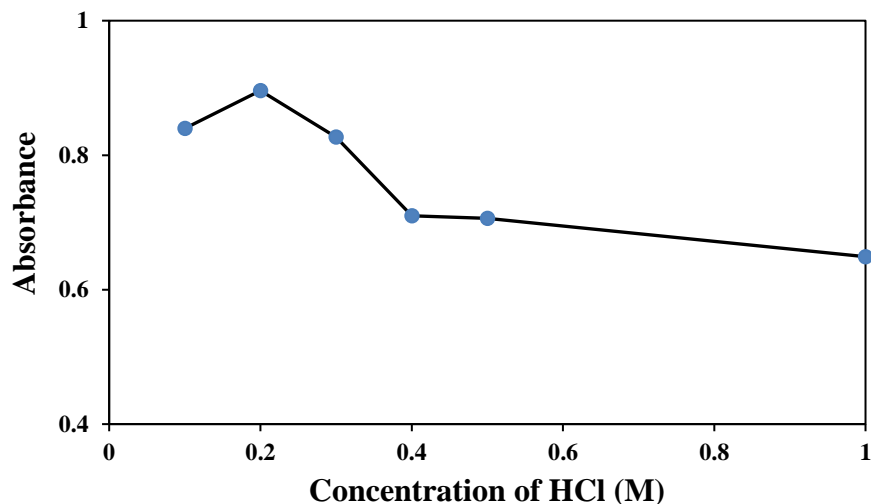


**Figure 2-4:** Effect of acidity on diazotization on the estimation of  $(5.0 \mu\text{g.mL}^{-1})$  SMZ.

### 5- Effect of sulfamic acid concentration

The optimum sulfamic acid concentration was estimated by adding 1.0 mL from various concentration (0.1-1.0) % (m/v) of sulfamic acid solution; it was found that 1.0 mL of 0.3 % (m/v) solution give the highest absorbance value. Sulfamic acid was added to remove the excess amount of nitrite; Figure 2-5 shows the effect of sulfamic acid concentration.

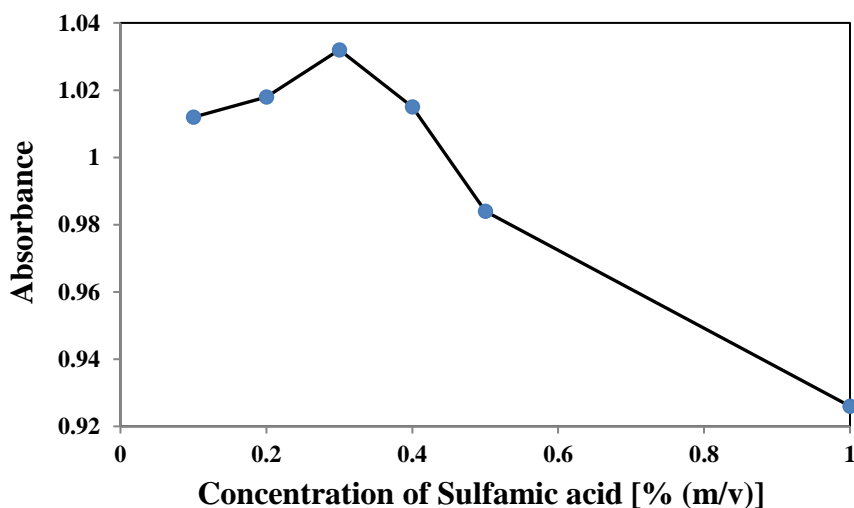


**Figure 2-5:** Effect of sulfamic acid concentration on the estimation of  $5.0 \mu\text{g.mL}^{-1}$  SMZ.

### 6- Effect of diphenylamine concentration

Concentration of diphenylamine ranged from (0.25-1.25) % (m/v) of 1.0 mL solutions were examined to obtain highest color intensity of the azo dye as shown in Figure 2-6, the investigations showed that 1.0 mL of 0.5 % DPA gave maximum and stable intensity, above this concentration, the absorbance remained unchanged.

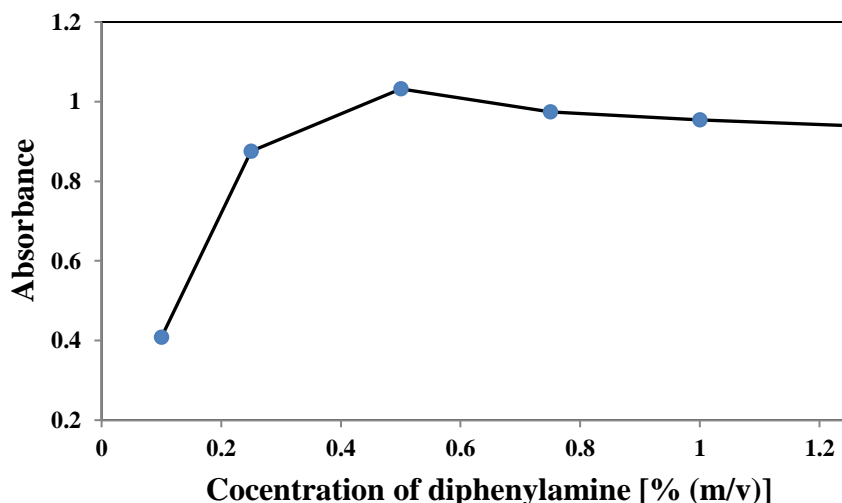


**Figure 2-6:** Effect of DPA concentration on the development of dye on the estimation of  $5.0 \mu\text{g}\cdot\text{mL}^{-1}$  SMZ.

### 7- Effect of coupling reaction time

The optimum time of coupling reaction time was determined by following the color azo-dye development at room temperature. The reaction mixture was allowed to stand for different intervals, and it was found that 10 minutes period was required for full color development; the color was stable for at least 1h, as indicated in Table 2-9.

**Table 2-9:** Effect of coupling reaction time.

<i>Time (min.)</i>	<i>Absorbance</i>
0	0.642
5	1.018
10	1.032
15	1.040
20	1.031
60	1.036

## 8- Effect of acidity

It was found that the optimum concentration of hydrochloric acid leading to a maximum intensity of the complex was 6.0 M. Concentrations below and above this value cause a decrease in absorbance; this may be attributed to the de-colorization of colored azo dye. Fig 2-7 shows the effect of acidity on color dye.

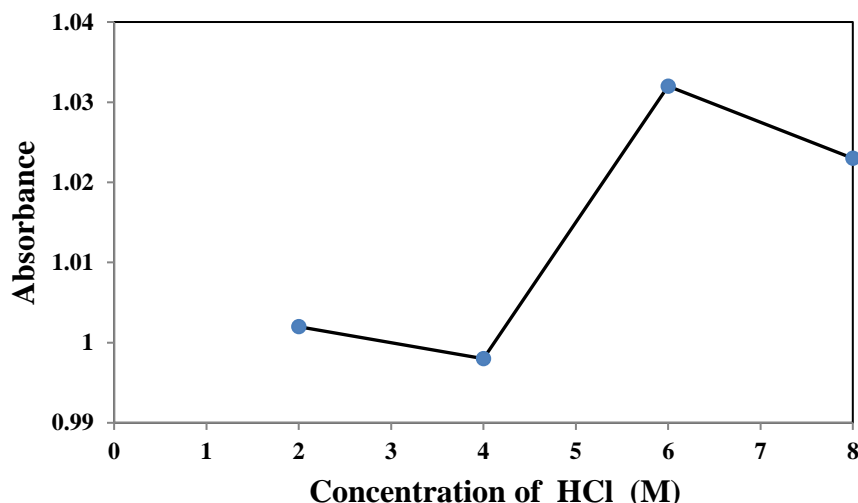


**Figure 2-7:** Effect of acidity on color dye on the estimation of  $5.0 \mu\text{g.mL}^{-1}$  SMZ.

## II- Simplex method

The simplex program was employed to find the optimum experimental conditions for the determination of (SMZ). The boundary conditions for the three variables delineated above, as recorded in (Table 2-5) together with the step values.

Four (n+1) arbitrary experimental conditions were chosen, by selecting the values of these parameters within specified boundaries for each, at which they affected the measured absorptions signal of the colored products (1-4 in Table 2-6) , the absorbencies of these four experiments were fed into the program.

The Simplex program starts to reflect the worst point through the centroid of other points to obtain a new point 5. An experiment was then performed utilizing the variable setting as a reflected point; because this value was better than that at point 3, the latter was rejected and replaced by point 5. A measured absorption signal was feeding again to the program and the process is repeated successively until optimum conditions were obtained similarly to those obtained by the univariate method. Figure 2-8 shows the progress of the simplex, which indicates

gradual improvement in the response function. Only 12 experiments were performed, enough to evaluate the proper conditions at maximum response function with the results given in (Table 2-10).

Step 5, 7, 9, 12 shows the same highest response function value obtained. To conclude, the optimum operating conditions for the determination of (SMZ) are 1.0 mL of each 0.20 % (m/v) sodium nitrite, 1.0 % (m/v) DPA and 0.90 M hydrochloric acid.

**Table 2-10:** Multivariate experiments (Simplex) for the determination of ( $5.0 \mu\text{g}\cdot\text{mL}^{-1}$ ) SMZ.

<i>Exp. No.</i>	<i>Conc. of sodium nitrite (% m/v)</i>	<i>Conc. of DPA (% m/v)</i>	<i>Conc. of hydrochloric acid (M)</i>	<i>Abs.</i>
1	0.01	0.25	0.20	0.788
2	0.02	0.40	0.40	0.878
3	0.10	0.60	0.80	0.904
4	0.16	0.75	0.50	0.918
5	0.20	1.00	0.90	0.995
6	0.20	1.00	1.00	0.988
7	0.20	1.00	0.90	0.995
8	0.18	0.90	0.60	0.978
9	0.20	1.00	0.90	0.995
10	0.19	1.00	0.90	0.975
11	0.20	1.00	0.80	0.970
12	0.20	1.00	0.90	0.995

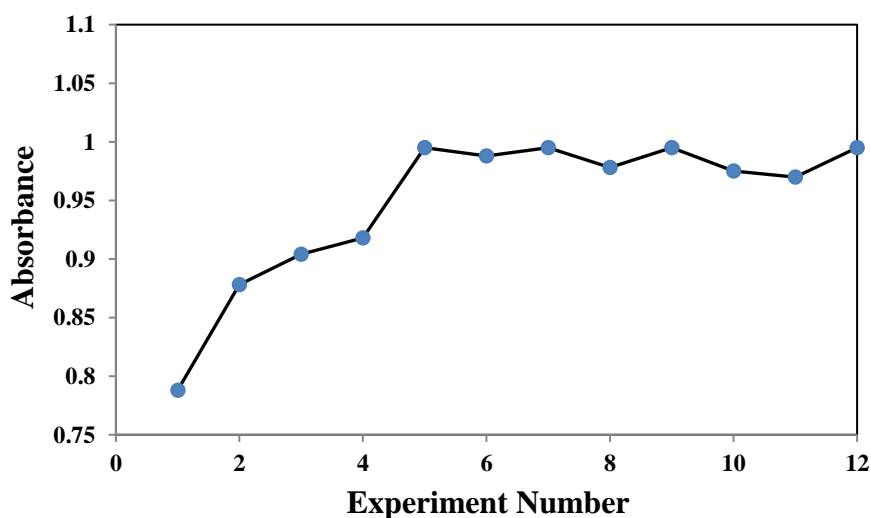


**Figure 2-8:** Response function progress for simplex.



### 2-3-3 Calibration curves and analytical data

#### I- Univariate method

The effect of concentration on the absorbance behavior at optimum conditions of univariate method was investigated using authentic standard. The results are shown in Figure 2-9.

Beer's law was obeyed in the range of 0.5-7.0  $\mu\text{g.mL}^{-1}$  of SMZ. The regression equation, correlation coefficient, molar absorptivity, Sandell's sensitivity and detection limit (DOL) and quantification of limit (QOL) are calculated and listed in Table 2-11.

**Table 2-11:** Optical characteristics and statistical data for the determination of SMZ by univariate method.

<i>Parameter</i>	<i>Value</i>
$\lambda_{\text{max}}$ (nm)	530.0
Color	Blue
Linearity range ( $\mu\text{g.mL}^{-1}$ )	0.5-7.0
Regression equation	$Y = 0.2043[\text{SMZ. } \mu\text{g.mL}^{-1}] - 0.001$
Calibration sensitivity ( $\text{mL.}\mu\text{g}^{-1}$ )	0.2043
Correlation coefficient (r)%	99.98
Correlation of linearity ( $r^2$ )%	99.97
Molar absorptivity ( $\text{L.mol}^{-1}.\text{cm}^{-1}$ )	$\epsilon = 5.1745 \times 10^4$
Sandell's sensitivity ( $\mu\text{g.cm}^{-2}$ )	4.8947
Detection limit ( $\mu\text{g.mL}^{-1}$ )	0.034
Quantification limit ( $\mu\text{g.mL}^{-1}$ )	0.104

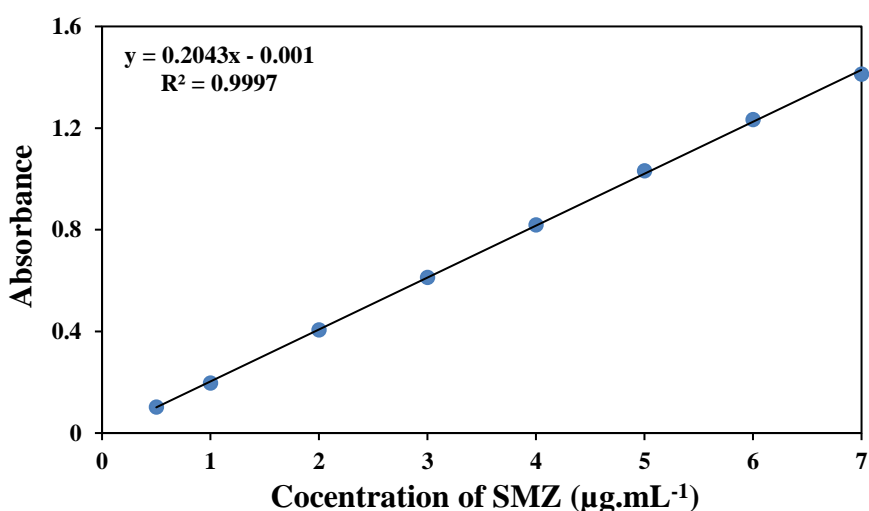


**Figure 2-9:** Calibration curve for the determination of SMZ by univariate optimal condition.

## II- Simplex method

Optical characteristics and statistical data for the regression equation of the simplex method are given in Table 2-12 and Figure 2-10.

The amino group of SMZ is diazotized with nitrous acid ( $\text{NaNO}_2/\text{HCl}$ ), thus the diazonium salt formed is coupled with DPA at temperature ( $0-5\text{ }^\circ\text{C}$ ) to yield the azo-dye, mechanism of sulfamethoxazole reaction with diphenylamine in an acidic medium can be represented in Scheme (2-3).

**Table 2-12:** Optical characteristics and statistical data for the determination of SMZ by simplex method.

<i>Parameter</i>	<i>Value</i>
$\lambda_{\text{max}}$ (nm)	530.0
Color	Blue
Linearity range ( $\mu\text{g.mL}^{-1}$ )	0.5-12.0
Regression equation	$Y=0.1959[\text{SMZ. } \mu\text{g.mL}^{-1}]-0.0083$
Calibration sensitivity ( $\text{mL. } \mu\text{g}^{-1}$ )	0.1959
Correlation coefficient (r)%	99.99
Correlation of linearity ( $r^2$ )%	99.98
Molar absorptivity ( $\text{L.mol}^{-1}.\text{cm}^{-1}$ )	$\epsilon =4.9617 \times 10^4$
Sandell's sensitivity ( $\mu\text{g.cm}^{-2}$ )	5.1047
Detection limit ( $\mu\text{g.mL}^{-1}$ )	0.036
Quantification limit ( $\mu\text{g.mL}^{-1}$ )	0.108

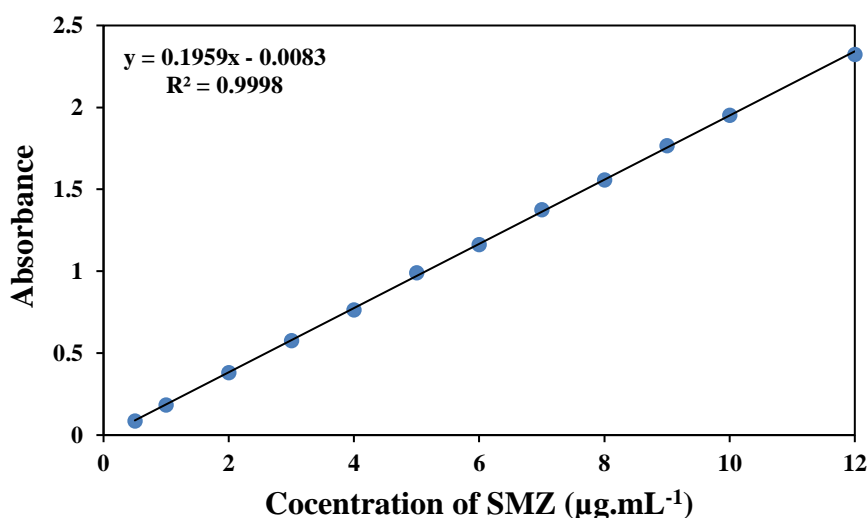
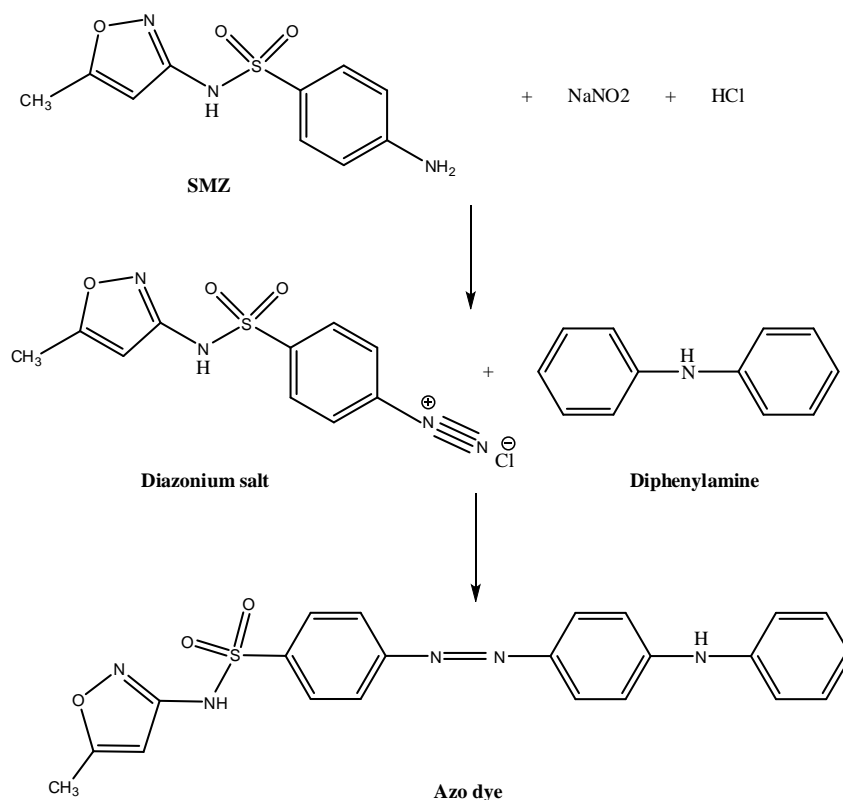


**Figure 2-10:** Calibration curve for the determination of SMZ by simplex optimal condition.



**Scheme 2-3:** The reaction mechanism for diazotization and reaction between SMZ and DPA.

#### 2-3-4 Precision and accuracy

The accuracy of the both methods were established by analyzing the pure drug at three concentration levels of five replicate analyses and the precision was examined by determining the coefficient of variation (C.V) % on the same solution of drug sample (Table 2-13). The low values of C.V % (0.139-0.424) and the range of error at the level (-0.550-0.275) indicate the high accuracy and precision of the proposed method.

**Table 2-13:** Evaluation of accuracy and precision for the determination of SMZ by proposed method.

	<i>Conc. of SMZ</i> ( $\mu\text{g.mL}^{-1}$ )		<i>Relative Error</i> %	<i>C.V*</i> %
	<i>Taken</i>	<i>Found*</i>		
<b>For univariate</b>	2.000	1.989	-0.550	0.190
	4.000	4.011	0.275	0.424
	6.000	6.014	0.233	0.369
<b>For simplex</b>	2.000	1.990	-0.500	0.139
	4.000	4.010	0.250	0.233
	6.000	6.013	0.216	0.224

\*Average of five determinations.

### 2-3-5 Interference study

To assess the analytical potential of the proposed method, the effect of some common excipients; sucrose, vanillin, glucose, lactose, and starch which often accompany drug, were examined by carrying out the determination of  $5.0 \mu\text{g.mL}^{-1}$  of SMZ in the presence of above compounds. The results presented in Table 2-14 indicate no interferences were found from any of the excipients studied in determination of SMZ.

**Table 2-14:** Percent recovery for  $5.0 \mu\text{g.mL}^{-1}$  of sulfamethoxazole in the presence of  $1000 \mu\text{g.mL}^{-1}$  of excipients.

<i>Excipients</i>	<i>Concentration</i> ( $\mu\text{g.mL}^{-1}$ )	<i>Sulfamethoxazole Conc. Taken (5.0 <math>\mu\text{g.mL}^{-1}</math>)</i>	
		<i>Conc. Found*</i> ( $\mu\text{g.mL}^{-1}$ )	<i>Recovery*</i> %
Sucrose	1000	5.02	100.40
Vanillin		4.94	98.80
Glucose		4.96	99.20
Lactose		4.92	98.40
Starch		5.06	101.20

\*Average of three determinations.

### 2-3-6 Application in pharmaceutical preparations by standard additions method (SAM)

Standard additions technique followed to check the validity of the proposed method has given good recoveries of the drug in pharmaceutical preparations suggesting a noninterference from pharmaceutical preparations. Hence, this method can be recommended for adoption in routine analysis of SMZ in quality control laboratories. The procedure is found in 2-2-10

Table 2-15 shows the result of recovery and coefficient of variation (C.V) for the standard additions method. Figure 2-11 to 2-18 shows the plot of determination of SMZ in syrup and tablet by standard additions method.

**Table 2-15:** Application of the proposed method to the SMZ concentration measurements pharmaceutical preparations by (SAM).

<i>Sample</i>	<i>Conc. taken</i> ( $\mu\text{g.mL}^{-1}$ )	<i>Conc.* found</i> ( $\mu\text{g.mL}^{-1}$ )	<i>Recovery</i> %	<i>C.V*</i> %
<b>Bactrim tablet</b> <b>(Roche-France)</b>	100.00	101.33	101.33	0.442
<b>Bactrim syrup</b> <b>(Roche-France)</b>	100.00	100.13	100.13	0.443

<i>Sample</i>	<i>Conc. taken</i> ( $\mu\text{g.mL}^{-1}$ )	<i>Conc.* found</i> ( $\mu\text{g.mL}^{-1}$ )	<i>Recovery</i> %	<i>C.V*</i> %
<b>Methoprim tablet</b> (NDI-Iraq)	100.00	96.54	96.54	0.867
<b>Cotrim syrup</b> (Asia-Syria)	100.00	101.00	101.00	0.469

\*Average of three determinations.

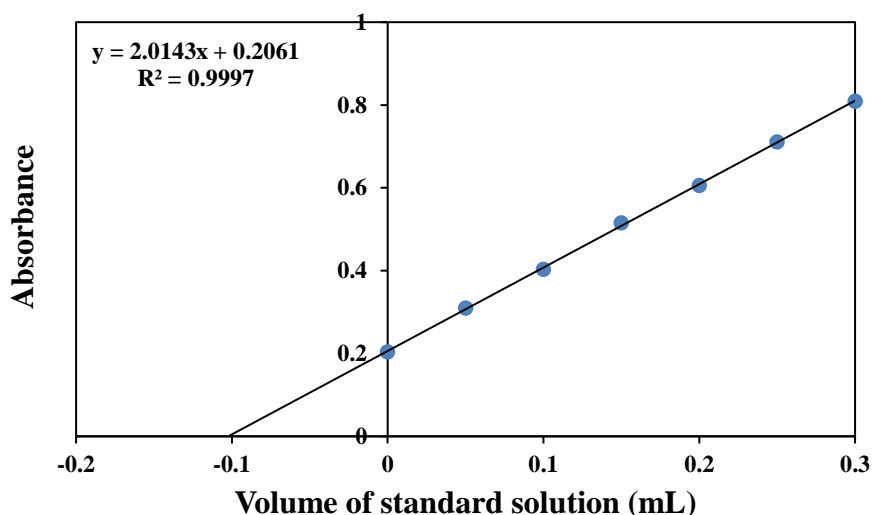


**Figure 2-11:** Determination of SMZ in tablet (Bactrim) by standard additions method level one, (0.1 mL from 100  $\mu\text{g.mL}^{-1}$  Bactrim tablet).

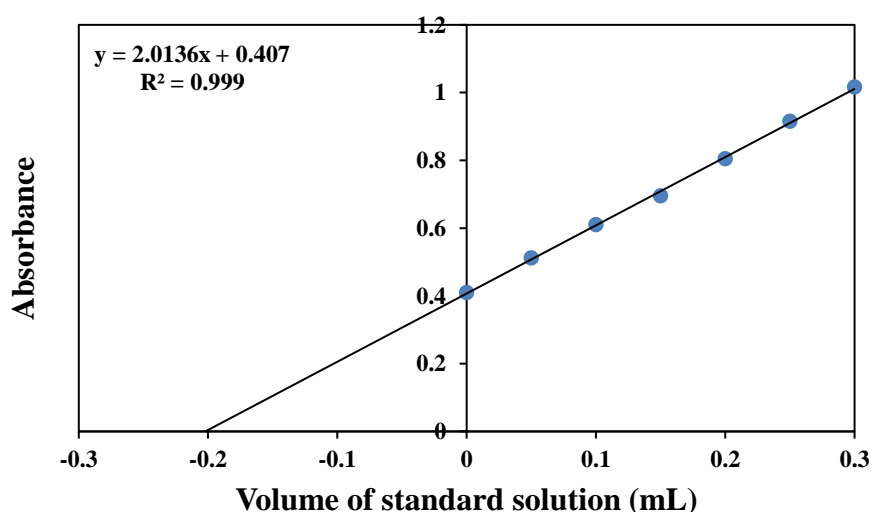


**Figure 2-12:** Determination of SMZ in tablet (Bactrim) by standard additions method level two, (0.2 mL from 100  $\mu\text{g.mL}^{-1}$  Bactrim tablet).

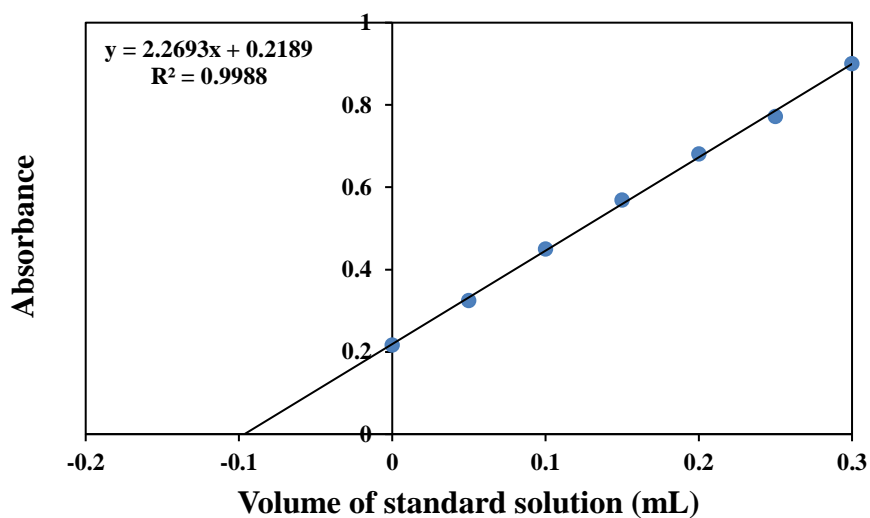


**Figure 2-13:** Determination of SMZ in tablet (Methoprim) by standard additions method level one, (0.1 mL from 100  $\mu\text{g}\cdot\text{mL}^{-1}$  Methoprim tablet).

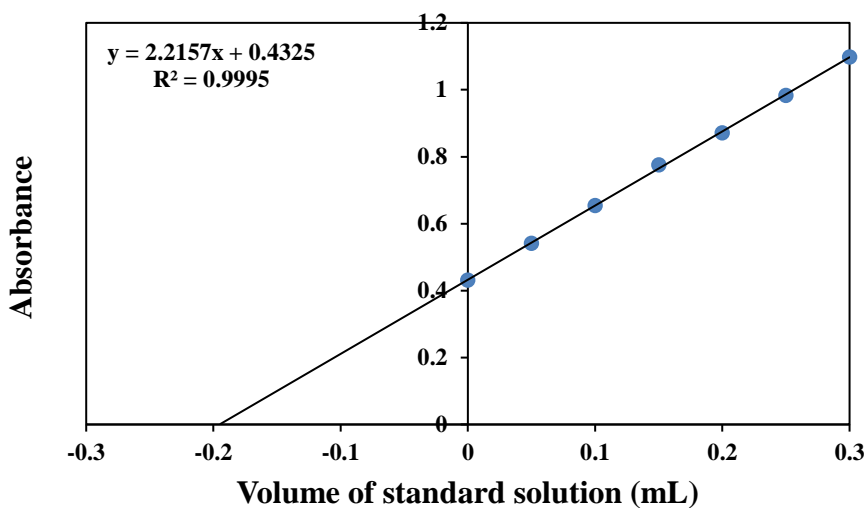


**Figure 2-14:** Determination of SMZ in tablet (Methoprim) by standard additions method level two, (0.2 mL from 100  $\mu\text{g}\cdot\text{mL}^{-1}$  Methoprim tablet).

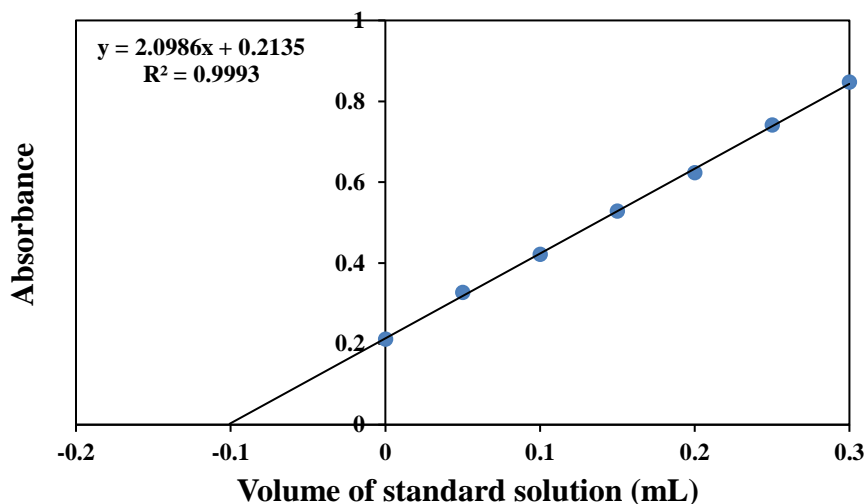


**Figure 2-15:** Determination of SMZ in syrup (Bactrim) by standard additions method level one, (0.1 mL from  $100 \mu\text{g}\cdot\text{mL}^{-1}$  Bactrim syrup).

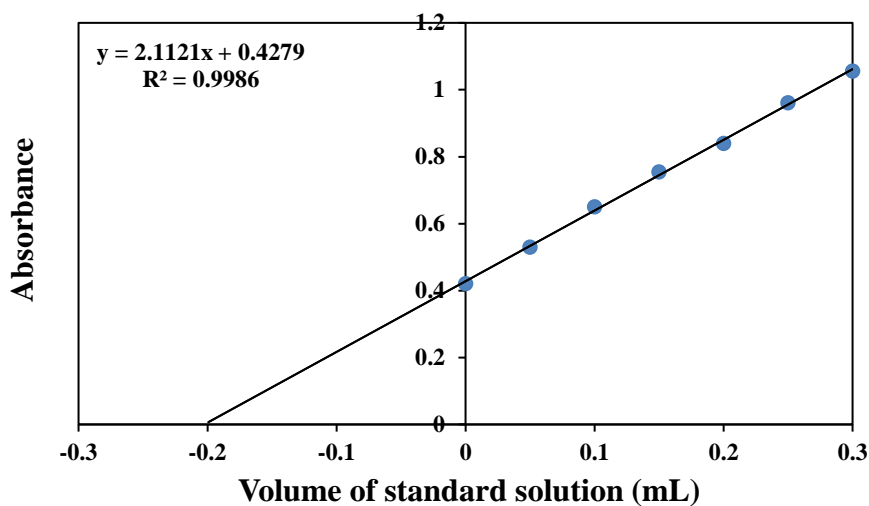


**Figure 2-16:** Determination of SMZ in syrup (Bactrim) by standard additions method level two, (0.2 mL from  $100 \mu\text{g}\cdot\text{mL}^{-1}$  Bactrim syrup).

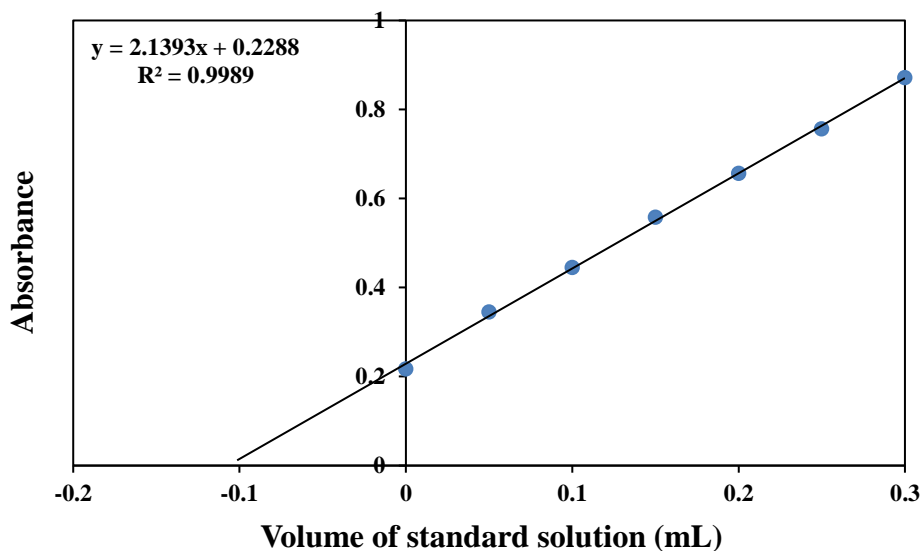


**Figure 2-17:** Determination of SMZ in syrup (Cotrim) by standard additions method level one, (0.1 mL from 100  $\mu\text{g}\cdot\text{mL}^{-1}$  Cotrim syrup).

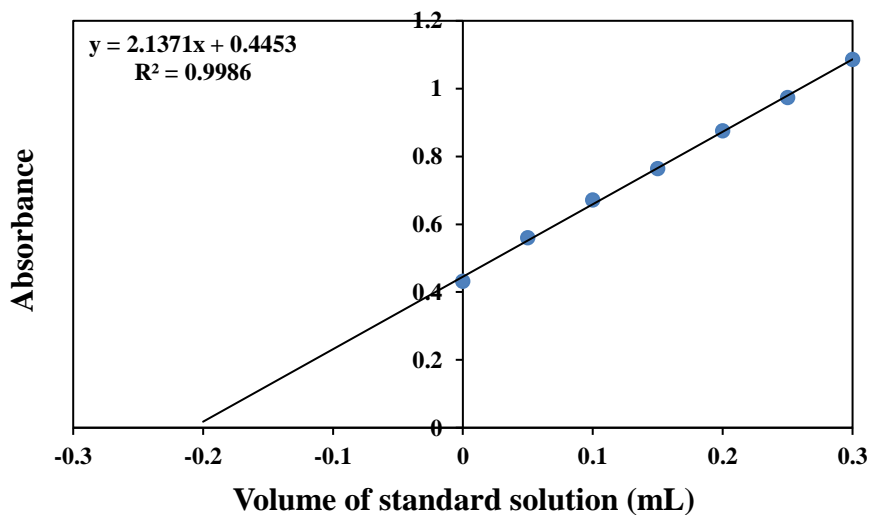


**Figure 2-18:** Determination of SMZ in syrup (Cotrim) by standard additions method level two, (0.2 mL from 100  $\mu\text{g}\cdot\text{mL}^{-1}$  Cotrim syrup).



## II- The Determination of sulfanilamide (SNA)

### 2-3-7 Absorption spectra

In order to get the optimum wavelength of maximum absorption ( $\lambda_{\max}$ ) of the colored azo dye formed in the proposed method,  $5.0 \mu\text{g.mL}^{-1}$  of SNA is taken and color has been developed by following the prescribed procedure, whereas the blank absorption was negligible in this record. Figure 2-19 shows the absorption spectrum for blank against D.W, and figure (2-20 and 2-21) show the absorption spectra for the primary test and optimum condition for univariate and simplex method respectively.

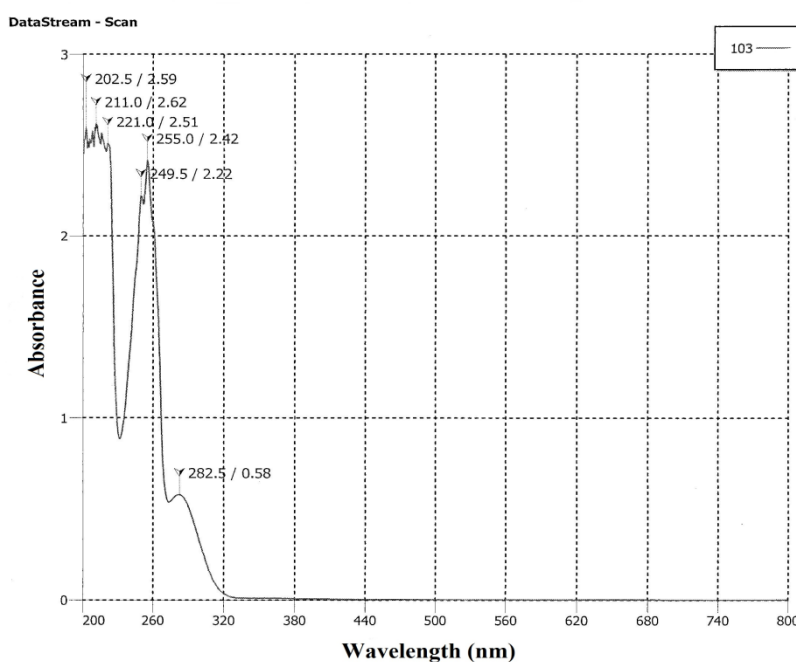


**Figure 2-19:** Absorption spectrum of blank solution against (D.W.) under the primary test.

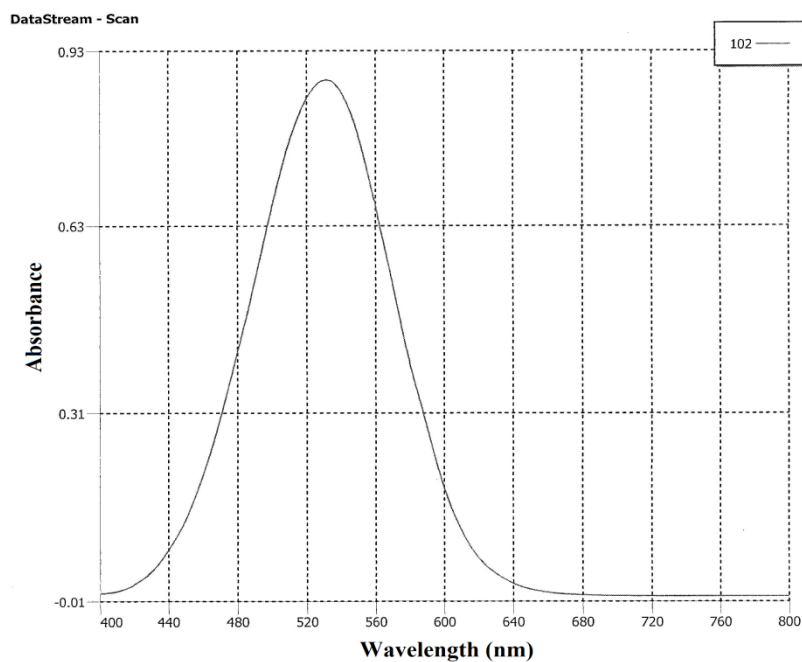


**Figure 2-20:** Absorption spectrum of (5 µg.mL<sup>-1</sup>) SNA-DPA against reagent blank under the primary test.

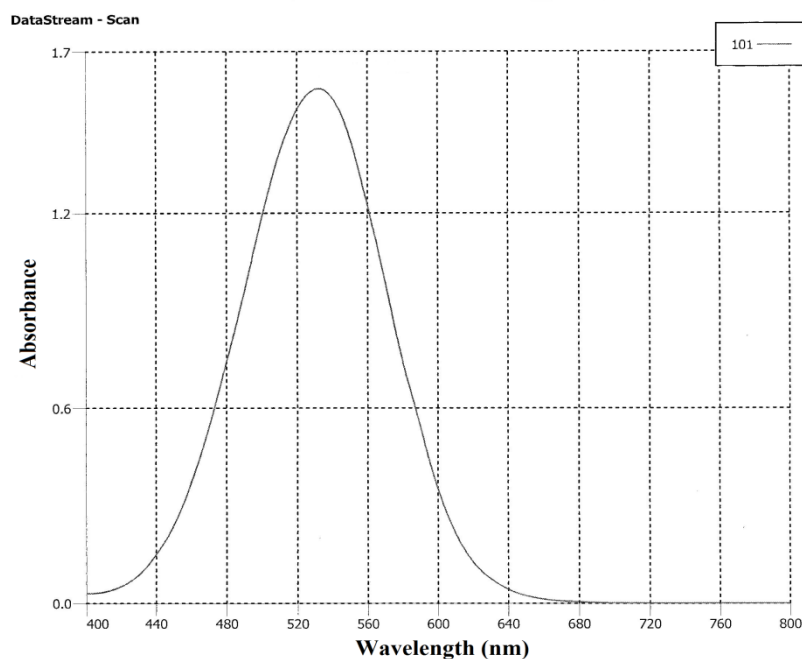


**Figure 2-21:** Absorption spectrum of (5 µg.mL<sup>-1</sup>) SNA-DPA against reagent blank under the optimum conditions, simplex method.

## 2-3-8 Optimization of reaction variables

### I- Univariate Method

Various parameters (diazotization reaction time, sodium nitrate concentration, hydrochloric acid concentration, sulfamic acid concentration, diphenylamine concentration and time of coupling reaction) were first optimized for the development of color dye, univariately by systematic study of the effects of each parameter in development of color product. The optimization steps were carried out by varying the parameters one at a time and controlling all others fixed.

#### 1- Effect of diazotization reaction time

It was found that the diazotization reaction was taking place instantaneous when the time required for diazotization reaction was studied in the range (0-20) min. at (0-5 °C). As listed in Table (2-16) the diazotized product was found to be decomposed with time therefore, diazotization was carried out instantaneously.

**Table 2-16:** Effect of diazotization reaction time.

<i>Time (min.)</i>	<i>Absorbance</i>
0	1.372
5	1.350
10	1.331
15	1.294
20	1.256

#### 2- Effect of sodium nitrite concentration

Sodium nitrite concentration for diazotization was optimized in the range of (0.02-0.20) % (m/v) (Figure 2-22). Maximum absorbance was observed when 1.0 mL of 0.14 % (m/v) sodium nitrite was added and the absorption of dye product was measured at 531.0 nm. Below and above this concentration the absorbance was decreased.

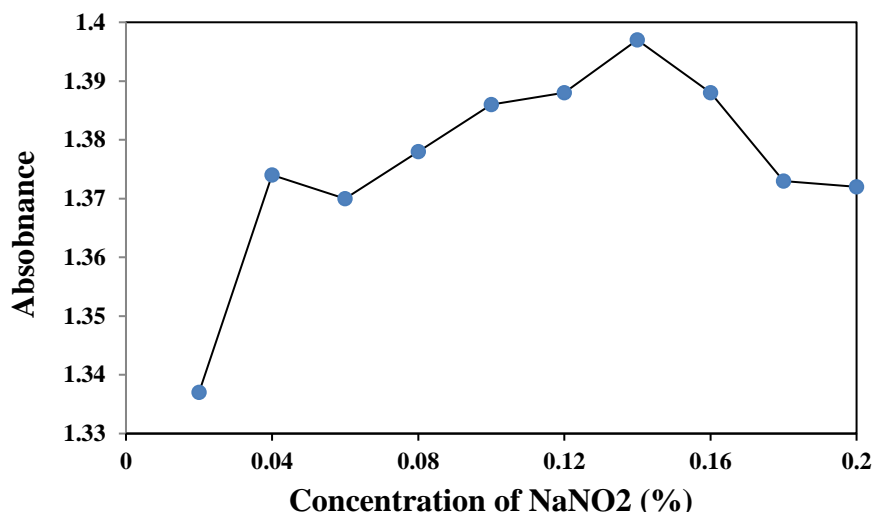


**Figure 2-22:** Effect of sodium nitrite on the color development of dye in the determination of  $5.0 \mu\text{g.mL}^{-1}$  of SNA.

### 3- Effect of different acidic solutions

Effect of many acids on diazotization reaction was studied such as  $\text{H}_2\text{SO}_4$ ,  $\text{HCl}$ ,  $\text{HNO}_3$ , and  $\text{CH}_3\text{COOH}$  with 1.0 M of concentration.  $\text{HCl}$  was responded for the stable diazotized product thus it was used for the following experiments (Table 2-17).

**Table 2-17:** Effect of different acids on diazotization of  $5 \mu\text{g.mL}^{-1}$  of SNA.

<i>Acidic solution (1.0 M)</i>	<i>Absorbance</i>
$\text{H}_2\text{SO}_4$	1.104
$\text{HCl}$	1.397
$\text{HNO}_3$	0.984
$\text{CH}_3\text{COOH}$	0.126

### 4- Effect of hydrochloric acid concentration

It was found that the absorbance of the formed azo dye product enhanced as the concentration hydrochloric acid was decreased in the studied range of the acid 1.0 mL of (0.20-2.0) M, Figure 2-23. Maximum absorption intensity was achieved when 1.0 mL of 0.8 M  $\text{HCl}$  was used, and this amount was used for subsequent work.

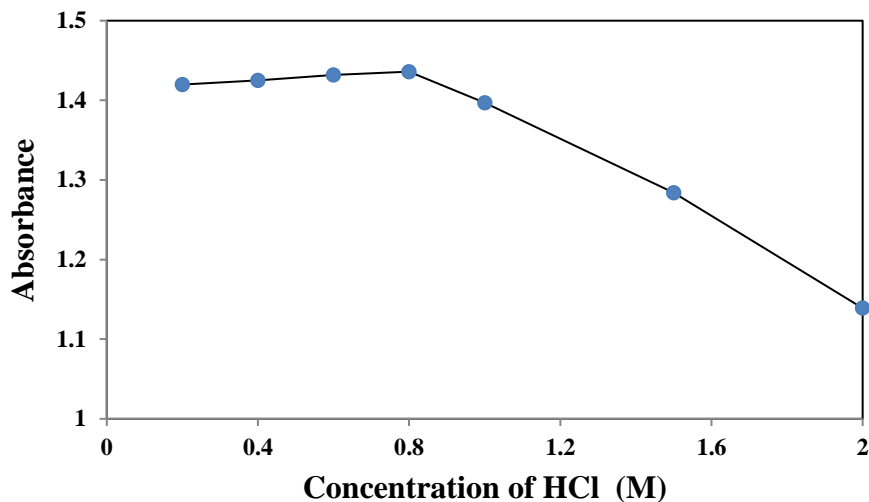


**Figure 2-23:** Effect of HCl concentration on the color development of dye in the determination of  $5.0 \mu\text{g}\cdot\text{mL}^{-1}$  of SNA.

### 5- Effect of sulfamic acid concentration

According to the results obtained upon studying the effect of the addition of 1.0 mL of (0.06-0.60) % (m/v) of sulfamic acid on the reaction product, the optimum amount was found to be 1.0 mL of 0.30 % (m/v) solution. The effect of sulfamic acid concentration is shown in Figure (2-24).

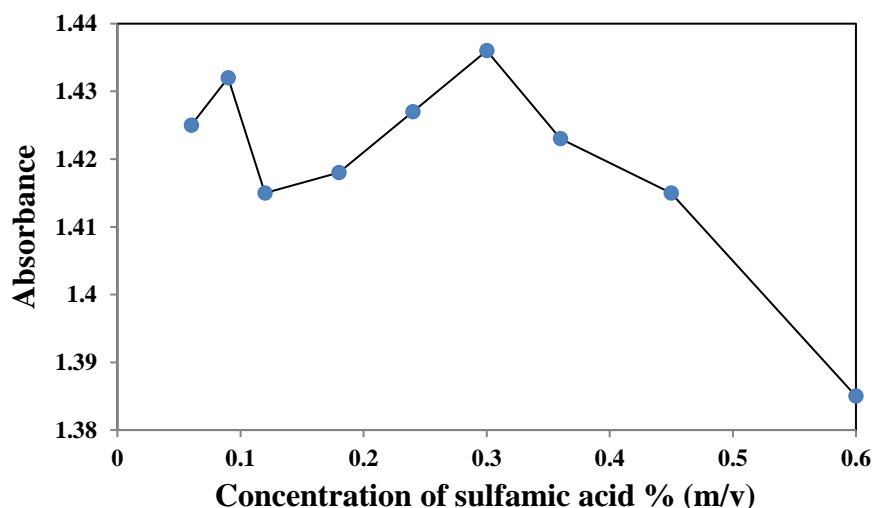


**Figure 2-24:** Effect of sulfamic acid concentration on the determination of ( $5.0 \mu\text{g}\cdot\text{mL}^{-1}$ ) of SNA.

### 6- Effect of reagent concentration

The effect of reagent concentration on the intensity of the color dye developed was tested using different concentration of DPA in the range (0.25-1.50) % (m/v) (Figure 2-25). The result shows that 1.0 mL of 1.0 % (m/v) of DPA solution was optimum for this method.

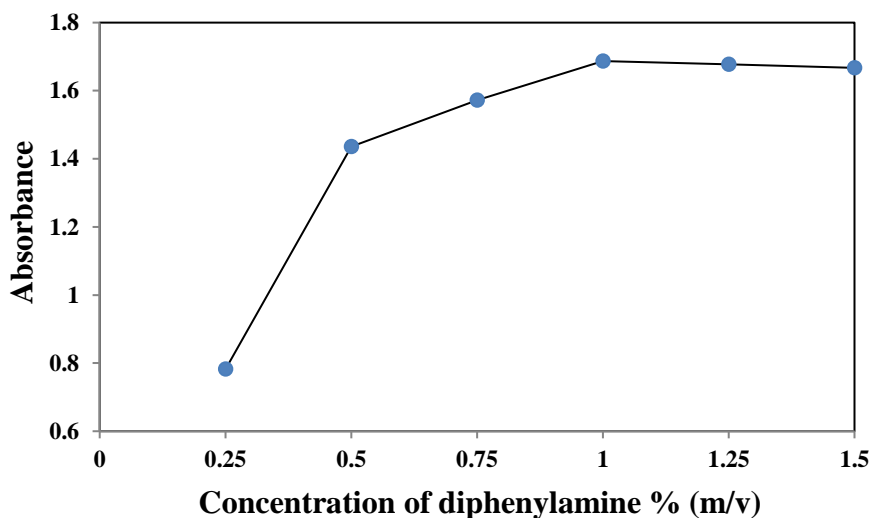


**Figure 2-25:** Effect of DPA concentration on the determination of (5.0  $\mu\text{g.mL}^{-1}$ ) of SNA.

### 7- Effect of coupling reaction time

The maximum time required for coupling reaction to be completed was found to be 3.0 min. at room temperature. After that period, the absorbance remained constant for at least 1.0 hours as presented in (Table 2-21).

**Table2-17:** Effect of coupling reaction time.

<i>Time (min.)</i>	<i>Absorbance</i>
0	1.233
2	1.626
3	1.687
5	1.683
10	1.685
15	1.684
20	1.683
60	1.680

### 8- Effect of acidity

It was found that the optimum concentration of hydrochloric acid leading to a maximum intensity of the complex was 6.0 M. Concentrations below and above this value cause a decrease in absorbance; this may be attributed to the de-colorization of colored azo dye. Figure 2-26 shows the effect of acidity on color dye.

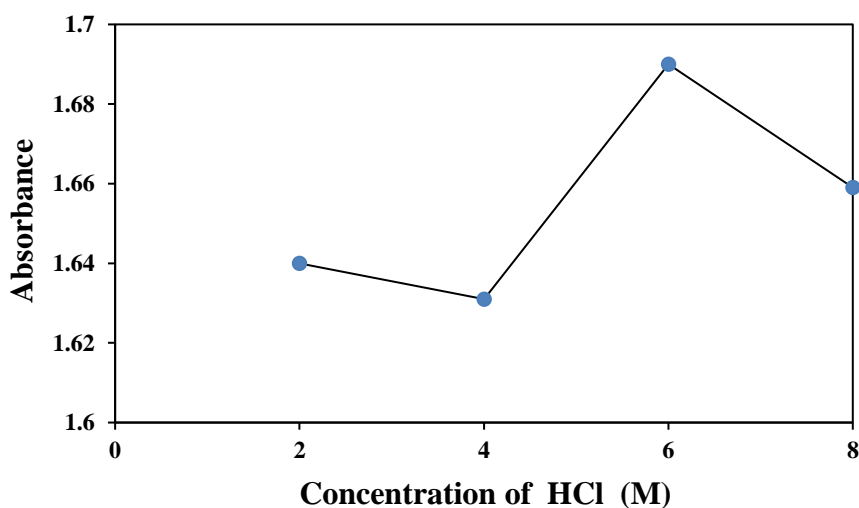


**Figure 2-26:** Effect of acidity on color dye on the estimation of 5.0  $\mu\text{g.mL}^{-1}$  SNA.

### II- Simplex Method

Simplex program was employed to find the optimum experimental conditions of three important parameters that considerably affect the colored product formation (viz the concentration of sodium nitrite, the concentration of DPA, and the coupling reaction time) for the determination of (SNA). The boundary conditions for the studied parameters delineated above, were first set as depicted in (Table 2-5) together with the step size values.

Four (number of studied parameters +1) arbitrary experimental conditions were chosen, by selecting the values of these parameters within specified boundaries for each, at which they affected the measured absorptions signal of the colored products (1-4 in Table 2-6), the absorbencies of these four experiments were fed into the program. Figure 2-27 shows the progress of the simplex, which indicates gradual improvement in the response function. Only 10 experiments were performed, enough to

evaluate the proper conditions at maximum response function with the results given in (Table 2-18). At step 8.0 the highest response function value was obtained. To conclude, the optimum operating conditions for the determination of (SNA) are 0.04 % (m/v) sodium nitrite, 1.0 % (m/v) DPA and 3.0 mints. coupling reaction Time.

**Table 2-18:** Multivariate experiments (Simplex) for the determination of ( $5.0 \mu\text{g.mL}^{-1}$ ) SNA.

<i>Exp. No.</i>	<i>Conc. of sodium nitrite (% m/v)</i>	<i>Conc. of DPA (% m/v)</i>	<i>Coupling reaction time (mint.)</i>	<i>Abs.</i>
1	0.04	0.50	4	1.669
2	0.20	0.25	3	0.742
3	0.08	1.00	2	1.659
4	0.16	1.25	1	1.190
5	0.04	1.25	3	1.686
6	0.04	0.75	4	1.670
7	0.04	0.25	4	1.186
8	0.04	1.00	3	1.710
9	0.04	0.25	4	1.186
10	0.04	1.25	2	1.669

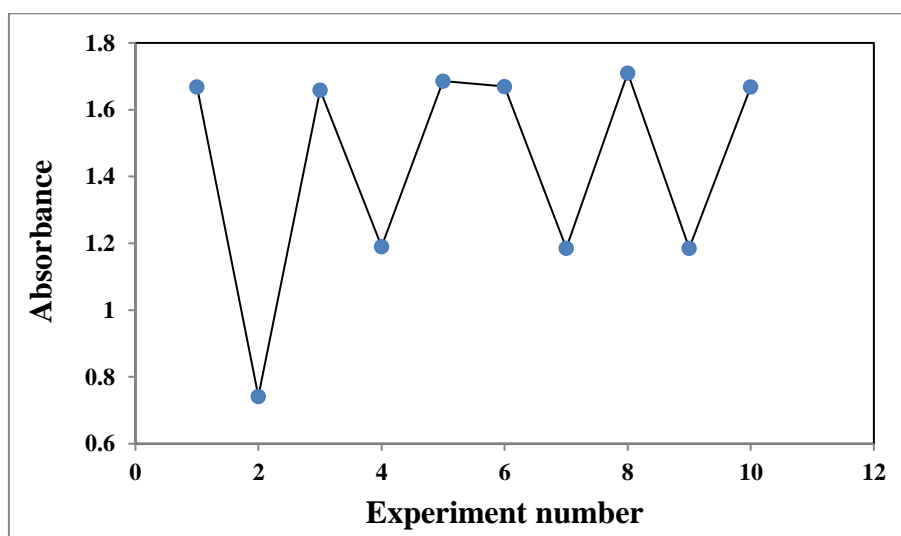


**Figure 2-27:** Response function progress for simplex.



### 2-3-9 Calibration curves and analytical data

#### I- Univariate method

According to the optimum experimental conditions, obtained via univariate method, linear calibration graph for sulfanilamide was obtained and shown in Figure 2-28, which shows that Beer's law is obeyed in the concentration range of (0.5-7.0)  $\mu\text{g.mL}^{-1}$ . The regression equation, correlation coefficient, molar absorptivity, Sandell's sensitivity and detection limit are given in Table 2-19.

**Table 2-19:** Optical characteristics and statistical data for the determination of SNA by univariate method.

<i>Parameter</i>	<i>Value</i>
$\lambda_{\text{max}}$ (nm)	531
Color	Blue
Linearity range ( $\mu\text{g.mL}^{-1}$ )	0.5-7.0
Regression equation	$Y=0.3313[\text{SNA. } \mu\text{g.mL}^{-1}]+0.0225$
Calibration sensitivity ( $\text{mL. } \mu\text{g}^{-1}$ )	0.3313
Correlation coefficient (r) %	99.99
Correlation of linearity ( $r^2$ ) %	99.98
Molar absorptivity ( $\text{L.mol}^{-1}.\text{cm}^{-1}$ )	$\epsilon = 5.7049 \times 10^4$
Sandell's sensitivity ( $\mu\text{g.cm}^{-2}$ )	3.0184
Detection limit ( $\mu\text{g.mL}^{-1}$ )	0.017
Quantification limit ( $\mu\text{g.mL}^{-1}$ )	0.050

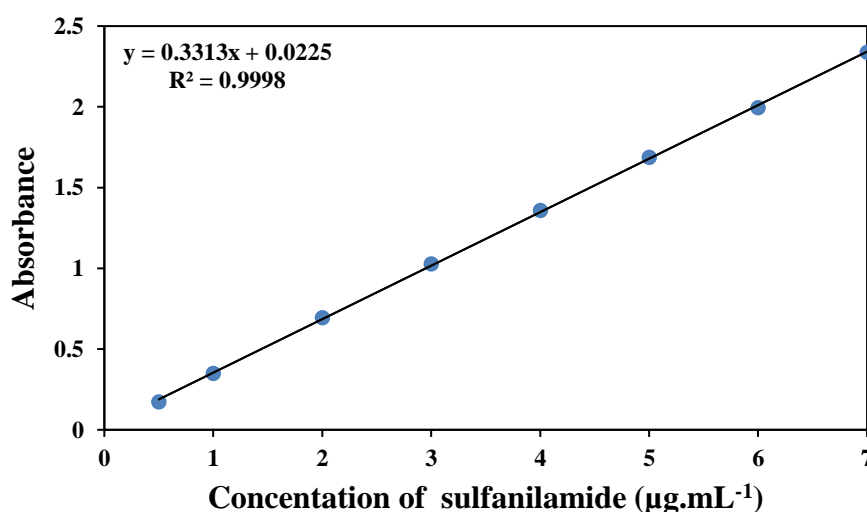


**Figure 2-28:** Calibration curve for the determination of SNA by univariate optimal condition.

## II- Simplex method

Table 2-20 and Figure 2-29 show the results for the calibration curve and statistical data. Better optical characteristics for calibration curve and statistical data were obtained under optimum conditions obtained by simplex optimization, in comparison with those obtained via univariate method.

**Table 2-20:** Optical characteristics and statistical data for the determination of SNA by simplex method.

<i>Parameter</i>	<i>Value</i>
$\lambda_{\max}$ (nm)	531
Color	Blue
Linearity range ( $\mu\text{g}.\text{mL}^{-1}$ )	0.5-7.0
Regression equation	$Y=0.3437[\text{SNA}.\mu\text{g}.\text{mL}^{-1}]+0.0091$
Calibration sensitivity ( $\text{mL}.\mu\text{g}^{-1}$ )	0.3437
Correlation coefficient (r) %	99.99
Correlation of linearity ( $r^2$ ) %	99.99
Molar absorptivity ( $\text{L}.\text{mol}^{-1}.\text{cm}^{-1}$ )	$\epsilon = 5.9185 \times 10^4$
Sandell's sensitivity ( $\mu\text{g}.\text{cm}^{-2}$ )	2.9095
Detection limit ( $\mu\text{g}.\text{mL}^{-1}$ )	0.016
Quantification limit ( $\mu\text{g}.\text{mL}^{-1}$ )	0.049

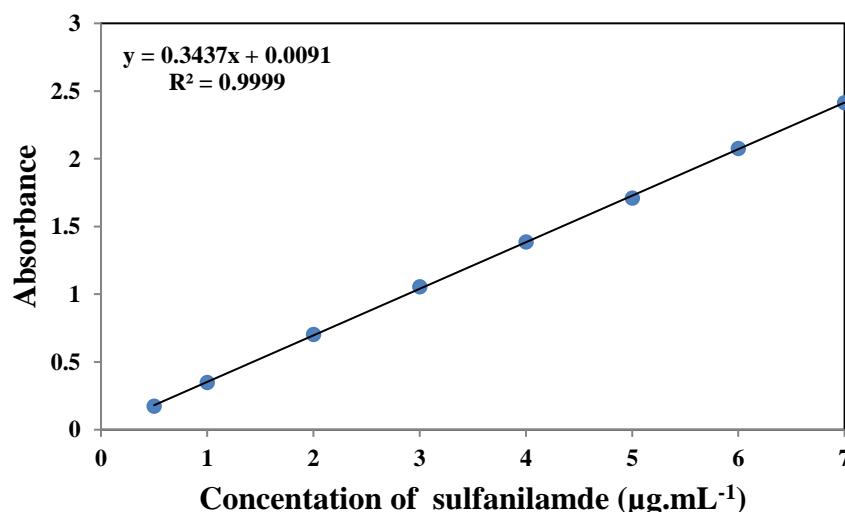
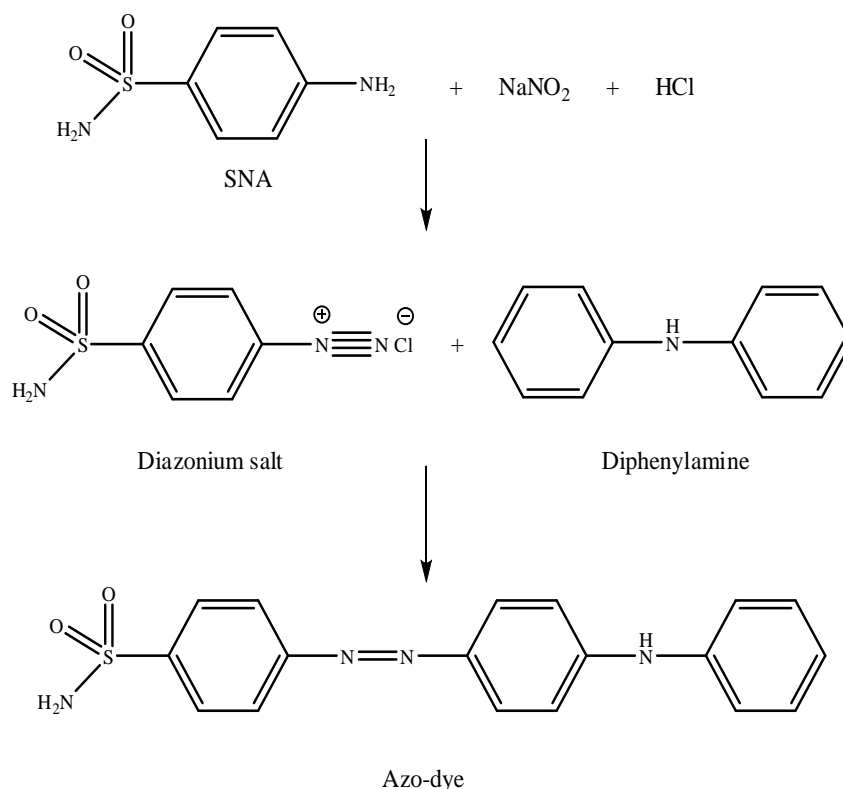


**Figure 2-29:** Calibration curve for the determination of SNA by simplex optimal condition.



**Scheme 2-4:** The reaction mechanism for diazotization and reaction between SNA and DPA

### 2-3-10 Precision and accuracy

The accuracy (in terms of relative error percent) and the precision (in term of coefficient of variation) of the proposed method under univariate and multivariate conditions were evaluated by doing five replicate analyses of SNA at three different levels of concentration within Beer's law range (Table 2-21). The results indicate good accuracy and precision of the proposed method at the studied concentration levels.

**Table 2-21:** accuracy and precision of the proposed method.

	Conc. of SNA ( $\mu\text{g.mL}^{-1}$ )		Relative Error %	C.V* %
	Taken	Found*		
For univariate	1.00	0.98	-0.020	1.822
	3.00	3.03	0.010	0.386
	5.00	4.99	-0.003	0.482
For simplex	1.00	0.99	-0.010	0.830
	3.00	3.03	0.010	0.333
	5.00	4.95	-0.010	0.149

\*mean of five replicate.

### 2-3-11 Interference study

The effect of various foreign species, which may be present in pharmaceutical products and affecting the reaction between the sulfanilamide and DPA, were studied. Optimum experimental conditions, for simplex optimization, were employed to determine  $5.0 \mu\text{g.mL}^{-1}$  concentration of SNA. Table 2-22 shows that the presence of  $1000 \mu\text{g.mL}^{-1}$  of the studied interfering excipient causes errors less than  $\pm 2 \%$ .

**Table 2-22:** Percent recovery for  $5.0 \mu\text{g.mL}^{-1}$  of sulfanilamide in the presence of  $1000 \mu\text{g.mL}^{-1}$  of excipients.

<i>Excipients</i>	<i>Concentration</i> ( $\mu\text{g.mL}^{-1}$ )	<i>Sulfanilamide Conc. Taken (<math>5.0 \mu\text{g.mL}^{-1}</math>)</i>	
		<i>Conc. *Found</i> ( $\mu\text{g.mL}^{-1}$ )	<i>Recovery*</i> %
Vanillin	1000	4.91	98.20
Glucose		5.10	102.00
Lactose		4.92	98.40
Starch		4.94	98.80
Sucrose		4.95	99.00

\*Average of three determinations.

### 2-3-12 Application in synthetic sample by standard additions method (SAM)

To increase the insurance, the proposed spectrophotometric method was applied for the determination of SNA in synthetic sample following the standard additions technique. Figures (2-30 and 2-31) show the standard additions plot and Table 2-23 shows the result of recovery and coefficient of variation for the method.

**Table 2-23:** Application of the simplex method to the SNA concentration measurements in synthetic sample by standard additions method.

<i>Sample</i>	<i>Conc. taken</i> ( $\mu\text{g.mL}^{-1}$ )	<i>Conc.* found</i> ( $\mu\text{g.mL}^{-1}$ )	<i>Recovery %</i>	<i>C.V*</i> %
<b>SNA in synthetic sample</b>	100.00	101.40	101.40	0.798
<b>SNA in synthetic sample</b>	200.00	202.60	101.30	0.202

\*Average of three determinations.

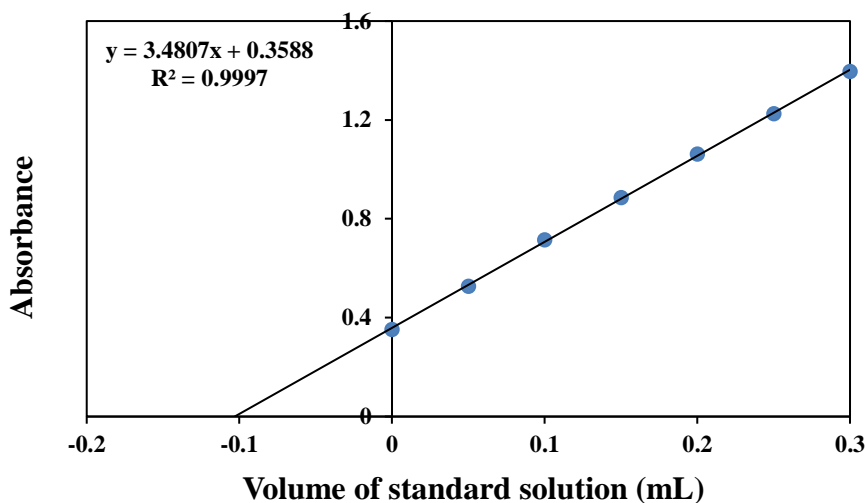


**Figure 2-30:** Determination of SNA in synthetic sample by standard additions method. Level one (0.1 mL from  $100 \mu\text{g}\cdot\text{mL}^{-1}$  synthetic sample).

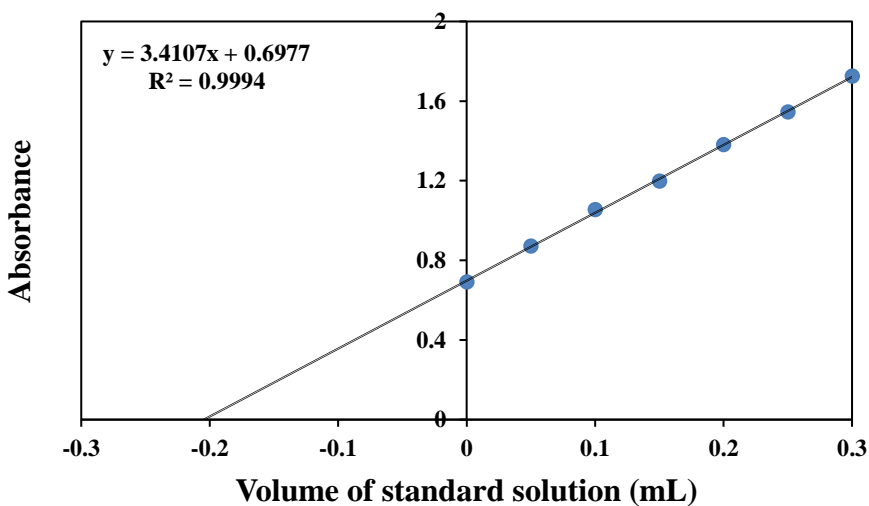


**Figure 2-31:** Determination of SNA in synthetic sample by standard additions method. Level two (0.2 mL from  $100 \mu\text{g}\cdot\text{mL}^{-1}$  synthetic sample).

Good recoveries of the drug present in studied sample indicate that non-interference from excipient.

# ***CHAPTER THREE***

***Determination of sulfamethoxazole  
and sulfanilamide by condensation  
reaction***

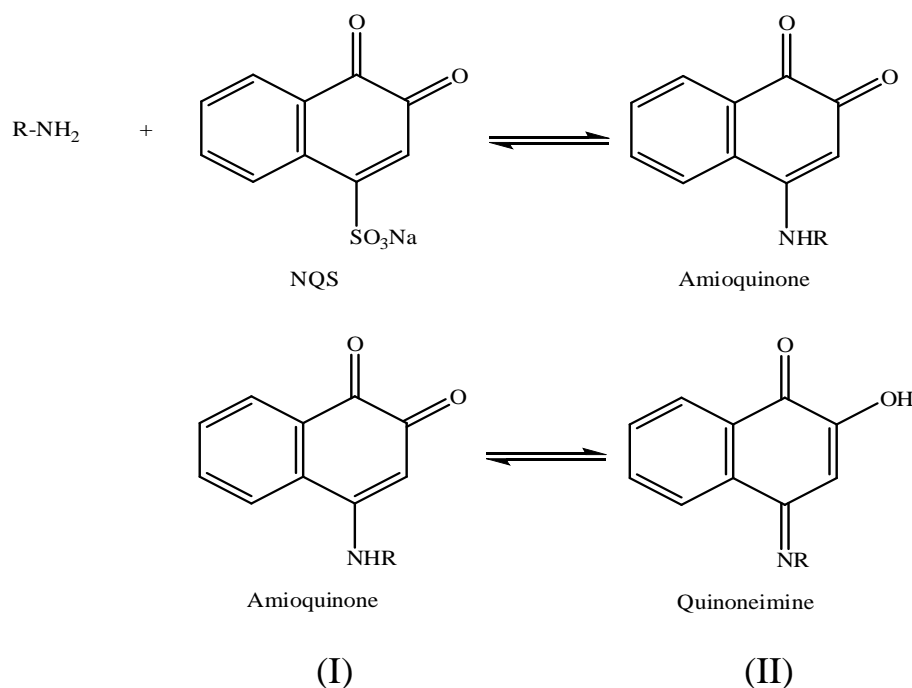
## Chapter Three

### 3 Determination of sulfamethoxazole and sulfanilamide by reaction with sodium 1, 2-Napthoquinon-4-Sulfonate (NQS)

#### 3-1 Introduction

##### 3-1-1 Condensation reaction

The reaction of sodium 1, 2-napthoquinone-4-sulphonate (NQS) with primary aromatic amine was reported by Boniger <sup>(113)</sup> since 1894. Replacement of the sulphonate group of the naphthoquinone sulphonic acid by an amino group gives N-alkylamino naphthoquinone <sup>(114)</sup>. This reaction has been applied to the characterization of primary aromatic amines and later formed the basis for colorimetric determinations of amino acids, sulfonamides, primary or secondary aliphatic and aromatic amines. In the case of primary amine, the adduct can be represented by either the amino quinone structure (I), the quinone imine structure (II) or an equilibrium mixture of the two obviously, only the quinone structure can be taken into account with a secondary amine.

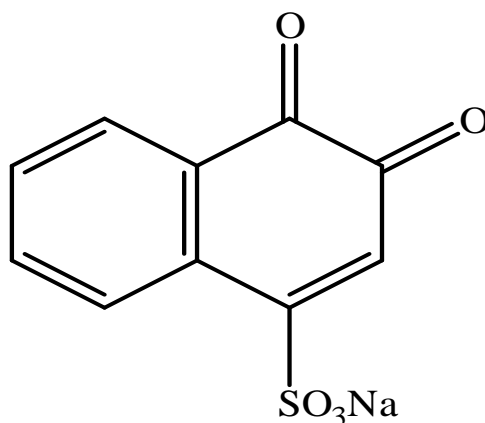


It may be concluded that, under the conventional analytical conditions, equilibrium between two forms (I and II) may intervene for the derivatives obtained from primary amines, but the quinone structure is mostly favored <sup>(115,116)</sup>. The applications of NQS for spectrophotometric

methods <sup>(117,118)</sup> as the chromogenic reagent are in good number and it is simplest reagent because of its well stability and the stability of colored complexes it formed with a series of reagents was been well utilized by good number of researchers.

### 3-1-2 Sodium 1, 2-naphthoquinone-4-sulfonate (NQS) <sup>(119,120,121)</sup>

The structure formula of sodium 1, 2-naphthoquinone-4-sulfonate (NQS) is shown in Scheme 3-1 and the general properties are listed below:



**Scheme 3-1:** The formula structure of sodium 1, 2-naphthoquinone-4-sulfonate (NQS).

<b>Chemical Name</b>	Sodium 3,4-dioxo-3,4-dihydronaphthalene-1-sulfonate
<b>Additional Name</b>	sodium 1,2-naphthoquinone-4-sulfonate
<b>Appearance</b>	Orange
<b>Molecular Formula</b>	C <sub>10</sub> H <sub>5</sub> NaO <sub>5</sub> S
<b>Molecular Weight (g.mol<sup>-1</sup>)</b>	260.20
<b>Melting Point</b>	289°C
<b>Uses</b>	Laboratory Reagent
<b>Solubility</b>	Soluble in water and cold water.
<b>Handling and Storage</b>	Keep container dry; Keep in a cool place, Keep container tightly closed, protected from the light.
<b>Stability</b>	The product is stable



### 3-1-3 Spectrophotometric determinations of some pharmaceutical preparations using condensation reaction

Various condensation reaction methods appeared in the literature for the assay of drugs with different reagents in pharmaceutical formulations Table 3-1 lists some of these.

**Table 3-1:** Spectrophotometric determinations of some pharmaceutical compounds using condensation reaction.

<i>Drug compounds (Trade Name) Chemical Nomenclature</i>	<i>Reagent</i>	<i><math>\lambda_{max}</math> (nm)</i>	<i>Linear dynamic range (<math>\mu\text{g.mL}^{-1}</math>)</i>	<i>Ref.</i>
<b>(Valacyclovir)</b> <i>L</i> -valine-2-[(2-amino-1,6-dihydro-6-oxo-9-hipurin-9-yl) methoxy] ethyl ester.	(NQS)	495	20-120,	
<b>(cefotaxime)</b> (6R, 7R)-3-[(acetyloxy) methyl]-7-[[[(2Z)-2-(2-aminothiazol-4-yl)-2-(methoxyimino) acetyl] amino]-8-oxo-5-thia-1-azabicyclo [4.2.0]oct-2-ene-2-carboxylate	1,2-naphtha quinone-4-sulfonate sodium salt	475	20-140	122
<b>(Reboxetine)</b> (2R)-rel-2-[(R)-(2-ethoxy phenoxy) phenyl methyl] morpholine	ethyl acetoacetate	400	0.5-3.0	123
<b>(Entacapone)</b> 2-cyano-3-(5-dihydroxyamino-3,4-dioxo-1-cyclohexa-1,5-dienyl)-N,N- diethyl-prop-2-enamide	(PDAC) p-dimethyl amino cinnamaldehyde, (PDAB) p-dimethyl amino benzaldehyde	524 415	10-50 50-250	124

<b>Drug compounds (Trade Name) Chemical Nomenclature</b>	<b>Reagent</b>	<b><math>\lambda_{max}</math> (nm)</b>	<b>Linear dynamic range (<math>\mu\text{g}\cdot\text{mL}^{-1}</math>)</b>	<b>Ref.</b>
<b>(Famciclovir)</b> 2-[2-(2-amino-9H-purin-9-yl) ethyl] - 1, 3-propanediol diacetate	(PDAB) P-dimethyl amino benzaldehyde.	480	2-10	125
	Vanillin.	470	2-10	
<b>(Bortezomib)</b> [(1R)-3-methyl-1-((2S)-3-phenyl-2-[(pyrazin-2-ylcarbonyl) amino] propanoyl) amino) butyl] boronic acid	Anthranilic acid.	485	2.5-12.5,	126
	2-chloro phenyl hydrazine.	560	2.5-12.5	
<b>(Ganciclovir)</b> 2-amino-1,9-[[2 - hydroxy -1-(hydroxymethyl) ethoxy] methyl]-6-H-purine-6-H-one	(PDAB) P-dimethyl amino cinnamaldehyde,	524.0	10-50,	127
	(MBTH) 3-methyl-2-benzothiazolinone hydrazone	611.8	50-250	
<b>Lisinopril</b>	<i>o</i> -phenylene diamine	399.5	2-30	128
<b>(Pramipexole dihydrochloride)</b> (S)-N <sup>6</sup> -propyl-4,5,6,7-tetrahydro-1,3-benzothiazole-2,6-diamine dihydrochloride	acetyl acetone and formaldehyde	455	5-150	129

## 3-2 Experimental

### 3-2-1 Instruments

As described in section 2-2-1.

### 3-2-2 Chemicals

As described in section 2-2-2.

### 3-2-3 Materials and reagents

\*Sodium 1, 2-Naphthoquinone-4-sulphonate (NQS) [0.5 % (m/v)]: prepared by dissolving 0.5 g of  $C_{10}H_5NaO_5S$  in 50.0 mL double distilled water and diluting to the mark in a 100 mL volumetric flask using distilled water.

\*Sodium hydroxide [0.01 M]: prepared by dissolving 0.2 g of NaOH in 100.0 mL double distilled water and diluting to the mark in a 500 mL volumetric flask.

\*Sodium tetraborate decahydrate (Borax) [0.03 M]: prepared by dissolving 0.57207 g of  $Na_2B_4O_7 \cdot 10H_2O$  in 25.0 mL double distilled water and diluting to the mark in a 50 mL volumetric flask.

\*Potassium hydroxide [0.01 M]: prepared by dissolving 0.0280 g of KOH in 25.0 mL double distilled water and diluting to the mark in a 50 mL volumetric flask.

\*Ammonium hydroxide [0.01 M]: prepared by taken 0.622 mL of concentrated  $NH_4OH$  and subsequent dilutions to the mark in a 500 mL volumetric flask with distilled water.

\*Sodium carbonate (Anhydrous) [0.01 M]: prepared by dissolving 0.0530 g of  $Na_2CO_3$  in 25.0 mL double distilled water and diluting to the mark in a 50 mL volumetric flask.

### 3-2-4 Preparation of standard drugs solutions

#### 1- Sulfamethoxazole (SMZ) stock solution ( $1000 \mu\text{g} \cdot \text{mL}^{-1}$ )

The standard solution of SMZ was prepared by dissolving accurate weighted 0.100 g of pure drug in 10 mL of 0.4 M HCl and further diluted to the mark in volumetric flask 100 mL with distilled water. Working solutions were freshly prepared by subsequent dilutions.

## **2- Sulfanilamide (SNA) stock solution (1000 $\mu\text{g}\cdot\text{mL}^{-1}$ )**

The standard solution of SNA was prepared by dissolving accurate weight 0.100 g of pure drug in 10 mL of 0.4 M HCl and further diluted to the mark in volumetric flask 100 mL with distilled water. Working solutions were freshly prepared by subsequent dilutions.

## **3- Preparation solution for the analysis of sulfamethoxazole in pharmaceutical preparations**

### **i. In tablets**

The content of 10 tablets was grinded and mixed well. A certain amount of the fine powder was accurately weighted to give an equivalent to 800 mg for tablets and the mean value of the weight of one tablet was calculated. An amount of the powder equivalent to about 0.0632 gm. was accurately weighted and transferred into 100 mL volumetric flask, about 10 mL of 0.4 M HCL was added and the solution was shaken swirled, left to stand for 5 mints and diluted to the mark in a volumetric flask 100 mL with distilled water to get 500  $\mu\text{g}\cdot\text{mL}^{-1}$  SMZ solutions. The solution was filtered by using Whatman filter paper No.41 to avoid any suspended or un-dissolved material before use, and the first portion of the filtrate was rejected. Working solutions were freshly prepared by subsequent dilutions with distilled water, and analyzed by the recommended procedure.

### **ii. In syrup**

Each 5 mL of the syrup contains (200 mg of sulfamethoxazole with 40 mg of trimethoprim). An accurately measured volume (1.25 mL) was transferred into a 100 mL volumetric flask, then added 10 mL of 0.4 M HCl swirled, left to stand for 5 mints and diluted to the mark with distilled water to get 500  $\mu\text{g}\cdot\text{mL}^{-1}$  SMZ solutions. The solution was filtered by using Whatman filter paper No.41 to avoid any suspended or un-dissolved material before use, and the first portion of the filtrate was rejected. Working solutions were freshly prepared by subsequent dilutions with distilled water, and analyzed by the recommended procedure.

### **3-2-5 Preparation of synthetic sulfanilamide drug sample**

1- To 0.02 g of the bulk drug, 0.005 g of interfering substance mixture (consisting of equal weights of each substance, namely, glucose, sucrose, lactose, starch soluble, and vanillin) was added.

2- 0.013 g of the resulted mixture was dissolved in 10 mL of 0.4 M HCl and diluted to the mark with distilled water in volumetric flask 100 mL in the same manner as used for the preparation standard drug to obtain  $100 \mu\text{g}\cdot\text{mL}^{-1}$ .

### **3-2-6 Primary experimental test**

The primary test for the condensation reaction of 200.0  $\mu\text{g}$  of SMZ and SNA separately with NQS in 10 mL volumetric flasks was done by adding 1.0 mL of 0.01M sodium hydroxide, followed by 1.0 mL 0.5% (m/v) NQS solution were added, then the mixture was shaken gently until the appearance of orange color, left to stand for 10 minutes and the content was diluted up to the mark with distilled water. The absorbance of the colored solution was measured for SMZ and SNA separately against the reagent blank and  $\lambda_{\text{max}}$  was extracted.

### **3-2-7 Optimization of experimental variables**

#### **I- Univariate method**

##### **1- Effect of different bases**

1.0 mL of aliquots standard solution containing 200.0  $\mu\text{g}$  of SMZ and SNA were transferred separately in a series of 10 mL volumetric flask. A volume of 1.0 mL of 0.01 M from different bases such as (NaOH,  $\text{Na}_2\text{B}_4\text{O}_7\cdot 10\text{H}_2\text{O}$ ,  $\text{NH}_4\text{OH}$ , KOH, and  $\text{Na}_2\text{CO}_3$ ) solution was added to each flasks, followed by 1.0 mL of 0.5 % (m/v) NQS solution was added. The mixture was then shaken gently until the appearance of orange color. Left to stand for 10 min., the contents were diluted up to the mark with distilled water. The absorbance of each solution was measured at 460.0 nm, 455.0 nm for SMZ and SNA respectively against the reagent blank.

##### **2- Effect of borax concentration**

1.0 mL of aliquots standard solution containing 200.0  $\mu\text{g}$  of SMZ and SNA were transferred in a series of 10 mL volumetric flasks. A volume

of 1.0 mL of (0.015, 0.03, 0.045, 0.060, and 0.075 M) borax solution was added to each flask, and then 1.0 mL of 0.50 % (m/v) NQS solution were added. The mixture was shaken gently until the appearance of orange color. Left to stand for 10 min., the contents were diluted up to the mark with distilled water and the absorbance of each solution was measured at 460.0 nm and 455.0 nm for SMZ and SNA respectively against the reagent blank.

### **3- Effect of NQS concentration**

1.0 mL of aliquots standard solution containing 200.0 µg of SMZ and SNA were transferred separately in a series of 10 mL volumetric flasks. Then 1.0 mL of 0.03 M borax solution was added to each flask, followed by 1.0 mL of (0.25, 0.50, 0.75, 1.00 and 1.25 % m/v) NQS solutions, the contents was shaken gently until the appearance of orange color. Left to stand for 10 min., the mixture was diluted up to the mark with distilled water, and the absorbance of each solution was measured at 460.0 nm and 455.0 nm for SMZ and SNA respectively against the reagent blank.

### **4- Effect of reaction time**

1.0 mL of aliquots standard solution containing 200.0 µg of SMZ and SNA were transferred separately in a series of 10 mL volumetric flasks. A volume of 1.0 mL of 0.03 M borax solution was added to each flask, followed by addition of 1.0 mL of 0.75 % (m/v) NQS for SMZ and 1.0 mL of 1.0 % (m/v) NQS for SNA solutions respectively. The mixture was shaken gently until the appearance of orange color. After (1-10 min.), the contents were diluted up to the mark with distilled water. The absorbance of each solution was measured at 460.0 nm and 455.0 nm for SMZ and SNA respectively against the reagent blank.

## **II- Multivariate method**

### **Experimental design and statistical analysis**

To find the optimal conditions for the estimation of sulfamethoxazole and sulfanilamide via condensation reaction with NQS, a central composite design was used.

The central composite design (CCD) with a quadratic model was employed. Three independent variables namely reagent concentration ( $X_1$ ), borax concentration ( $X_2$ ), reaction time ( $X_3$ ) was chosen. Each independent variable had three levels which were -1, 0 and +1.

A total 20 different combinations (including six replicates of center point each signified the coded value 0) were chosen in random order according to a CCD configuration for three factors. The coded values of independent variables were found from equations:

For sulfamethoxazole:

$$X_1 = (X_1 - 0.750) / 0.500$$

$$X_2 = (X_2 - 0.045) / 0.030$$

$$X_3 = (X_3 - 5.500) / 4.500$$

For sulfanilamide:

$$X_1 = (X_1 - 0.750) / 0.500$$

$$X_2 = (X_2 - 0.045) / 0.030$$

$$X_3 = (X_3 - 5.500) / 4.500$$

and are given in Table 3-2 for SMZ and SNA.

**Table 3-2:** Un coded and coded levels of the independent variables for the determination of SMZ and SNA.

<i>Drug</i>	<i>Independent variable</i>	<i>Coded unit</i>		
		<i>-1</i>	<i>0</i>	<i>1</i>
<b>SMZ</b>	Reagent conc. (%)	0.250	0.750	1.250
	Borax conc. (M)	0.015	0.045	0.075
	Reaction time (min.)	1.000	5.500	10.000
<b>SNA</b>	Reagent conc. (%)	0.250	0.750	1.250
	Borax conc. (M)	0.015	0.045	0.075
	Reaction time (min.)	1.000	5.500	10.000

Tables 3-3 and 3-4 list results of the study made according to the central composite design and the experimental points used according to the design for SMZ and SNA respectively.

**Table 3-3:** The central composite design with three independent variables (un code variables) for SMZ.

<i>Exp. No.</i>	<i>Reagent conc. (% m/v)</i>	<i>Borax conc. (M)</i>	<i>Reaction time (min.)</i>
1	0.750	0.045	10.0
2	1.250	0.045	5.5
3	0.750	0.045	5.5
4	0.750	0.045	5.5
5	1.250	0.075	10.0
6	0.250	0.045	5.5
7	0.750	0.075	5.5
8	0.750	0.045	1.0
9	0.750	0.045	5.5
10	0.750	0.045	5.5
11	0.250	0.075	1.0
12	1.250	0.075	1.0
13	0.250	0.015	10.0
14	0.750	0.045	5.5
15	0.250	0.015	1.0
16	1.250	0.015	10.0
17	0.750	0.045	5.5
18	0.250	0.075	10.0
19	0.750	0.015	5.5
20	1.250	0.015	1.0



**Table3-4:** The central composite design with three independent variables (un code variables) for SNA.

<i>Exp. No.</i>	<i>Reagent conc. (% m/v)</i>	<i>Borax conc. (M)</i>	<i>Reaction time (min.)</i>
1	0.750	0.045	10.0
2	1.250	0.045	5.5
3	0.750	0.045	5.5
4	0.750	0.045	5.5
5	1.250	0.075	10.0
6	0.250	0.045	5.5
7	0.750	0.075	5.5
8	0.750	0.045	1.0
9	0.750	0.045	5.5
10	0.750	0.045	5.5
11	0.250	0.075	1.0
12	1.250	0.075	1.0
13	0.250	0.015	10.0
14	0.750	0.045	5.5
15	0.250	0.015	1.0
16	1.250	0.015	10.0
17	0.750	0.045	5.5
18	0.250	0.075	10.0
19	0.750	0.015	5.5
20	1.250	0.015	1.0

### 3-2-8 General recommended procedures

#### 1- Assay procedure for determination of sulfamethoxazole

##### I. Univariate method

Aliquots of the standard solution ( $1000 \mu\text{g.mL}^{-1}$ ) containing (50-500)  $\mu\text{g}$  of sulfamethoxazole were transferred into a series of 10 mL volumetric flasks. A volume of 1.0 mL of 0.03 M borax solution was added to each flask, followed by 1.0 mL of 0.75 % (m/v) NQS solution was added, then the mixture was shaken gently until the appearance of orange color. The solution was left to stand for 3.0 min., and the contents were diluted up to

the mark with distilled water. The absorbance of each solution was measured at 460.0 nm against the reagent blank.

## **II. Design of experiment method**

Aliquots of the standard solution ( $1000 \mu\text{g.mL}^{-1}$ ) containing (50-500)  $\mu\text{g}$  of sulfamethoxazole were transferred into a series of 10 mL volumetric flasks. A volume of 1.0 mL of 0.05 M borax solution was added to each flask, followed by 1.0 mL of 0.90 % (m/v) NQS solution was added, then the mixture was shaken gently until the appearance of orange color, left to stand for 5.717 min., and the contents were diluted up to the mark with distilled water. The absorbance of each solution was measured at 460.0 nm against the reagent blank.

## **2- Assay procedure for determination of sulfanilamide**

### **I. Univariate method**

Aliquots of the standard solution ( $1000 \mu\text{g.mL}^{-1}$ ) containing (50-300)  $\mu\text{g}$  of sulfanilamide were transferred into a series of 10 mL volumetric flasks. A volume of 1.0 mL of 0.03 M borax solution was added to each flask, followed by 1.0 mL of 1.0 % (m/v) NQS solutions were added, and then the mixture was shaken gently until the appearance of orange color. Left to stand for 3.0 min., and the contents were diluted up to the mark with distilled water. The absorbance of each solution was measured at 455.0 nm against the reagent blank.

### **II. Design of experiment method**

Aliquots of the standard solution ( $1000 \mu\text{g.mL}^{-1}$ ) containing (5.0-30.0)  $\mu\text{g}$  of sulfanilamide were transferred into a series of 10 mL volumetric flasks. A volume of 1.0 mL of 0.036 M borax solution was added to each flask, followed by 1.0 mL of 0.975 % (m/v) NQS solutions were added, and then the mixture was shaken gently until the appearance of orange color, then left to stand for 22.0 sec., and the contents were diluted up to the mark with distilled water. The absorbance of each solution was measured at 455.0 nm against the reagent blank.

### **3-2-9 Procedure for synthetic sulfanilamide drug sample**

Aliquots of the synthetic sample ( $1000 \mu\text{g.mL}^{-1}$ ) containing (50, 100, 200)  $\mu\text{g}$  of sulfanilamide were transferred into a series of 10 mL volumetric flasks. A volume of 1.0 mL of 0.036 M borax solution was added to each flask, followed by 1.0 mL of 0.975 % (m/v) NQS solutions were added, and then the mixture was shaken gently until the appearance of orange color. Left to stand for 22.0 sec., and the contents were diluted up to the mark with distilled water. The absorbance of each solution was measured at 455.0 nm against the reagent blank.

### **3-2-10 Determination of SMZ drug in pharmaceutical preparation by standard additions method (SAM)**

- 1- Preparation of SMZ stock solution  $1000 \mu\text{g.mL}^{-1}$  according to the method of preparation which is previously mentioned.
- 2- Prepare solution of commercial pharmaceutical preparation (syrup or tablets) concentration of  $500 \mu\text{g.mL}^{-1}$  according to the method of preparation which is previously mentioned.
- 3- Preparation of (7) solutions in 10 mL volumetric flask for measurements by adding 0.1, 0.2, 0.3 mL of solution commercial pharmaceutical preparation (syrup or tablets) from ( $500 \mu\text{g.mL}^{-1}$ ) commercial pharmaceutical preparation, and added (0, 0.05, 0.10, 0.15, 0.20, 0.25, and 0.30 mL) of ( $1000 \mu\text{g.mL}^{-1}$ ) standard solution of SMZ drug. A volume of 1.0 mL of 0.05 M borax solution was added to each flask, followed by 1.0 mL of 0.90 % (m/v) NQS solutions were added, and then the mixture was shaken gently until the appearance of orange color. Left to stand for 5.717 min., and the contents were diluted up to the mark with distilled water. The absorbance of each solution was measured at 460.0 nm against the reagent blank.

## **3-3 Results and discussion**

### **I- The determination of sulfamethoxazole**

#### **3-3-1 Absorption spectra**

According to the procedure, the absorption spectrum of the product produced by the condensation reaction between SMZ and NQS was recorded, and the maximum absorption wavelength of product is at 460.0

nm against reagent blank under the primary test and optimization conditions for univariate and DOE methods as can be seen in Figure 3-2. And the spectrum of reagent blank against D.W. in Figure 3-1.

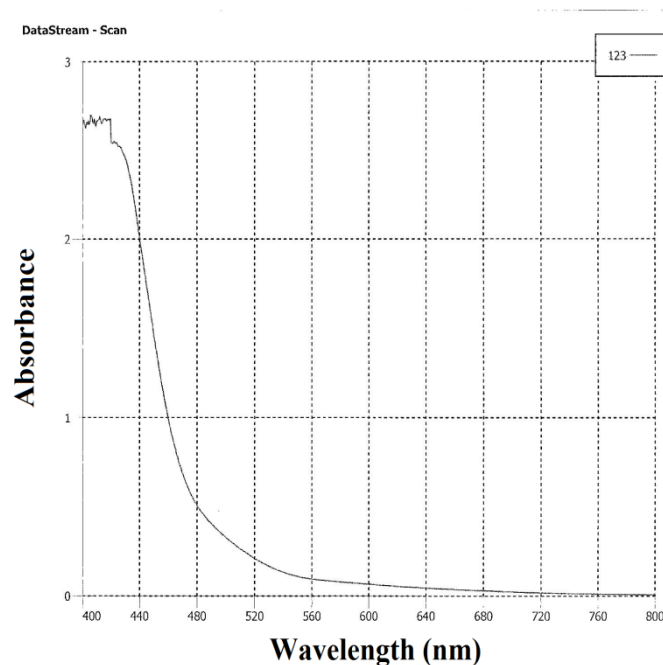


**Figure 3-1:** Absorption spectrum of blank solution against (D.W.) under the primary test and optimization condition.

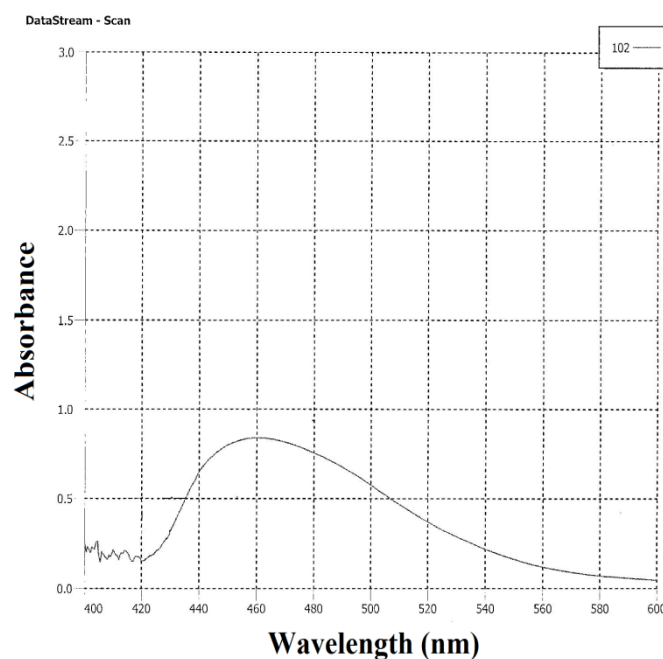


**Figure 3-2:** Absorption spectrum of (30 µg.mL<sup>-1</sup>) SMZ against the reagent blank under the primary test and optimization condition.

### 3-3-2 Optimization of reaction variables

#### I- Univariate method

For the development of maximum color intensity of dye, various experimental parameters via (effect of different bases, effect of borax concentration, effect of NQS concentration, and effect of reaction time) which influence the formation of the colored dye were necessary optimized. The optimization was done by studying one parameter while keeping the others fixed.

#### 1- Effect of different bases

1.0 mL of aliquots standard solution containing 200.0  $\mu\text{g}$  of SMZ were transferred in a series of 10 mL volumetric flasks. A volume of 1.0 mL of 0.01 M from different bases such as (NaOH,  $\text{Na}_2\text{B}_4\text{O}_7 \cdot 10\text{H}_2\text{O}$ ,  $\text{NH}_4\text{OH}$ , KOH, and  $\text{Na}_2\text{CO}_3$ ) was added to each flask followed by 1.0 mL of 0.5 % (m/v) NQS solution were added, then the mixture was shaken gently until the appearance of orange color. Left to stand for 10 min., before dilution to the mark with (D.W.), the absorbance of each solution was measured at 460.0 nm against the reagent blank. Borax was the most suitable alkaline medium for a maximum absorbance for the method and was used in all subsequent experiments (Table 3-5).

**Table 3-5:** Effect of different bases on condensation reaction.

<i>Alkaline solution (0.01M)</i>	<i>Absorbance</i>
NaOH	0.285
$\text{Na}_2\text{B}_4\text{O}_7 \cdot 10\text{H}_2\text{O}$	0.311
$\text{NH}_4\text{OH}$	0.246
KOH	0.238
$\text{Na}_2\text{CO}_3$	0.163

#### 2- Effect of borax concentration

1.0 mL of aliquots standard solution containing 200.0  $\mu\text{g}$  of SMZ was transferred in a series of 10 mL volumetric flask. A volume of 1.0 mL of (0.015, 0.030, 0.045, 0.060, 0.075 M) borax solution was added to each flasks, followed by 1.0 mL of 0.50 % (m/v) NQS solutions were added, then the mixture was shaken gently until the appearance of orange color. Left to stand for 10 min., and the contents were diluted up to the mark

with distilled water. The absorbance of each solution was measured at 460.0 nm against the reagent blank. It was found that 1.0 mL of 0.03 M borax solution gives a maximum absorbance for the method and was used in all subsequent experiments as shown in Figure 3-3.

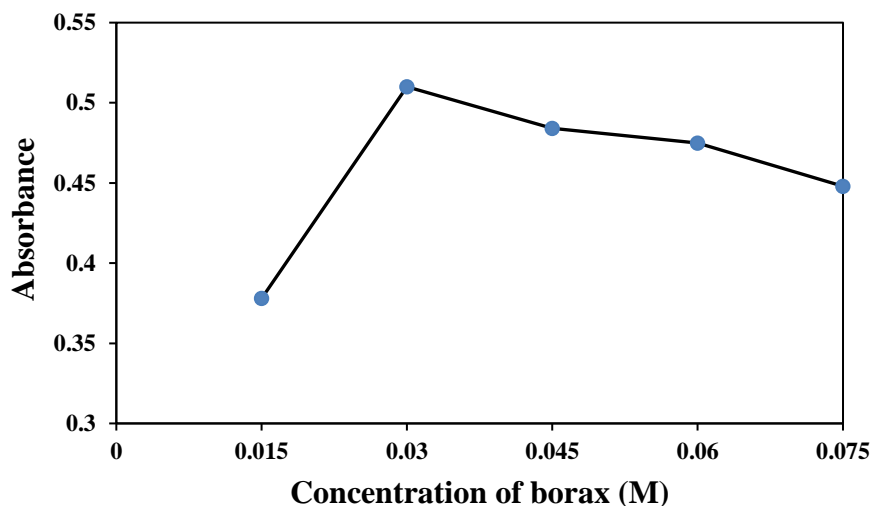


**Figure 3-3:** Effect of 1.0 mL of borax concentration on the color development of dye on the determination of ( $20.0 \mu\text{g.mL}^{-1}$ ) SMZ.

### 3- Effect of NQS concentration

1.0 mL of aliquots standard solution containing  $200.0 \mu\text{g}$  of SMZ was transferred in a series of 10 mL volumetric flasks. A volume of 1.0 mL of 0.03 M borax solution was added to each flask, followed by 1.0 mL of (0.25, 0.50, 0.75, 1.00 and 1.25 % m/v) NQS solutions were added, then the mixture was shaken gently until the appearance of orange color. Left to stand for 10 min., and the contents were diluted up to the mark with distilled water. The absorbance of each solution was measured at 460.0 nm against the reagent blank. It was found that 1.0 mL of 0.75 % (m/v) gives a maximum absorbance for the method and was used in all subsequent experiments as shown in Figure 3-4.

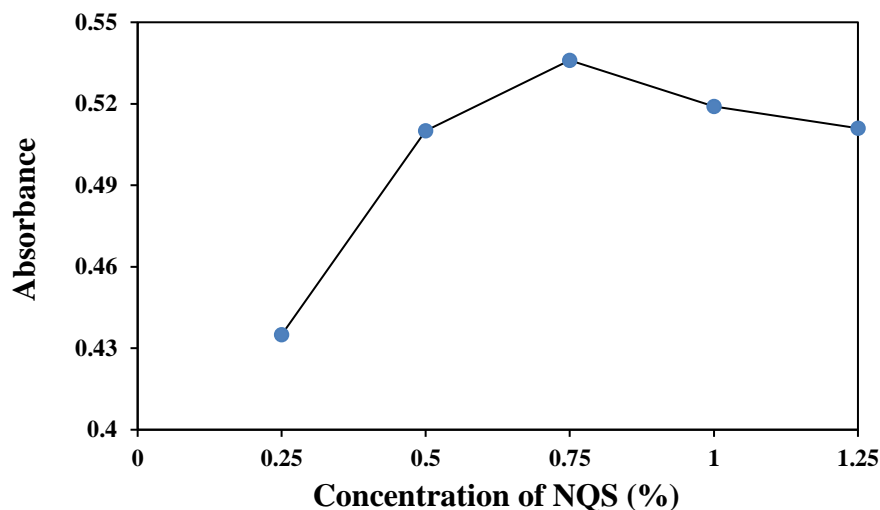


**Figure 3-4:** Effect of 1.0 mL of NQS concentration on the color development of dye on the determination of ( $20.0 \mu\text{g}\cdot\text{mL}^{-1}$ ) SMZ.

#### 4- Effect of reaction time

1.0 mL of aliquots of standard solution containing  $200.0 \mu\text{g}$  of SMZ was transferred in a series of 10 mL volumetric flasks. A volume of 1.0 mL of 0.03 M borax solution was added to each flask, followed by 1.0 mL of 0.75 % (m/v) NQS solutions, and then the mixture were shaken gently until the appearance of orange color. Left to stand (1-10 min.) and the contents were diluted up to the mark with distilled water. The absorbance of each solution was measured at 460.0 nm against the reagent blank. It was found that 3.0 min. is required for a maximum absorbance for the reaction and was used in all subsequent experiments as shown in Table 3-6.

**Table 3-6:** Effect of coupling reaction time.

<i>Time (min.)</i>	<i>Absorption</i>
1	0.510
2	0.531
3	0.545
5	0.537
8	0.539
10	0.533
60	0.538

## II- Design of experiment method

Optimum experimental conditions have been studied using multivariate experimental design. The most three critical variables (reagent concentration, borax concentration, and reaction time) were examined using a central composite design; three levels of each selected variable were required to test for the curvature of the response. The values of these variables were chosen within specified boundaries for each at which they affected the measured absorption of the colored products as shown in Table (3-2).

The number of experiments required to investigate the previously noted three parameters at three levels would be 27 ( $3^3$ ). However, this was reduced to 20 using a central experimental design. Response surface model was applied to study the effect of the three variables, (reagent concentration, borax concentration, and reaction time) on the absorbance of SMZ-NQS complex and generate an optimal and robust response surface. A second order polynomial linear-quadratic equation was used to express the absorption as a function of independent variables namely, reagent concentration, borax concentration, and reaction time.

$$\text{Absorbance} = \beta_0 + \beta_1^* (\text{Reg. conc.}) + \beta_2^* (\text{Borax conc.}) + \beta_3^* (\text{Reaction time}) + \beta_4^* (\text{Reg. conc.})^2 + \beta_5^* (\text{Borax conc.})^2 + \beta_6^* (\text{Reaction time})^2.$$

Table 3-7 shows the study of optimum conditions according to central composite design and the experimental points used according to the design.



**Table 3-7:** The central composite design with three independent variables (un coded variables) and their experimental absorption values of (30  $\mu\text{g.mL}^{-1}$ ) SMZ-NQS complex.

<i>Exp. No.</i>	<i>Reagent conc. (% m/v)</i>	<i>Borax conc. (M)</i>	<i>Reaction time (min.)</i>	<i>Abs.</i>
1	0.750	0.045	10.0	0.834
2	1.250	0.045	5.5	0.845
3	0.750	0.045	5.5	0.835
4	0.750	0.045	5.5	0.835
5	1.250	0.075	10.0	0.870
6	0.250	0.045	5.5	0.684
7	0.750	0.075	5.5	0.827
8	0.750	0.045	1.0	0.862
9	0.750	0.045	5.5	0.835
10	0.750	0.045	5.5	0.835
11	0.250	0.075	1.0	0.444
12	1.250	0.075	1.0	0.860
13	0.250	0.015	10.0	0.728
14	0.750	0.045	5.5	0.835
15	0.250	0.015	1.0	0.739
16	1.250	0.015	10.0	0.504
17	0.750	0.045	5.5	0.835
18	0.250	0.075	10.0	0.494
19	0.750	0.015	5.5	0.720
20	1.250	0.015	1.0	0.546

The coefficients of the response surface equation were determined by **STATISTICA 10.0** software (**Stat. Soft. Inc., release 2011**), the results are listed in Table 3-8.

Optimum conditions that were developed from central composite design for the determination of sulfamethoxazole via condensation reaction with NQS were calculated mathematically and the results are 1.0 mL of 0.90 % (m/v) for the reagent concentration, 1.0 mL of 0.050 M for borax concentration and 5.717 minute for the reaction time. Figures 3-5, 3-6, and 3-7 give the imagine of response surface model if one of the three variables is remained constant.

**Table 3-8:** Regression coefficients, P (or probability for absorption of SMZ- NQS).

<i>Variable</i>	<i>Regression coefficient</i>	<i>Standard error of coefficient</i>	<i>t-value</i>	<i>P</i>
Constant	0.3028	0.1461	2.0731	0.0586
Reg. conc.	0.6783	0.4453	1.5234	0.1516
(Reg. conc.) <sup>2</sup>	-0.3807	0.2924	-1.3021	0.2155
Borax conc.	9.4782	7.4209	1.2772	0.2239
(Borax conc.) <sup>2</sup>	-95.7576	81.2231	-1.1789	0.2595
Reaction time	0.0059	0.0406	0.1448	0.8871
(Reaction time) <sup>2</sup>	-0.0006	0.0036	-0.1598	0.8755

Fitted Surface; Variable: Var4  
3 factors, 1 Blocks, 20 Runs

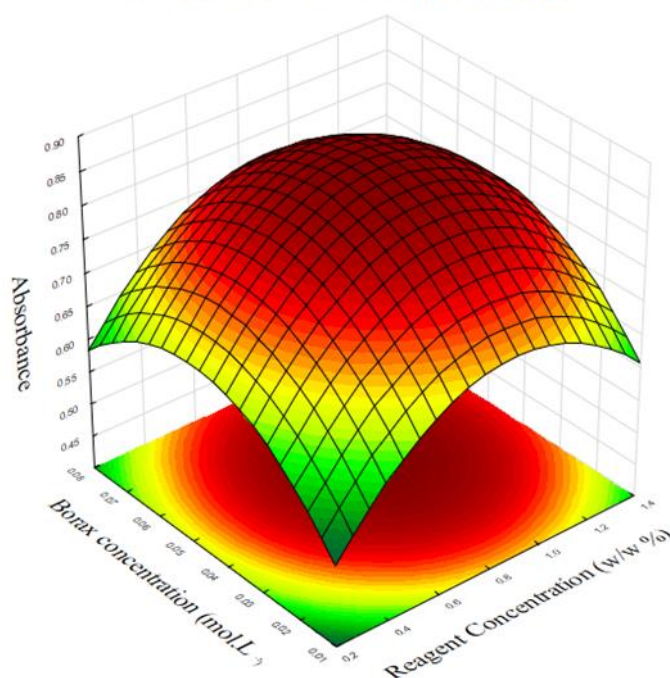


**Figure 3-5:** The response surface for the absorbance of SMZ-NQS complex as a function of reagent concentration and borax concentration (at constant optimum value of reaction time, 5.717 min.).

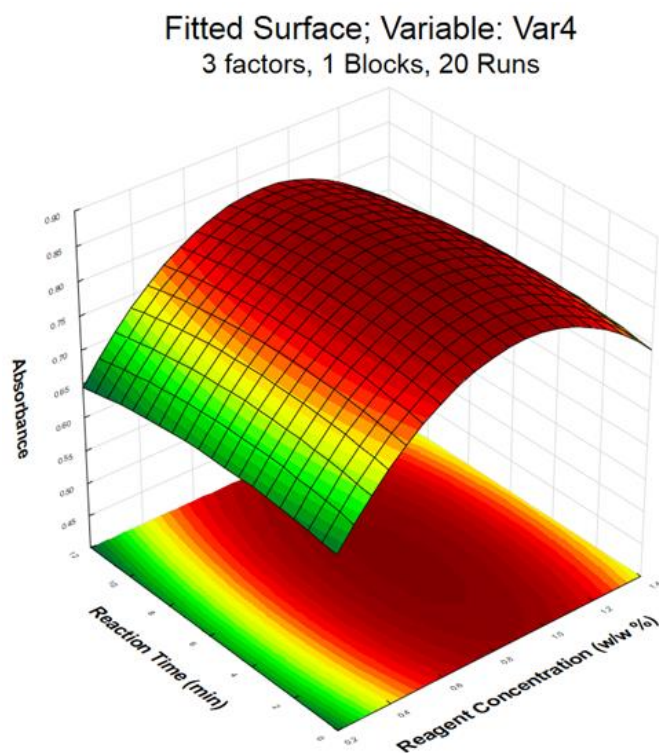


**Figure 3-6:** The response surface for the absorbance of SMZ-NQS complex as a function of reagent concentration and reaction time (at constant optimum value of borax concentration, 0.05 M).

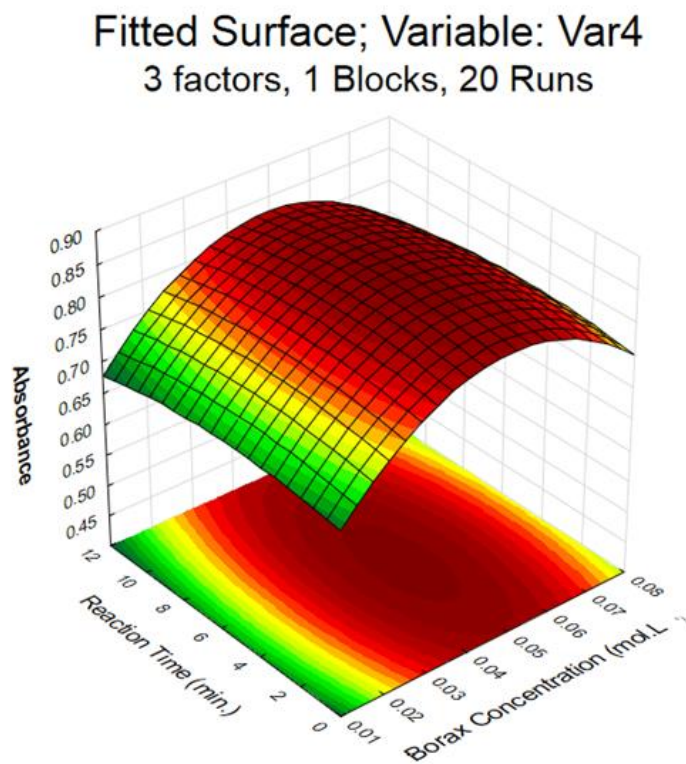


**Figure 3-7:** The response surface for the absorbance of SMZ-NQS complex as a function of borax concentration and reaction time (at constant optimum value of reagent concentration, 0.9 % m/v).

### 3-3-3 Calibration curves and analytical data

#### I- Univariate method

In order to test whether the colored species formed in univariate method adhere to Beer's law, the absorbance at appropriate wavelengths of a set of solutions containing varying amounts of SMZ and specified amounts of reagents were recorded against the corresponding reagent blanks.

The Beer's law plots were recorded graphically (Figure 3-8). A linear correlation was found between absorbance at  $\lambda_{\max}$  and concentration ranges (5-50)  $\mu\text{g.mL}^{-1}$  of SMZ. Sensitivity parameters such as molar absorptivity, correlation coefficient ( $r$ ), Sandell's sensitivity, detection limit are presented in Table 3-9.

**Table 3-9:** Optical characteristics and statistical data for the determination of SMZ by univariate method.

<i>Parameter</i>	<i>Value</i>
$\lambda_{\max}$ (nm)	460.0
Color	Orange
Linearity range ( $\mu\text{g.mL}^{-1}$ )	5.0-50.0
Regression equation	$Y=0.0268[\text{SMZ. } \mu\text{g.mL}^{-1}]+0.0152$
Calibration sensitivity ( $\text{mL. } \mu\text{g}^{-1}$ )	0.0268
Correlation coefficient ( $r$ )%	99.98
Correlation of linearity ( $r^2$ )%	99.97
Molar absorptivity ( $\text{L. mol}^{-1}.\text{cm}^{-1}$ )	$\epsilon =6.7878 \times 10^4$
Sandell's sensitivity ( $\mu\text{g.cm}^{-2}$ )	3.7314
Detection limit ( $\mu\text{g.mL}^{-1}$ )	0.3755
Quantification limit ( $\mu\text{g.mL}^{-1}$ )	1.1380

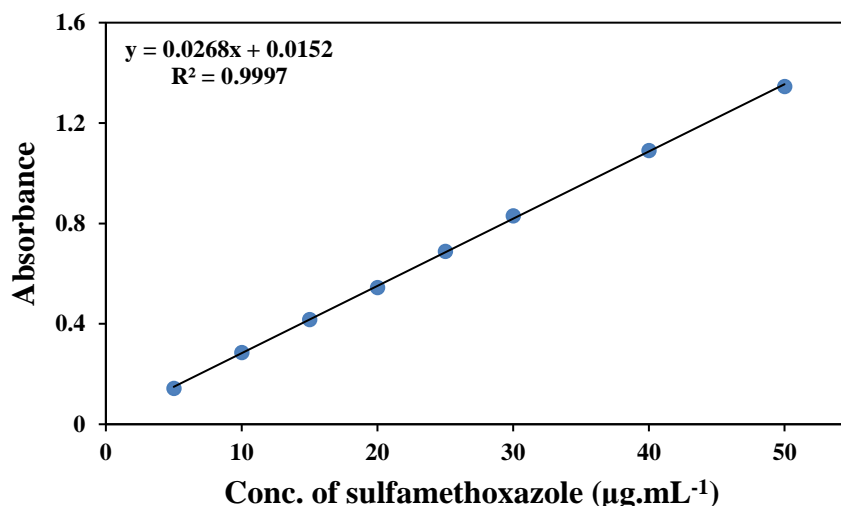


**Figure 3-8:** Calibration curve for the determination of SMZ by univariate optimal condition.

## II- Design of experiment method

The optical characteristics such as maximum absorption, Beer's law limits, molar absorptivity and Sandell's sensitivity for the proposed method are summarized in Table 3-10 and Figure 3-9. Condensation reaction of sulfamethoxazole with NQS in an alkaline medium to form orange color product represented in Scheme (3-2).

**Table 3-10:** Optical characteristics and statistical data for the determination of SMZ by DOE method.

<i>Parameter</i>	<i>Value</i>
$\lambda_{\max}$ (nm)	460.0
Color	Orange
Linearity range ( $\mu\text{g.mL}^{-1}$ )	5.0-50.0
Regression equation	$Y=0.0280[\text{SMZ. } \mu\text{g.mL}^{-1}]+0.0165$
Calibration sensitivity ( $\text{mL. } \mu\text{g}^{-1}$ )	0.0280
Correlation coefficient (r)%	99.98
Correlation of linearity ( $r^2$ )%	99.97
Molar absorptivity ( $\text{L. mol}^{-1}.\text{cm}^{-1}$ )	$\epsilon =7.0918 \times 10^4$
Sandell's sensitivity ( $\mu\text{g.cm}^{-2}$ )	3.5714
Detection limit ( $\mu\text{g.mL}^{-1}$ )	0.3594
Quantification limit ( $\mu\text{g.mL}^{-1}$ )	1.0893

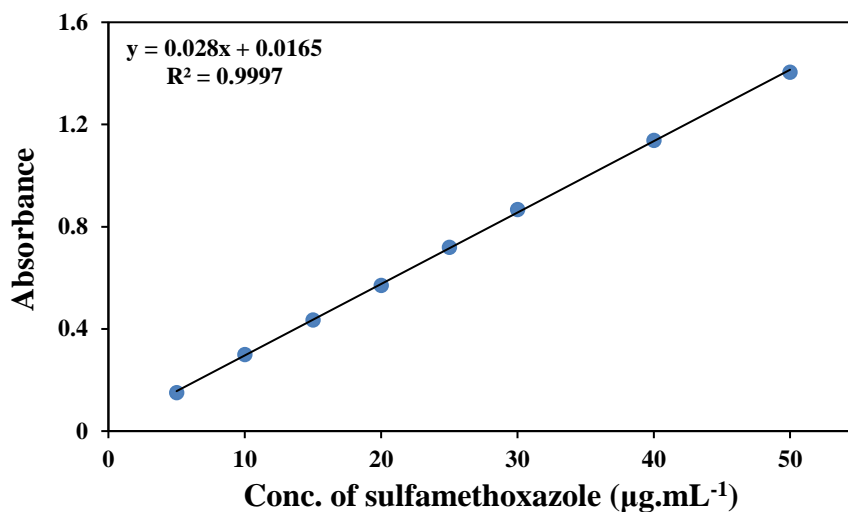
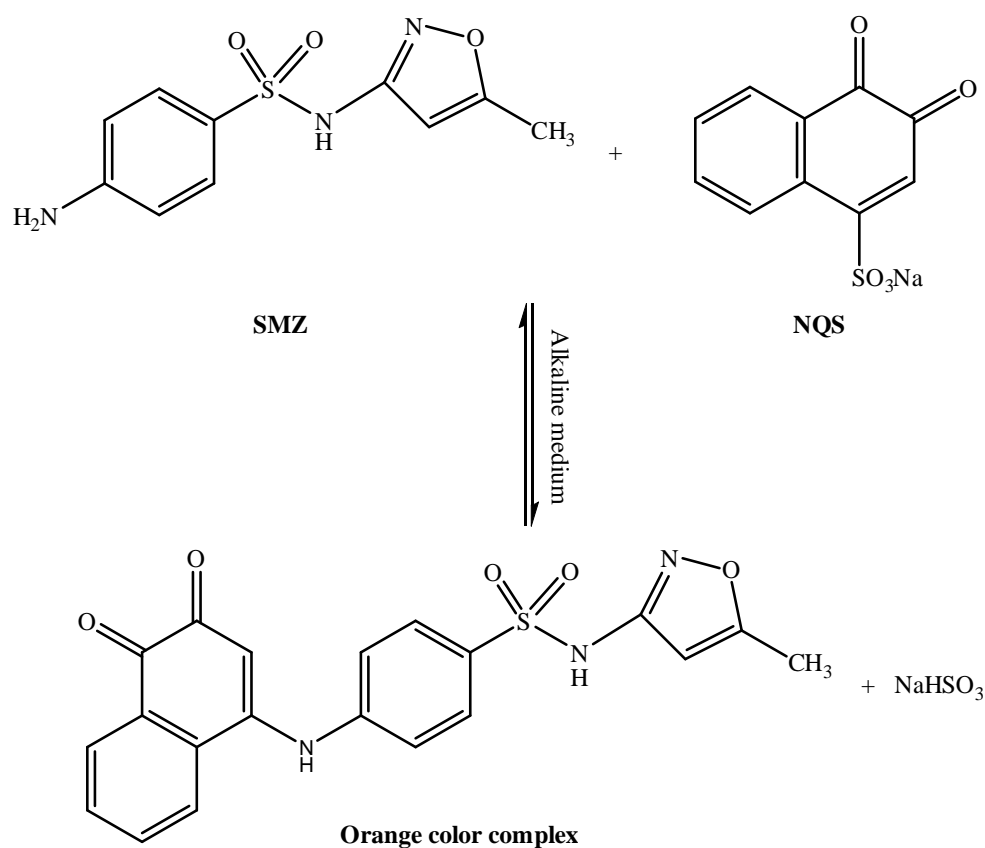


**Figure 3-9:** Calibration curve for the determination of SMZ by DOE optimal condition.



**Scheme 3-2:** The reaction mechanism for the condensation reaction between SMZ and NQS.

**3-3-4 Precision and accuracy**

Accuracy of the method was done by relative error % and precision was evaluated by coefficient of variation (C.V) %. Three different concentration levels of SMZ were analyzed in five replicates.

Lower values of relative error and coefficient of variation signifies the accuracy and precision of the method. The results of accuracy and precision for univariate and DOE are listed in Table 3-11.

**Table 3-11:** Evaluation of accuracy and precision for the determination of SMZ by proposed methods.

	<i>Conc. of SMZ (<math>\mu\text{g.mL}^{-1}</math>)</i>		<i>Relative Error %</i>	<i>C.V* %</i>
	<i>Taken</i>	<i>Found*</i>		
<b>For univariate</b>	10.0	10.022	0.220	1.377
	20.0	19.746	-1.270	1.026
	30.0	30.119	0.396	0.692
<b>For DOE</b>	10.0	10.039	0.388	1.718
	20.0	19.953	-0.234	0.710
	30.0	30.139	0.462	0.528

\*Average of five determinations.

**3-3-5 Interference study**

In pharmaceutical analysis, it is important to test the selectivity towards the excipients added to the pharmaceutical preparations. Commonly encountered excipients such as (vanillin, glucose, lactose, starch, and sucrose) did not interfere in the determination of SMZ and did not have an effect on the reaction between the SMZ and NQS. 20.0  $\mu\text{g.mL}^{-1}$  of SMZ was analyzed and design of experiment method was used for analyzing (Table 3-12).

**Table 3-12:** Percent recovery for 20.0  $\mu\text{g.mL}^{-1}$  of sulfamethoxazole in the presence of different concentration of excipients.

<i>Excipients</i>	<i>Concentration</i> ( $\mu\text{g.mL}^{-1}$ )	<i>Sulfamethoxazole conc. taken</i> (20 $\mu\text{g.mL}^{-1}$ )	
		<i>Conc. Found*</i> ( $\mu\text{g.mL}^{-1}$ )	<i>Recovery*</i> %
Vanillin	1000	20.102	100.51
Glucose		20.132	100.66
Lactose		19.874	99.37
Starch		20.184	100.92
Sucrose		20.151	100.75

\*Average of three determinations.

### 3-3-6 Application in pharmaceutical preparation by standard additions method (SAM)

Standard additions technique followed to check the validity of the proposed method has given good recoveries of the drug in pharmaceutical preparations suggesting a noninterference from pharmaceutical preparations. Hence, this method can be recommended for adoption in routine analysis of SMZ in quality control laboratories. The procedure is found in 3-2-10.

Table 3-13 shows the result of recovery and coefficient of variation (C.V) for the standard additions method. Figures 3-10 to 3-17 show the plot of determination of SMZ in syrup and tablet by standard additions method.

**Table 3-13:** Application of the proposed method to the SMZ concentration measurements in pharmaceutical preparation by (SAM).

<i>Sample</i>	<i>Conc. taken</i> ( $\mu\text{g.mL}^{-1}$ )	<i>Conc.* found</i> ( $\mu\text{g.mL}^{-1}$ )	<i>Recovery*</i> %	<i>C.V*</i> %
<b>Bactrim tablet</b> (Roche-France)	500.00	504.74	100.95	0.093
<b>Bactrim syrup</b> (Roche-France)	500.00	504.70	100.94	0.109
<b>Methoprim tablet</b> (NDI-Iraq)	500.00	510.68	102.136	0.243
<b>Cotrim syrup</b> (Asia-Syria)	500.00	506.40	101.28	0.100

\*Average of three determinations.



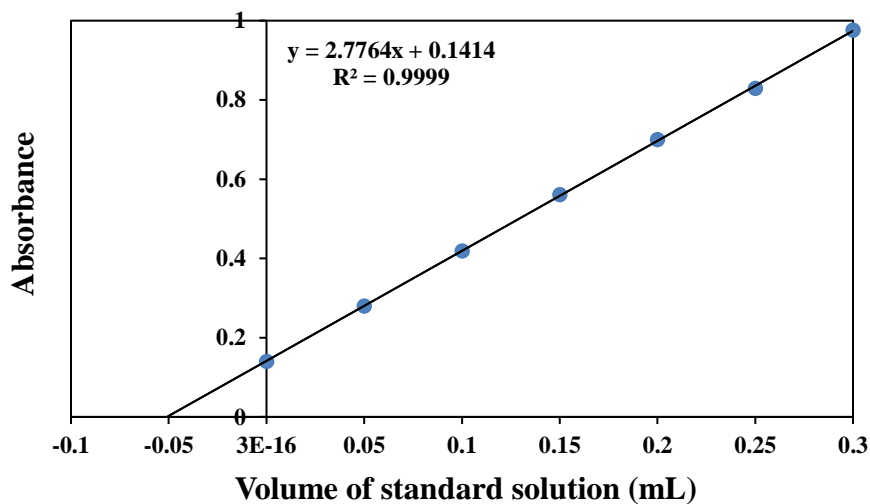


**Figure 3-10:** Determination of SMZ in pharmaceutical preparation (Bactrim syrup) sample by standard additions method, (level one 0.1 mL from  $500 \mu\text{g}\cdot\text{mL}^{-1}$ )

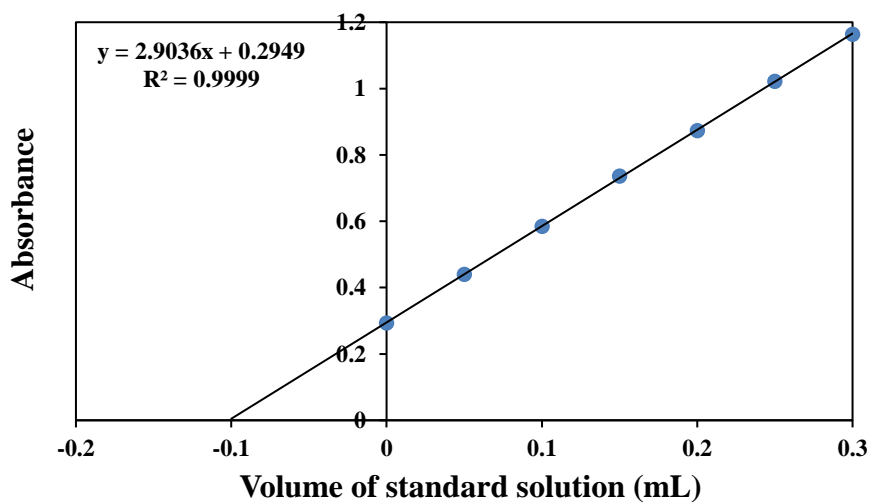


**Figure 3-11:** Determination of SMZ in pharmaceutical preparation (Bactrim syrup) sample by standard additions method, (level two 0.2 mL from  $500 \mu\text{g}\cdot\text{mL}^{-1}$ )

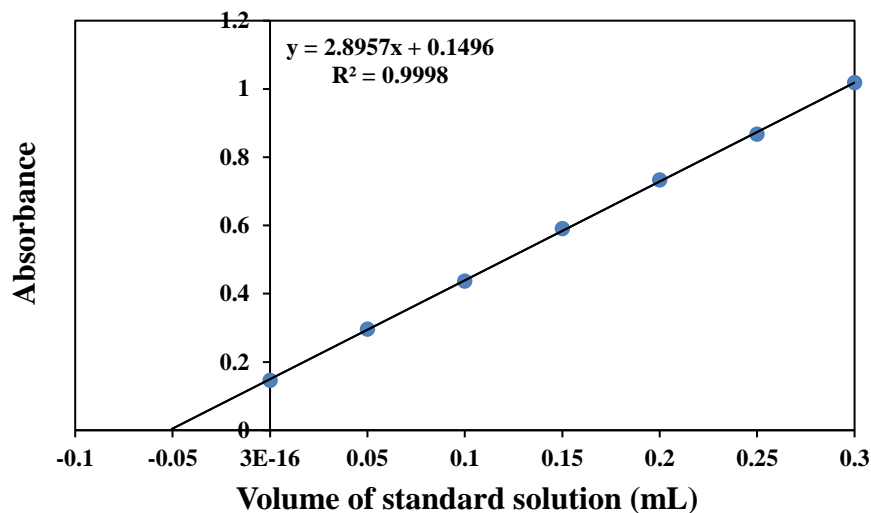


**Figure 3-12:** Determination of SMZ in pharmaceutical preparation (Bactrim tablet) sample by standard additions method, (level one 0.1 mL from  $500 \mu\text{g.mL}^{-1}$ )

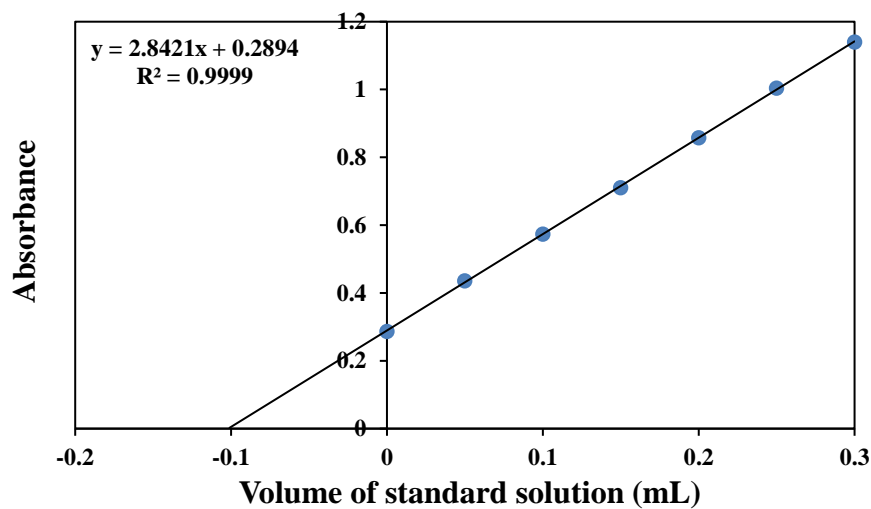


**Figure 3-13:** Determination of SMZ in pharmaceutical preparation (Bactrim tablet) sample by standard additions method, (level two 0.2 mL from  $500 \mu\text{g.mL}^{-1}$ )

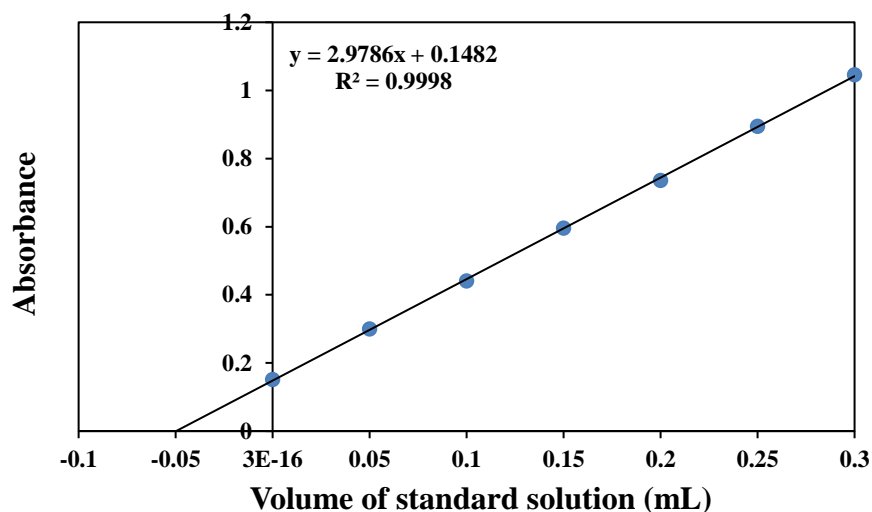


**Figure 3-14:** Determination of SMZ in pharmaceutical preparation (Cotrim syrup) sample by standard additions method, (level one 0.1 mL from 500  $\mu\text{g}\cdot\text{mL}^{-1}$ )

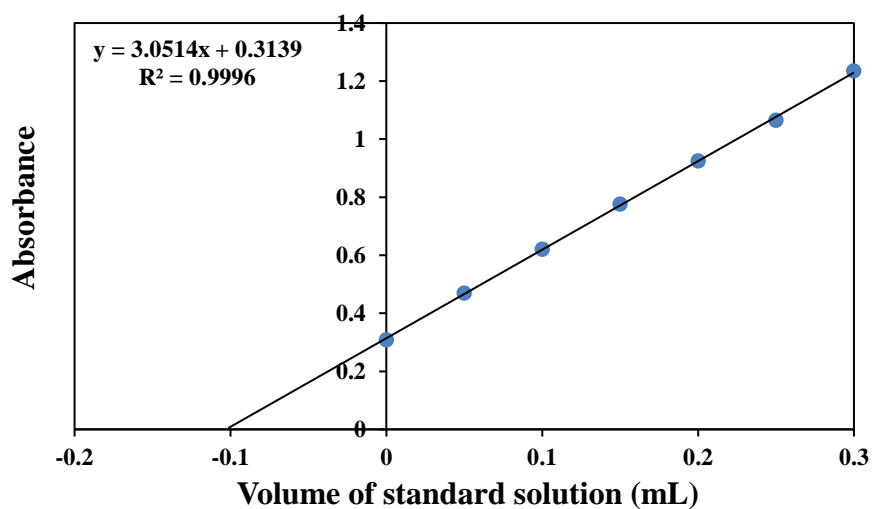


**Figure 3-15:** Determination of SMZ in pharmaceutical preparation (Cotrim syrup) sample by standard additions method, (level two 0.2 mL from 500  $\mu\text{g}\cdot\text{mL}^{-1}$ )

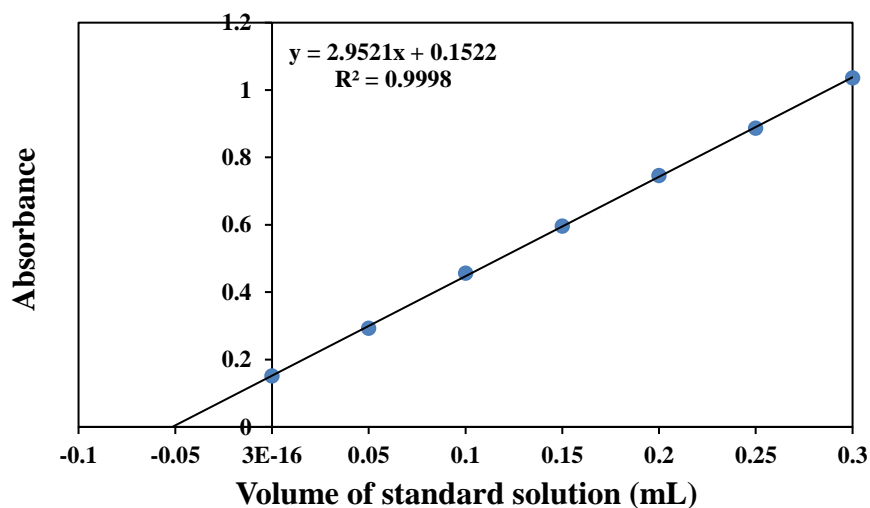


**Figure 3-16:** Determination of SMZ in pharmaceutical preparation (Methoprim tablet) sample by standard additions method, (level one 0.1 mL from  $500 \mu\text{g}\cdot\text{mL}^{-1}$ )

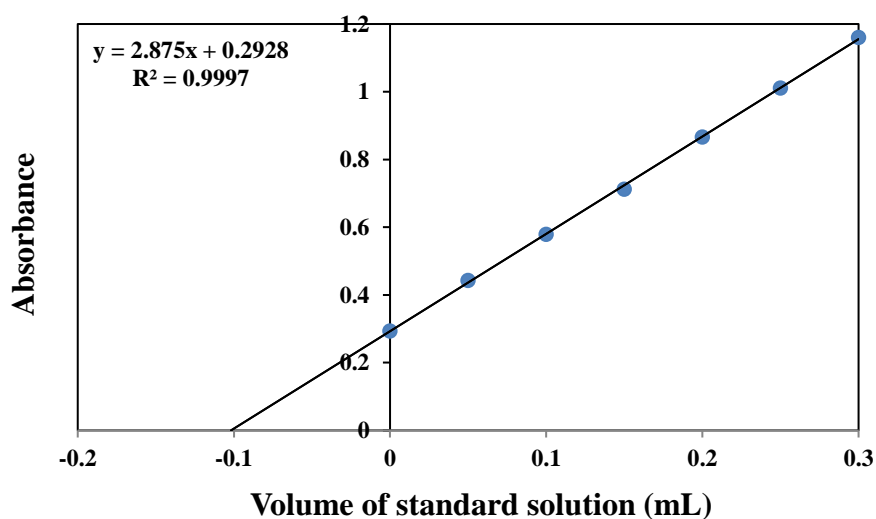


**Figure 3-17:** Determination of SMZ in pharmaceutical preparation (Methoprim tablet) sample by standard additions method, (level two 0.2 mL from  $500 \mu\text{g}\cdot\text{mL}^{-1}$ )

## II- The Determination of sulfanilamide

### 3-3-7 Absorption spectra

The reaction of sulfanilamide with NQS yield orange color dye complex showing the maximum absorption at 455.0 nm against reagent blank in Figure (3-19) and the absorbance of reagent blank against (D.W.) in Figure (3-18).

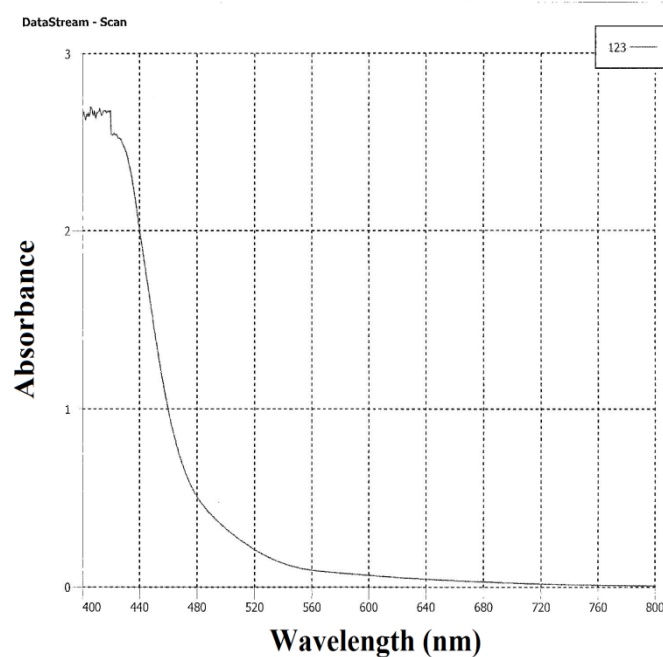


**Figure 3-18:** Absorption spectrum of blank solution against (D.W.) under the primary test and optimization condition.

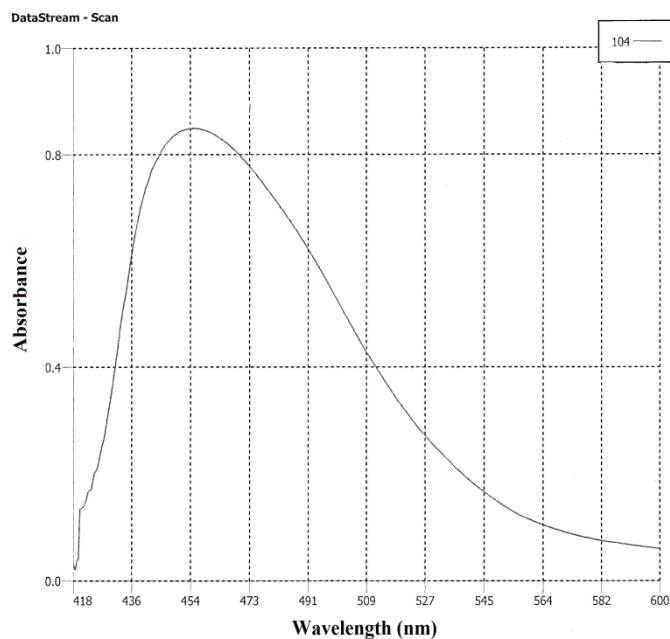


**Figure 3-19:** Absorption spectrum of ( $20 \mu\text{g.mL}^{-1}$ ) SNA against the reagent blank under the primary test and optimization condition.

### 3-3-8 Optimization of reaction variables

#### I-Univariate method

The optimum conditions for the univariate method were established by varying single parameter such as (effect of different bases, effect of borax concentration, effect of NQS concentration, and effect of reaction time) at one time while keeping the others fixed and observing the effect produced on the absorbance of the colored dye.

#### 1- Effect of different bases

1.0 mL of aliquots standard solution containing  $200.0 \mu\text{g}$  of SNA was transferred in a series of 10 mL volumetric flasks. A volume of 1.0 mL of 0.01 M from different bases such as (NaOH,  $\text{Na}_2\text{B}_4\text{O}_7 \cdot 10\text{H}_2\text{O}$ ,  $\text{NH}_4\text{OH}$ , KOH, and  $\text{Na}_2\text{CO}_3$ ) solution was added to each flask, and then 1.0 mL of 0.5 % (m/v) NQS solutions were added. The mixture was shaken gently until the appearance of orange color. Left to stand for 10 min., the contents were diluted up to the mark with distilled water. The absorbance of each solution was measured at 455.0 nm against the reagent blank. Borax was the most suitable alkaline medium for a maximum absorbance

for the method and was used in all subsequent experiments as shown in Table (3-14).

**Table 3-14:** Effect of different bases on condensation reaction.

<i>Alkaline solution (0.01 M)</i>	<i>Absorbance</i>
NaOH	0.541
Na <sub>2</sub> B <sub>4</sub> O <sub>7</sub> .10H <sub>2</sub> O	0.583
NH <sub>4</sub> OH	0.512
KOH	0.438
Na <sub>2</sub> CO <sub>3</sub>	0.350

## 2- Effect of borax concentration

1.0 mL of aliquots standard solution containing 200.0 µg of SNA was transferred in a series of 10 mL volumetric flasks. A volume of 1.0 mL of (0.015, 0.030, 0.045, 0.060, and 0.075 M) borax solution was added to each flask, and then 1.0 mL of 0.50 % (m/v) NQS solutions were added. The mixture was shaken gently until the appearance of orange color. Left to stand for 10 min., the contents were diluted up to the mark with distilled water, and the absorbance of each solution was measured at 455.0 nm against the reagent blank. It was found that 1.0 mL of 0.03 M borax solution gives a maximum absorbance for the method and was used in all subsequent experiments, as shown in Figure 3-20.

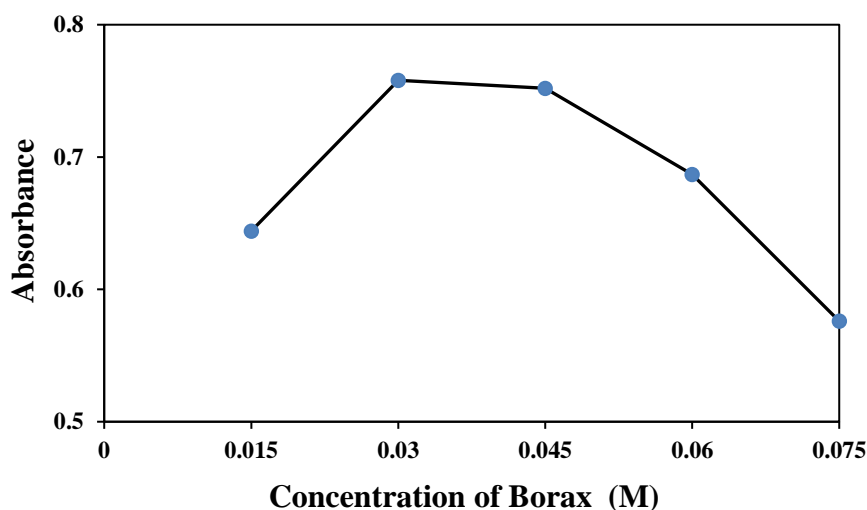


**Figure 3-20:** Effect of borax concentration on the color development of dye on the estimation of (20 µg.mL<sup>-1</sup>) SNA.

### 3- Effect of NQS concentration

1.0 mL of aliquots standard solution containing 200.0  $\mu\text{g}$  of SNA was transferred in a series of 10 mL volumetric flasks, then 1.0 mL of 0.03 M borax solution was added to each flask, and then 1.0 mL of (0.25, 0.50, 0.75, 1.00 and 1.25 % m/v) NQS solution, then the contents was shaken gently until the appearance of orange color. Left to stand for 10 min., the mixture was diluted up to the mark with distilled water, and the absorbance of each solution was measured at 455.0 nm against the reagent blank. It was found that 1.0 mL of 1.0 % (m/v) NQS gives a maximum absorbance for the method and was used in all subsequent experiments, as shown in Figure 3-21.

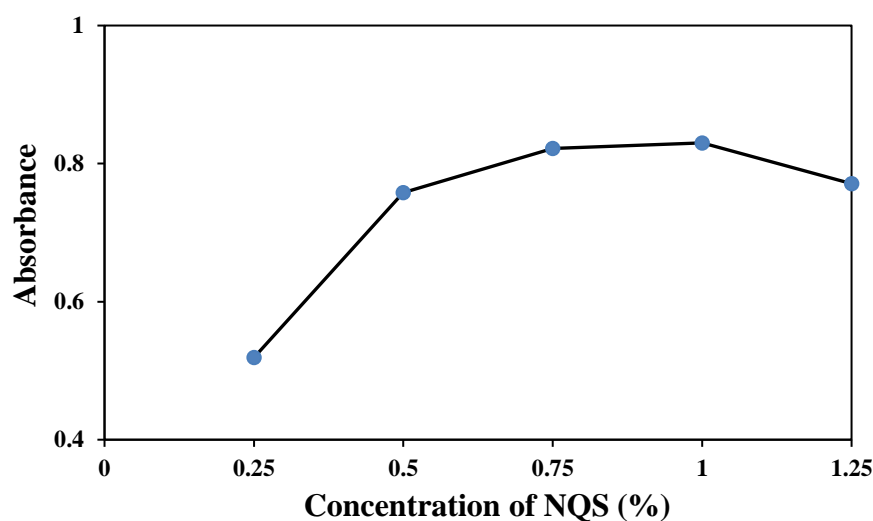


**Figure 3-21:** Effect of 1.0 mL of NQS concentration on the color development of dye on the determination of ( $20.0 \mu\text{g.mL}^{-1}$ ) SNA.

### 4- Effect of reaction time

1.0 mL of aliquots standard solution containing 200.0  $\mu\text{g}$  of SNA was transferred in a series of 10 mL volumetric flasks. A volume of 1.0 mL of 0.03M borax solution was added to each flask, and then 1.0 mL of 1.0% (m/v) NQS solution, then the contents was shaken gently until the appearance of orange color. Left to stand (1-10 min.), the mixture was diluted up to the mark with distilled water, and the absorbance of each solution was measured at 455.0 nm against the reagent blank. It was found that (5.0 min.) for a maximum absorbance for the method and was used in all subsequent experiments, as shown in Table 3-15.



**Table 3-15:** Effect of coupling reaction time.

<i>Time (min.)</i>	<i>Absorption</i>
1	0.768
2	0.801
3	0.821
4	0.825
5	0.830
6	0.825
8	0.828
10	0.830
60	0.826

## II- Design of experiment method

Optimum experimental conditions have been studied using multivariate experimental design. The most three critical variables (reagent concentration, borax concentration, and reaction time) were examined using a central composite design; three levels of each selected variable were required to test for the curvature of the response. The values of these variables were chosen within specified boundaries for each at which they affected the measured absorption of the colored products as shown in Table (3-2).

The number of experiments required to investigate the previously noted three parameters at three levels would be 27 ( $3^3$ ). However, this was reduced to 20 using a central experimental design. Response surface model was applied to study the effect of the three variables, reagent concentration, borax concentration, and reaction time on the absorbance of SNA-NQS complex and generate an optimal and robust response surface. A second order polynomial linear-quadratic equation was used to express the absorption as a function of independent variables namely, reagent concentration, borax concentration, and reaction time.

$$\text{Absorbance} = \beta_0 + \beta_1^* (\text{Reg. conc.}) + \beta_2^* (\text{Borax conc.}) + \beta_3^* (\text{Reaction time}) + \beta_4^* (\text{Reg. conc.})^2 + \beta_5^* (\text{Borax conc.})^2 + \beta_6^* (\text{Reaction time})^2.$$

Table 3-16 shows the study of optimum conditions according to central composite design and the experimental points used according to the design.

**Table 3-16:** The central composite design with three independent variables (un coded variables) and their experimental absorption values of 20  $\mu\text{g.mL}^{-1}$  SNA-NQS complex.

<i>Exp. No.</i>	<i>Reagent conc. (% m/v)</i>	<i>Borax conc. (M)</i>	<i>Reaction time (min.)</i>	<i>Abs.</i>
1	0.750	0.045	10.0	0.825
2	1.250	0.045	5.5	0.823
3	0.750	0.045	5.5	0.832
4	0.750	0.045	5.5	0.832
5	1.250	0.075	10.0	0.848
6	0.250	0.045	5.5	0.538
7	0.750	0.075	5.5	0.713
8	0.750	0.045	1.0	0.826
9	0.750	0.045	5.5	0.832
10	0.750	0.045	5.5	0.832
11	0.250	0.075	1.0	0.232
12	1.250	0.075	1.0	0.812
13	0.250	0.015	10.0	0.766
14	0.750	0.045	5.5	0.832
15	0.250	0.015	1.0	0.667
16	1.250	0.015	10.0	0.612
17	0.750	0.045	5.5	0.832
18	0.250	0.075	10.0	0.288
19	0.750	0.015	5.5	0.741
20	1.250	0.015	1.0	0.633

The coefficients of the response surface equation were determined by **STATISTICA 10.0** software (Stat. Soft. Inc, release 2011), the results are listed in Table 3-17.

Optimum conditions that were developed from central composite design for the determination of sulfanilamide via condensation reaction with NQS were calculated mathematically and the results are 1.0 mL of 0.975 % (m/v) for the reagent concentration, 1.0 mL of 0.036 M for borax concentration and 22.0 seconds for reaction time.

Figures 3-22, 3-23, and 3-24 give the imagine of response surface model if one of the three variables is remained constant.

**Table 3-17:** Regression coefficients, P (or probability for absorption of SNA- NQS).

<i>Variable</i>	<i>Regression coefficient</i>	<i>Standard error of coefficient</i>	<i>t-value</i>	<i>P</i>
Constant	0.1957	0.1603	1.2203	0.2440
Reg. conc.	1.0729	0.4887	2.1953	0.0469
(Reg. conc.) <sup>2</sup>	-0.5504	0.3210	-1.7147	0.1101
Borax conc.	7.3558	8.1457	0.9030	0.3829
(Borax conc.) <sup>2</sup>	-101.2121	89.1558	-1.1352	0.2768
Reaction time	-0.0003	0.0446	-0.0060	0.9953
(Reaction time) <sup>2</sup>	0.0004	0.0040	0.0923	0.9278

Fitted Surface; Variable: Absorbance  
3 factors, 1 Blocks, 20 Runs

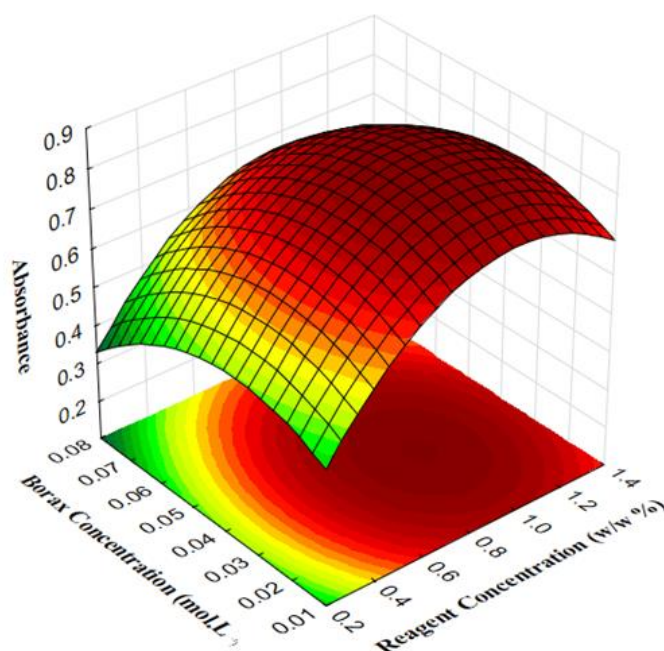


**Figure 3-22:** The response surface for the absorbance of SNA-NQS complex as a function of reagent concentration and borax concentration (at constant optimum value of reaction time, 22.0 sec.).

Fitted Surface; Variable: Absorbance  
3 factors, 1 Blocks, 20 Runs

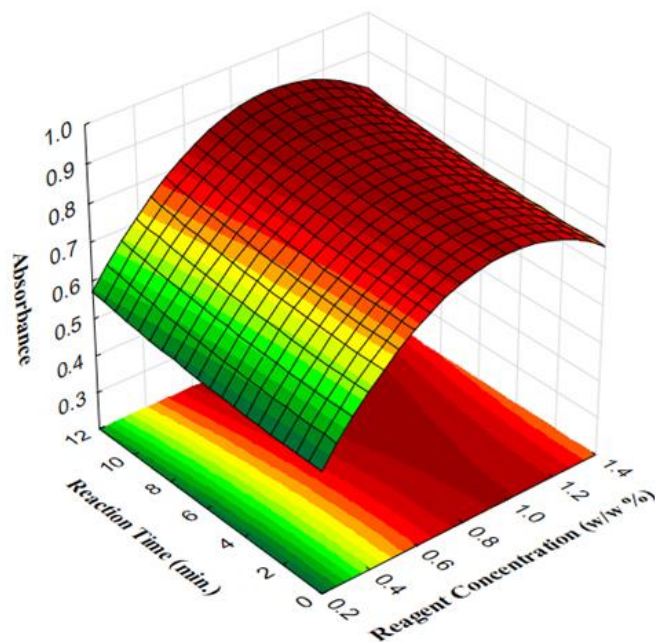


**Figure 3-23:** The response surface for the absorbance of SNA-NQS complex as a function of reagent concentration and reaction time (at constant optimum value of borax concentration, 0.036 M).

Fitted Surface; Variable: Absorbance  
3 factors, 1 Blocks, 20 Runs

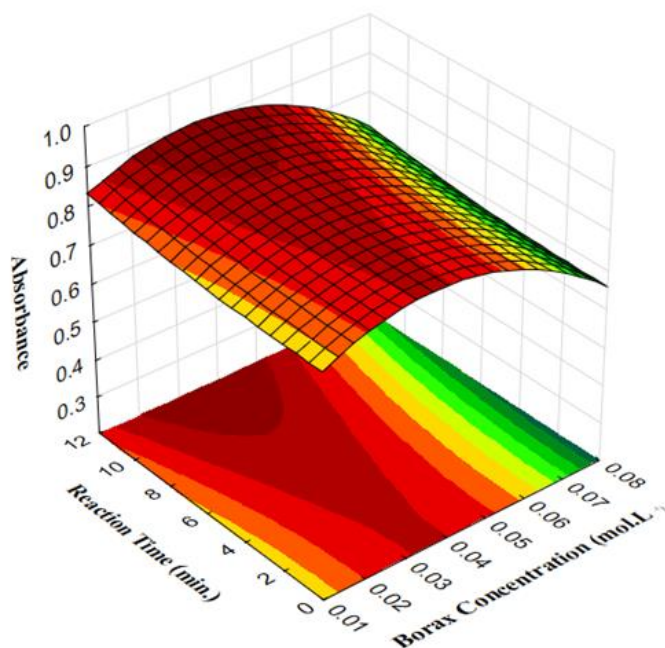


**Figure 3-24:** The response surface for the absorbance of SNA-NQS complex as a function of borax concentration and reaction time (at constant optimum value of reagent concentration, 0.975 % m/v).

### 3-3-9 Calibration curves and analytical data

#### I- Univariate method

In univariate method, sulfanilamide obeys the Beer's law over the range of (5.0-30.0)  $\mu\text{g.mL}^{-1}$ . Linear regression analysis was used to calculate the slope, intercept and correlation of linearity ( $r^2$ ) of calibration line. The molar absorptivity, Sandell's sensitivity, and limit of detection were also computed from the calibration graphs. Optical parameters were listed in Table 3-18 and shown in Figure 3-25.

**Table 3-18:** Optical characteristics and statistical data for the determination of SNA by univariate method.

<i>Parameter</i>	<i>Value</i>
$\lambda_{\text{max}}$ (nm)	455.0
Color	Orange
Linearity range ( $\mu\text{g.mL}^{-1}$ )	5.0-30.0
Regression equation	$Y=0.0404[\text{SNA. } \mu\text{g.mL}^{-1}]+0.0301$
Calibration sensitivity ( $\text{mL. } \mu\text{g}^{-1}$ )	0.0404
Correlation coefficient (r) %	99.98
Correlation of linearity ( $r^2$ ) %	99.97
Molar absorptivity ( $\text{L. mol}^{-1}.\text{cm}^{-1}$ )	$\varepsilon = 6.9568 \times 10^4$
Sandell's' sensitivity ( $\mu\text{g.cm}^{-2}$ )	2.4753
Detection limit ( $\mu\text{g.mL}^{-1}$ )	0.546
Quantification limit ( $\mu\text{g.mL}^{-1}$ )	1.654

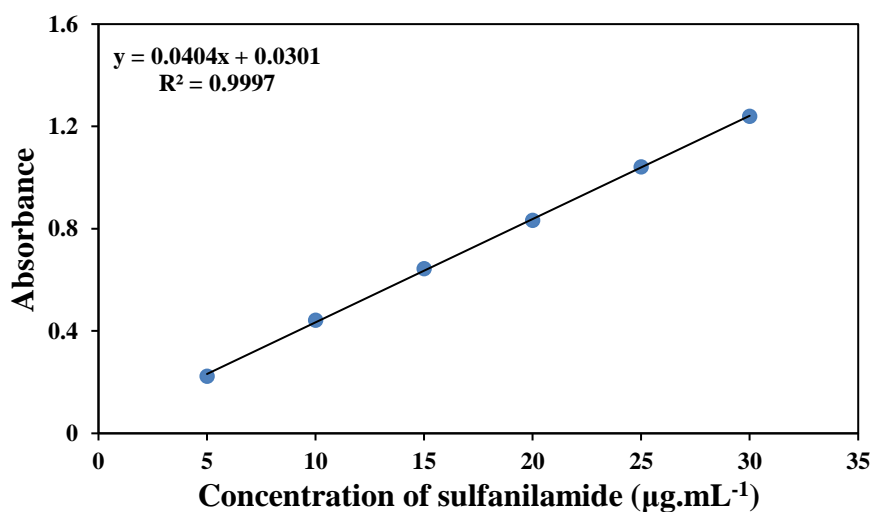


**Figure 3-25:** Calibration curve for the determination of SNA by univariate optimal condition.

## II- Design of experiment method

For the design of experiment (DOE) optical characteristics and statistical data for the determination of sulfanilamide also were calculated and the results appeared in Table 3-19 and Figure 3-26. Condensation reaction of sulfanilamide with NQS was represented in Scheme (3-3).

**Table 3-19:** Optical characteristics and statistical data for the determination of SNA by DOE method.

<i>Parameter</i>	<i>Value</i>
$\lambda_{\max}$ (nm)	455
Color	Orange
Linearity range ( $\mu\text{g}.\text{mL}^{-1}$ )	5.0-30.0
Regression equation	$Y=0.0411[\text{SNA}.\mu\text{g}.\text{mL}^{-1}]+0.0347$
Calibration sensitivity ( $\text{mL}.\mu\text{g}^{-1}$ )	0.0411
Correlation coefficient (r) %	99.99
Correlation of linearity ( $r^2$ ) %	99.99
Molar absorptivity ( $\text{L}.\text{mol}^{-1}.\text{cm}^{-1}$ )	$\epsilon=7.0774\times 10^4$
Sandell's sensitivity ( $\mu\text{g}.\text{cm}^{-2}$ )	2.4330
Detection limit ( $\mu\text{g}.\text{mL}^{-1}$ )	0.536
Quantification limit ( $\mu\text{g}.\text{mL}^{-1}$ )	1.626

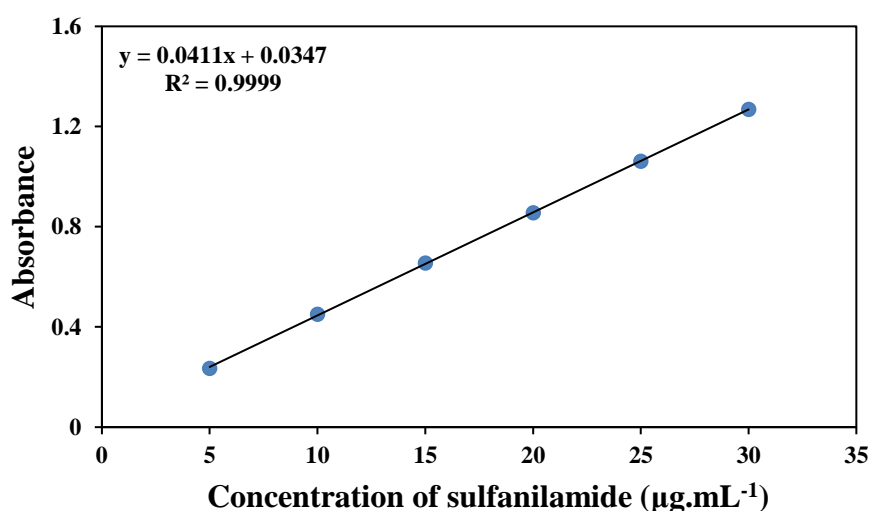
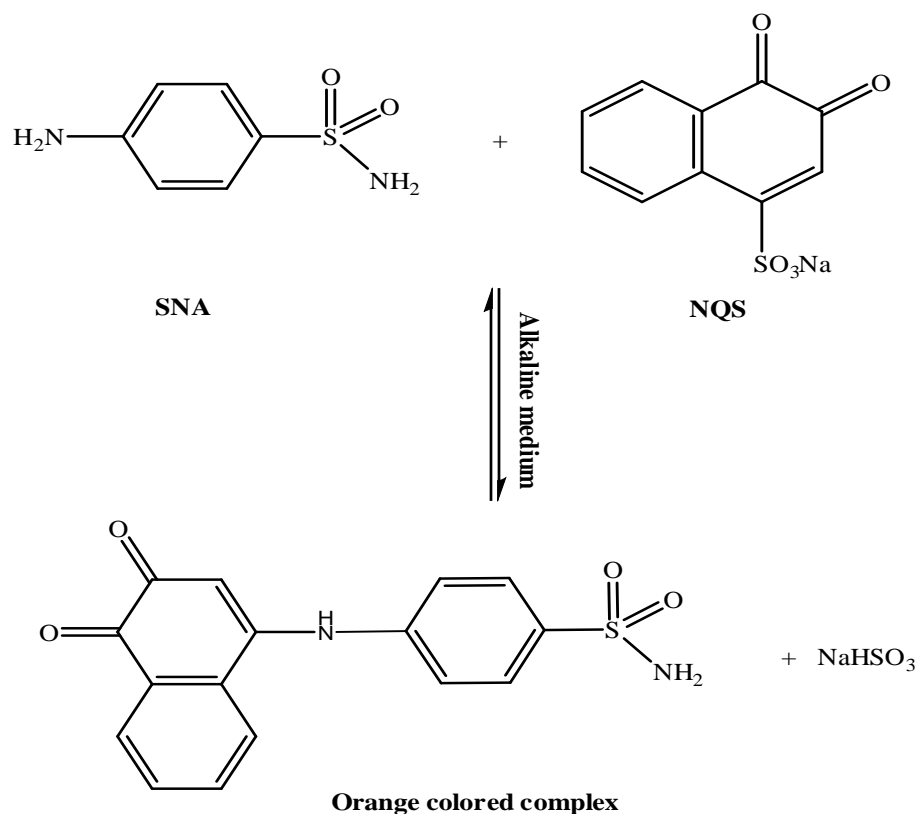


**Figure 3-26:** Calibration curve for the determination of SNA by DOE optimal condition.



**Scheme 3-3:** The reaction mechanism for the condensation reaction between SNA and NQS.

### 3-3-10 Precision and accuracy

The accuracy and precision of the proposed (univariate and DOE) methods were ascertained from the absorbance values obtained by actual determination of five replicates of a three level amounts of SNA within the Beer's law limits. The coefficient of variation and percent relative error were calculated for the proposed methods recorded in Table 3-20.

**Table 3-20:** Evaluation of accuracy and precision for the determination of SNA by proposed method.

	<i>Conc. of SNA</i> ( $\mu\text{g.mL}^{-1}$ )		<i>Relative Error</i> %	<i>C.V*</i> %
	<i>Taken</i>	<i>Found*</i>		
<b>For univariate</b>	5.0	4.968	-0.640	1.381
	10.0	9.993	-0.070	0.991
	20.0	19.790	-1.050	0.542
<b>For DOE</b>	5.0	5.043	0.860	2.127
	10.0	10.157	1.570	0.429
	20.0	19.958	-0.210	0.367

\*Average of five determinations.

**3-3-11 Interference Study**

Under optimum conditions of DOE method, the effect of excipients usually present in the formulations (vanillin, glucose, lactose, starch, and sucrose) for the assay of  $20.0 \mu\text{g.mL}^{-1}$  of SNA were investigated. The commonly used excipients present in formulations did not interfere even if they were present in excess amount than they usually exist Table (3-21).

**Table 3-21:** Percent recovery for  $20.0 \mu\text{g.mL}^{-1}$  of sulfanilamide in the presence of different concentration of Excipients.

<i>Excipients</i>	<i>Concentration</i> ( $\mu\text{g.mL}^{-1}$ )	<i>Sulfanilamide Conc. Taken</i> ( $20.0 \mu\text{g.mL}^{-1}$ )	
		<i>Conc. Found*</i> ( $\mu\text{g.mL}^{-1}$ )	<i>Recovery*</i> %
Vanillin	1000	19.971	99.85
Glucose		20.046	100.23
Lactose		19.912	99.56
Starch		19.731	98.65
Sucrose		20.086	100.43

\*Average of three determinations

**3-3-12 Application in synthetic sample**

Synthetic sample of sulfanilamide was successfully analyzed by the proposed method. The results obtained for the determination of SNA in its synthetic sample by the proposed methods are presented in Table 3-22.

**Table 3-22:** Application of the proposed method to the SNA concentration measurements in synthetic sample.

<i>Sample</i>	<i>Conc. taken</i> ( $\mu\text{g.mL}^{-1}$ )	<i>Conc.*</i> <i>found</i> ( $\mu\text{g.mL}^{-1}$ )	<i>Recovery</i> %	<i>C.V*</i> %
SNA	5.0	5.042	100.832	0.4827
	10.0	10.126	101.266	0.2573
	20.0	19.980	99.900	0.0512

\*Average of three determinations.

The obtained results are in good agreement with each other and provide no interference of additive and excipients in proposed analytical method.



### 3-3-13 Application in synthetic sample by standard additions method (SAM)

The proposed method also could be useful and suitable for the determination of SNA in synthetic sample by standard addition method. The data presented in Table 3-23 reveals the good recovery and coefficient of variation. Figure 3-27 shows the plot of standard addition method for the determination of SNA.

**Table 3-23:** Application of the proposed method to the SNA concentration measurements in synthetic sample (SNA) by (SAM).

<i>Sample</i>	<i>Conc. taken</i> ( $\mu\text{g.mL}^{-1}$ )	<i>Conc.*</i> <i>found</i> ( $\mu\text{g.mL}^{-1}$ )	<i>Recovery</i> %	<i>C.V*</i> %
SNA (synthetic sample)	500.00	505.266	101.0532	0.2180

\*Average of three determinations.

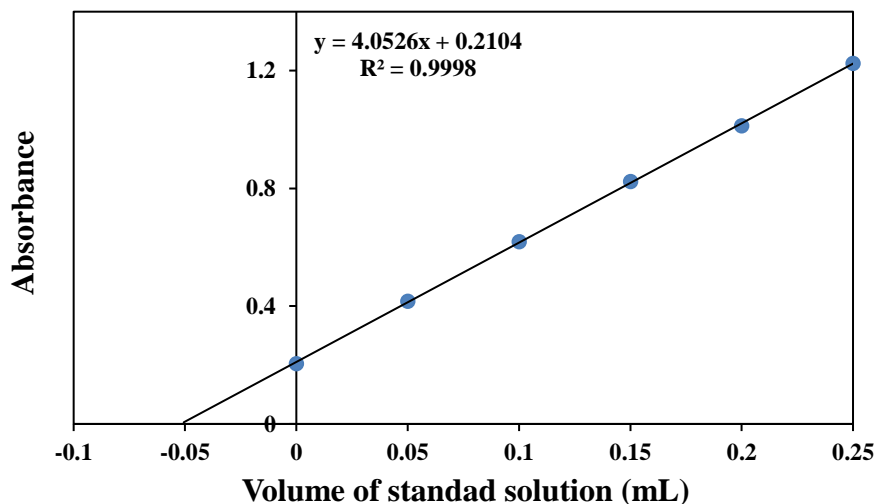


**Figure 3-27:** Determination of SNA in synthetic sample by standard additions method.

# ***CHAPTER FOUR***

***Simultaneous determination of  
sulfamethoxazole and  
sulfanilamide***

## Chapter Four

### 4- Simultaneous determination of sulfamethoxazole and sulfanilamide

#### 4-1 Simultaneous determination of sulfamethoxazole and sulfanilamide by derivative spectrophotometry

##### 4-1-1 Introduction

In 1953 derivative mode was first introduced and applied for IR-spectroscopy and since that time the technique has continued to progress especially in incorporation with other methods such as multi component analysis of mixtures and multi-wavelength measurements <sup>(130,131)</sup>.

Recently, especially after the introduction of digital computer in spectroscopy, differentiation of spectra becomes a widely used technique particularly in infra-red, fluorescence, reflectance spectrophotometry and UV/VIS absorption and referred to as derivative spectroscopy <sup>(132)</sup>.

Generally, the first- and second-order derivative spectra were initially employed, but with progress made in modern electronics, most commercial spectrophotometers have been fitted with derivative modules to resolve higher-order differentiation ( $n > 2$ ) of signals.

Because of the fact that the amplitude of the  $n^{\text{th}}$  derivative of a peak-shaped signal is inversely proportional to the  $n^{\text{th}}$  power of the width of the peak, differentiation may be employed as a general way to discriminate against broad spectral features in favor of narrow components. This is the basis for the application of differentiation as a method of correction for background signals in quantitative spectrophotometric analysis. Very often in the practical applications of spectrophotometry to the analysis of complex samples, the spectral bands of the analyte (i.e. the compound to be measured) are superimposed on a broad, gradually curved background. Background of this type can be reduced by differentiation. Derivative methods have been used in analytical spectroscopy for three main purposes:

- a) Spectral discrimination, as a qualitative fingerprinting technique to accentuate small structural differences between nearly identical spectra;
- b) Spectral resolution enhancement, as a technique for increasing the apparent resolution of overlapping spectral bands in order to more easily determine the number of bands and their wavelengths;

c) Quantitative analysis, as a technique for the correction for irrelevant background absorption and as a way to facilitate multicomponent analysis <sup>(133)</sup>.

The term derivative mode refers to spectra that are obtained by plotting the first or higher order derivative of absorbance with respect to wavelength as a function of wavelength (Fig. 4-1).

The principle of operation of this technique is based on the measurement of the changes in intensity or absorbance manually or automatically by certain instrument. The approach is based on the idea that the wavelength scan rate,  $(\frac{d\lambda}{dt})$  is constant, and then the derivative of the intensity with respect to the wavelength;  $(\frac{dI}{d\lambda})$  is proportional to the derivative of the intensity with respect to the time,  $(dI/dt)$ , which is measured by means of its electronic differentiation <sup>(131,134)</sup>.

$$\left(\frac{dI}{d\lambda}\right) = \left(\frac{dI}{dt}\right) / \left(\frac{d\lambda}{dt}\right)$$

Regardless of the odd unit, derivative spectra possess the same relation to the concentration of the absorption species as that in the original normal (zero order) spectrum i.e. Beer's law is obeyed. In addition, concentration measurement of an analyte in the presence of interference or of two or more analytes in mixture can sometimes be made more easily or more accurately using derivative methods <sup>(130,135)</sup>.

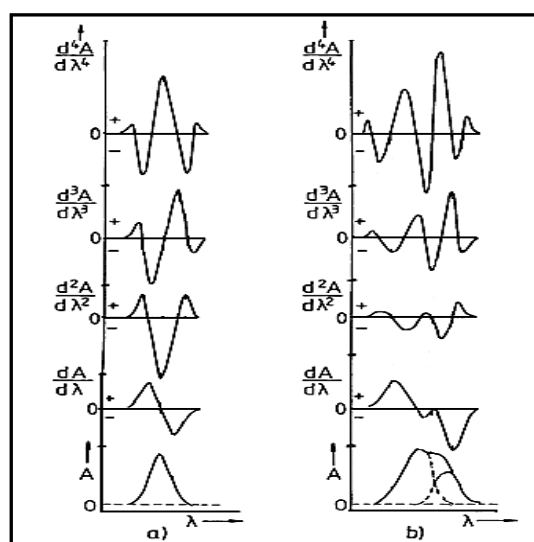


**Figure 4-1:** Differentiation of computed Gaussian analytical bands.

- a) Fundamental curve and its first- to fourth-order derivatives,
- b) Fundamental curve and first- to fourth -order derivatives of two superposed Gaussian bands. The overlapping peaks become separated by this manipulation.

The most important applications of derivative spectrophotometric technique in analytical chemistry are:

1. Inorganic analysis <sup>(136,137)</sup>.
2. Determination of ionization constant of some compounds <sup>(138)</sup>.
3. Organic and pharmaceutical analysis <sup>(139)</sup>.
4. Determination of drug partition coefficient between lipid bi-layers and water <sup>(140)</sup>.
5. Clinical analysis <sup>(141)</sup>.
6. Food analysis <sup>(142)</sup>.

#### 4-1-2 Spectrophotometric determinations of some pharmaceutical

Derivative spectrophotometric method was initially utilized for simultaneous determination of metal ion mixture and its applications have been extend to other analytical fields among them is for pharmaceutical compounds <sup>(143)</sup>.

The determination of some drugs which have an importance in therapy is an analytical problem in the quality control of the pharmaceutical industry. Derivative spectrophotometric method is one of the analytical techniques that have a great utility for resolving drug mixtures with overlapping spectra. Moreover, derivative methods have been applied successfully to the determination of drugs in the presence of their degradation products <sup>(134)</sup>. Table 4-1 shows the analytical characteristics of these methods for simultaneous determination of some pharmaceutical compounds.

**Table 4-1:** Analytical characteristics of derivative methods for simultaneous determination of some pharmaceutical compounds.

<i>Pharmaceutical compounds</i>	<i><math>\lambda</math> max (nm)</i>	<i>Derivative order and Application Remarks</i>	<i>Ref. No.</i>
<b>Imipramine</b>	240.2	1 <sup>st</sup> , Presence of Iminodi-benzyl as an impurity.	144
<b>Haloperidol</b>	255.2	1 <sup>st</sup> , Presence of methyl Paraben and Propyl Paraben.	145
<b>Pyridoxine</b>	306	1 <sup>st</sup> , Presence of Multivitamin Preparations.	146
<b>Cephalothin, Clavulanic Acid</b>	270, 236.75	1 <sup>st</sup> , Normal Saline	147
<b>Asprin, Acetaminophen, Ascorbic Acid</b>	291.3 221.8 262.5	1 <sup>st</sup> , Per Afebry effervescent tablets	148

<i>Pharmaceutical compounds</i>	<i><math>\lambda</math> max (nm)</i>	<i>Derivative order and Application Remarks</i>	<i>Ref. No.</i>
<b>Dorzolamide HCl, Timolol Maleate</b>	250.3, 315.8 242.9, 223.5	1 <sup>st</sup> , Eye Drops	149
<b>Pseudoephedrine, Acrivastine</b>	270.6, 288	1 <sup>st</sup> , 2nd, Mixture of Capsules	150
<b>Propyphenazone, Caffeine</b>	230, 256	4 <sup>th</sup> , Mixture of Commercial Tablets	151

### 4-1-3 Experimental

#### 4-1-3-1 Instrumentation

The instruments used are described in section 2-2-1; however, the spectra of the studied compounds were recorded using Cecil CE 7200 & shimadzu 1800 under different instrumental parameters, finally a spectral band width of 1.8 nm, a response time of 5 seconds a scan speed of 1 nm.sec<sup>-1</sup> and a wavelength range of 190-350 nm were used. The resulted absorption data were plotted and manipulated by Shimadzu 1800 software to obtain the first and second derivatives.

#### 4-1-3-2 Chemicals

All chemicals used in this investigation are described in section 2-2-2.

#### 4-1-3-3 Pharmaceutical compounds

Table 2-3, section 2-2-2, illustrates the used pharmaceutical compounds and their manufacturers.

#### 4-1-3-4 Reagents

The procedures used for the preparation of all reagents and the solutions of the pharmaceutical preparations which are used throughout the investigation are given in section 2-2-3, the pharmaceutical preparations measures according to the general recommended procedures (used the pharmaceutical preparations of sulfamethoxazole when we want to determine it with the stander of sulfanilamide and vice versa).

#### 4-1-3-5 General recommended procedures

##### 1. Assay procedure for the determination of sulfamethoxazole or sulfanilamide

Aliquots, of sulfamethoxazole standard solution containing 50-500  $\mu\text{g}$  (or sulfanilamide standard solution containing 50-500  $\mu\text{g}$ ), was transferred into a series of 10 mL volumetric flasks; and diluted to the mark with 0.02 M HCl. The spectrum for each solution was recorded against a reagent blank, prepared similarly without the addition of (sulfamethoxazole or sulfanilamide). Each zero order spectrum was then manipulated to get its first derivative (D1) and second derivative (D2).

##### 2. Assay procedure for the determination of each drug in the presence of the other

Aliquots, of sulfamethoxazole standard solution containing 50-500  $\mu\text{g}$  (or sulfanilamide standard solution containing 50-500  $\mu\text{g}$ ), was transferred into a series of 10 mL volumetric flask containing aliquots of (20-500  $\mu\text{g}$ ) of sulfanilamide solutions (or aliquots of 20-500  $\mu\text{g}$  of sulfamethoxazole solutions); the mixture was then diluted to the mark with 0.02 M HCl. The spectrum for each solution was recorded against a reagent blank. The recorded spectra were then manipulated to get D1 and D2.

#### 4-1-4 Results and discussions

Derivative spectroscopy is a useful tool to give some improvement to the selectivity of the UV/VIS spectrophotometry. As the name suggests, the technique consists of plotting the rate of change of the absorbance spectrum versus wavelength, this will give a plot having one or more maxima, and minima and the graph may pass through zero on the ordinate. As a result, the technique can be used to identify peak maxima and minima and this is termed a first-derivative spectrum.

When second derivative spectrum is recorded (by derivatizing the absorbance spectrum twice); the spectrum can be thought of as an inverted spectrum with respect to first derivative spectrum. Sharp peaks will be made even sharper and broad peaks (and broad background features) will become flattened and so the technique can be used both as a peak-enhancement and background-rejection tool.

The derivative spectrum, like its absorbance counterpart, still contains quantitative information. If two points are consistently used on the spectrum and the difference in their values on the ordinate is taken, this can be plotted against concentration and a linear relationship is

established therefore, derivative spectra represent an alternative presentation of the original data <sup>(152)</sup>.

#### 4-1-4-1 Absorption spectra

The absorption spectra for sulfamethoxazole and sulfanilamide in addition to the spectrum of their mixture were recorded against solvent blank solution. Figure 4-2 shows the absorption spectrum of sulfamethoxazole, with two maxima at wavelengths 197 nm and 266 nm, while the absorption spectrum of sulfanilamide shows two maximum absorptions at 198.0 nm and 258.0 nm. On the other hand, the mixture of sulfamethoxazole and sulfanilamide shows two maxima at wavelengths at 198.0 nm and 260.0 nm, which may be related to the absorption maxima of the two individual components.

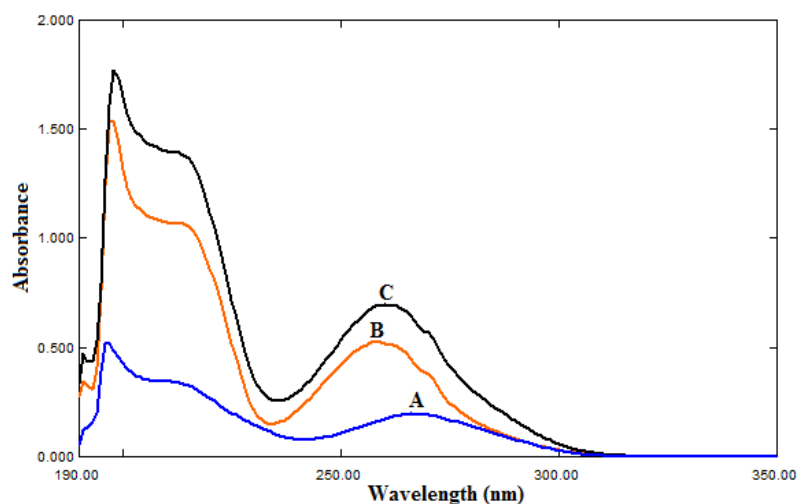


**Figure 4-2:** Absorption spectra of: (A)  $5.0 \mu\text{g}\cdot\text{mL}^{-1}$  sulfamethoxazole, (B)  $20.0 \mu\text{g}\cdot\text{mL}^{-1}$  sulfanilamide, and (C) a mixture of  $5.0 \mu\text{g}\cdot\text{mL}^{-1}$  sulfamethoxazole and  $20.0 \mu\text{g}\cdot\text{mL}^{-1}$  sulfanilamide.

#### 4-1-4-2 First and second derivative modes

It is obvious that there is a large overlap of the spectra of sulfamethoxazole and sulfanilamide, therefore, the direct determination of using zero order absorption measurements, when they are present in same solution, is very difficult using conventional methods.

Derivative spectrophotometric technique, as mentioned before, is of a particular utility in the determination of the concentration of single component in such mixtures, with large spectral overlapping. For this reason, derivative spectrophotometric methods have been applied. Both



first and second order modes were tested, the results obtained show that these techniques could successfully applied when the measurements are carried out under optimum selected conditions.

To select the derivative order, the first, second, third and fourth derivative spectra of Sulfamethoxazole and Sulfanilamide were recorded. The investigation reveals that first and second order spectra were simple and gave results of highest accuracy and detection limits.

The first and second order derivative spectra of sulfamethoxazole and sulfanilamide and for their mixture are shown in Figures 4-3 and 4-4 respectively.

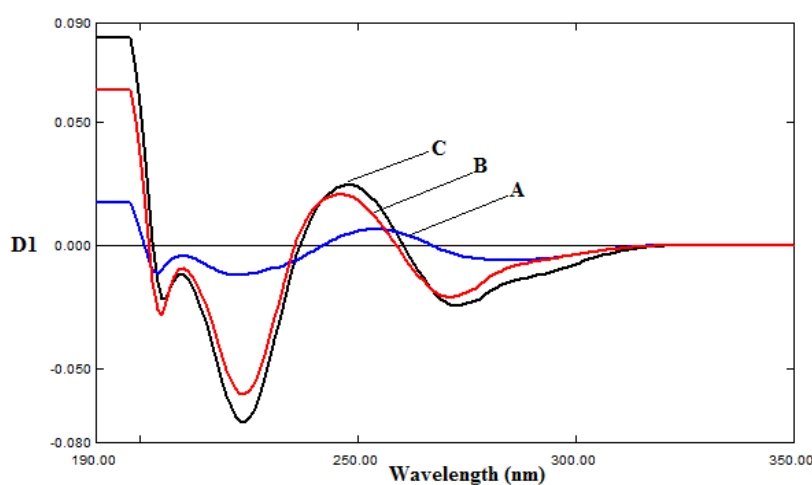


**Figure 4-3:** First derivative spectra of: (A) 5.0 µg.mL<sup>-1</sup> sulfamethoxazole, (B) 20.0 µg.mL<sup>-1</sup> sulfanilamide, and (C) mixture of 5.0 µg.mL<sup>-1</sup> sulfamethoxazole and 20.0 µg.mL<sup>-1</sup> sulfanilamide.

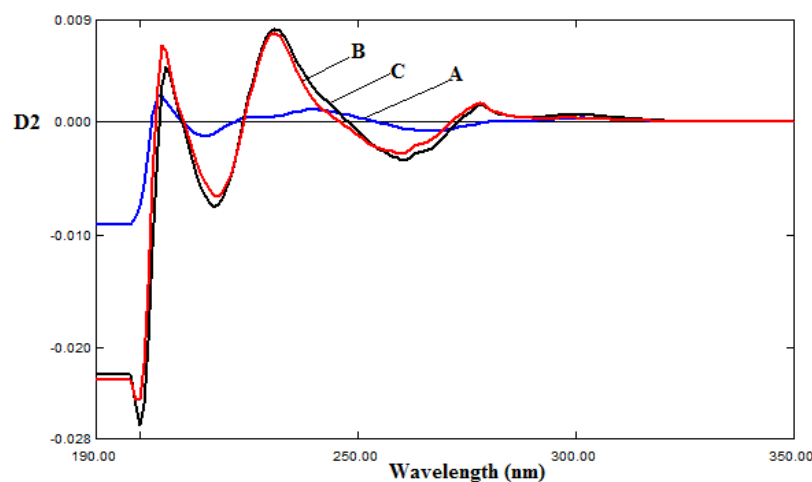
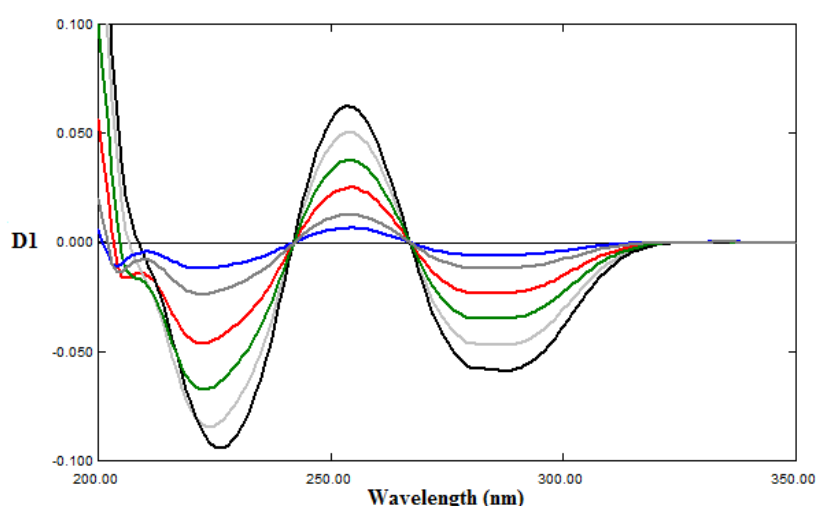


**Figure 4-4:** Second derivative spectra of (A) 5 µg.mL<sup>-1</sup> sulfamethoxazole, (B) 20 µg.mL<sup>-1</sup> sulfanilamide, and (C) mixture of 5 µg.mL<sup>-1</sup> sulfamethoxazole and 20 µg.mL<sup>-1</sup> sulfanilamide.

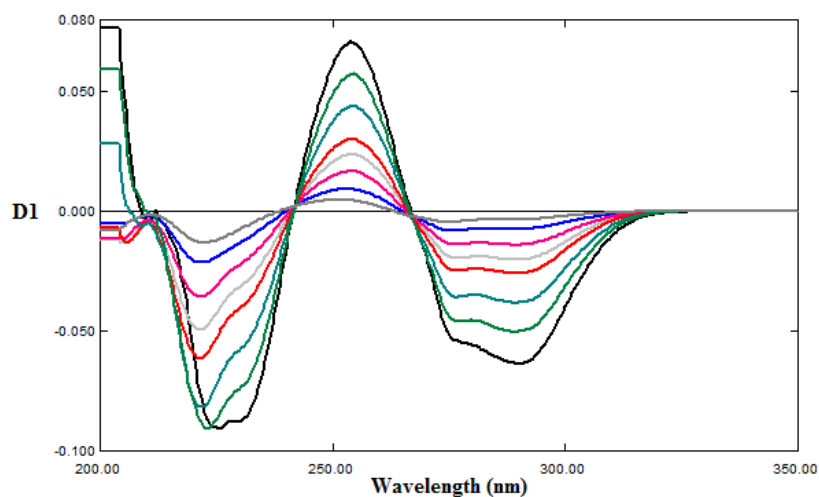
#### 4-1-4-3 Calibration graphs for sulfamethoxazole

Under the optimum instrumental operating conditions, the (peak-to-base line), zero-crossing, peak to peak technique which were graphically found in addition to the calculated area under peak were used to utilize the D1 and D2 spectra for quantitative analyses of sulfamethoxazole individually and in its mixture with sulfanilamide. Figures 4-5 to 4-11 show first order spectra for sets of solutions containing different amounts of sulfamethoxazole ( $2\text{--}50\ \mu\text{g.mL}^{-1}$ ) in the presence of different amounts ( $0, 2, 5, 10, 15, 20, 30\ \mu\text{g.ml}^{-1}$ ) of sulfanilamide.

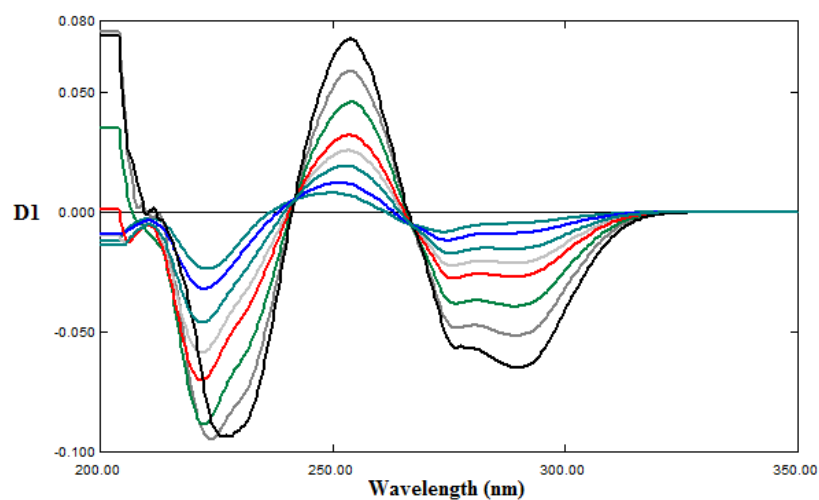
The results obtained, with the first derivative measurements, indicate that when the concentration of sulfanilamide is kept constant and the concentration of sulfamethoxazole varied, the peak amplitudes are measured at peak-to-baseline ( $223, 254, 287\ \text{nm}$ ), peak to peak height between ( $223\text{--}254\ \text{nm}$ ), ( $254\text{--}287\ \text{nm}$ ). Moreover, the height at the zero cross of sulfanilamide at ( $235.62, 258.72\ \text{nm}$ ), height-to-height of the two zero crosses between ( $235.62\text{--}258.72\ \text{nm}$ ) and area under peak between ( $241.95\text{--}267.04\ \text{nm}$ ), ( $267.04\text{--}330\ \text{nm}$ ) were found to be in proportion to the sulfamethoxazole concentration. Therefore, calibration plots were constructed for the assay of sulfamethoxazole in the presence of sulfanilamide at the mentioned wavelengths by plotting the measured values (as signals) against the concentration of sulfamethoxazole (Figures 4-12 to 4-32).



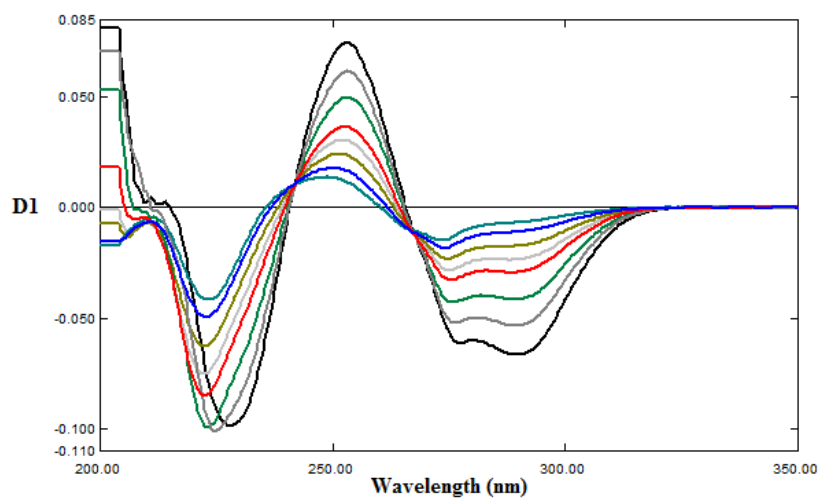
**Figure 4-5:** First derivative spectra of ( $5\text{--}50\ \mu\text{g.mL}^{-1}$ ) sulfamethoxazole.



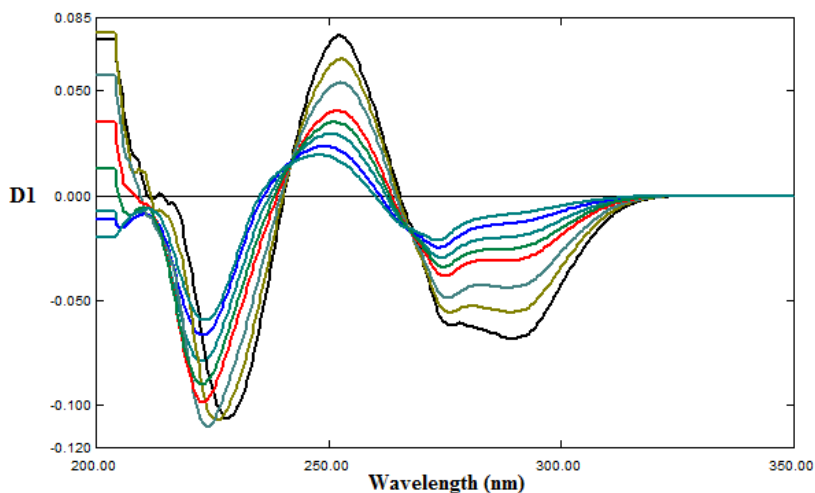
**Figure 4-6:** First derivative spectra of mixture contain (2-50  $\mu\text{g} \cdot \text{mL}^{-1}$ ) Sulfamethoxazole in the presence of (2  $\mu\text{g} \cdot \text{mL}^{-1}$ ) Sulfanilamide.



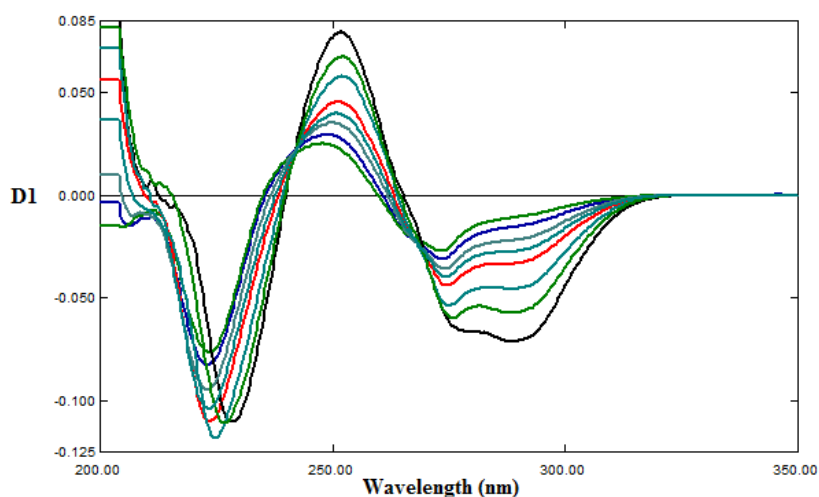
**Figure 4-7:** First derivative spectra mixture contain of (2 - 50  $\mu\text{g} \cdot \text{mL}^{-1}$ ) Sulfamethoxazole in the presence of (5  $\mu\text{g} \cdot \text{mL}^{-1}$ ) Sulfanilamide.



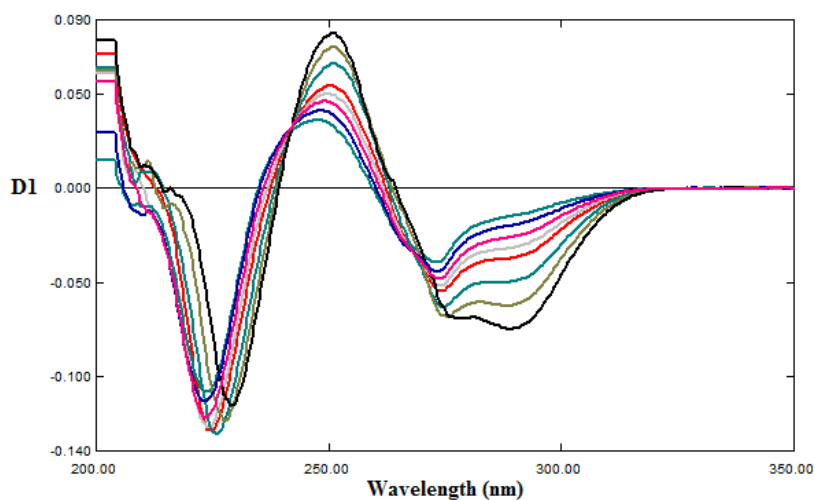
**Figure 4-8:** First derivative spectra of mixture contain (2-50  $\mu\text{g} \cdot \text{mL}^{-1}$ ) sulfamethoxazole in the presence of (10  $\mu\text{g} \cdot \text{mL}^{-1}$ ) sulfanilamide.



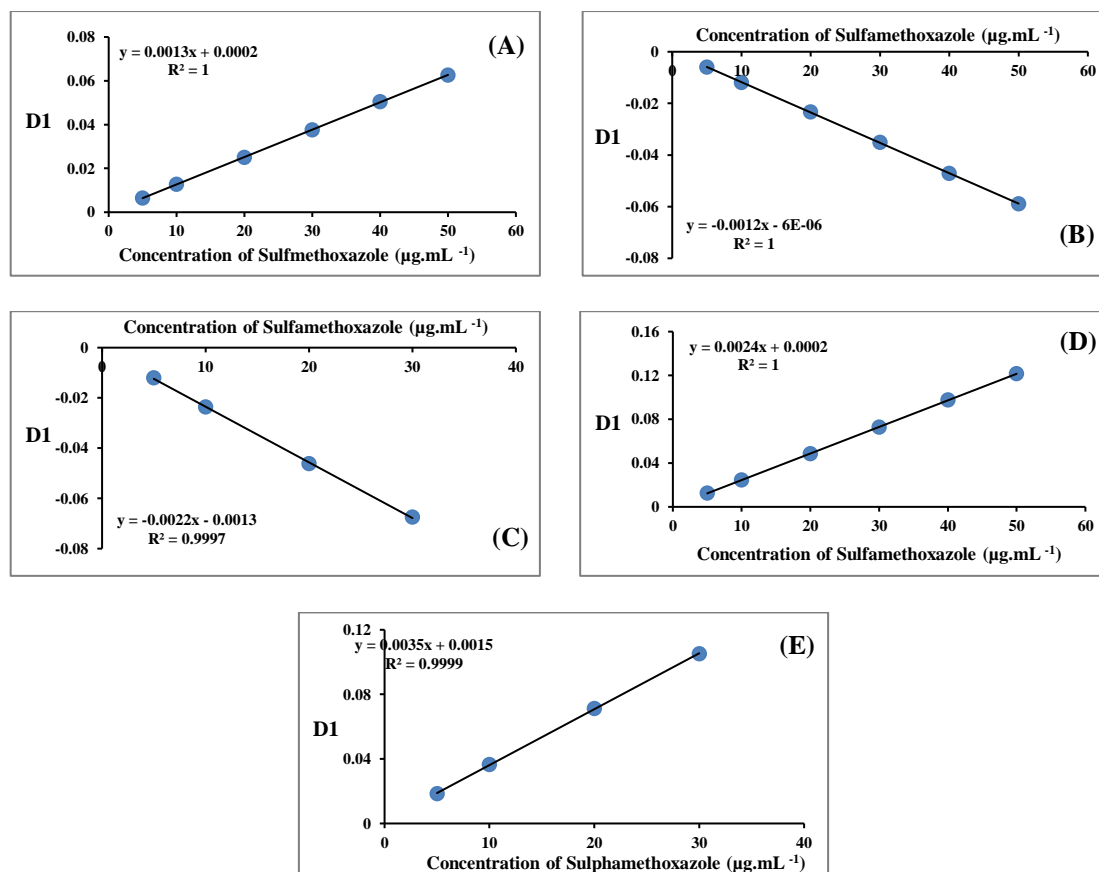
**Figure 4-9:** First derivative spectra of mixture contain (2-50  $\mu\text{g.mL}^{-1}$ ) Sulfamethoxazole in the presence of (15  $\mu\text{g.mL}^{-1}$ ) Sulfanilamide.



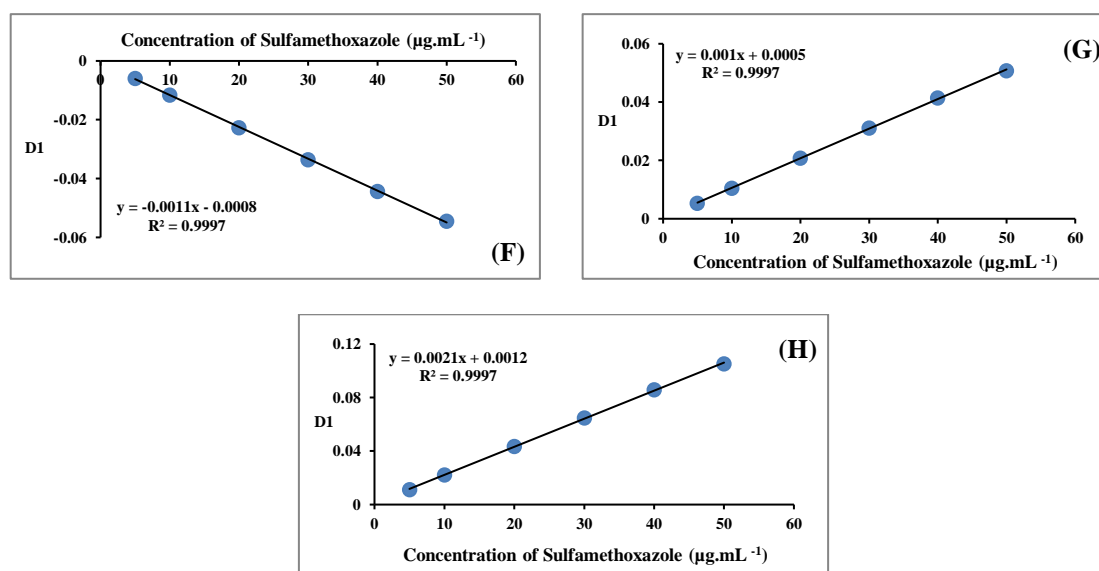
**Figure 4-10:** First derivative spectra of mixture contain (2-50  $\mu\text{g.mL}^{-1}$ ) Sulfamethoxazole in the presence of (20  $\mu\text{g.mL}^{-1}$ ) Sulfanilamide.



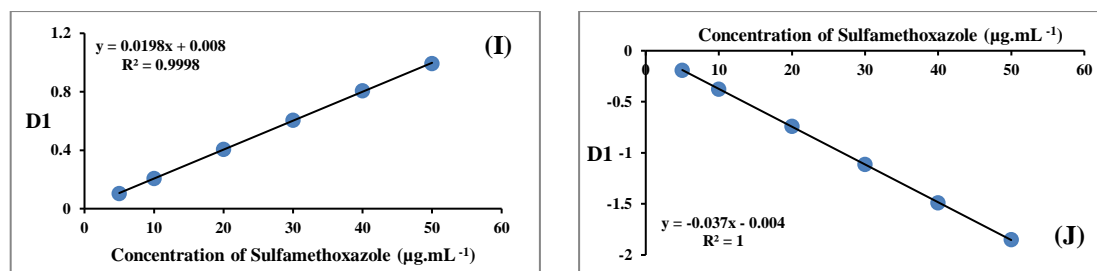
**Figure 4-11:** First derivative spectra of mixture contain (2-50  $\mu\text{g.mL}^{-1}$ ) Sulfamethoxazole in the presence of (30  $\mu\text{g.mL}^{-1}$ ) Sulfanilamide.



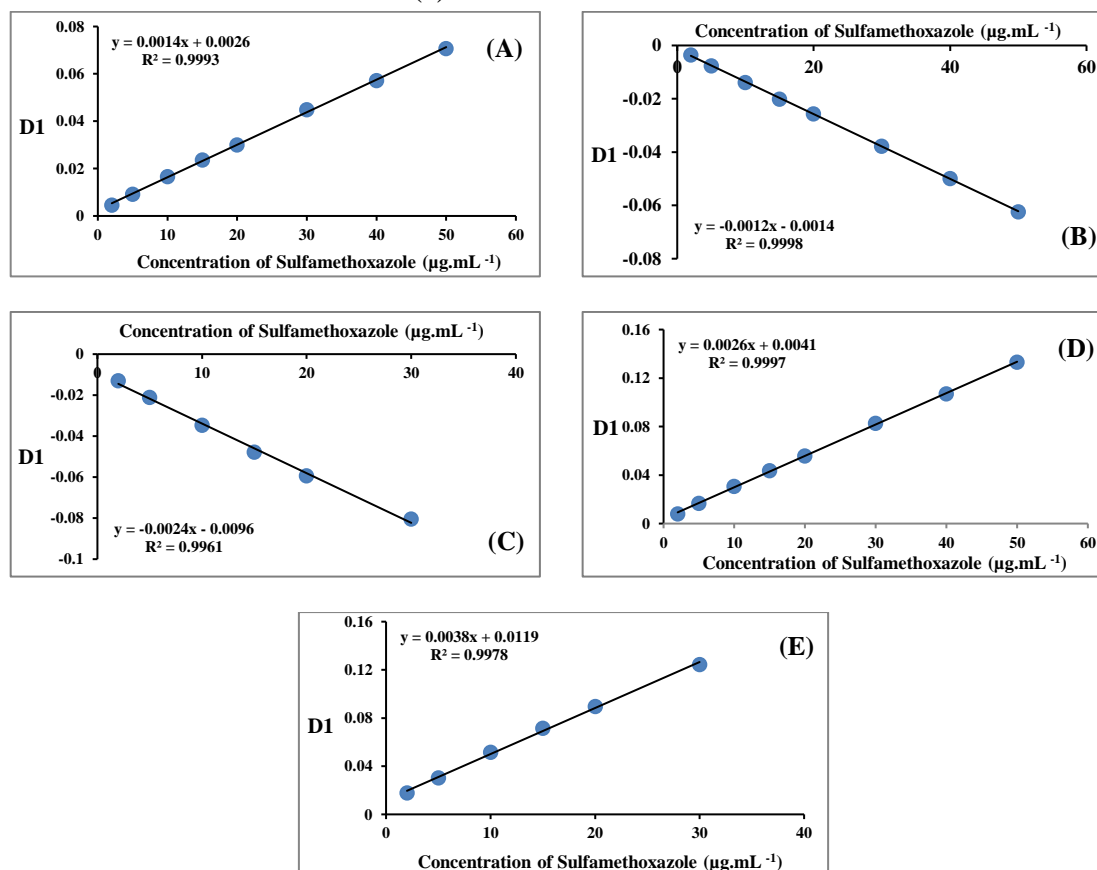
**Figure 4-12:** Calibration curves obtained via first derivative spectra of sulfamethoxazole for peak-to-baseline at (A) 254 nm, (B) 287 nm, (C) 223 nm, (D) peak to peak between (254-287 nm) and (E) peak to peak between (223-254 nm).



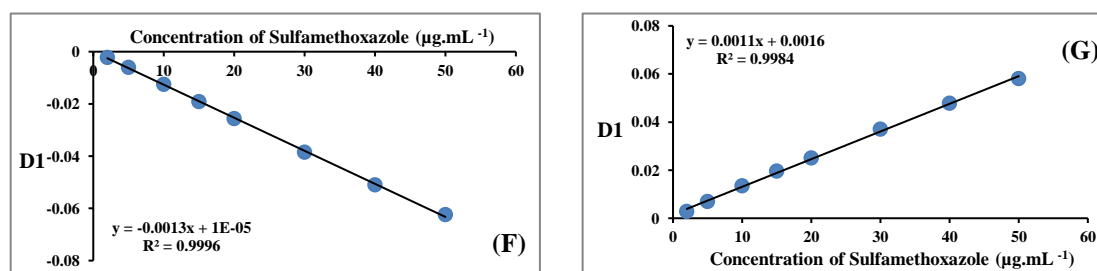
**Figure 4-13:** Calibration curves obtained via first derivative spectra of Sulfamethoxazole for height at zero cross at (F) 235.62 nm, (G) 258.72 nm and (H) height-to-height between (235.62-285.72 nm).

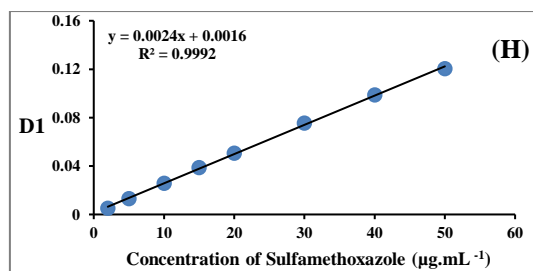


**Figure 4-14:** Calibration curves obtained via first derivative spectra of Sulfamethoxazole for peak area at the interval (I) 241.95 nm to 267.04 nm and (J) 267.04 nm to 330 nm.

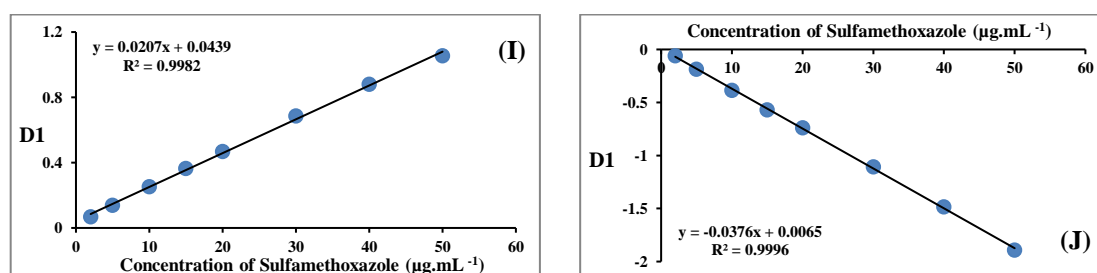


**Figure 4-15:** Calibration curves obtained via first derivative spectra of mixture of Sulfamethoxazole ( $2\text{-}50 \mu\text{g.mL}^{-1}$ ) in the presence of ( $2 \mu\text{g.mL}^{-1}$ ) Sulfanilamide, for peak-to-baseline at (A) 254 nm, (B) 287 nm, (C) 223 nm, (D) peak to peak between (254-287 nm) and (E) peak to peak between (223-254 nm).

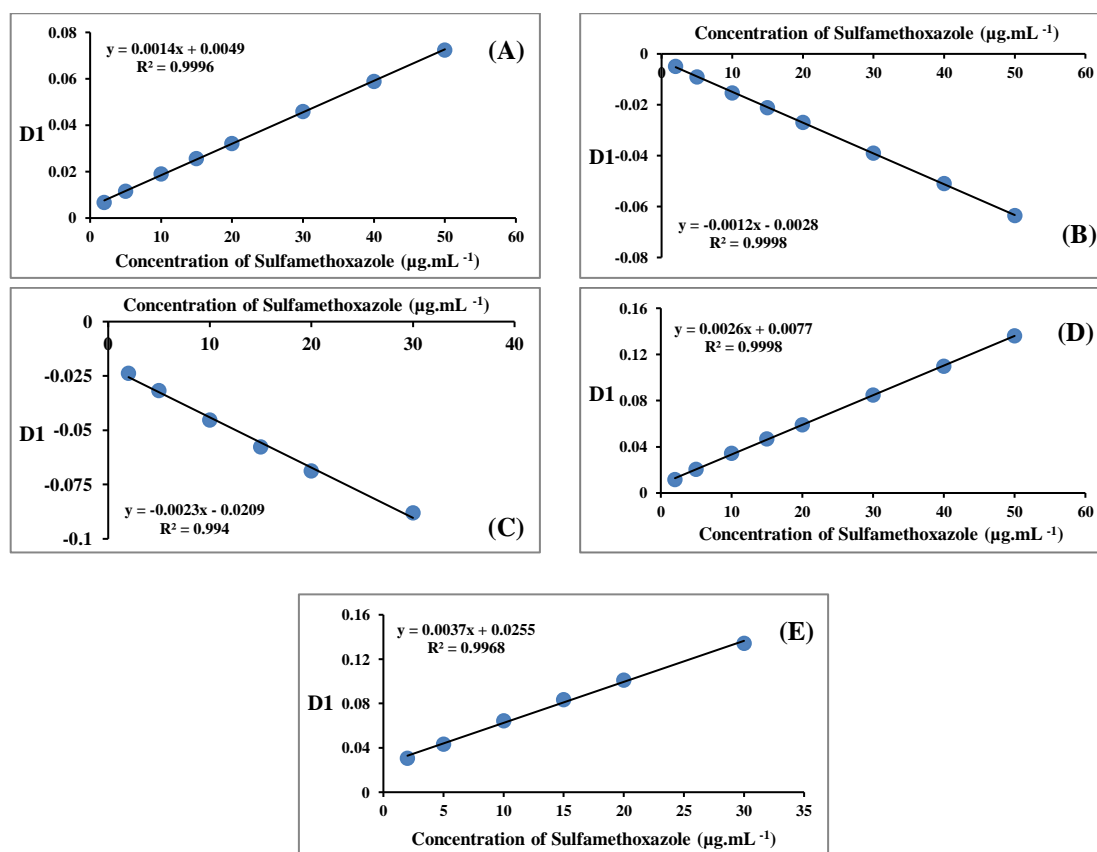




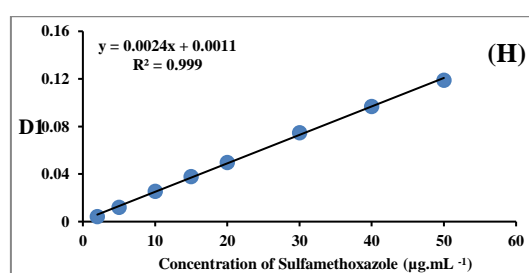
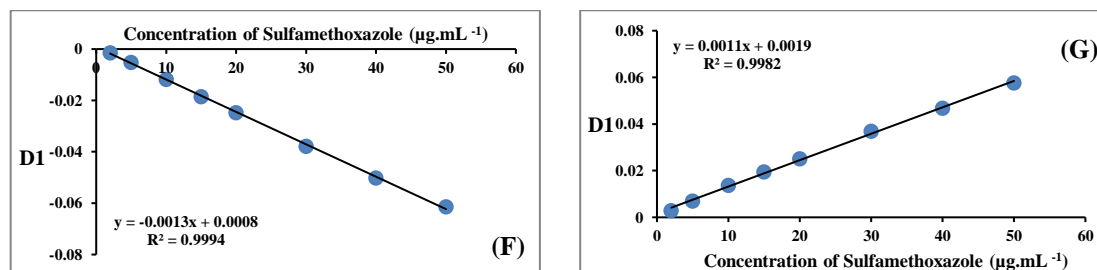
**Figure 4-16:** Calibration curves obtained via first derivative spectra of mixture of Sulfamethoxazole (2-50 µg.mL<sup>-1</sup>) in the presence of (2 µg.mL<sup>-1</sup>) Sulfanilamide, for height at zero cross at (F) 235.62 nm, (G) 258.72 nm and (H) height to height between (235.62-285.72 nm).



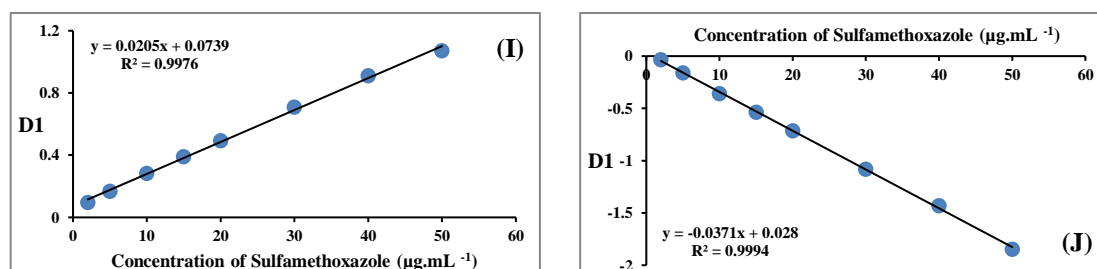
**Figure 4-17:** Calibration curves obtained via first derivative spectra of mixture of Sulfamethoxazole (2-50 µg.mL<sup>-1</sup>) in the presence of (2 µg.mL<sup>-1</sup>) Sulfanilamide, for peak area at the interval (I) 241.95 nm to 267.04 nm and (J) 267.04 nm to 330 nm.



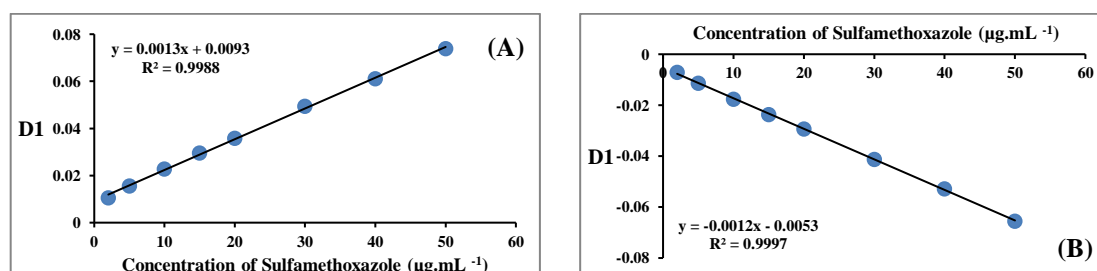
**Figure 4-18:** Calibration curves obtained via first derivative spectra of mixture of Sulfamethoxazole ( $2-50 \mu\text{g.mL}^{-1}$ ) in the presence of ( $5 \mu\text{g.mL}^{-1}$ ) Sulfanilamide, for peak-to-baseline at (A) 254 nm, (B) 287 nm, (C) 223 nm, (D) peak to peak between (254-287 nm) and (E) peak to peak between (223-254 nm).



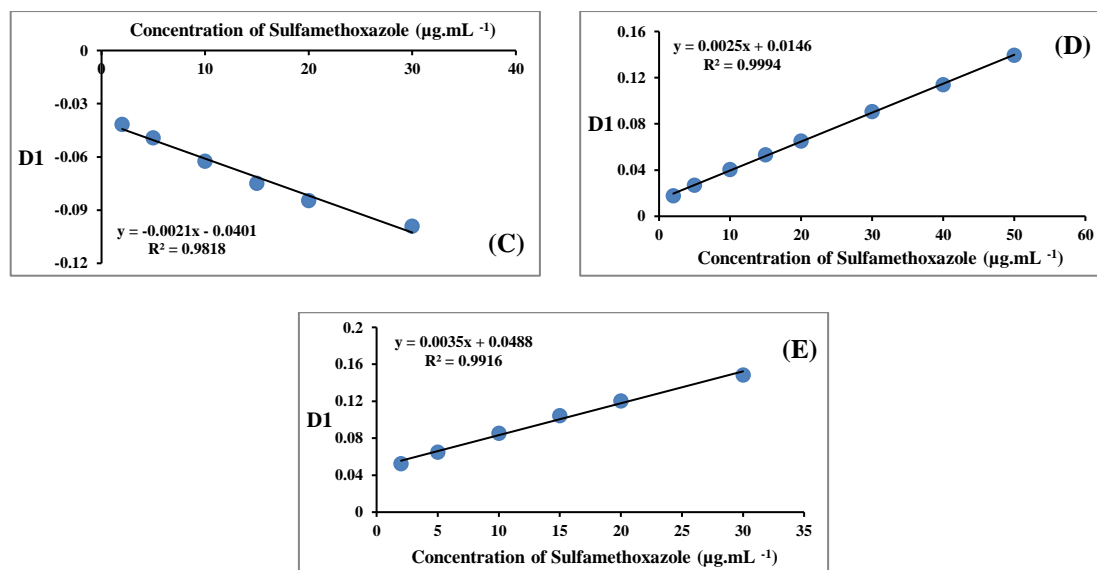
**Figure 4-19:** Calibration curves obtained via first derivative spectra of mixture of Sulfamethoxazole ( $2-50 \mu\text{g.mL}^{-1}$ ) in the presence of ( $5 \mu\text{g.mL}^{-1}$ ) Sulfanilamide, for height at zero cross at (F) 235.62 nm, (G) 258.72 nm and (H) height to height between (235.62-285.72 nm).



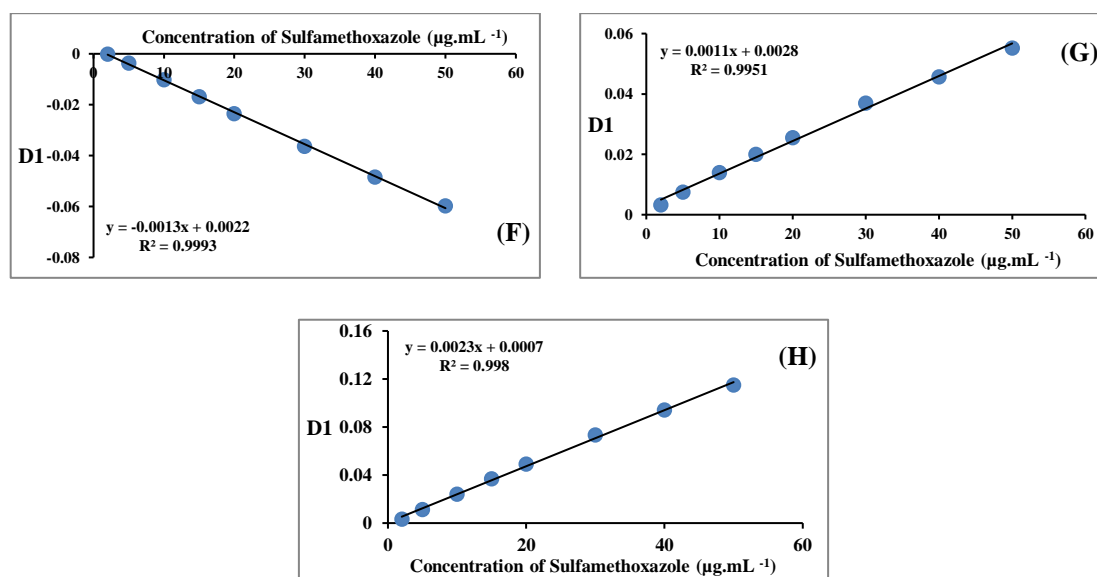
**Figure 4-20:** Calibration curves obtained via first derivative spectra of mixture of Sulfamethoxazole ( $2-50 \mu\text{g.mL}^{-1}$ ) in the presence of ( $5 \mu\text{g.mL}^{-1}$ ) Sulfanilamide, for peak area at the interval (I) 241.95 nm to 267.04 nm and (J) 267.04 nm to 330 nm.



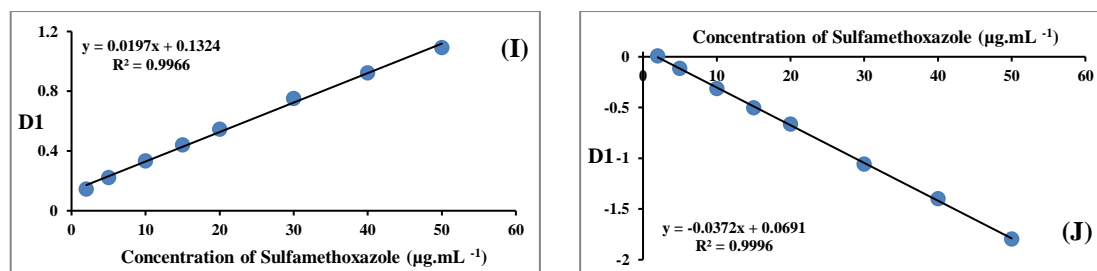




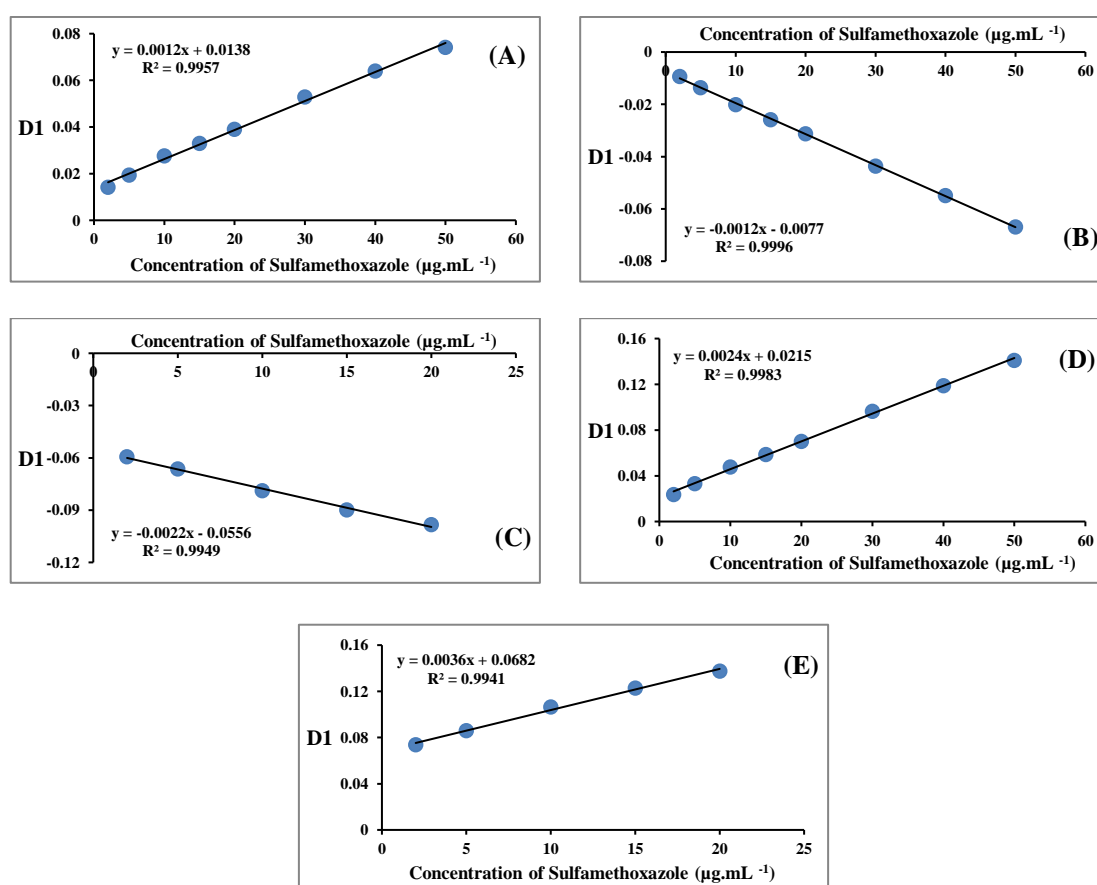
**Figure 4-21:** Calibration curves obtained via first derivative spectra of mixture of Sulfamethoxazole (2-50 µg.mL<sup>-1</sup>) in the presence of (10 µg.mL<sup>-1</sup>) Sulfanilamide, for peak-to-baseline at (A) 254 nm, (B) 287 nm, (C) 223 nm, (D) peak to peak between (254-287 nm) and (E) peak to peak between (223-254 nm).



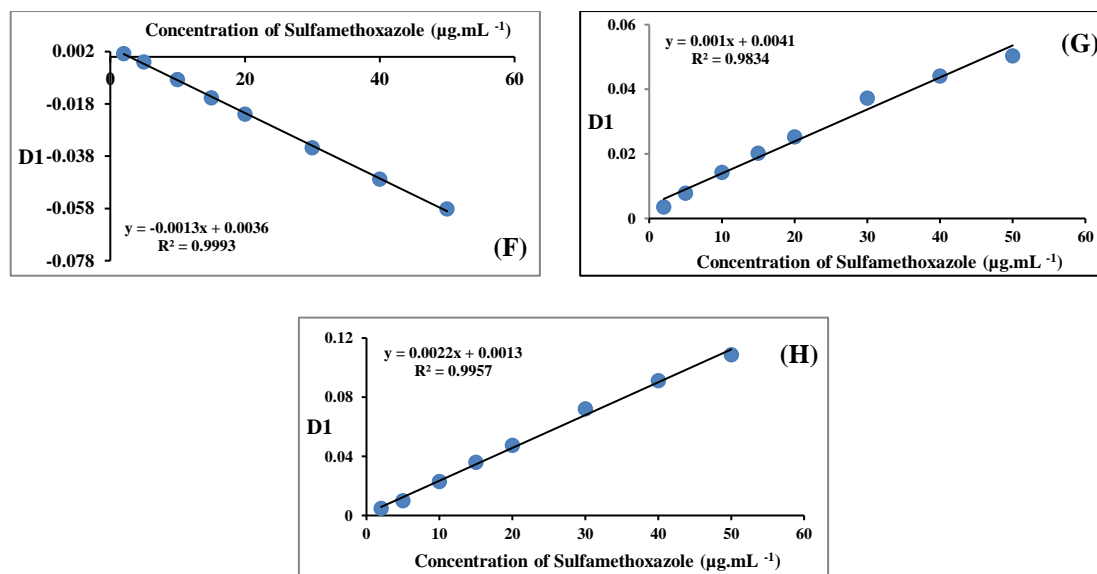
**Figure 4-22:** Calibration curves obtained via first derivative spectra of mixture of Sulfamethoxazole (2-50 µg.mL<sup>-1</sup>) in the presence of (10 µg.mL<sup>-1</sup>) Sulfanilamide, for height at zero cross at (F) 235.62 nm, (G) 258.72 nm and (H) height to height between (235.62-285.72 nm).



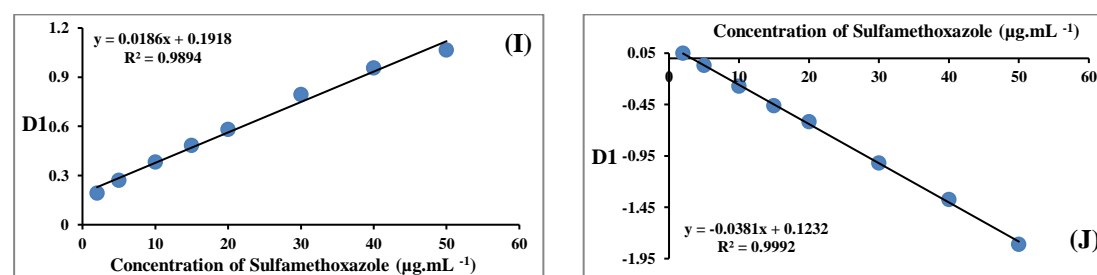
**Figure 4-23:** Calibration curves obtained via first derivative spectra of mixture of Sulfamethoxazole (2-50 µg.mL<sup>-1</sup>) in the presence of (10 µg.mL<sup>-1</sup>) Sulfanilamide, for peak area at the interval (I) 241.95 nm to 267.04 nm and (J) 267.04 nm to 330 nm.



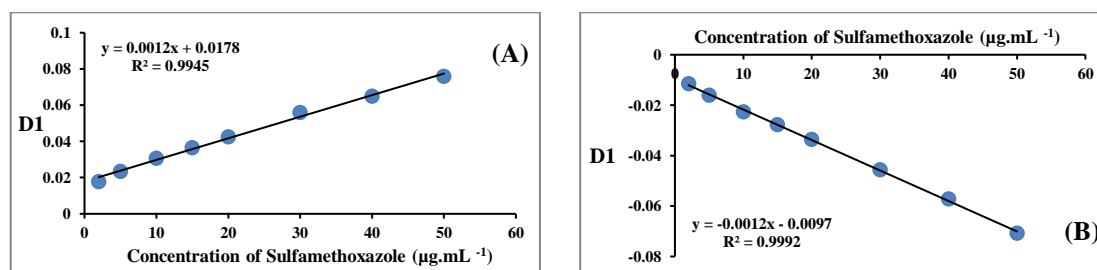
**Figure 4-24:** Calibration curves obtained via first derivative spectra of mixture of Sulfamethoxazole (2-50 µg.mL<sup>-1</sup>) in the presence of (15 µg.mL<sup>-1</sup>) Sulfanilamide, for peak-to-baseline at (A) 254 nm, (B) 287 nm, (C) 223 nm, (D) peak to peak between (254-287 nm) and (E) peak to peak between (223-254 nm).



**Figure 4-25:** Calibration curves obtained via first derivative spectra of mixture of Sulfamethoxazole ( $2\text{-}50 \mu\text{g.mL}^{-1}$ ) in the presence of ( $15 \mu\text{g.mL}^{-1}$ ) Sulfanilamide, for height at zero cross at (F) 235.62 nm, (G) 258.72 nm and (H) height to height between (235.62-285.72 nm).



**Figure 4-26:** Calibration curves obtained via first derivative spectra of mixture of Sulfamethoxazole ( $2\text{-}50 \mu\text{g.mL}^{-1}$ ) in the presence of ( $15 \mu\text{g.mL}^{-1}$ ) Sulfanilamide, for peak area at the interval (I) 241.95 nm to 267.04 nm and (J) 267.04 nm to 330 nm.



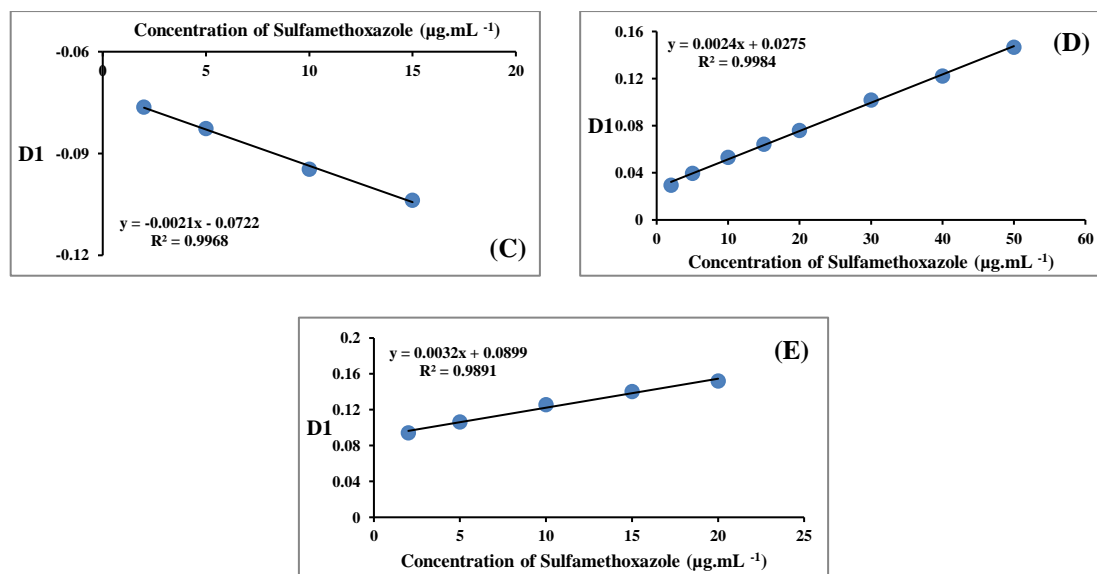


**Figure 4-27:** Calibration curves obtained via first derivative spectra of mixture of Sulfamethoxazole ( $2\text{-}50 \mu\text{g.mL}^{-1}$ ) in the presence of ( $20 \mu\text{g.mL}^{-1}$ ) Sulfanilamide, for peak-to-baseline at (A) 254 nm, (B) 287 nm, (C) 223 nm, (D) peak to peak between (254-287 nm) and (E) peak to peak between (223-254 nm).

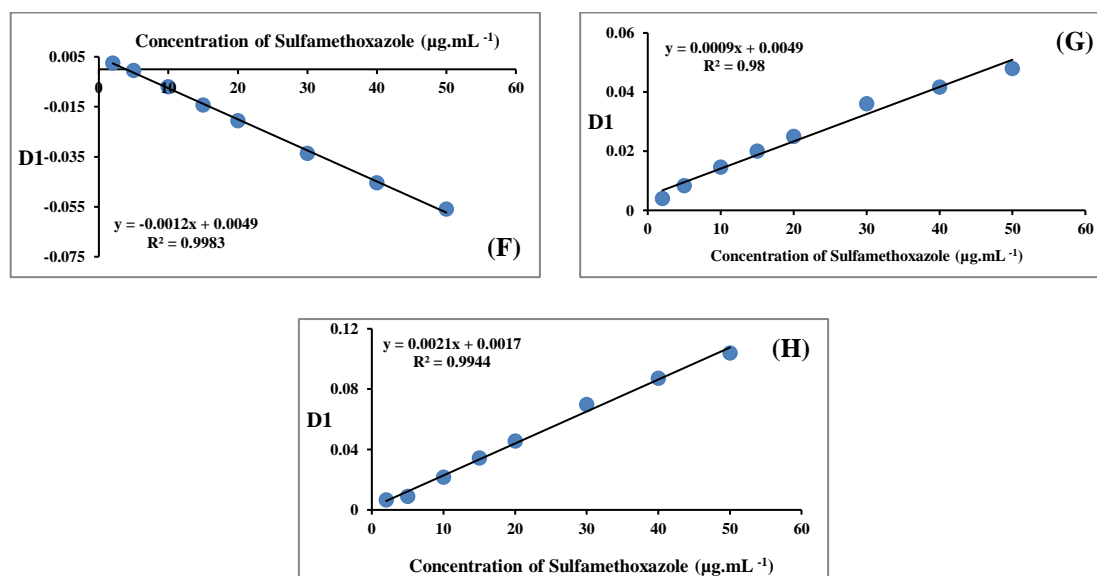


**Figure 4-28:** Calibration curves obtained via first derivative spectra of mixture of Sulfamethoxazole ( $2\text{-}50 \mu\text{g.mL}^{-1}$ ) in the presence of ( $20 \mu\text{g.mL}^{-1}$ ) Sulfanilamide, for height at zero cross at (F) 235.62 nm, (G) 258.72 nm and (H) height to height between (235.62-285.72 nm).

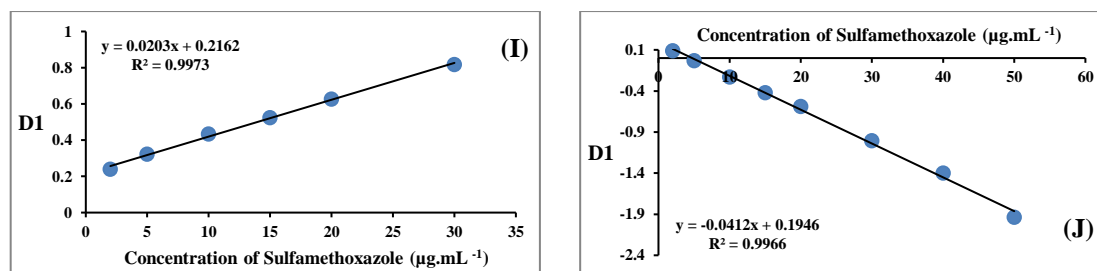


**Figure 4-29:** Calibration curves obtained via first derivative spectra of mixture of Sulfamethoxazole ( $2\text{-}50\ \mu\text{g.mL}^{-1}$ ) in the presence of ( $20\ \mu\text{g.mL}^{-1}$ ) Sulfanilamide, for peak area at the interval (I)  $241.95\ \text{nm}$  to  $267.04\ \text{nm}$  and (J)  $267.04\ \text{nm}$  to  $330\ \text{nm}$ .

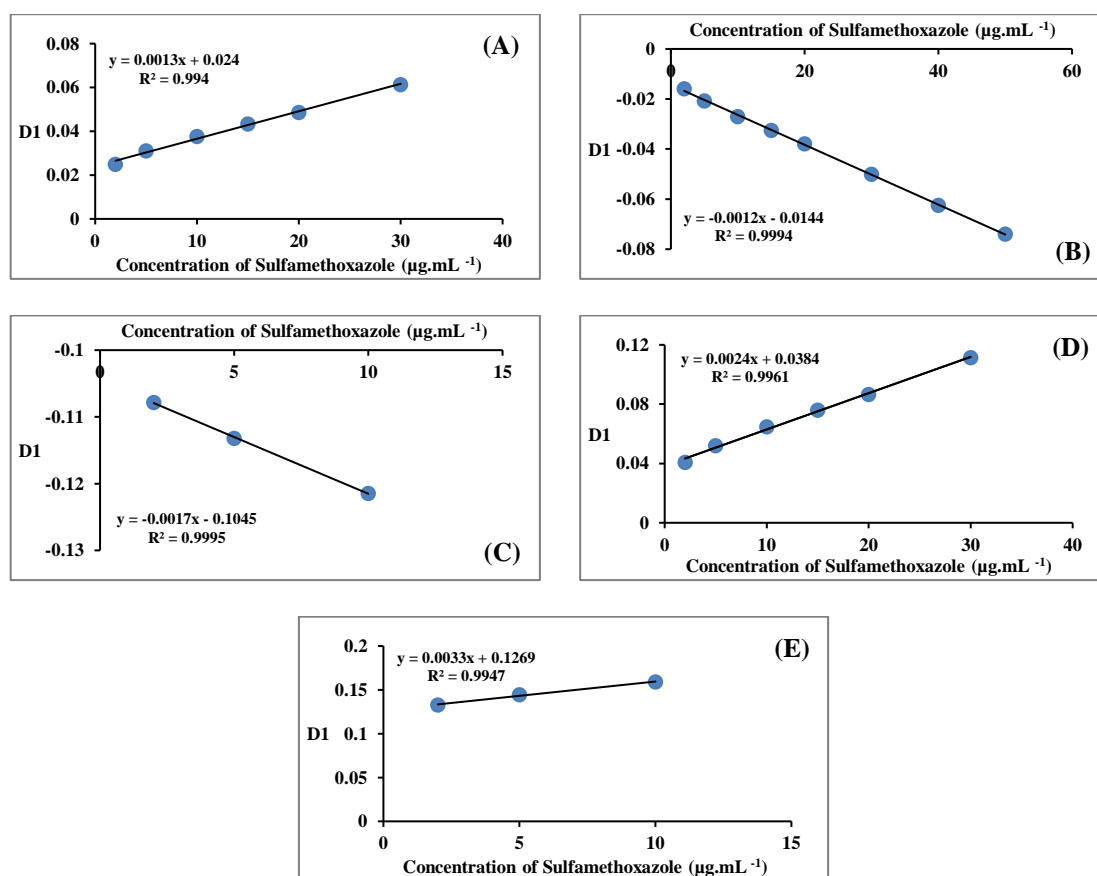


**Figure 4-30:** Calibration curves obtained via first derivative spectra of mixture of Sulfamethoxazole ( $2\text{-}50\ \mu\text{g.mL}^{-1}$ ) in the presence of ( $30\ \mu\text{g.mL}^{-1}$ ) Sulfanilamide, for peak-to-baseline at (A)  $254\ \text{nm}$ , (B)  $287\ \text{nm}$ , (C)  $223\ \text{nm}$ , (D) peak to peak between ( $254\text{-}287\ \text{nm}$ ) and (E) peak to peak between ( $223\text{-}254\ \text{nm}$ ).

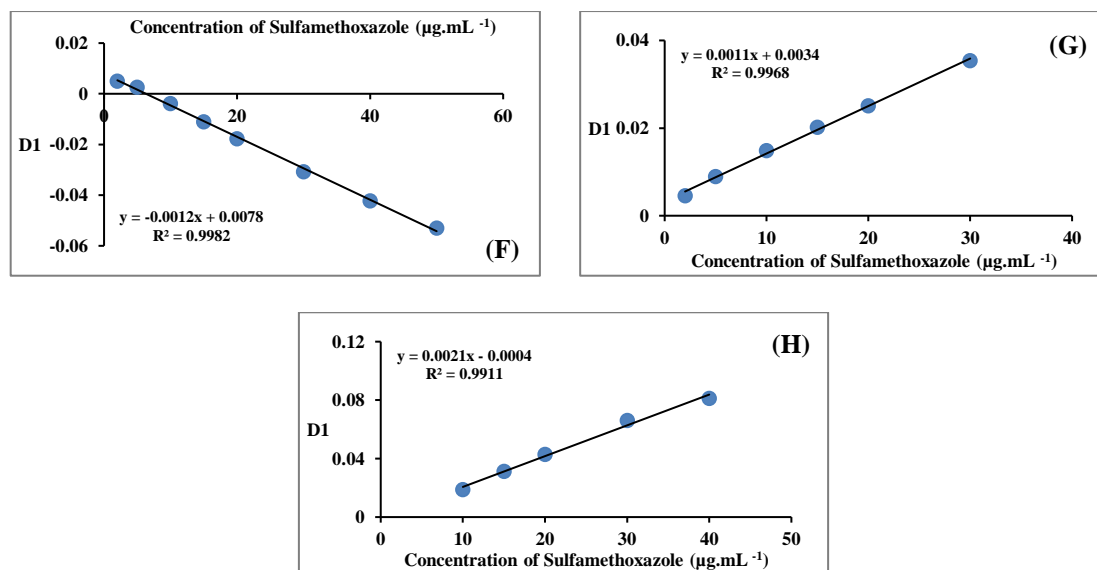


**Figure 4-31:** Calibration curves obtained via first derivative spectra of mixture of Sulfamethoxazole ( $2\text{-}50 \mu\text{g.mL}^{-1}$ ) in the presence of ( $30 \mu\text{g.mL}^{-1}$ ) Sulfanilamide, for height at zero cross at (F)  $235.62 \text{ nm}$ , (G)  $258.72 \text{ nm}$  and (H) height to height between ( $235.62\text{-}285.72 \text{ nm}$ ).

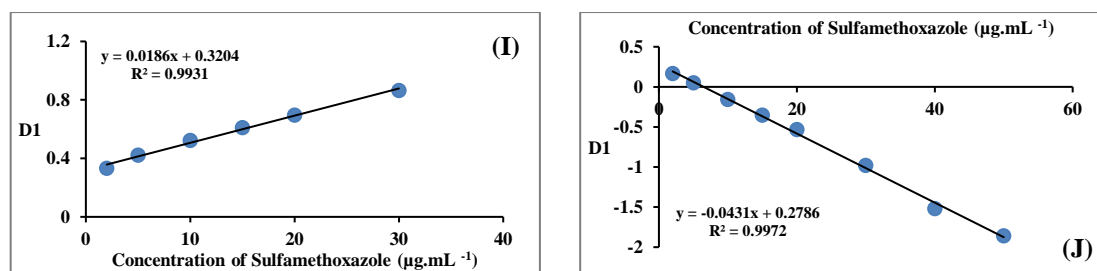


**Figure 4-32:** Calibration curves obtained via first derivative spectra of mixture of Sulfamethoxazole ( $2\text{-}50 \mu\text{g.mL}^{-1}$ ) in the presence of ( $30 \mu\text{g.mL}^{-1}$ ) Sulfanilamide, for peak area at the interval (I)  $241.95 \text{ nm}$  to  $267.04 \text{ nm}$  and (J)  $267.04 \text{ nm}$  to  $330 \text{ nm}$ .

The careful inspection of the second derivative spectra obtained for the mentioned mixtures of sulfamethoxazole and sulfanilamide shows that peak to baseline at ( $239.5, 263.5, 267.75, 301, 215 \text{ nm}$ ), height to baseline at zero cross at ( $245.86, 271.28 \text{ nm}$ ), peak to peak between ( $239.5\text{-}264.25 \text{ nm}$ ), ( $239.5\text{-}267.75 \text{ nm}$ ), ( $271.28\text{-}301 \text{ nm}$ ), ( $215\text{-}239.5 \text{ nm}$ ), height to height at two zero cross ( $245.86\text{-}271.28 \text{ nm}$ ) in addition to peak area at the interval between ( $254.12\text{-}281 \text{ nm}$ ), ( $286.95\text{-}329.5 \text{ nm}$ ), ( $221.75\text{-}254.12 \text{ nm}$ ) measurements at specified wavelength could be used to quantify the exact concentration of sulfamethoxazole in the presence of sulfanilamide. Figures 4-33 – 4-39 show the calculated second derivative spectra of sulfamethoxazole alone and with different mixtures of the cited drugs while, Figures 4-40 – 4-67 represent the calibration graphs

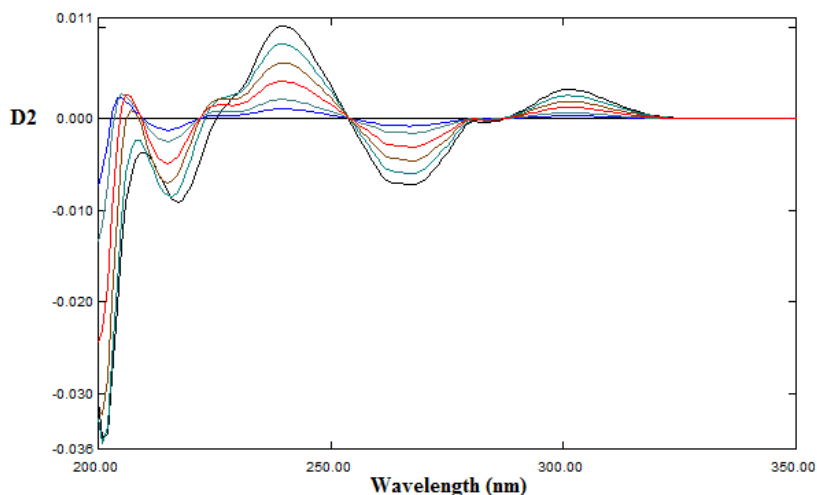


**Figure 4-33:** Second derivative spectra of (5-50  $\mu\text{g.mL}^{-1}$ ) sulfamethoxazole.

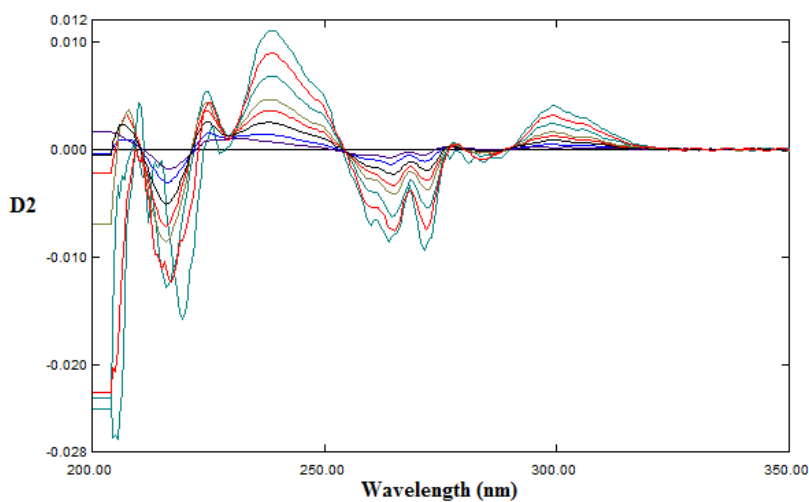


**Figure 4-34:** Second derivative spectra of mixture contain (2-50  $\mu\text{g.mL}^{-1}$ ) sulfamethoxazole in the presence of (2  $\mu\text{g.mL}^{-1}$ ) sulfanilamide.

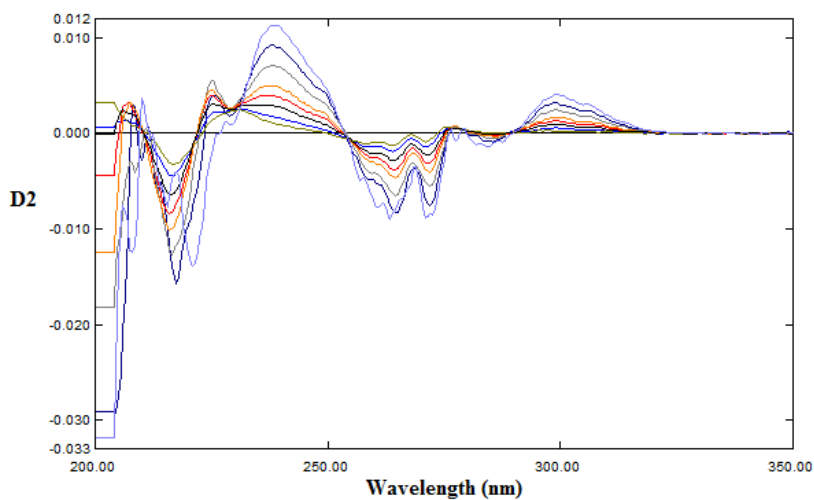


**Figure 4-35:** Second derivative spectra of mixture contain (2-50  $\mu\text{g.mL}^{-1}$ ) sulfamethoxazole in the presence of (5  $\mu\text{g.mL}^{-1}$ ) sulfanilamide.

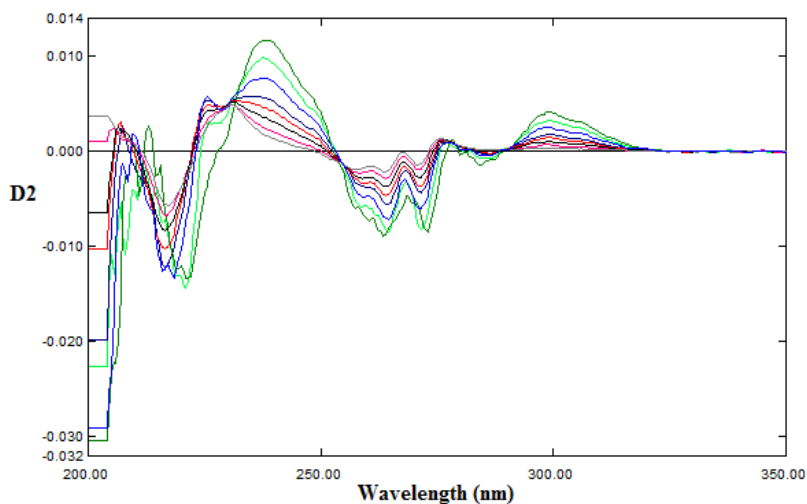


**Figure 4-36:** Second derivative spectra of mixture contain (2-50  $\mu\text{g.mL}^{-1}$ ) sulfamethoxazole in the presence of (10  $\mu\text{g.mL}^{-1}$ ) sulfanilamide.

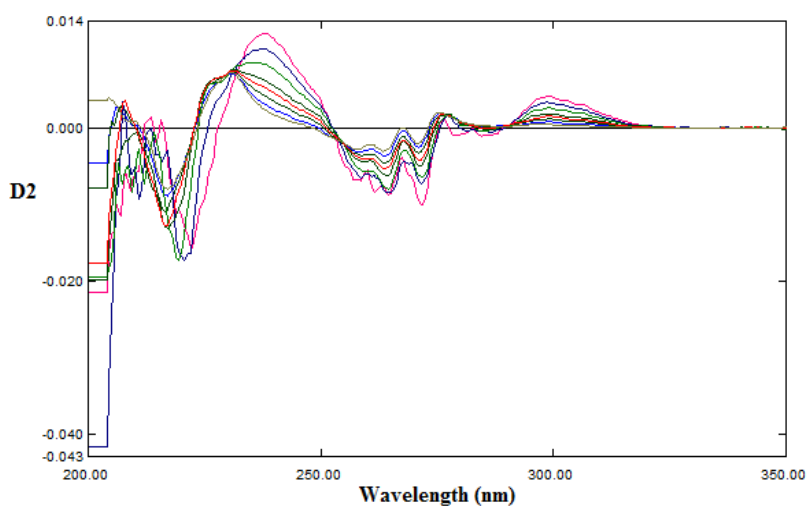


**Figure 4-37:** Second derivative spectra of mixture contain (2-50  $\mu\text{g.mL}^{-1}$ ) sulfamethoxazole in the presence of (15  $\mu\text{g.mL}^{-1}$ ) sulfanilamide.

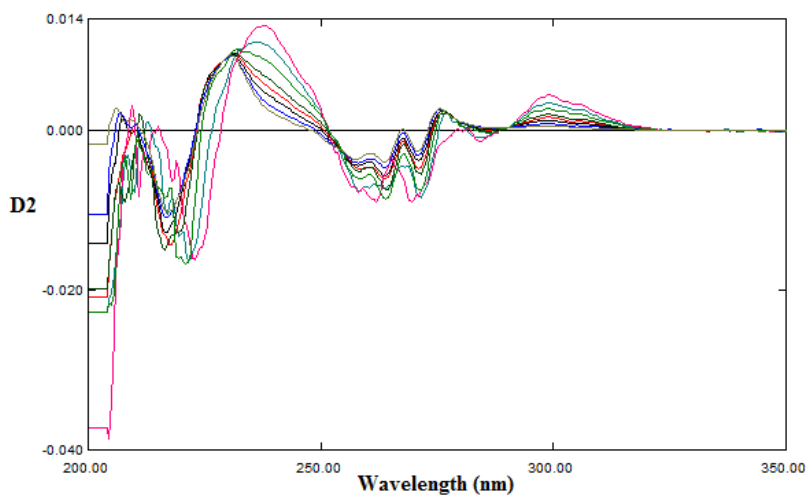


**Figure 4-38:** Second derivative spectra of mixture contain (2-50  $\mu\text{g.mL}^{-1}$ ) sulfamethoxazole in the presence of (20  $\mu\text{g.mL}^{-1}$ ) sulfanilamide.



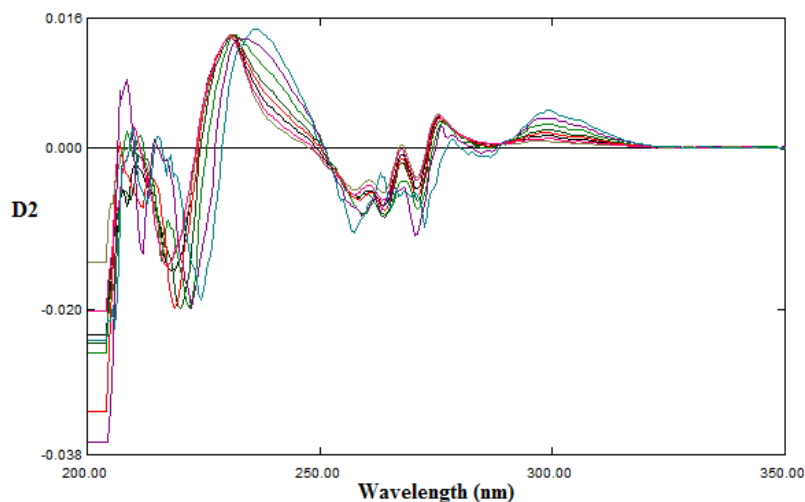


**Figure 4-39:** Second derivative spectra of mixture contain (2-50  $\mu\text{g.mL}^{-1}$ ) sulfamethoxazole in the presence of (30  $\mu\text{g.mL}^{-1}$ ) sulfanilamide.

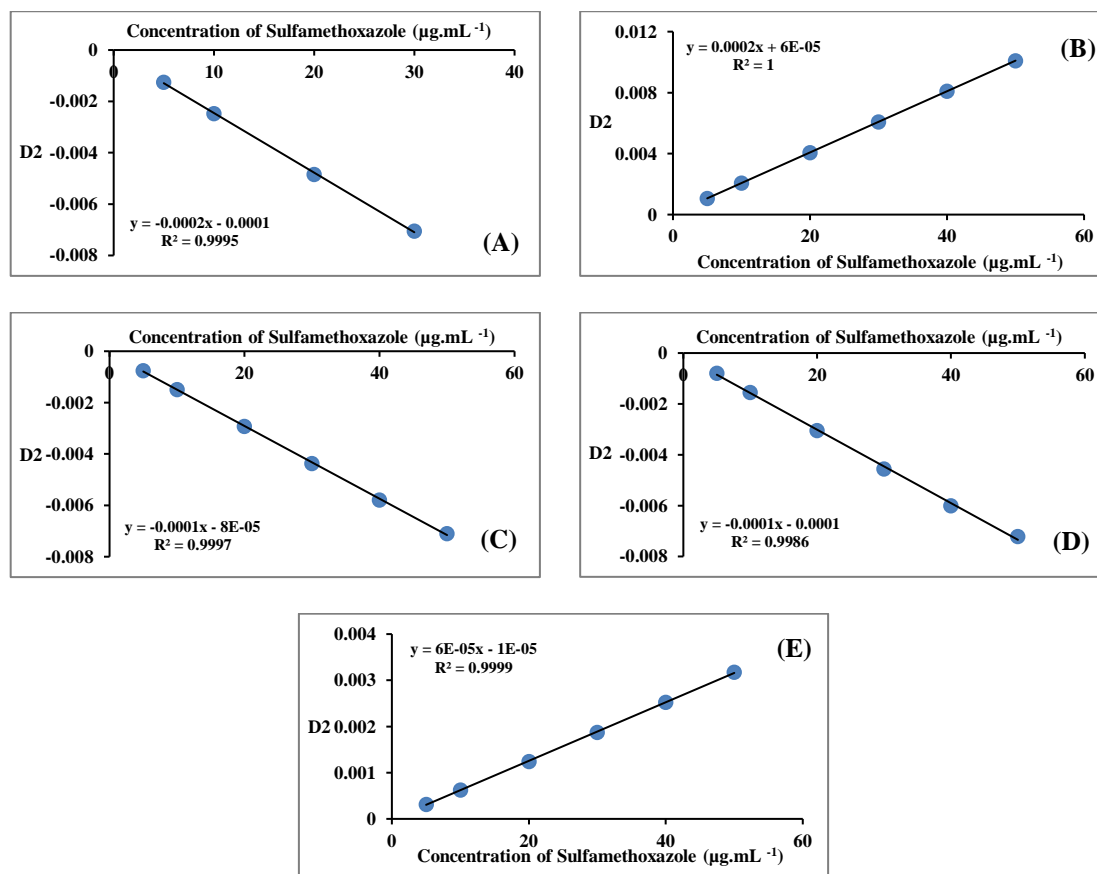


**Figure 4-40:** Calibration curves obtained via second derivative spectra of sulfamethoxazole for peak-to-baseline at (A) 215 nm, (B) 239.5 nm, (C) 264.25 nm, (D) 267.75 nm and (E) 301 nm.

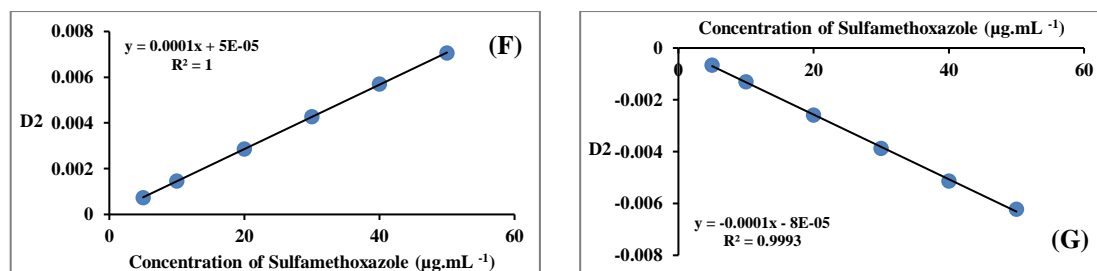


**Figure 4-41:** Calibration curves obtained via second derivative spectra of sulfamethoxazole for height at zero cross at (F) 245.86 nm and (G) 271.28 nm.

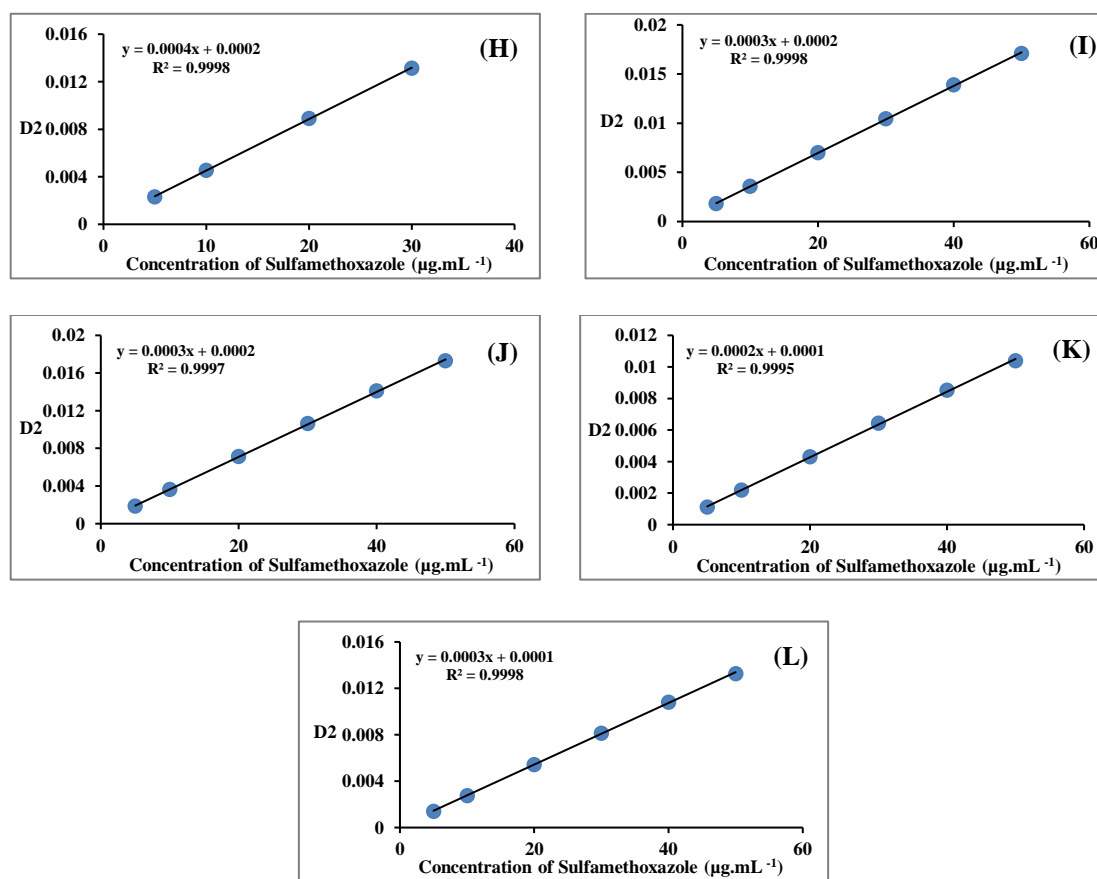


**Figure 4-42:** Calibration curves obtained via second derivative spectra of sulfamethoxazole for peak to peak, between (H) (215-239.5 nm), (I) (239.5-264.25 nm), (J) (239.5-267.75 nm), (K) (271.28-301 nm) and (L) height to height at zero cross (245.86-271.28 nm).

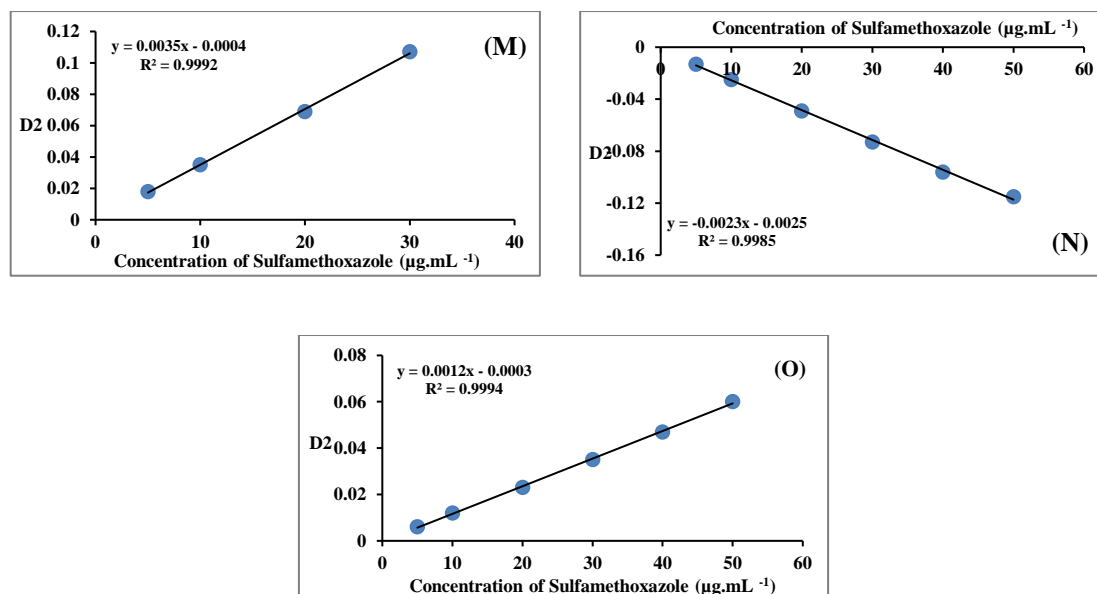


**Figure 4-43:** Calibration curves obtained via second derivative spectra of sulfamethoxazole for peak area at the interval (M) 221.75 nm to 254.12 nm, (N) 254.12 nm to 281 nm and (O) 286.86 nm to 329.5 nm.

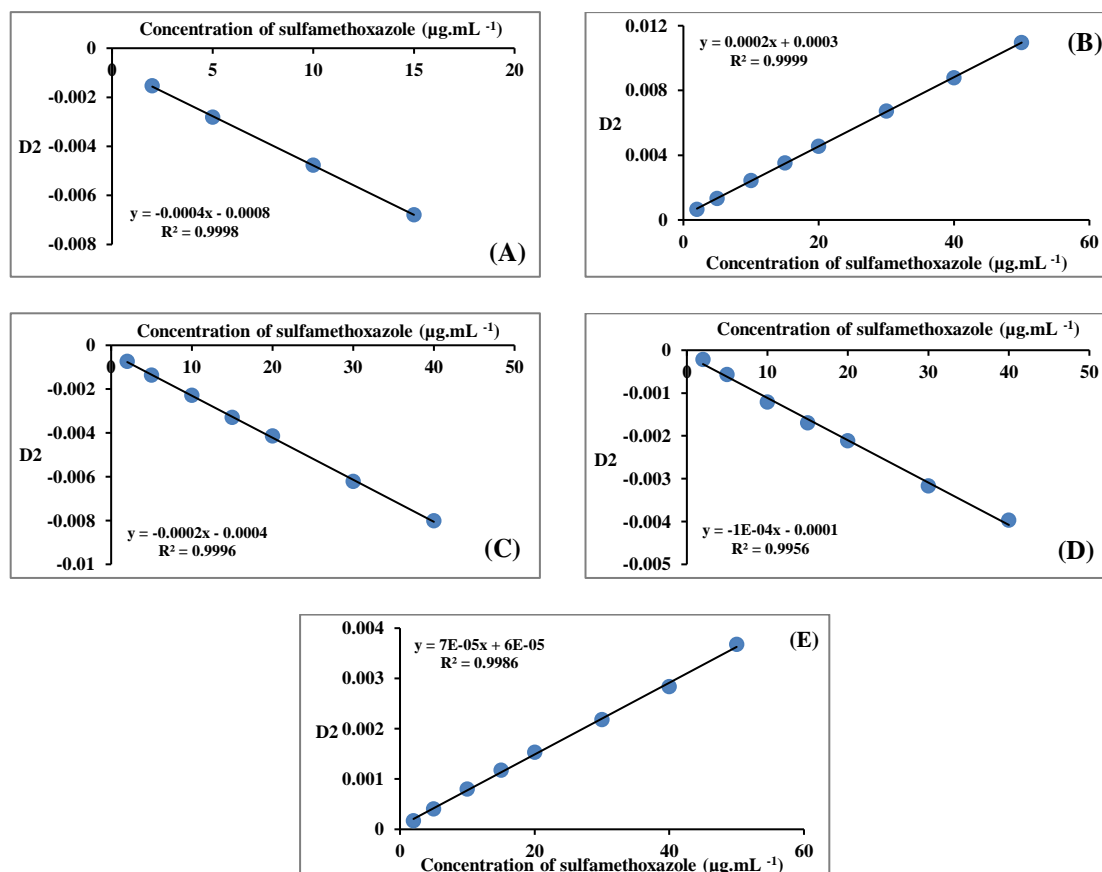


**Figure 4-44:** Calibration curves obtained via second derivative spectra of mixture of Sulfamethoxazole (2-50 µg.mL<sup>-1</sup>) in the presence of (2 µg.mL<sup>-1</sup>) Sulfanilamide, for peak-to-baseline at (A) 215 nm, (B) 239.5 nm, (C) 264.25 nm, (D) 267.75 nm and (E) 301 nm.

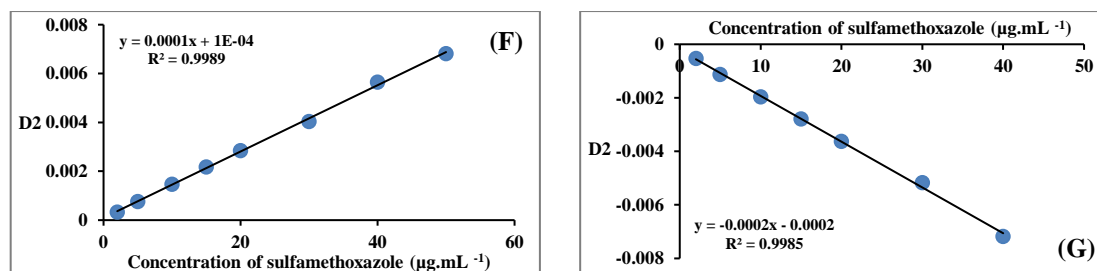


**Figure 4-45:** Calibration curves obtained via second derivative spectra of mixture of Sulfamethoxazole ( $2\text{-}50 \mu\text{g.mL}^{-1}$ ) in the presence of ( $2 \mu\text{g.mL}^{-1}$ ) Sulfanilamide, for height at zero cross at (F) 245.86 nm and (G) 271.28 nm.

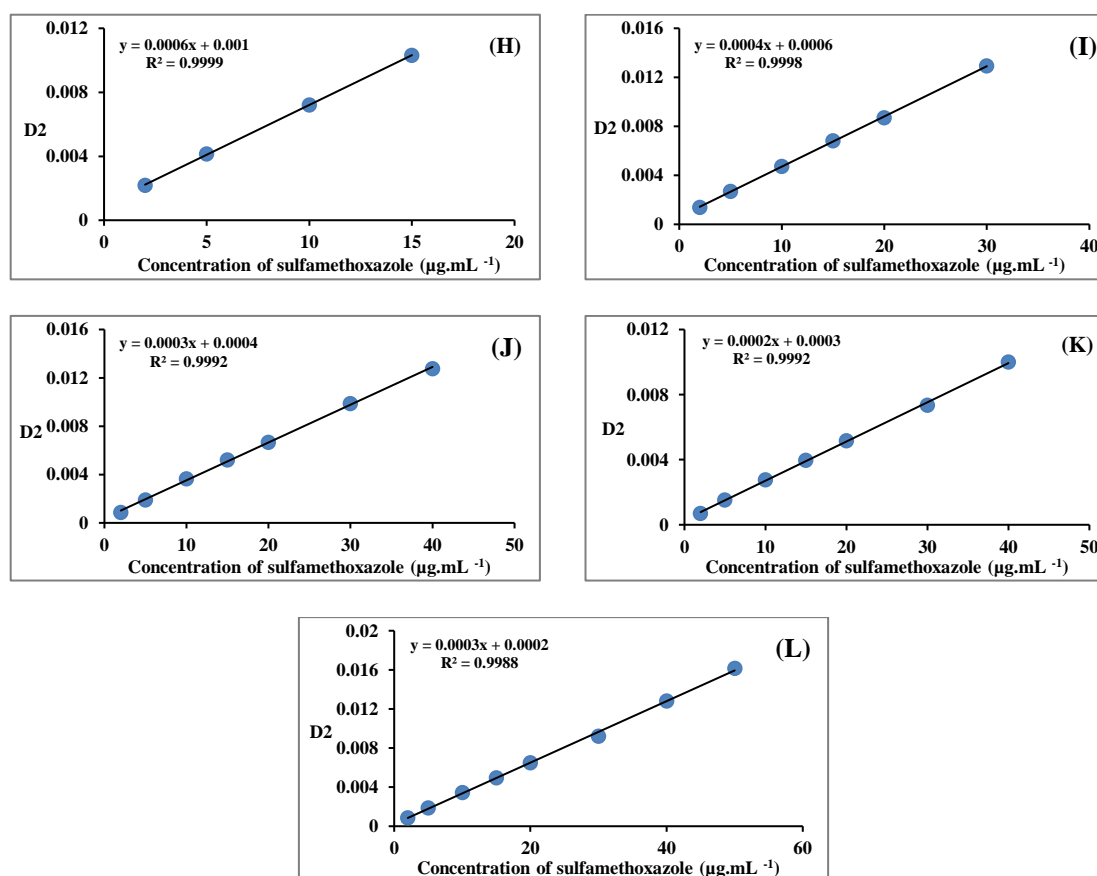


**Figure 4-46:** Calibration curves obtained via second derivative spectra of mixture of Sulfamethoxazole ( $2\text{-}50 \mu\text{g.mL}^{-1}$ ) in the presence of ( $2 \mu\text{g.mL}^{-1}$ ) Sulfanilamide, for peak to peak between (H) (215-239.5 nm), (I) (239.5-264.25 nm), (J) (239.5-267.75 nm), (K) (271.28-301 nm) and (L) height to height at zero cross (245.86-271.28 nm).

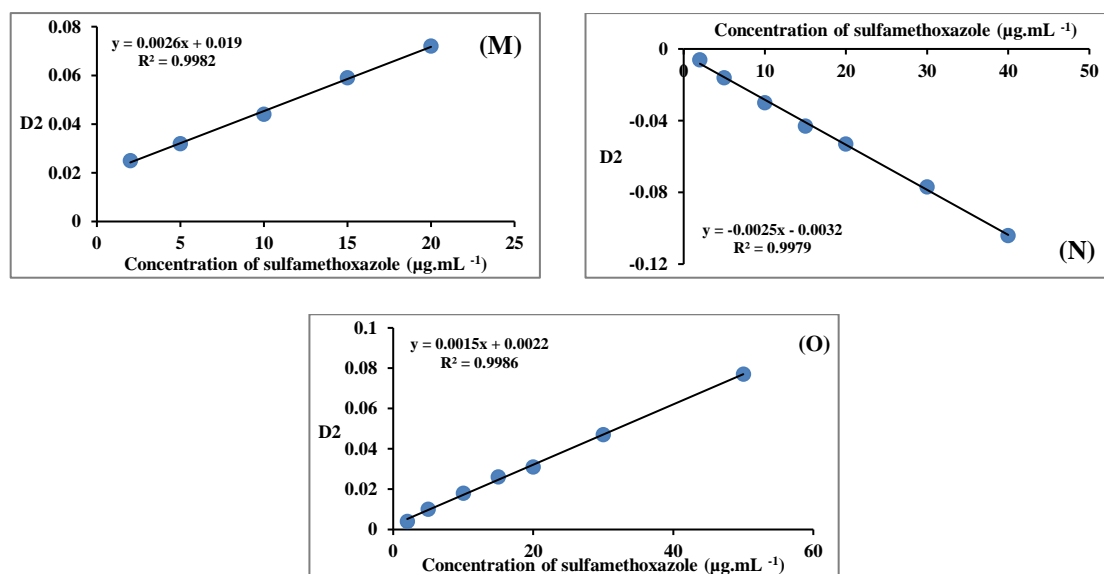


**Figure 4-47:** Calibration curves obtained via second derivative spectra of mixture of Sulfamethoxazole (2-50 µg.mL<sup>-1</sup>) in the presence of (2 µg.mL<sup>-1</sup>) Sulfanilamide, for peak area at the interval (M) 221.75 nm to 254.12 nm, (N) 254.12 nm to 281 nm and (O) 286.86 nm to 329.5 nm.

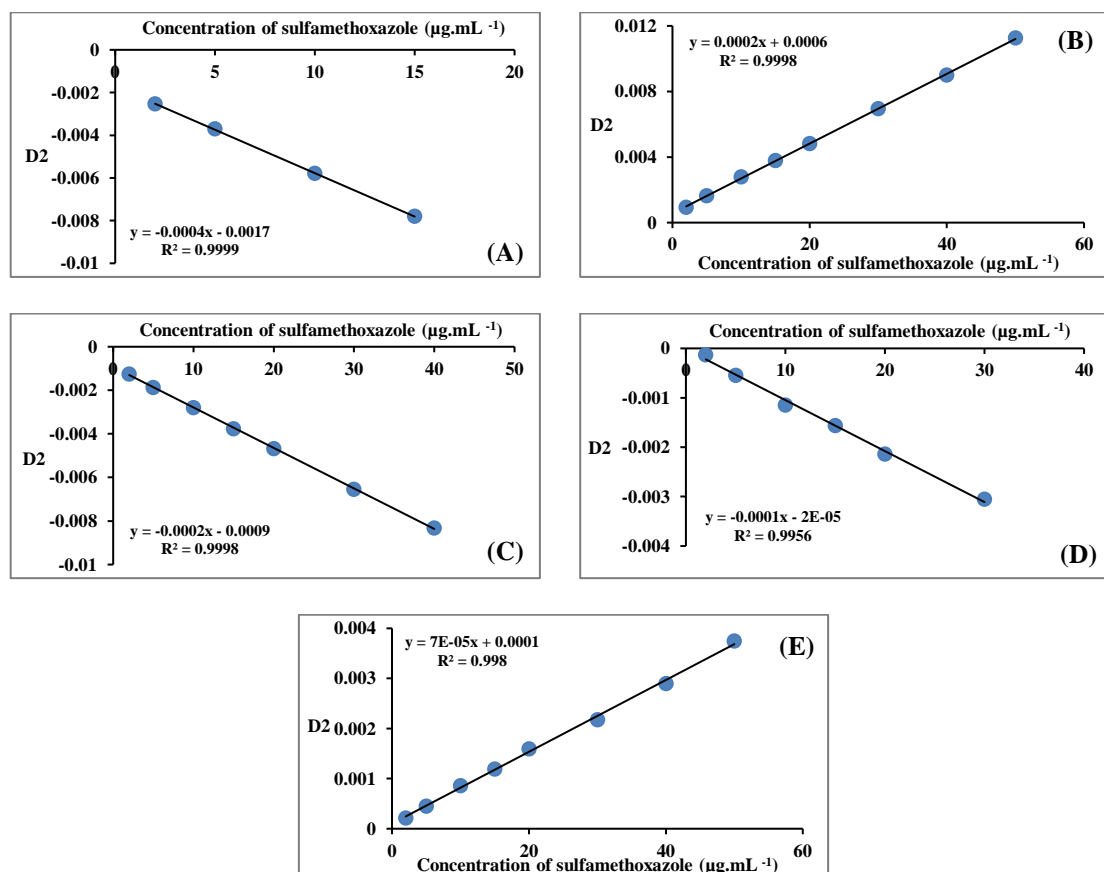


**Figure 4-48:** Calibration curves obtained via second derivative spectra of mixture of Sulfamethoxazole (2-50 µg.mL<sup>-1</sup>) in the presence of (5 µg.mL<sup>-1</sup>) Sulfanilamide, for peak-to-baseline at (A) 215 nm, (B) 239.5 nm, (C) 264.25nm, (D) 267.75 nm and (E) 301 nm.

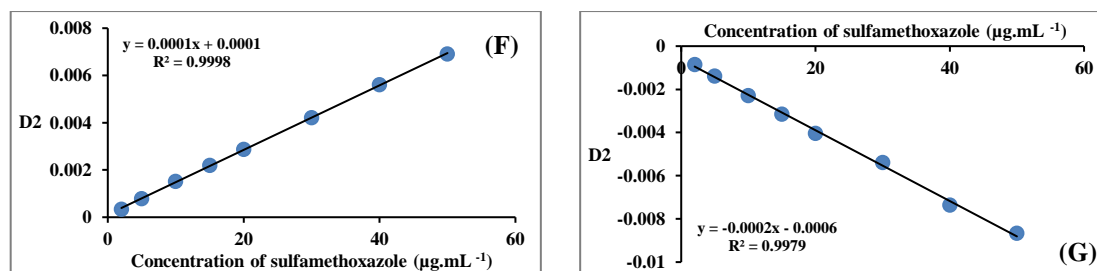


**Figure 4-49:** Calibration curves obtained via second derivative spectra of mixture of Sulfamethoxazole ( $2\text{-}50 \mu\text{g.mL}^{-1}$ ) in the presence of ( $5 \mu\text{g.mL}^{-1}$ ) Sulfanilamide, for height at zero cross at (F) 245.86 nm and (G) 271.28 nm.

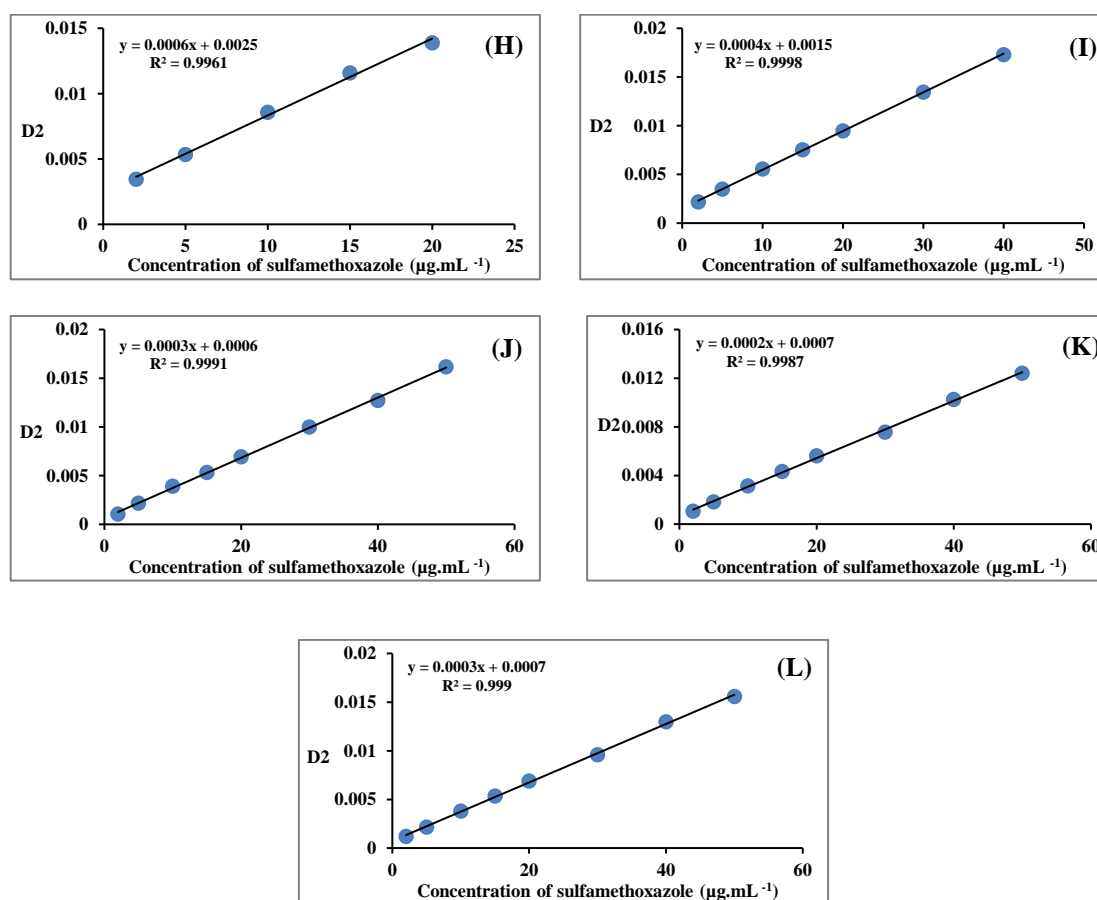


**Figure 4-50:** Calibration curves obtained via second derivative spectra of mixture of sulfamethoxazole ( $2\text{-}50 \mu\text{g.mL}^{-1}$ ) in the presence of ( $5 \mu\text{g.mL}^{-1}$ ) sulfanilamide, for peak to peak between (H) (215-239.5 nm), (I) (239.5-264.25 nm), (J) (239.5-267.7 5 nm), (K) (271.28-301 nm) and (L) height to height at zero cross (245.86-271.28 nm).

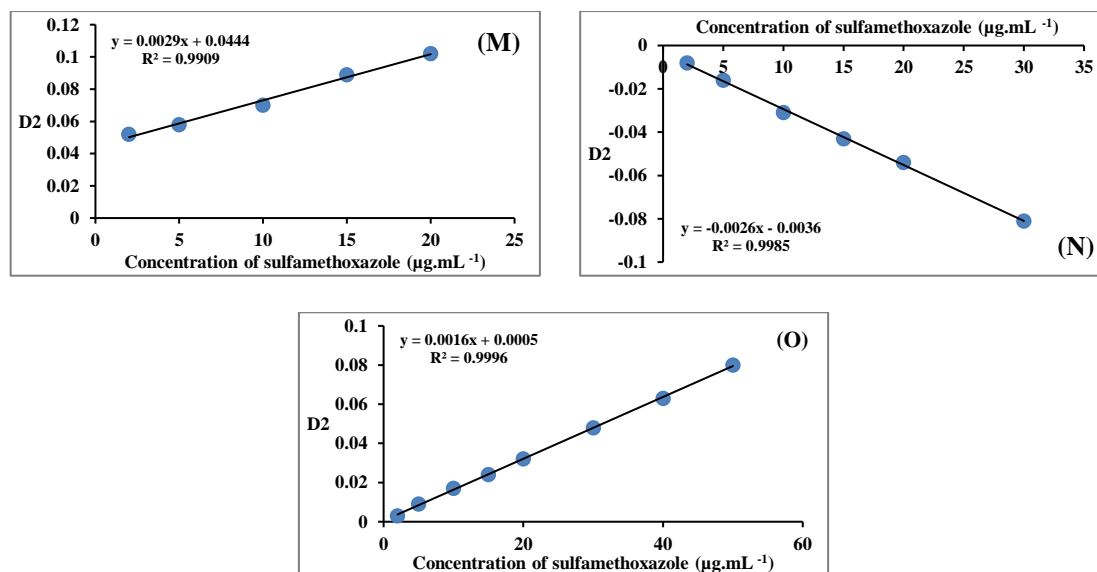


**Figure 4-51:** Calibration curves obtained via second derivative spectra of mixture of Sulfamethoxazole ( $2\text{-}50 \mu\text{g.mL}^{-1}$ ) in the presence of ( $5 \mu\text{g.mL}^{-1}$ ) Sulfanilamide, for peak area at the interval (M) 221.75 nm to 254.12 nm, (N) 254.12 nm to 281 nm and (O) 286.86 nm to 329.5 nm.

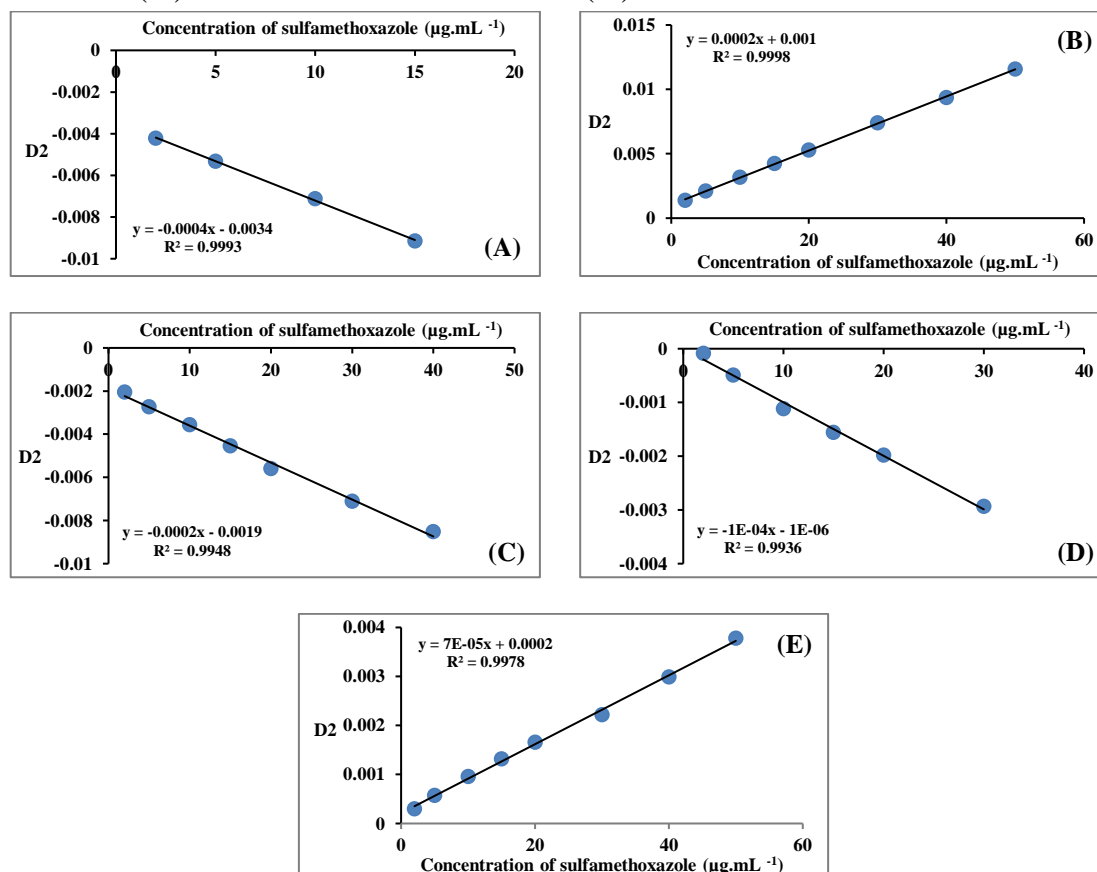


**Figure 4-52:** Calibration curves obtained via second derivative spectra of mixture of Sulfamethoxazole ( $2\text{-}50 \mu\text{g.mL}^{-1}$ ) in the presence of ( $10 \mu\text{g.mL}^{-1}$ ) Sulfanilamide, for peak-to-baseline at (A) 215 nm, (B) 239.5 nm, (C) 264.25 nm, (D) 267.75 nm and (E) 301 nm.

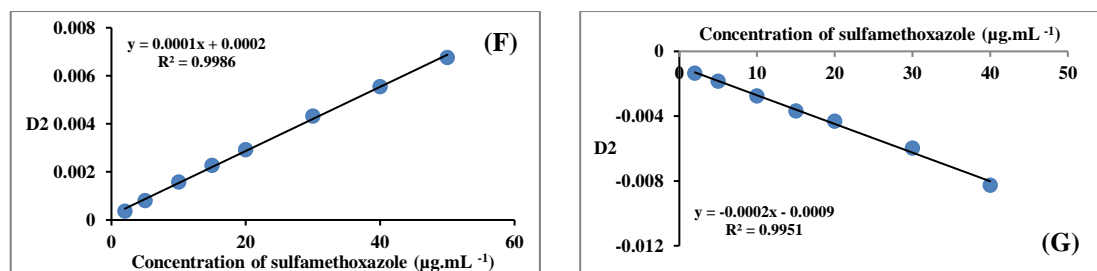


**Figure 4-53:** Calibration curves obtained via second derivative spectra of mixture of Sulfamethoxazole ( $2\text{-}50 \mu\text{g.mL}^{-1}$ ) in the presence of ( $10 \mu\text{g.mL}^{-1}$ ) Sulfanilamide, for height at zero cross at (F) 245.86 nm and (G) 271.28 nm.

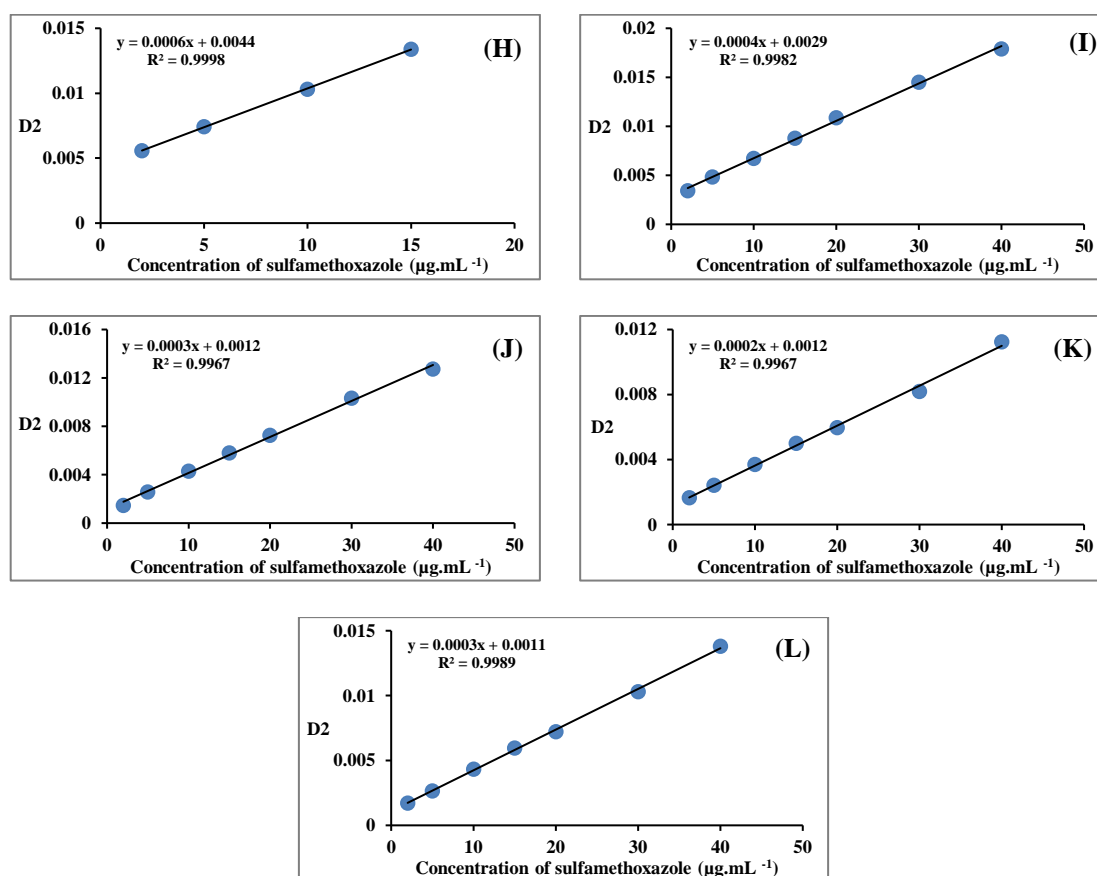


**Figure 4-54:** Calibration curves obtained via second derivative spectra of mixture of sulfamethoxazole ( $2\text{-}50 \mu\text{g.mL}^{-1}$ ) in the presence of ( $10 \mu\text{g.mL}^{-1}$ ) sulfanilamide, for peak to peak between (H) (215-239.5 nm), (I) (239.5-264.25 nm), (J) (239.5-267.75 nm), (K) (271.28-301 nm) and (L) height to height at zero cross (245.86-271.28 nm).



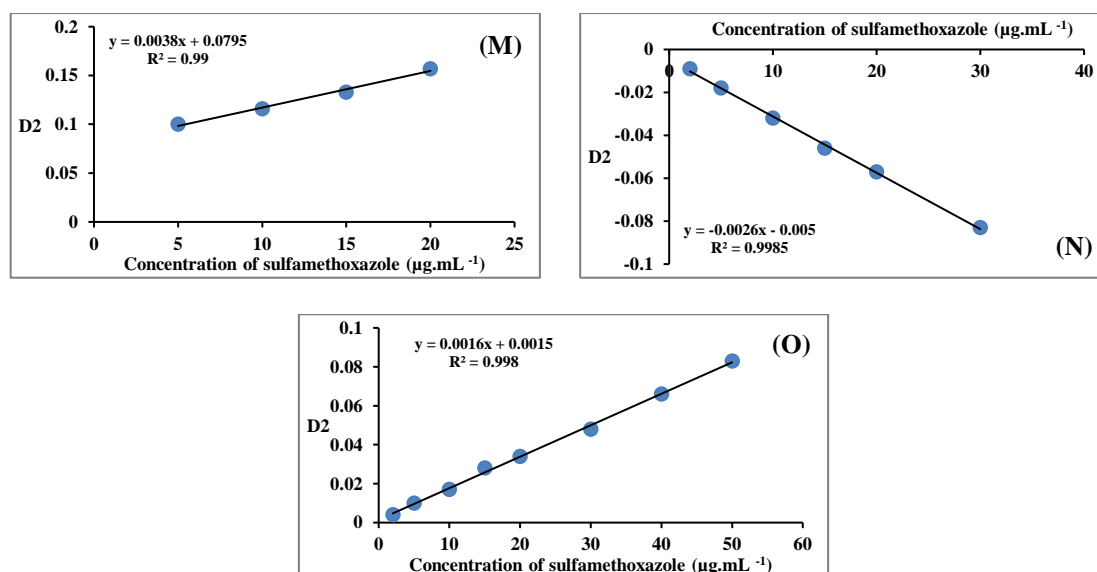


**Figure 4-55:** Calibration curves obtained via second derivative spectra of mixture of Sulfamethoxazole (2-50 µg.mL<sup>-1</sup>) in the presence of (10 µg.mL<sup>-1</sup>) Sulfanilamide, for peak area at the interval (M) 221.75 nm to 254.12 nm, (N) 254.12 nm to 281 nm and (O) 286.86 nm to 329.5 nm.

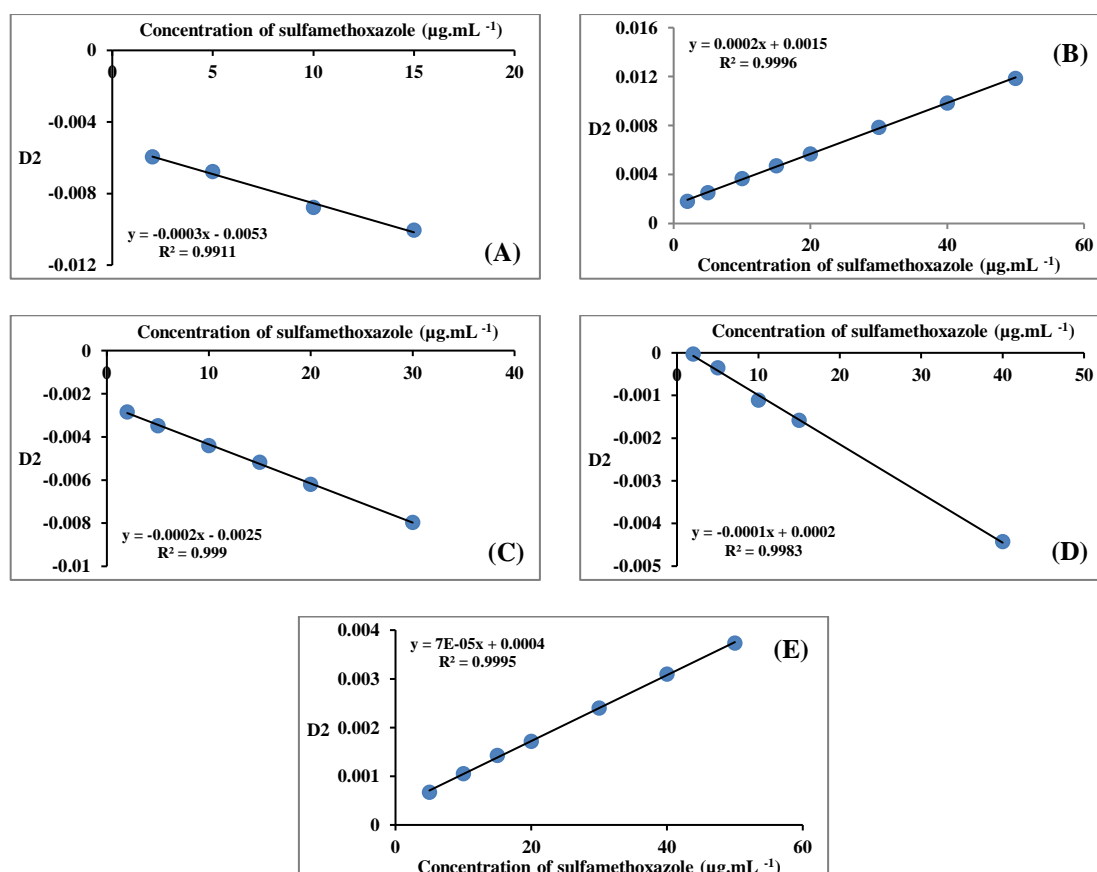


**Figure 4-56:** Calibration curves obtained via second derivative spectra of mixture of Sulfamethoxazole (2-50 µg.mL<sup>-1</sup>) in the presence of (15 µg.mL<sup>-1</sup>) Sulfanilamide, for peak-to-baseline at (A) 215 nm, (B) 239.5 nm, (C) 264.25 nm, (D) 267.75 nm and (E) 301 nm.

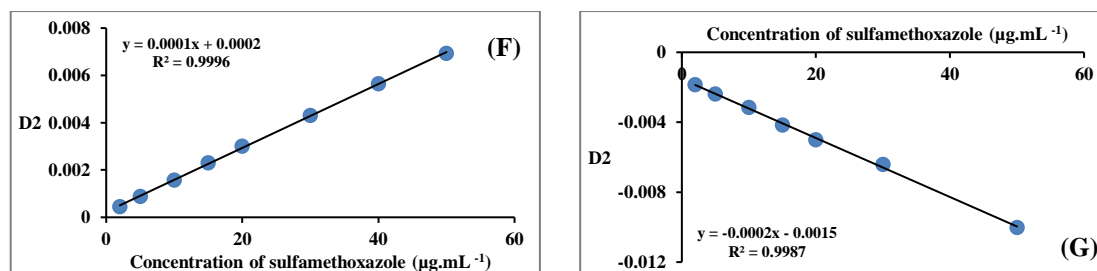


**Figure 4-57:** Calibration curves obtained via second derivative spectra of mixture of Sulfamethoxazole ( $2\text{-}50\ \mu\text{g.mL}^{-1}$ ) in the presence of ( $15\ \mu\text{g.mL}^{-1}$ ) Sulfanilamide, for height at zero cross at (F)  $245.86\ \text{nm}$  and (G)  $271.28\ \text{nm}$ .

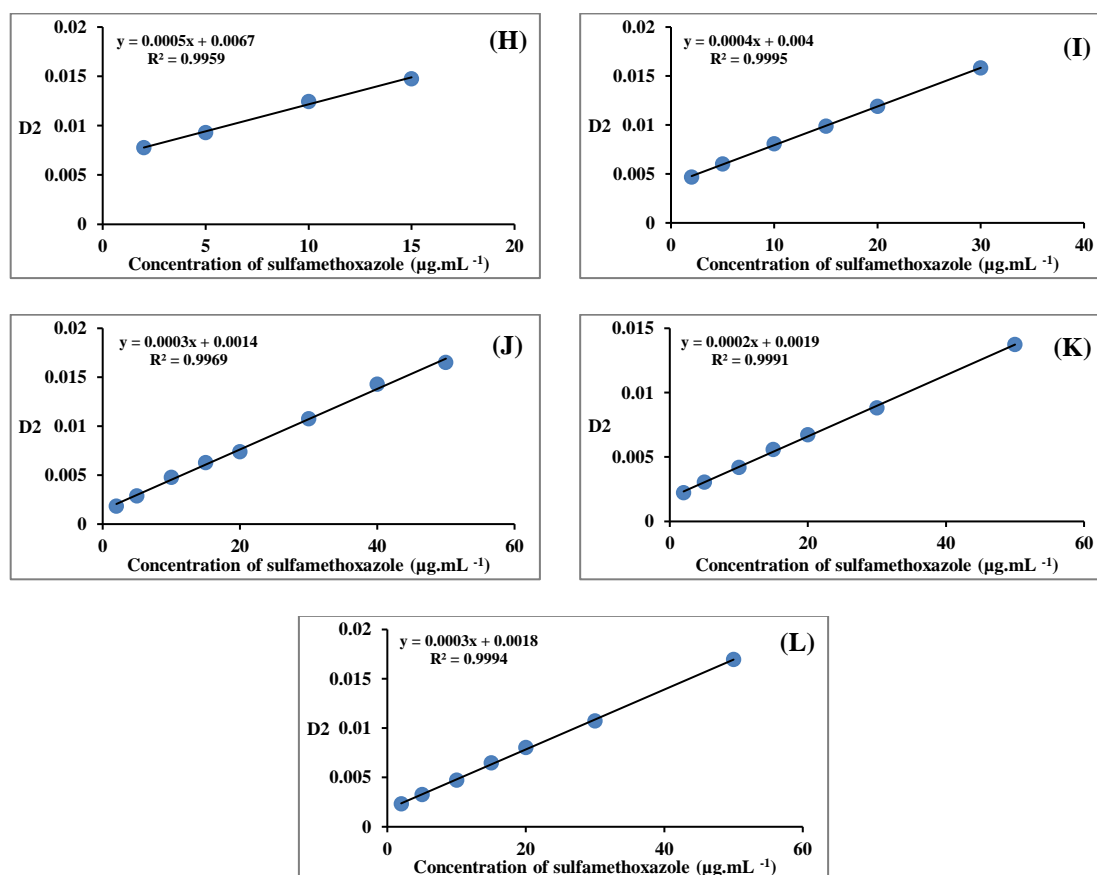


**Figure 4-58:** Calibration curves obtained via second derivative spectra of mixture of sulfamethoxazole ( $2\text{-}50\ \mu\text{g.mL}^{-1}$ ) in the presence of ( $15\ \mu\text{g.mL}^{-1}$ ) sulfanilamide, for peak to peak between (H) ( $215\text{-}239.5\ \text{nm}$ ), (I) ( $239.5\text{-}264.25\ \text{nm}$ ), (J) ( $239.5\text{-}267.75\ \text{nm}$ ), (K) ( $271.28\text{-}301\ \text{nm}$ ) and (L) height to height at zero cross ( $245.86\text{-}271.28\ \text{nm}$ ).

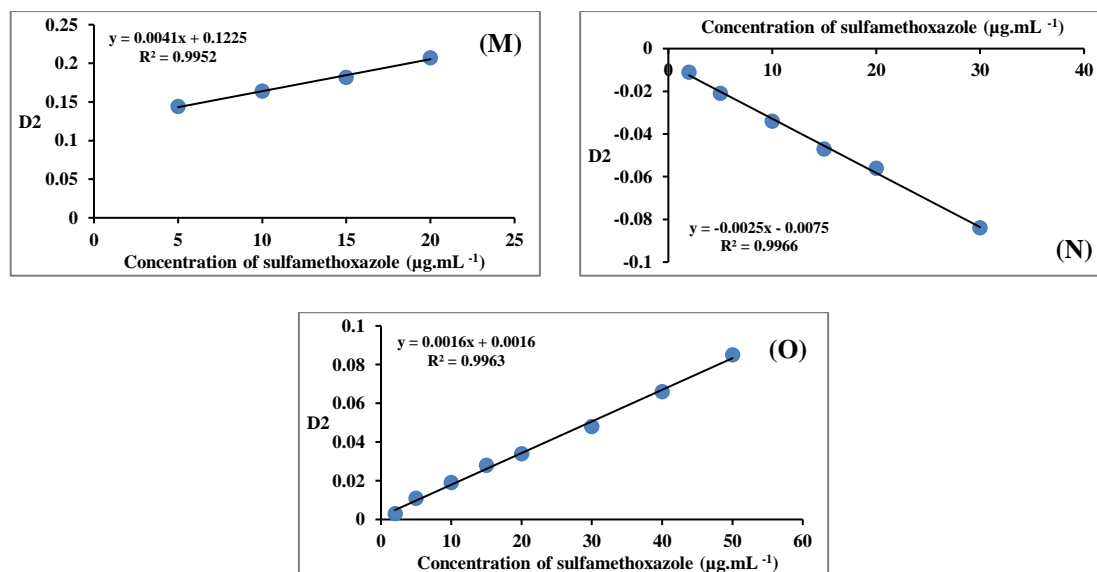


**Figure 4-59:** Calibration curves obtained via second derivative spectra of mixture of Sulfamethoxazole (2-50 µg.mL<sup>-1</sup>) in the presence of (15 µg.mL<sup>-1</sup>) Sulfanilamide, for peak area at the interval (M) 221.75 nm to 254.12 nm, (N) 254.12 nm to 281 nm and (O) 286.86 nm to 329.5 nm

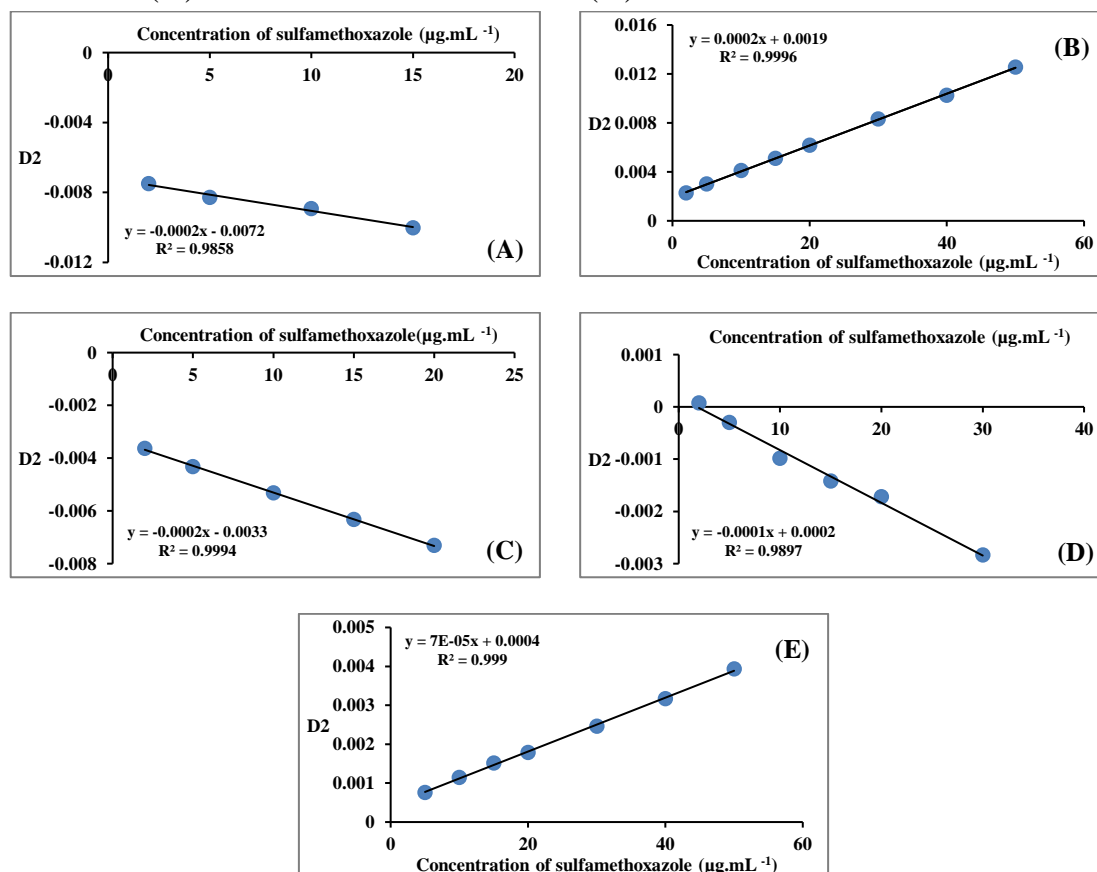


**Figure 4-60:** Calibration curves obtained via second derivative spectra of mixture of Sulfamethoxazole (2-50 µg.mL<sup>-1</sup>) in the presence of (20 µg.mL<sup>-1</sup>) Sulfanilamide, for peak-to-baseline at (A) 215 nm, (B) 239.5 nm, (C) 264.25 nm, (D) 267.75 nm and (E) 301 nm.

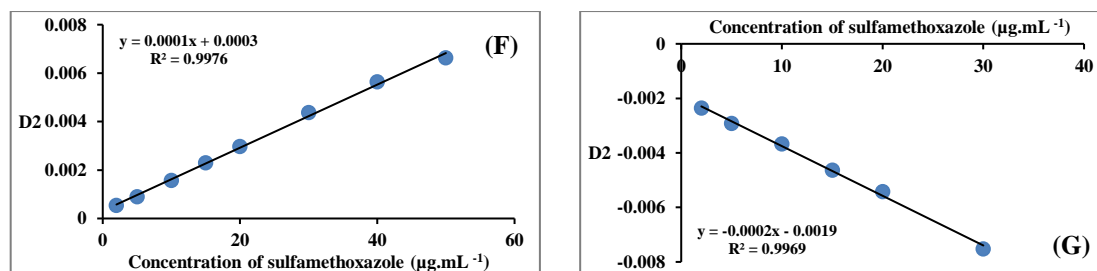


**Figure 4-61:** Calibration curves obtained via second derivative spectra of mixture of Sulfamethoxazole (2-50 µg.mL<sup>-1</sup>) in the presence of (20 µg.mL<sup>-1</sup>) Sulfanilamide, for height at zero cross at (F) 245.86 nm and (G) 271.28 nm.

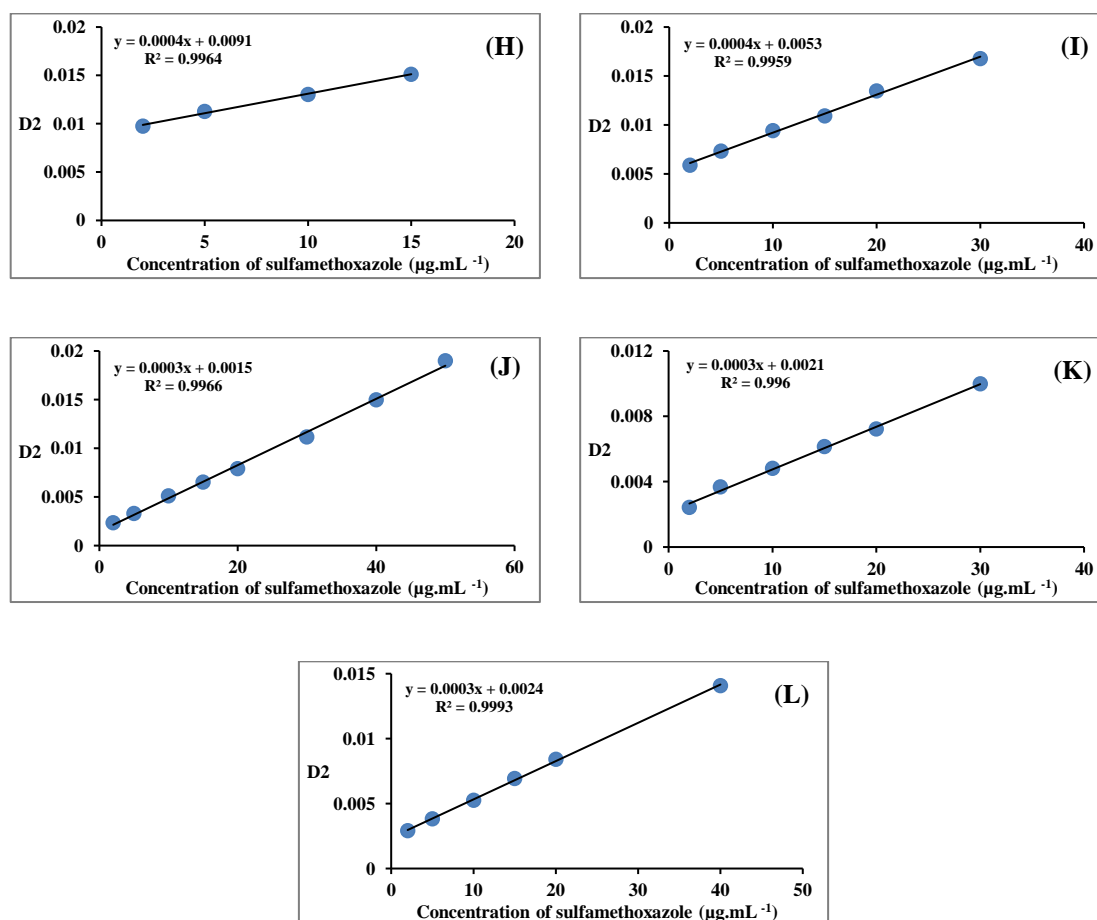


**Figure 4-62:** Calibration curves obtained via second derivative spectra of mixture of sulfamethoxazole (2-50 µg.mL<sup>-1</sup>) in the presence of (20 µg.mL<sup>-1</sup>) sulfanilamide, for peak to peak between (H) (215-239.5 nm), (I) (239.5-264.25 nm), (J) (239.5-267.7 5 nm), (K) (271.28-301 nm) and (L) height to height at zero cross (245.86-271.28 nm).

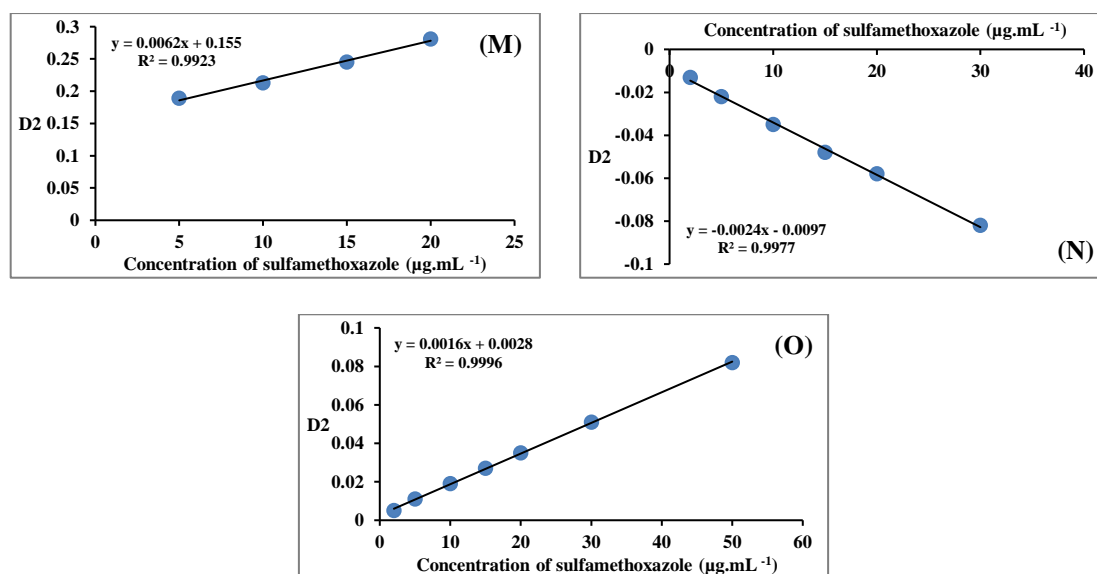


**Figure 4-63:** Calibration curves obtained via second derivative spectra of mixture of Sulfamethoxazole ( $2\text{-}50\ \mu\text{g.mL}^{-1}$ ) in the presence of ( $20\ \mu\text{g.mL}^{-1}$ ) Sulfanilamide, for peak area at the interval (M) 221.75 nm to 254.12 nm, (N) 254.12 nm to 281 nm and (O) 286.86 nm to 329.5 nm.

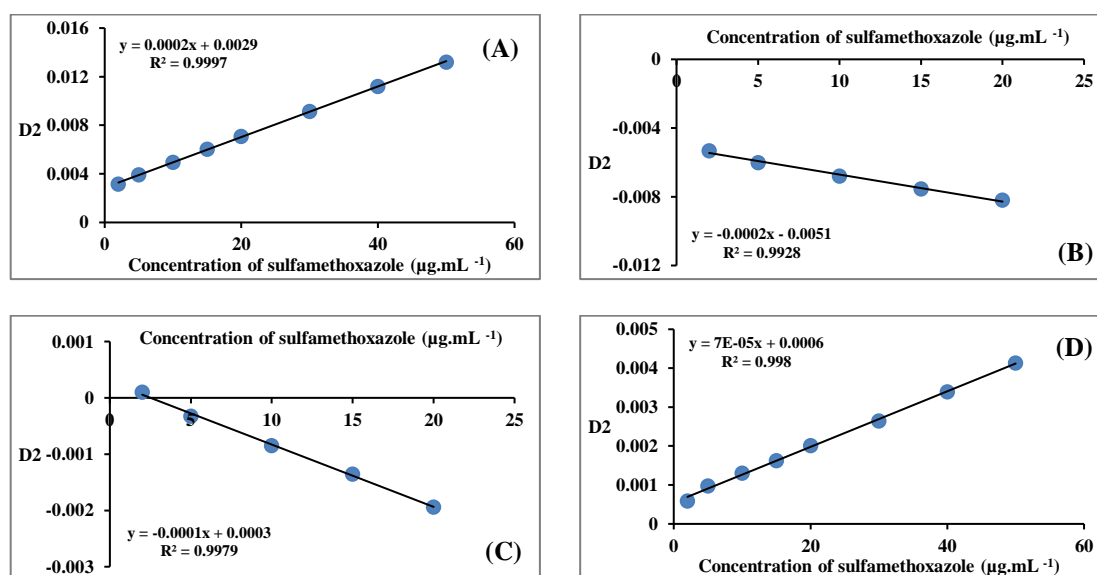


**Figure 4-64:** Calibration curves obtained via second derivative spectra of mixture of Sulfamethoxazole ( $2\text{-}50\ \mu\text{g.mL}^{-1}$ ) in the presence of ( $30\ \mu\text{g.mL}^{-1}$ ) Sulfanilamide, for peak-to-baseline at (A) 239.5 nm, (B) 264.25 nm, (C) 267.75 nm and (D) 301 nm.

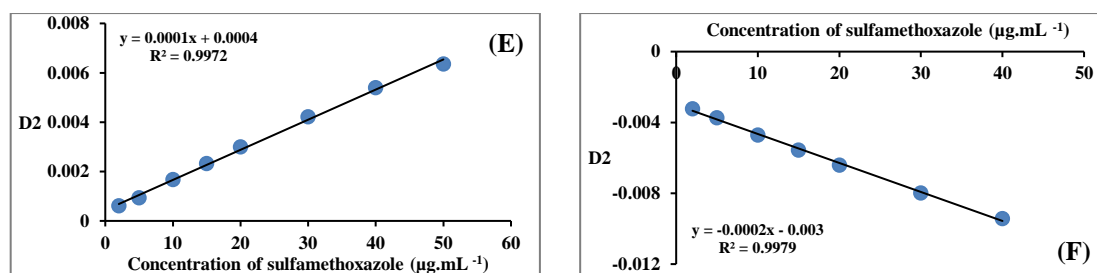


**Figure 4-65:** Calibration curves obtained via second derivative spectra of mixture of Sulfamethoxazole ( $2\text{-}50 \mu\text{g.mL}^{-1}$ ) in the presence of ( $30 \mu\text{g.mL}^{-1}$ ) Sulfanilamide, for height at zero cross at (E)  $245.86 \text{ nm}$  and (F)  $271.28 \text{ nm}$ .

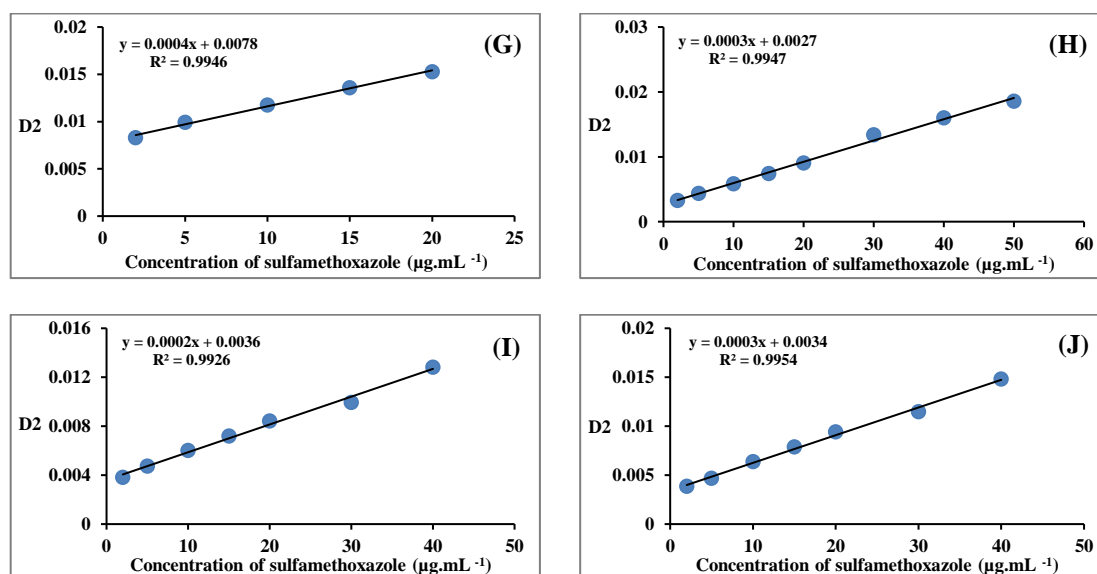


**Figure 4-66:** Calibration curves obtained via second derivative spectra of mixture of sulfamethoxazole ( $2\text{-}50 \mu\text{g.mL}^{-1}$ ) in the presence of ( $30 \mu\text{g.mL}^{-1}$ ) sulfanilamide, for peak to peak between ((G)) ( $239.5\text{-}264.25 \text{ nm}$ ), (H) ( $239.5\text{-}267.75 \text{ nm}$ ), (I) ( $271.28\text{-}301 \text{ nm}$ ) and (J) height to height at zero cross ( $245.86\text{-}271.28 \text{ nm}$ ).

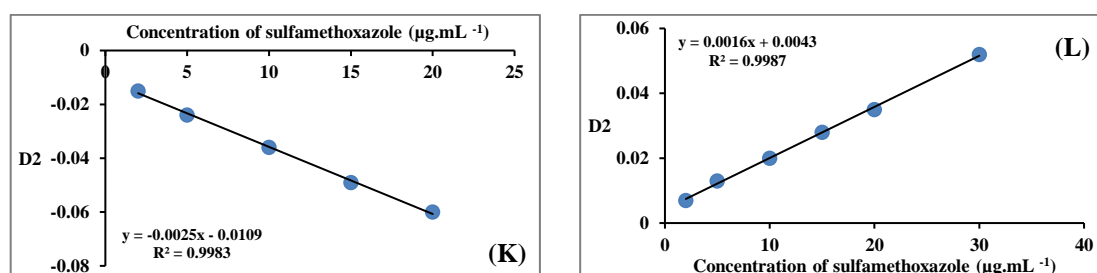


**Figure 4-67:** Calibration curves obtained via second derivative spectra of mixture of Sulfamethoxazole ( $2\text{-}50 \mu\text{g.mL}^{-1}$ ) in the presence of ( $30 \mu\text{g.mL}^{-1}$ ) Sulfanilamide, for peak area at the interval (K)  $254.12 \text{ nm}$  to  $281 \text{ nm}$  and (L)  $286.86 \text{ nm}$  to  $329.5 \text{ nm}$ .

Summarize all the results for sulfamethoxazole analysis by using first and second derivative technique in table 4-2.

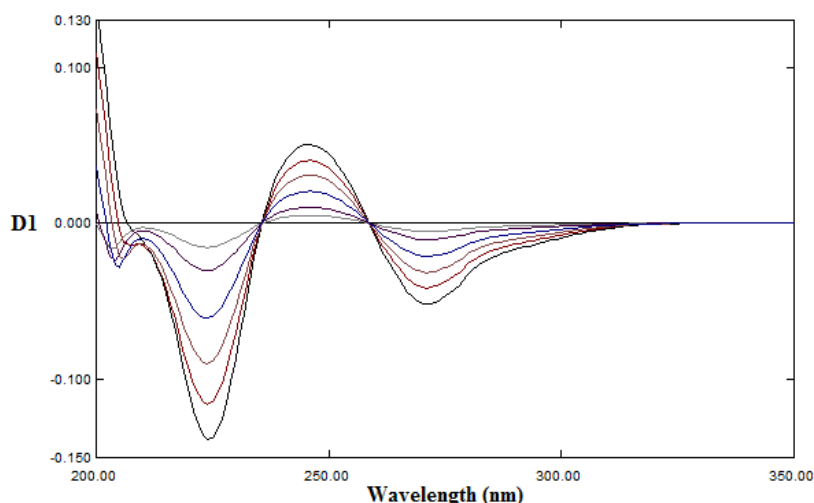
**Table 4-2:** Statistical analysis for the determination of sulfamethoxazole using first and second derivative spectrophotometric technique.

<i>Order of derivative</i>	<i>Mode of calculation</i>	$\lambda$ (nm)	<i>Regression equation</i>	<i>R</i>	<i>Slope</i>
<b>First</b>	Peak to base line	254	$Y = 0.0013x + 0.0002$	1.0000	0.0013
	Peak to base line	287	$Y = -0.0012x - 6E-06$	1.0000	-0.0012
	Peak to base line	223	$Y = -0.0022x - 0.0013$	0.9998	-0.0022
	Peak to peak	254-287	$Y = 0.0024x + 0.0002$	1.0000	0.0024
	Peak to peak	223-254	$Y = 0.0035x + 0.0015$	0.9999	0.0035
	Zero cross	235.62	$Y = -0.0011x - 0.0008$	0.9998	-0.0011
	Zero cross	258.72	$Y = 0.001x + 0.0005$	0.9998	0.001
	Height to height at zero cross	235.62-258.72	$Y = 0.0021x + 0.0012$	0.9998	0.0021
	Peak area	241.95-267.04	$Y = 0.0198x + 0.008$	0.9999	0.0198
	Peak area	267.04-330	$Y = -0.037x - 0.004$	1.0000	-0.037
<b>Second</b>	Peak to base line	215	$Y = -0.0002x - 0.0001$	0.9997	-0.0002
	Peak to base line	239.5	$Y = 0.0002x + 6E-05$	1.0000	0.0002
	Peak to base line	264.25	$Y = -0.0001x - 8E-05$	0.9998	-0.0001
	Peak to base line	267.75	$Y = -0.0001x - 0.0001$	0.9992	-0.0001
	Peak to base line	301	$Y = 6E-05x - 1E-05$	0.9999	$6 \times 10^{-5}$
	Zero cross	245.86	$Y = 0.0001x + 5E-05$	1.0000	0.0001
	Zero cross	271.28	$Y = -0.0001x - 8E-05$	0.9996	-0.0001
	Peak to peak	215-239.5	$Y = 0.0004x + 0.0002$	0.9998	0.0004
	Peak to peak	239.5-264.25	$Y = 0.0003x + 0.0002$	0.9998	0.0003
	Peak to peak	239.5-267.75	$Y = 0.0003x + 0.0002$	0.9998	0.0003
	Peak to peak	271.28-301	$Y = 0.0002x + 0.0001$	0.9997	0.0002
	Height to height at zero cross	245.86-271.28	$Y = 0.0003x + 0.0001$	0.9998	0.0003
	Peak area	221.75-254.12	$Y = 0.0035x - 0.0004$	0.9995	0.0035
	Peak area	254.12-281	$Y = -0.0023x - 0.0025$	0.9992	-0.0023
	Peak area	286.86-329.5	$Y = 0.0012x - 0.0003$	0.9996	0.0012

#### 4-1-4-4 Calibration graphs for sulfanilamide

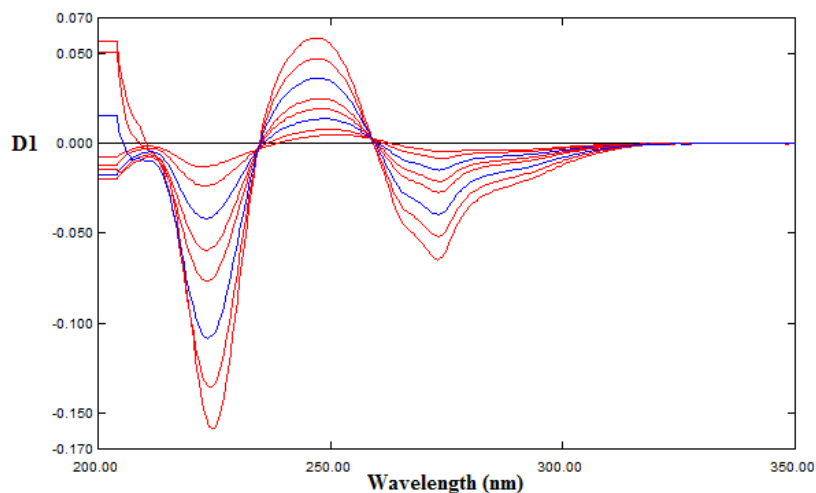
Calibration curves were constructed for the assay of sulfanilamide via UV-spectrophotometric method operated under the mentioned optimum conditions for D1 and D2 modes in selected ranges of wavelengths. The same ideas used previously to utilize derivative modes for the quantitative analysis of sulfamethoxazole are used (i.e. peak-to- base line, peak-to-peak, zero crossing and area under peak measurements).

The recorded spectra using D1 mode for a set of solutions containing (5-50  $\mu\text{g.mL}^{-1}$ ) sulfanilamide with different spiked concentrations of sulfamethoxazole (0, 2, 5, 10, 15, 20, 30  $\mu\text{g.mL}^{-1}$ ) are shown in Figures 4-68 – 4-74. The procedure showed good results over the studied range of concentration depending on peak-to-baseline, height at zero cross, peak to peak, height to height at zero cross and area under the peak measurements (Figures 4-75 and 4-95), and show plotted calibration curves.

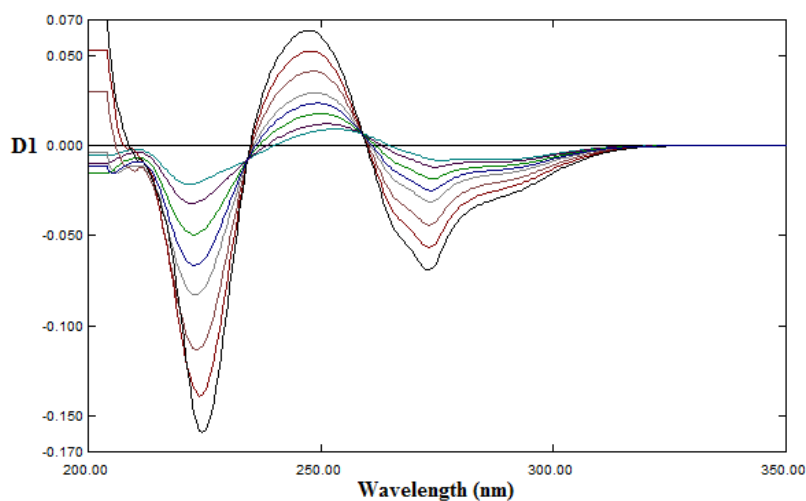


**Figure 4-68:** First derivative spectra of (5-50  $\mu\text{g.mL}^{-1}$ ) sulfanilamide.

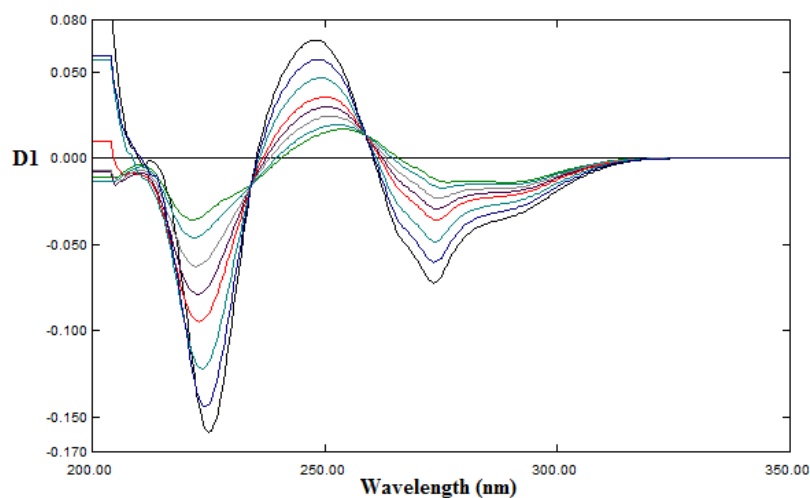




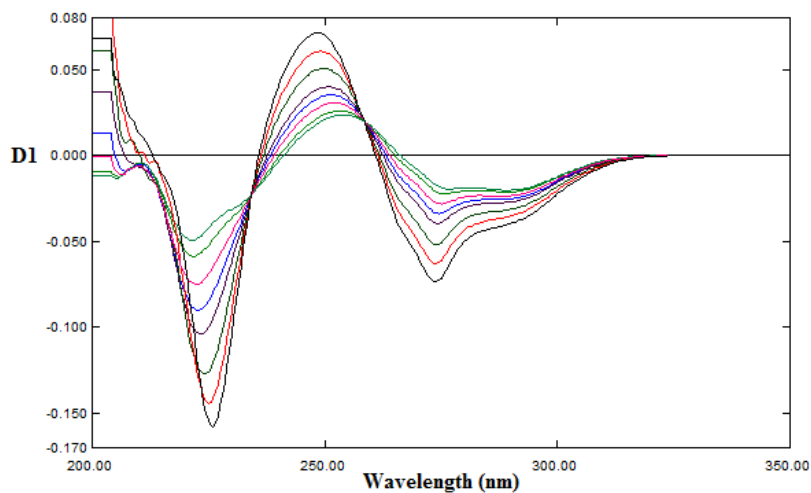
**Figure 4-69:** First derivative spectra of (5-50  $\mu\text{g.mL}^{-1}$ ) sulfanilamide in the presence of (2  $\mu\text{g.mL}^{-1}$ ) sulfamethoxazole.



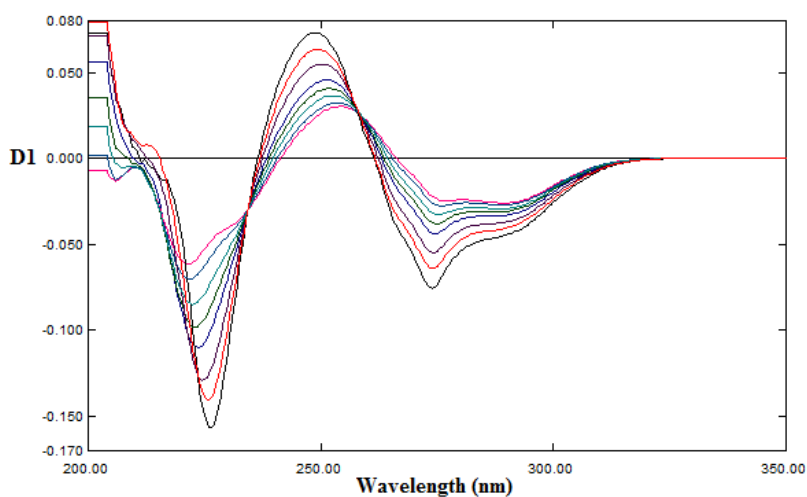
**Figure 4-70:** First derivative spectra of (5 - 50  $\mu\text{g.mL}^{-1}$ ) sulfanilamide in the presence of (5  $\mu\text{g.mL}^{-1}$ ) sulfamethoxazole.



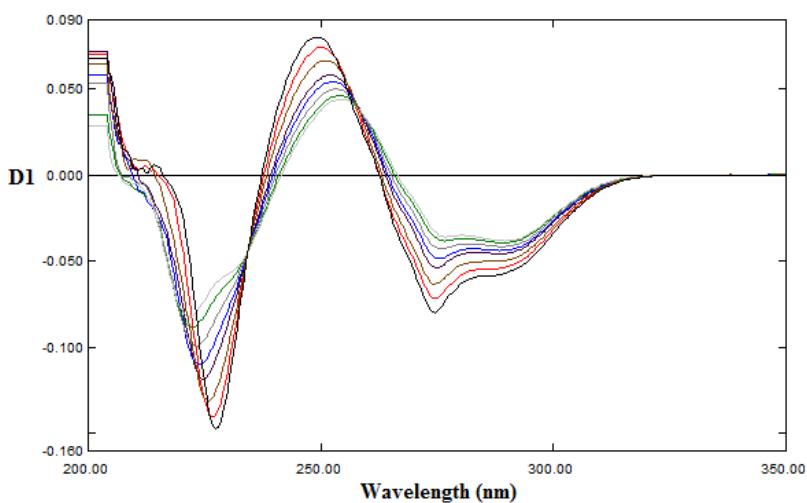
**Figure 4-71:** First derivative spectra of (5 - 50  $\mu\text{g.mL}^{-1}$ ) sulfanilamide in the presence of (10  $\mu\text{g.mL}^{-1}$ ) sulfamethoxazole.



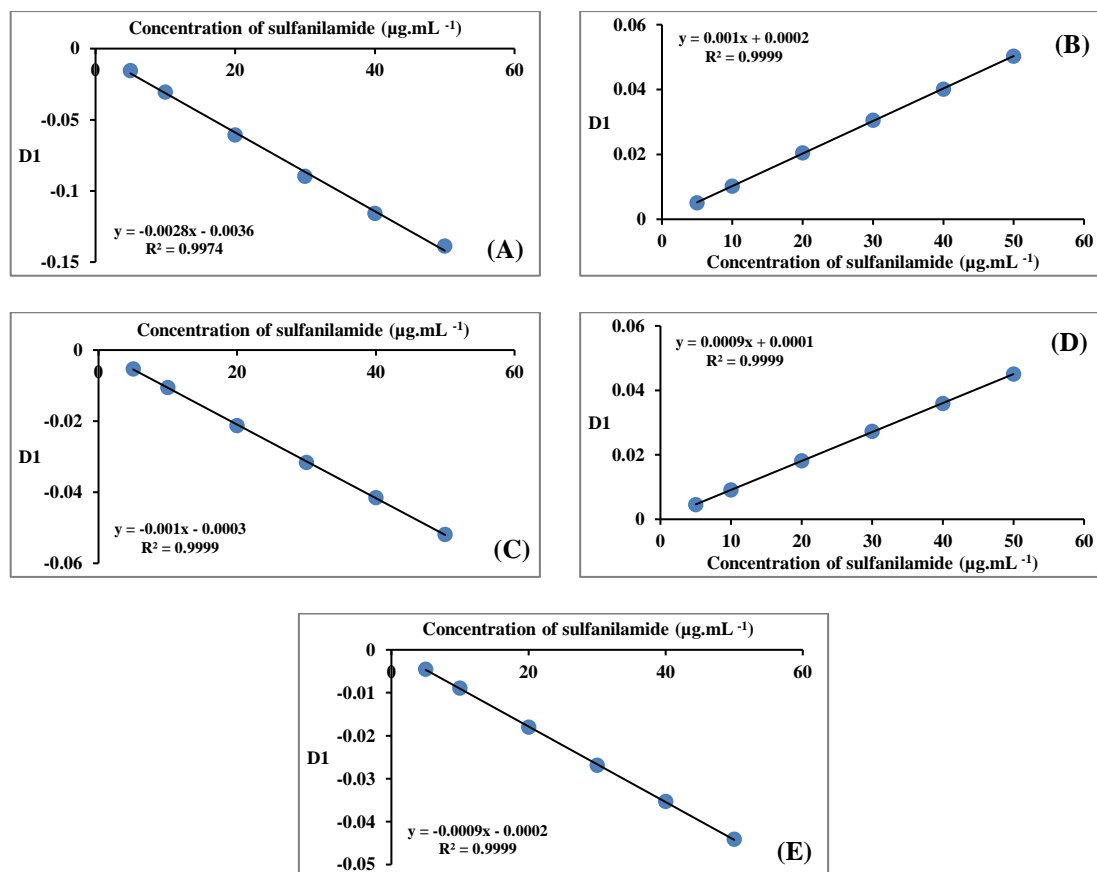
**Figure 4-72:** First derivative spectra of (5 - 50  $\mu\text{g.mL}^{-1}$ ) sulfanilamide in the presence of (15  $\mu\text{g.mL}^{-1}$ ) sulfamethoxazole.



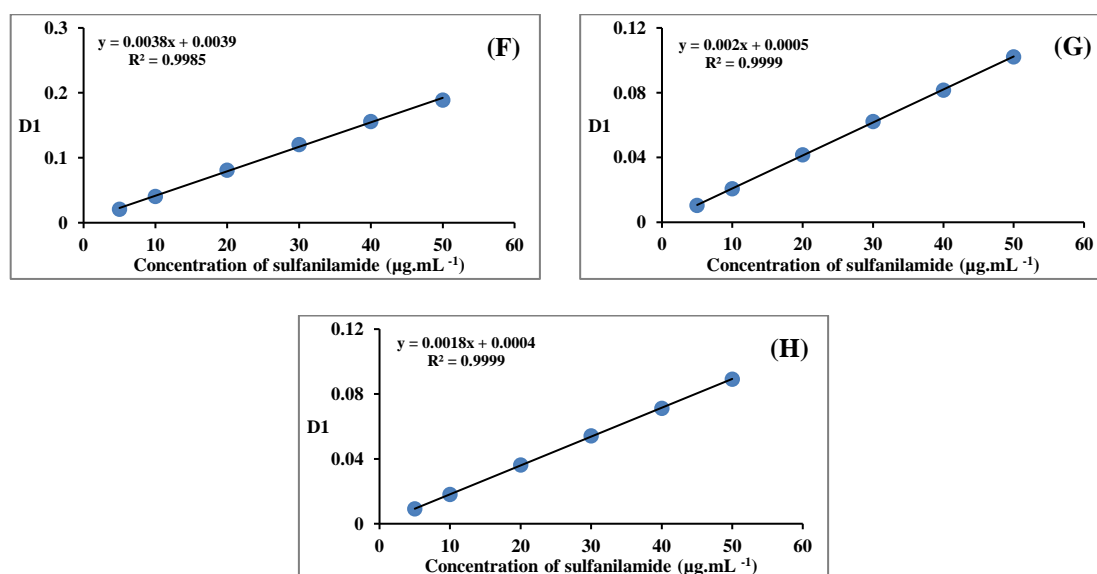
**Figure 4-73:** First derivative spectra of (5 - 50  $\mu\text{g.mL}^{-1}$ ) sulfanilamide in the presence of (20  $\mu\text{g.mL}^{-1}$ ) sulfamethoxazole.



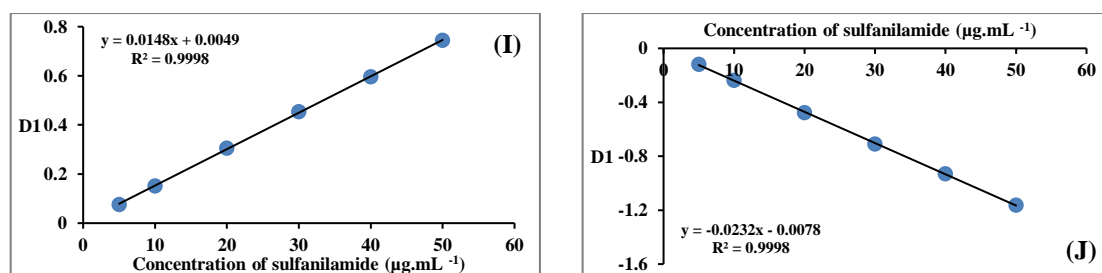
**Figure 4-74:** First derivative spectra of (5 - 50  $\mu\text{g.mL}^{-1}$ ) sulfanilamide in the presence of (30  $\mu\text{g.mL}^{-1}$ ) sulfamethoxazole.



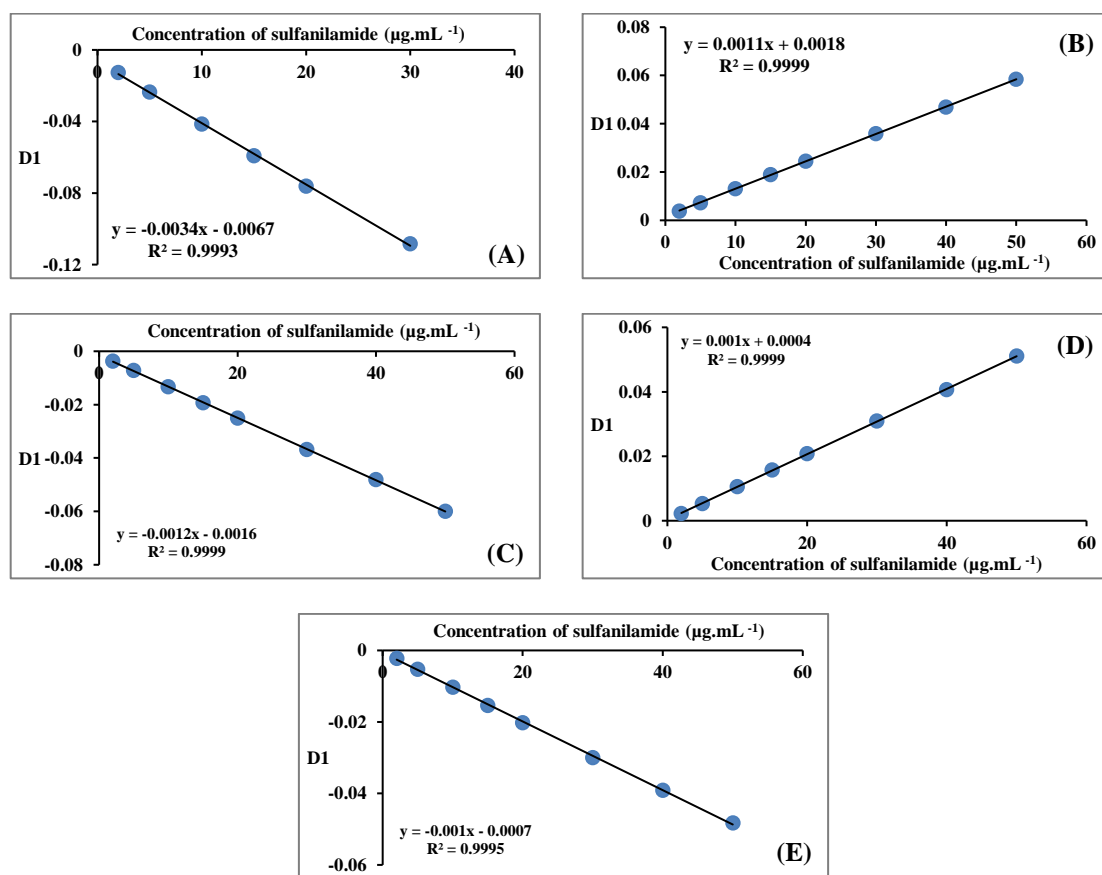
**Figure 4-75:** Calibration curves obtained via first derivative spectra of sulfanilamide for peak-to-baseline at (A) 224 nm, (B) 246 nm, (C) 271 nm, (D) height at zero cross at 241.95 nm and (E) height at zero cross at 267.04 nm.



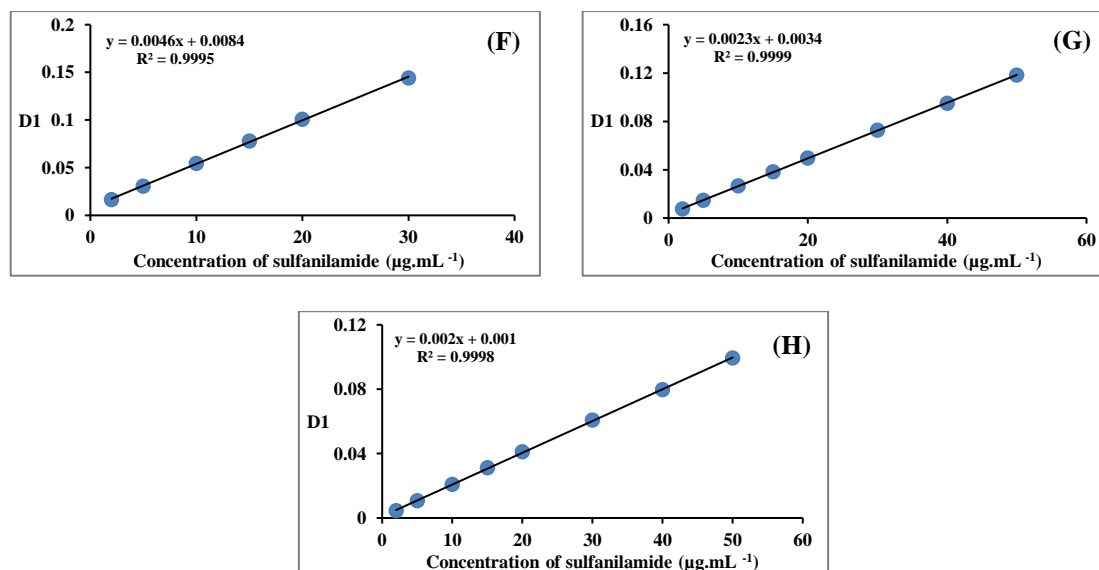
**Figure 4-76:** Calibration curves obtained via first derivative spectra of sulfanilamide for peak to peak between (F) (224-246 nm), (G) (246-271 nm) and (H) height-to-height between (241.95-271 nm).



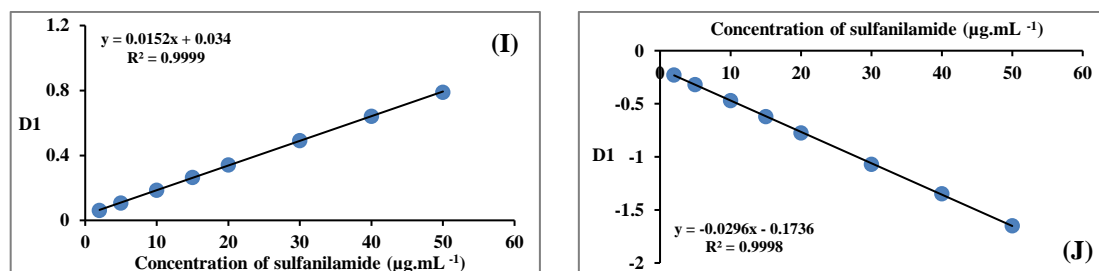
**Figure 4-77:** Calibration curves obtained via first derivative spectra of sulfanilamide for peak area at the interval (I) 235.62 nm to 258.72 nm and (J) 258.72 nm to 331 nm.



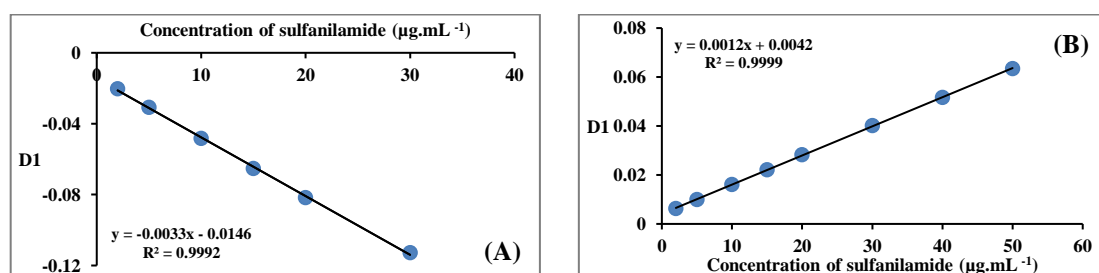
**Figure 4-78:** Calibration curves obtained via first derivative spectra of mixture of sulfanilamide ( $2\text{-}50 \mu\text{g.mL}^{-1}$ ) in the presence of ( $2 \mu\text{g.mL}^{-1}$ ) sulfamethoxazole, for peak-to-baseline at (A) 224 nm, (B) 246 nm, (C) 271 nm, (D) height at zero cross at 241.95 nm and (E) height at zero cross at 267.04 nm.

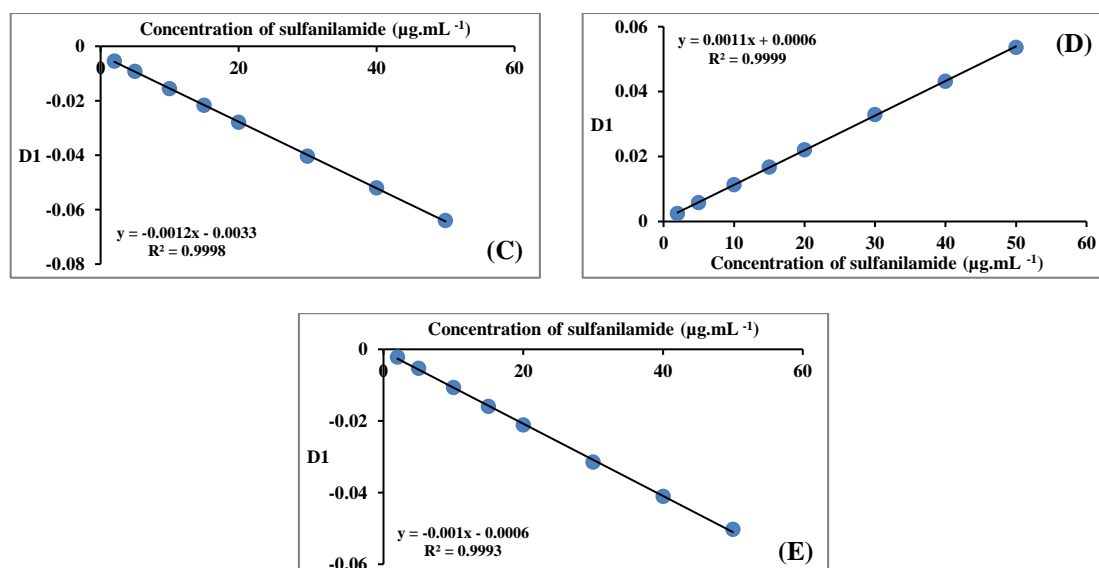


**Figure 4-79:** Calibration curves obtained via first derivative spectra of mixture of sulfanilamide (2-50  $\mu\text{g.mL}^{-1}$ ) in the presence of (2  $\mu\text{g.mL}^{-1}$ ) sulfamethoxazole, for peak to peak between (F) (224-246 nm), (G) (246-271 nm) and (H) height-to-height between (241.95-271 nm).

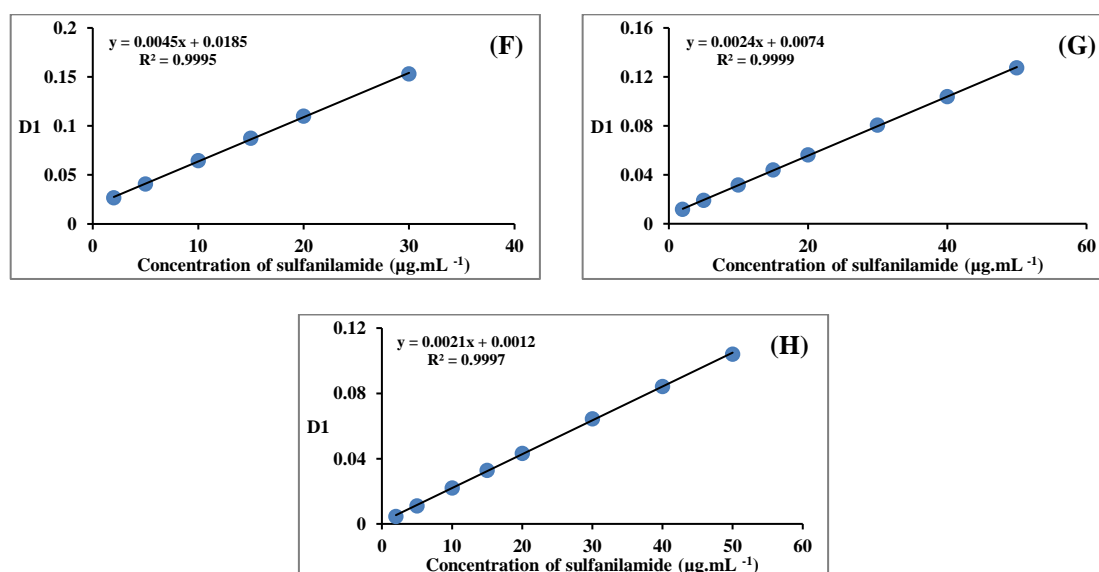


**Figure 4-80:** Calibration curves obtained via first derivative spectra of mixture of sulfanilamide (2-50  $\mu\text{g.mL}^{-1}$ ) in the presence of (2  $\mu\text{g.mL}^{-1}$ ) sulfamethoxazole, for peak area at the interval (I) 235.62 nm to 258.72 nm and (J) 258.72 nm to 331 nm.

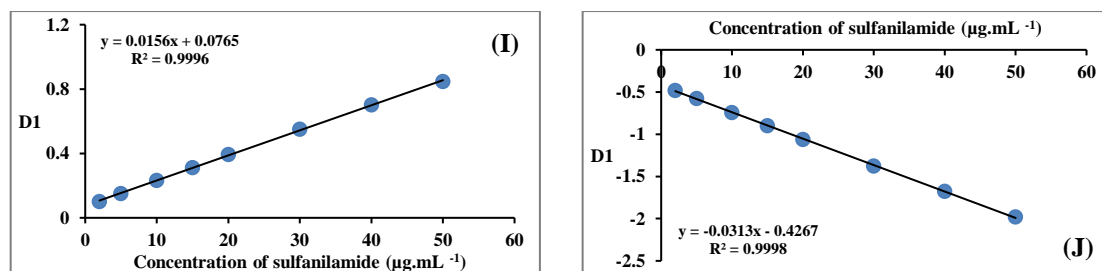




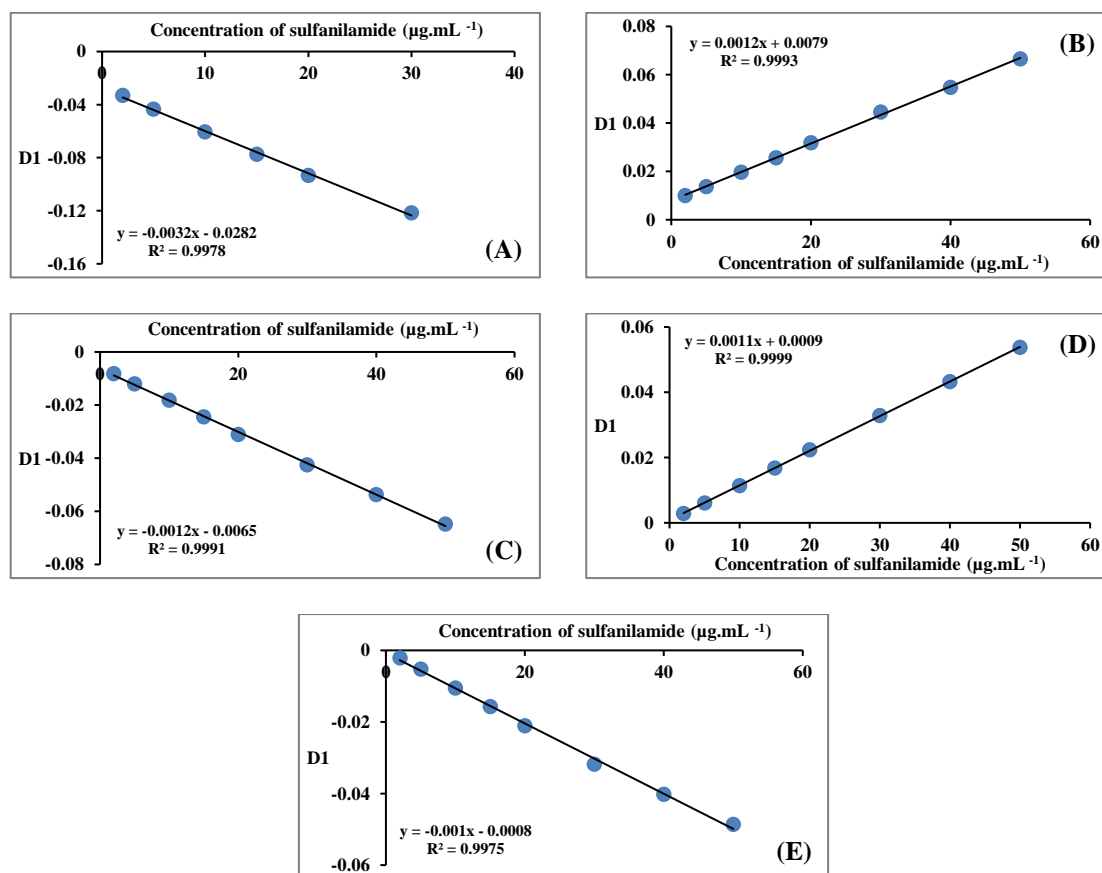
**Figure 4-81:** Calibration curves obtained via first derivative spectra of mixture of sulfanilamide ( $2\text{-}50 \mu\text{g.mL}^{-1}$ ) in the presence of ( $5 \mu\text{g.mL}^{-1}$ ) sulfamethoxazole, for peak-to-baseline at (A) 224 nm, (B) 246 nm, (C) 271 nm, (D) height at zero cross at 241.95 nm and (E) height at zero cross at 267.04 nm.



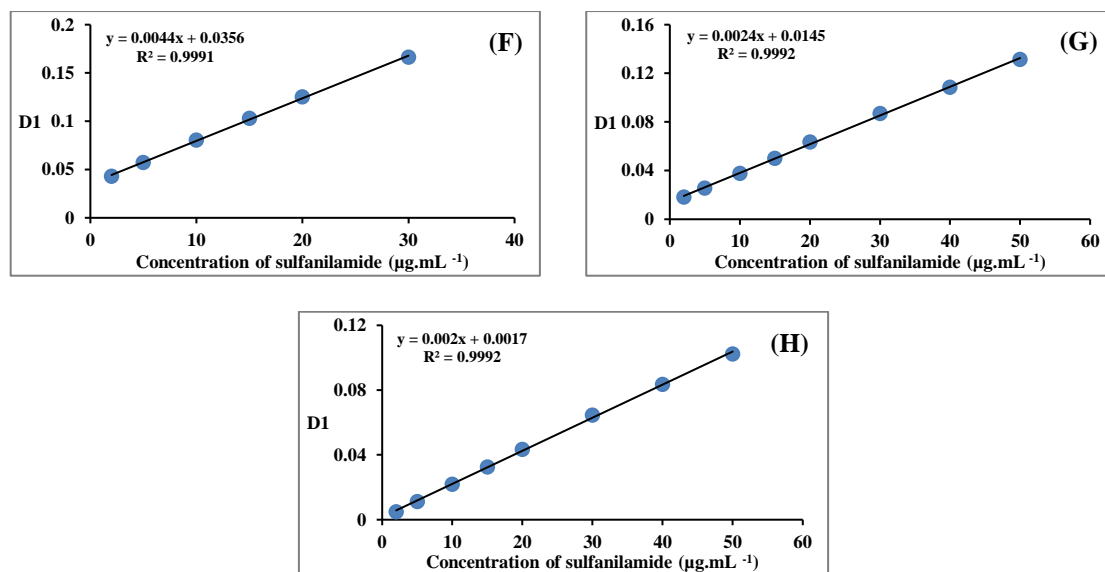
**Figure 4-82:** Calibration curves obtained via first derivative spectra of mixture of sulfanilamide ( $2\text{-}50 \mu\text{g.mL}^{-1}$ ) in the presence of ( $5 \mu\text{g.mL}^{-1}$ ) sulfamethoxazole, for peak to peak between (F) (224-246 nm), (G) (246-271 nm) and (H) height-to-height between (241.95-271 nm).



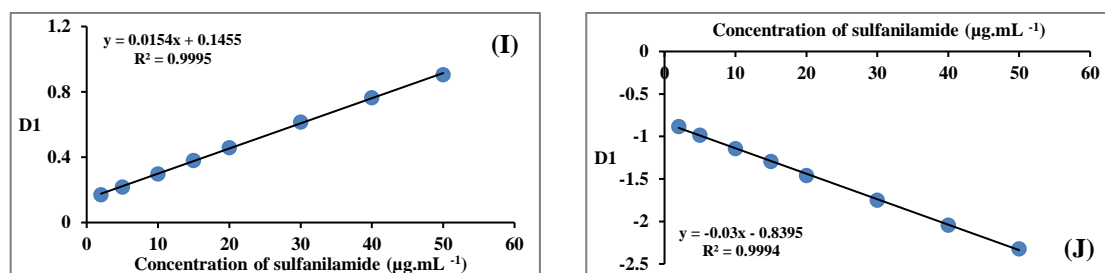
**Figure 4-83:** Calibration curves obtained via first derivative spectra of mixture of sulfanilamide ( $2\text{-}50\ \mu\text{g.mL}^{-1}$ ) in the presence of ( $5\ \mu\text{g.mL}^{-1}$ ) sulfamethoxazole, for peak area at the interval (I)  $235.62\ \text{nm}$  to  $258.72\ \text{nm}$  and (J)  $258.72\ \text{nm}$  to  $331\ \text{nm}$ .



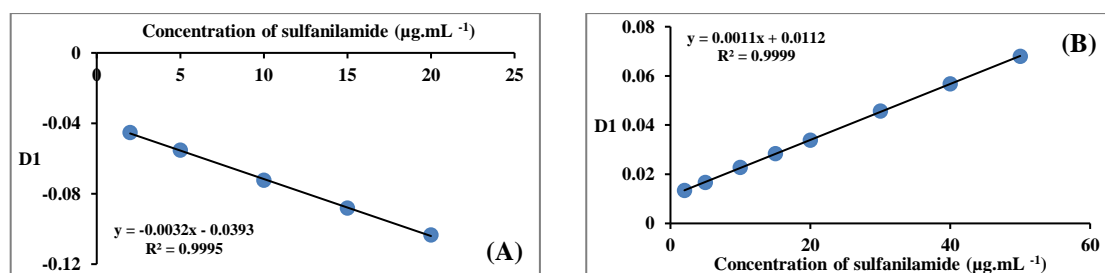
**Figure 4-84:** Calibration curves obtained via first derivative spectra of mixture of sulfanilamide ( $2\text{-}50\ \mu\text{g.mL}^{-1}$ ) in the presence of ( $10\ \mu\text{g.mL}^{-1}$ ) sulfamethoxazole, for peak-to-baseline at (A)  $224\ \text{nm}$ , (B)  $246\ \text{nm}$ , (C)  $271\ \text{nm}$ , (D) height at zero cross at  $241.95\ \text{nm}$  and (E) height at zero cross at  $267.04\ \text{nm}$ .



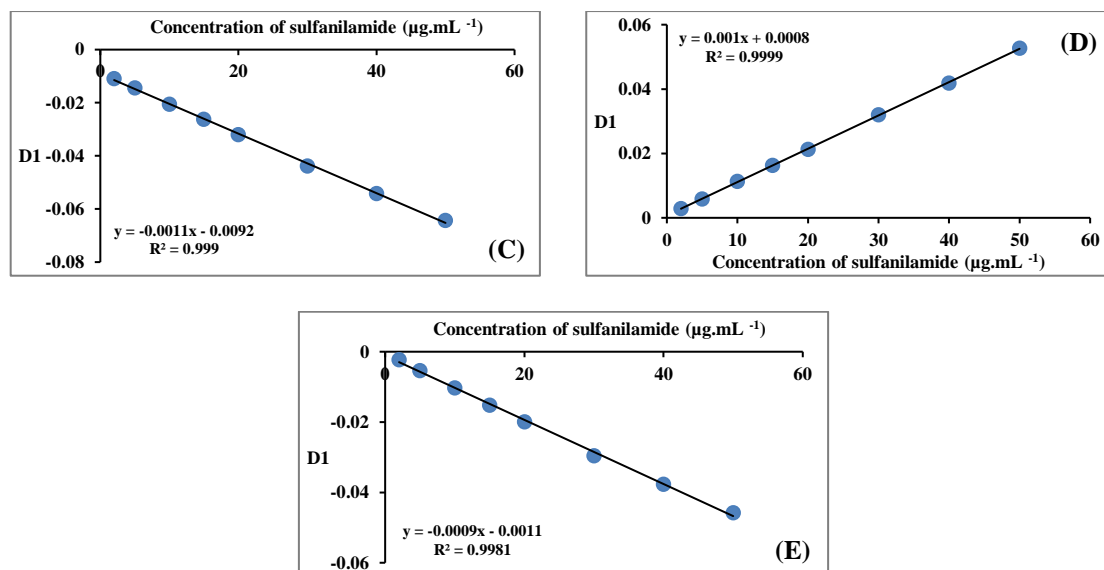
**Figure 4-85:** Calibration curves obtained via first derivative spectra of mixture of sulfanilamide (2-50  $\mu\text{g.mL}^{-1}$ ) in the presence of (10  $\mu\text{g.mL}^{-1}$ ) sulfamethoxazole, for peak to peak between (F) (224-246 nm), (G) (246-271 nm) and (H) height-to-height between (241.95-271 nm).



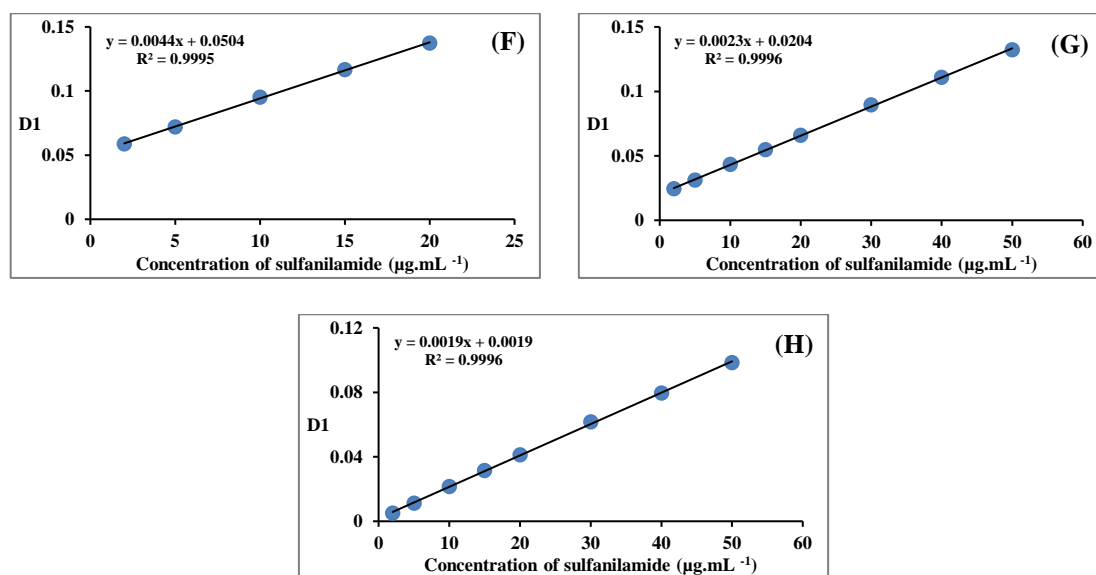
**Figure 4-86:** Calibration curves obtained via first derivative spectra of mixture of sulfanilamide (2-50  $\mu\text{g.mL}^{-1}$ ) in the presence of (10  $\mu\text{g.mL}^{-1}$ ) sulfamethoxazole, for peak area at the interval (I) 235.62 nm to 258.72 nm and (J) 258.72 nm to 331 nm.



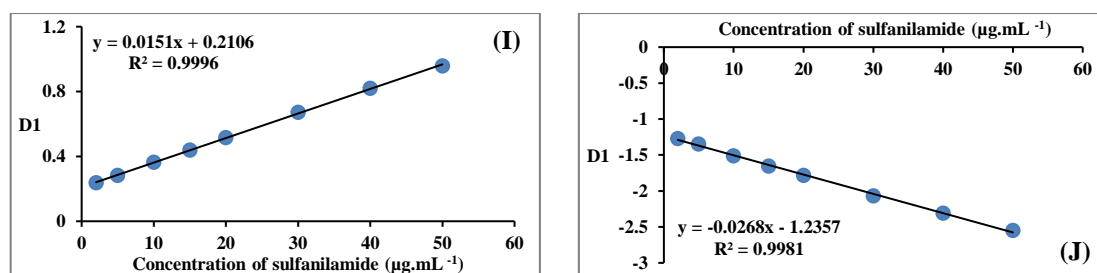




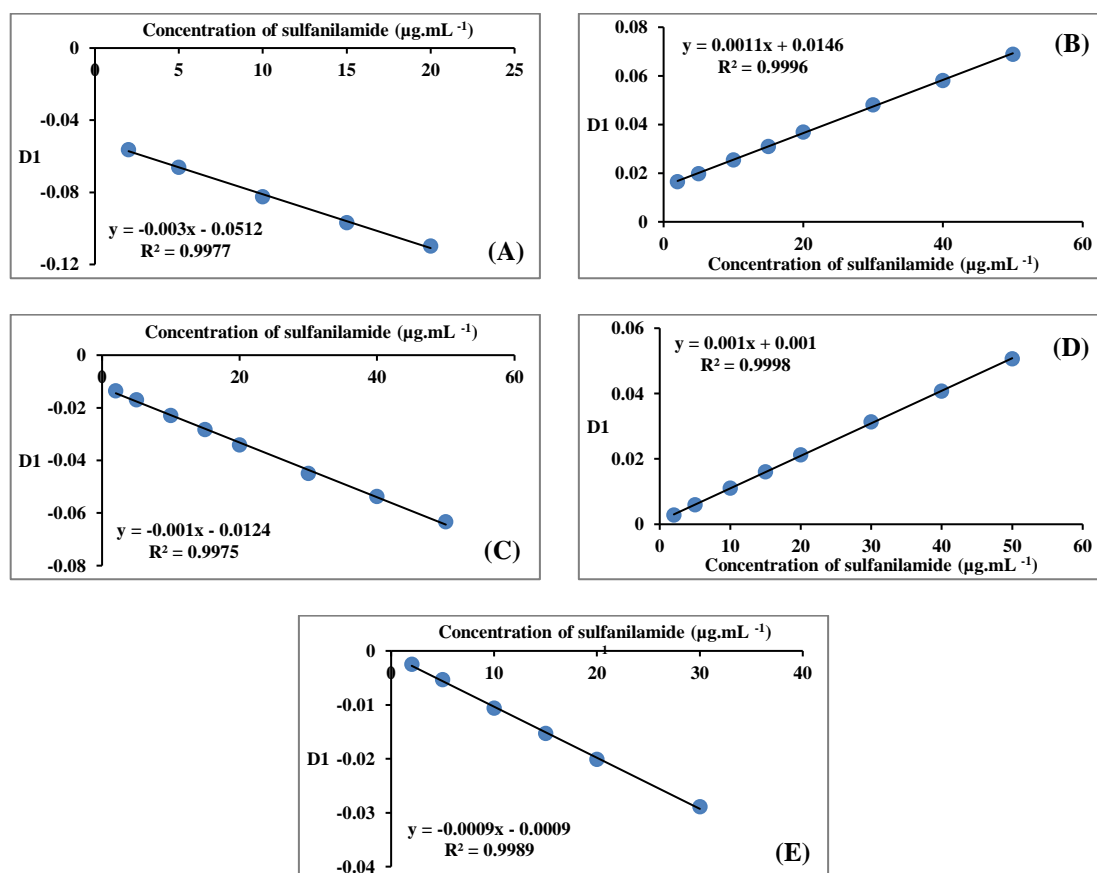
**Figure 4-87:** Calibration curves obtained via first derivative spectra of mixture of sulfanilamide ( $2\text{-}50 \mu\text{g.mL}^{-1}$ ) in the presence of ( $15 \mu\text{g.mL}^{-1}$ ) sulfamethoxazole, for peak-to-baseline at (A) 224 nm, (B) 246 nm, (C) 271 nm, (D) height at zero cross at 241.95 nm and (E) height at zero cross at 267.04 nm.



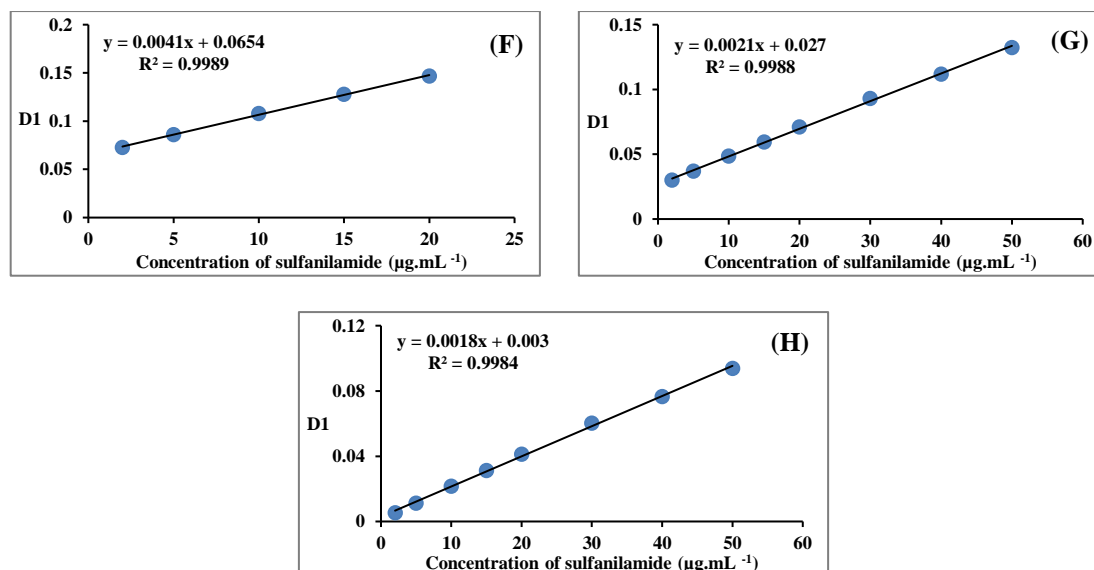
**Figure 4-88:** Calibration curves obtained via first derivative spectra of mixture of sulfanilamide ( $2\text{-}50 \mu\text{g.mL}^{-1}$ ) in the presence of ( $15 \mu\text{g.mL}^{-1}$ ) sulfamethoxazole, for peak to peak between (F) (224-246 nm), (G) (246-271 nm) and (H) height-to-height between (241.95-271 nm).



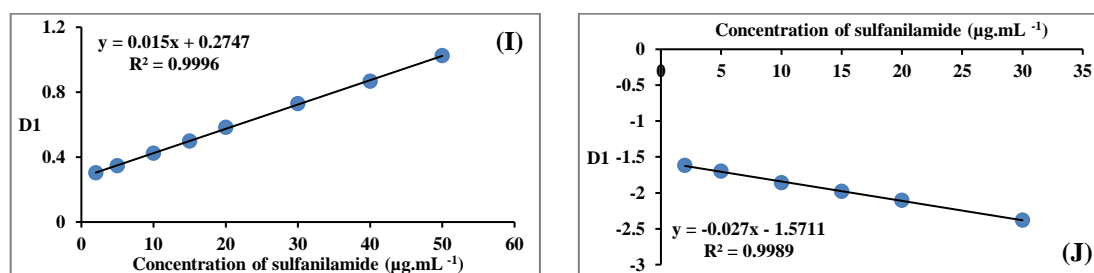
**Figure 4-89:** Calibration curves obtained via first derivative spectra of mixture of sulfanilamide (2-50  $\mu\text{g.mL}^{-1}$ ) in the presence of (15  $\mu\text{g.mL}^{-1}$ ) sulfamethoxazole, for peak area at the interval (I) 235.62 nm to 258.72 nm and (J) 258.72 nm to 331 nm.



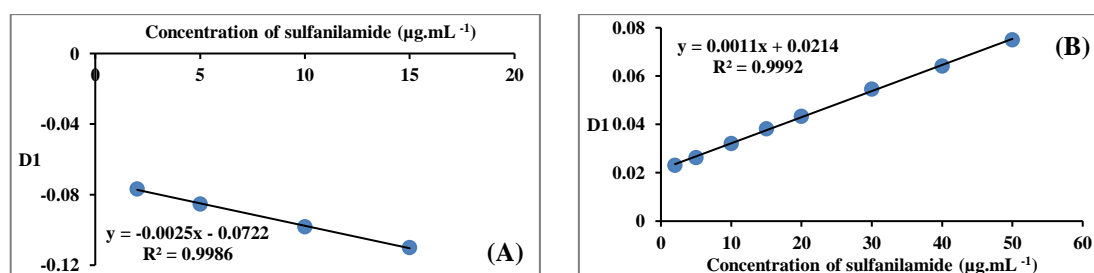
**Figure 4-90:** Calibration curves obtained via first derivative spectra of mixture of sulfanilamide (2-50  $\mu\text{g.mL}^{-1}$ ) in the presence of (20  $\mu\text{g.mL}^{-1}$ ) sulfamethoxazole, for peak-to-baseline at (A) 224 nm, (B) 246 nm, (C) 271 nm, (D) height at zero cross at 241.95 nm and (E) height at zero cross at 267.04 nm.



**Figure 4-91:** Calibration curves obtained via first derivative spectra of mixture of sulfanilamide (2-50  $\mu\text{g.mL}^{-1}$ ) in the presence of (20  $\mu\text{g.mL}^{-1}$ ) sulfamethoxazole, for peak to peak between (F) (224-246 nm), (G) (246-271 nm) and (H) height-to-height between (241.95-271 nm).



**Figure 4-92:** Calibration curves obtained via first derivative spectra of mixture of sulfanilamide (2-50  $\mu\text{g.mL}^{-1}$ ) in the presence of (20  $\mu\text{g.mL}^{-1}$ ) sulfamethoxazole, for peak area at the interval (I) 235.62 nm to 258.72 nm and (J) 258.72 nm to 331 nm.



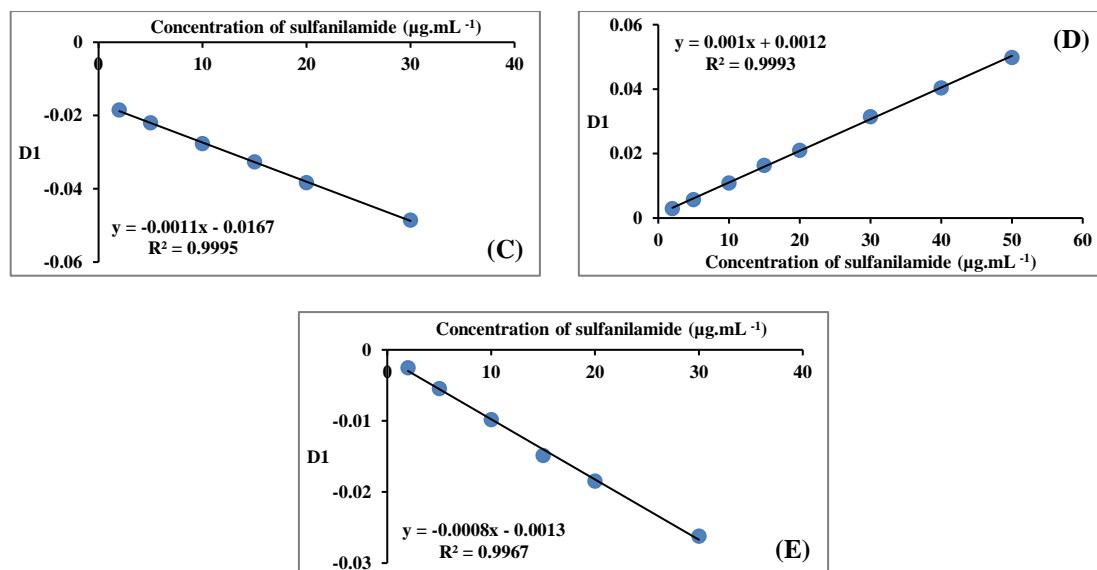


**Figure 4-93:** Calibration curves obtained via first derivative spectra of mixture of sulfanilamide (2-50  $\mu\text{g.mL}^{-1}$ ) in the presence of (30  $\mu\text{g.mL}^{-1}$ ) sulfamethoxazole, for peak-to-baseline at (A) 224 nm, (B) 246 nm, (C) 271 nm, (D) height at zero cross at 241.95 nm and (E) height at zero cross at 267.04 nm.

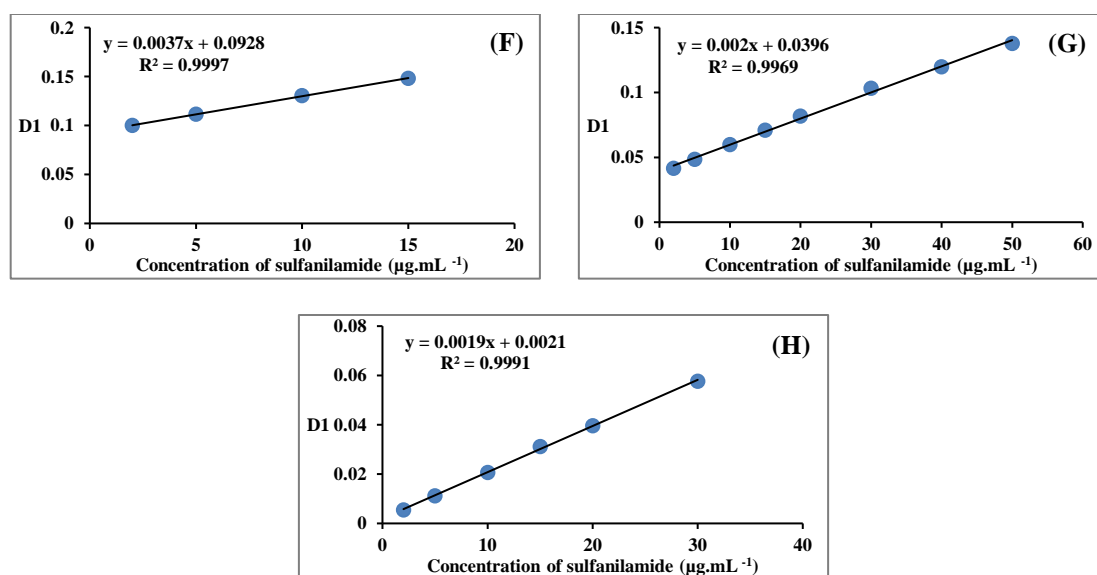


**Figure 4-94:** Calibration curves obtained via first derivative spectra of mixture of sulfanilamide (2-50  $\mu\text{g.mL}^{-1}$ ) in the presence of (30  $\mu\text{g.mL}^{-1}$ ) sulfamethoxazole, for peak to peak between (F) (224-246 nm), (G) (246-271 nm) and (H) height-to-height between (241.95-271 nm).

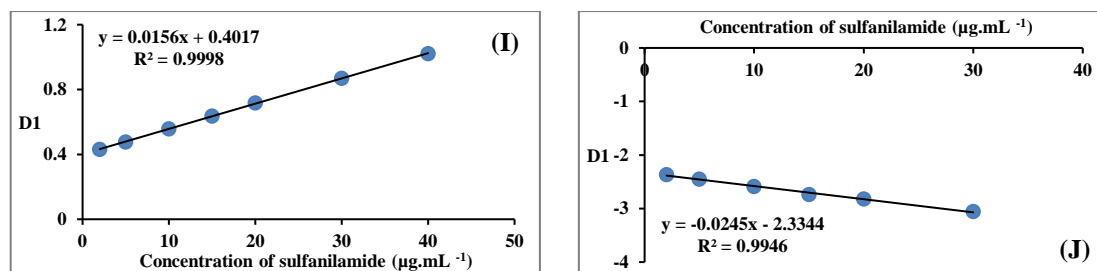


**Figure 4-95:** Calibration curves obtained via first derivative spectra of mixture of sulfanilamide ( $2\text{--}50\ \mu\text{g.mL}^{-1}$ ) in the presence of ( $30\ \mu\text{g.mL}^{-1}$ ) sulfamethoxazole, for peak area at the interval (I)  $235.62\ \text{nm}$  to  $258.72\ \text{nm}$  and (J)  $258.72\ \text{nm}$  to  $331\ \text{nm}$ .

Moreover, the second derivative spectra of the same sets of solutions (i.e. containing ( $5\text{--}50\ \mu\text{g.mL}^{-1}$ ) sulfanilamide with different spiked concentrations of sulfamethoxazole ( $0, 2, 5, 10, 15, 20, 30\ \mu\text{g.mL}^{-1}$ ) were also recorded and attempts were made to utilize them for finding the concentrations of the drug. Figures 4-96 – 4-102 show the D2 spectra for different concentrations of sulfanilamide and for its mixtures with sulfamethoxazole.

Measurements of peak-to-baseline, zero cross, peak to peak, height at zero cross and height to height at zero cross values in addition to peak area, at accurately selected regions in the recorded spectra, were carried out. Calibration plots were constructed when the measured values were plotted against the concentration of sulfanilamide (Figures 4-103 to 4-123). Excellent calibration relations were obtained.

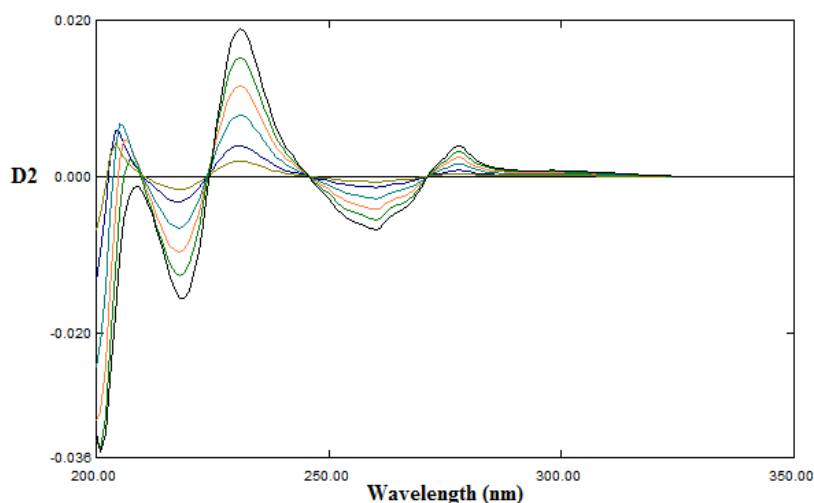


**Figure 4-96:** Second derivative spectra of ( $5\text{--}50\ \mu\text{g.mL}^{-1}$ ) sulfanilamide.

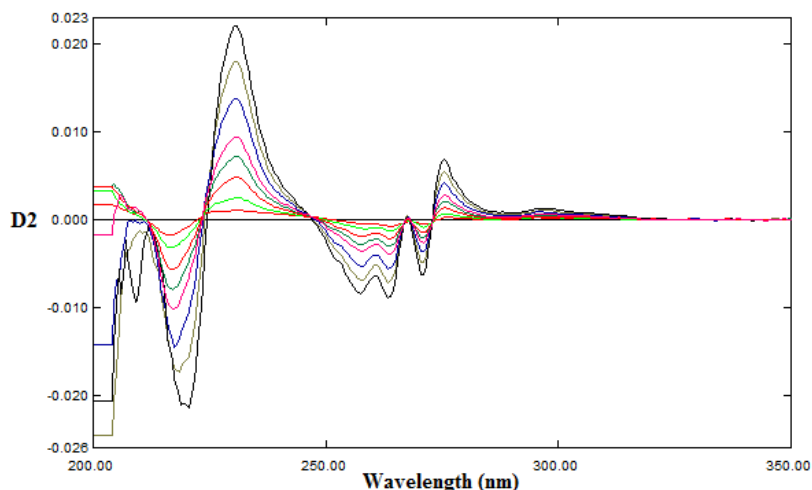


**Figure 4-97:** Second derivative spectra of (2-50  $\mu\text{g.mL}^{-1}$ ) sulfanilamide in the presence of (2  $\mu\text{g.mL}^{-1}$ ) sulfamethoxazole.

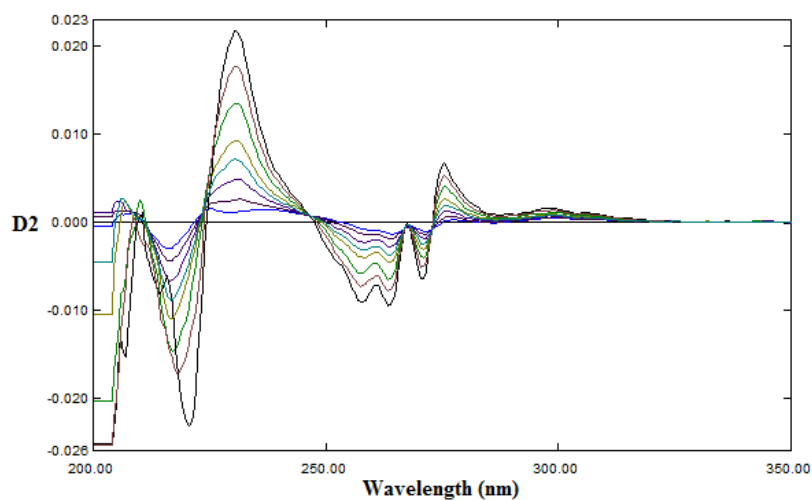


**Figure 4-98:** Second derivative spectra of (2-50  $\mu\text{g.mL}^{-1}$ ) sulfanilamide in the presence of (5  $\mu\text{g.mL}^{-1}$ ) sulfamethoxazole.

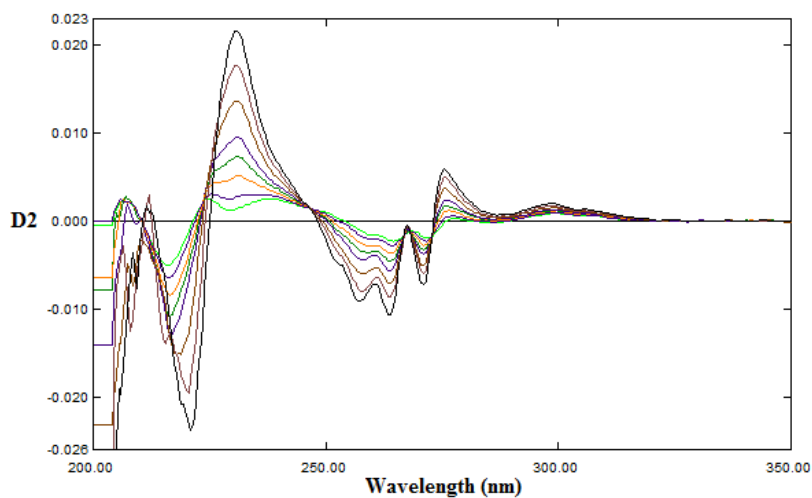


**Figure 4-99:** Second derivative spectra of (2-50  $\mu\text{g.mL}^{-1}$ ) sulfanilamide in the presence of (10  $\mu\text{g.mL}^{-1}$ ) sulfamethoxazole.

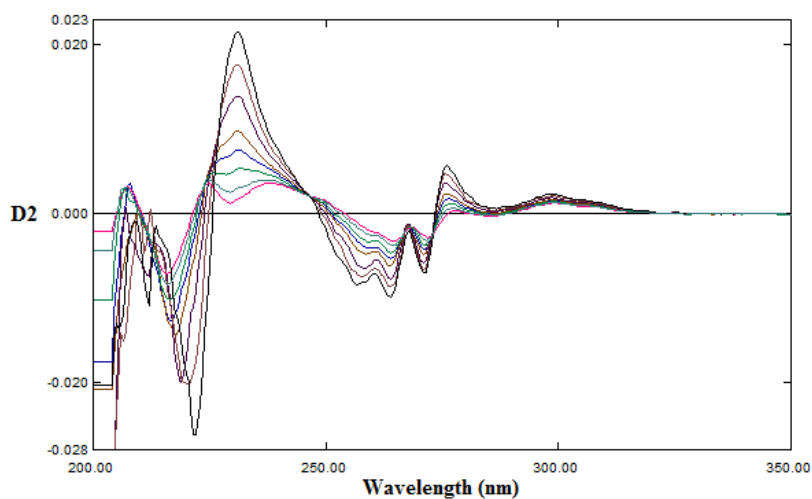


**Figure 4-100:** Second derivative spectra of (2-50  $\mu\text{g.mL}^{-1}$ ) sulfanilamide in the presence of (15  $\mu\text{g.mL}^{-1}$ ) sulfamethoxazole.

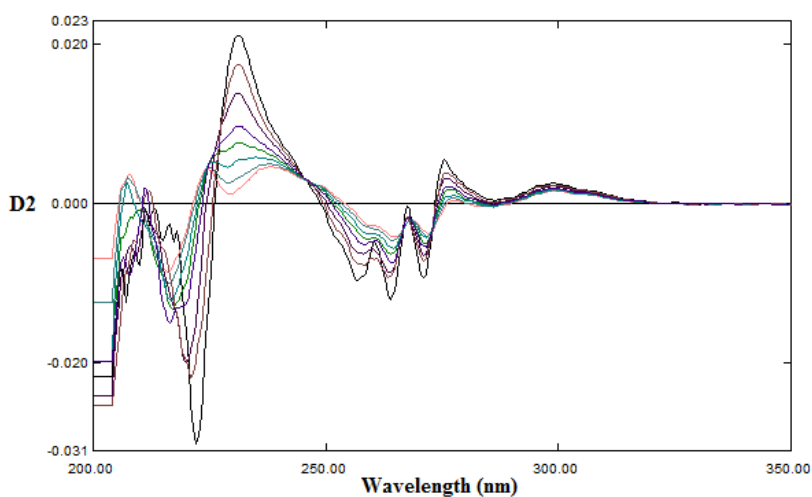


**Figure 4-101:** Second derivative spectra of (2-50  $\mu\text{g.mL}^{-1}$ ) sulfanilamide in the presence of (20  $\mu\text{g.mL}^{-1}$ ) sulfamethoxazole.

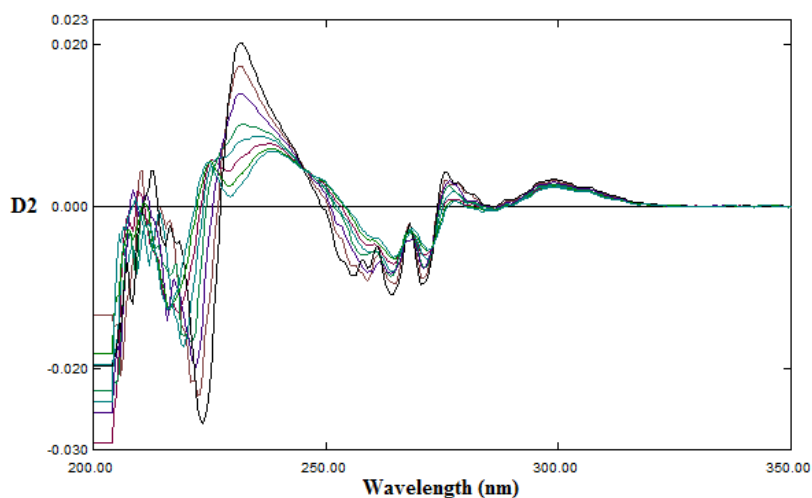


**Figure 4-102:** Second derivative spectra of (2-50  $\mu\text{g.mL}^{-1}$ ) sulfanilamide in the presence of (30  $\mu\text{g.mL}^{-1}$ ) sulfamethoxazole.

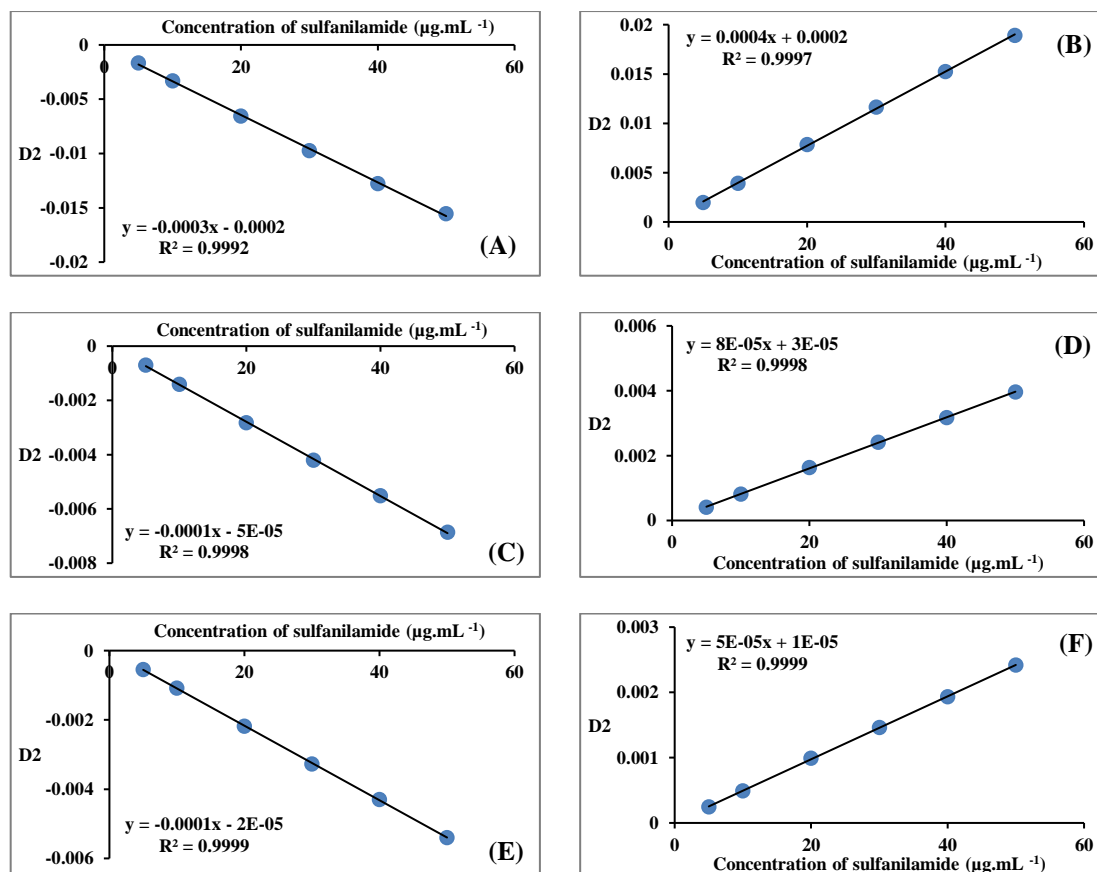


**Figure 4-103:** Calibration curves obtained via second derivative spectra of sulfanilamide for peak-to-baseline at (A) 218 nm, (B) 231 nm, (C) 260 nm, (D) 278 nm, (E) height at zero cross at 254 nm and (F) height at zero cross at 281 nm.

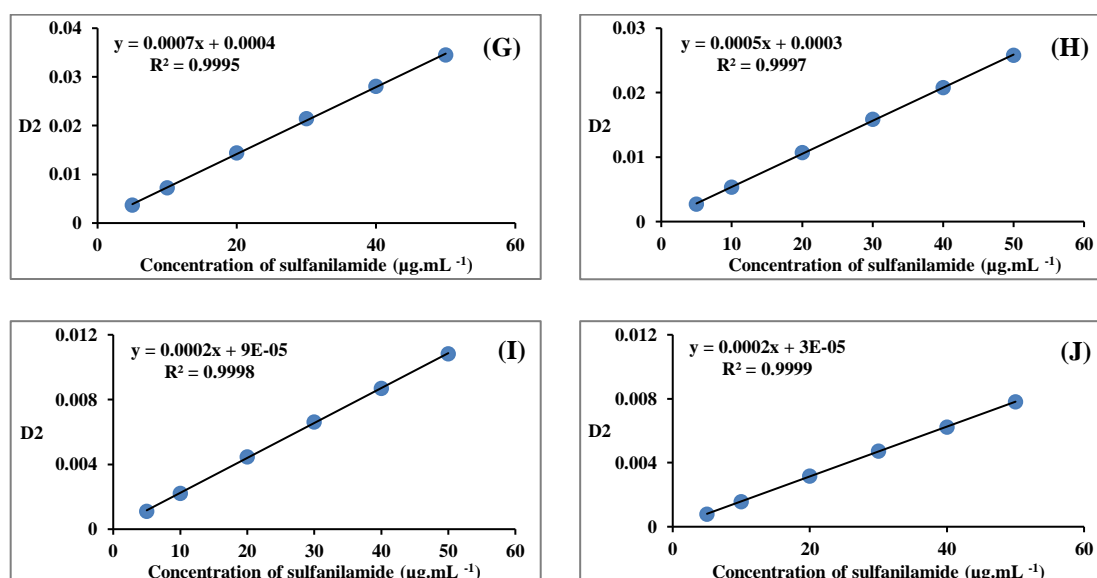


**Figure 4-104:** Calibration curves obtained via second derivative spectra of sulfanilamide for peak to peak (G) 218-231 nm, (H) 231-260 nm, (I) 260-278 nm and (J) height to height at zero cross 254-281 nm.



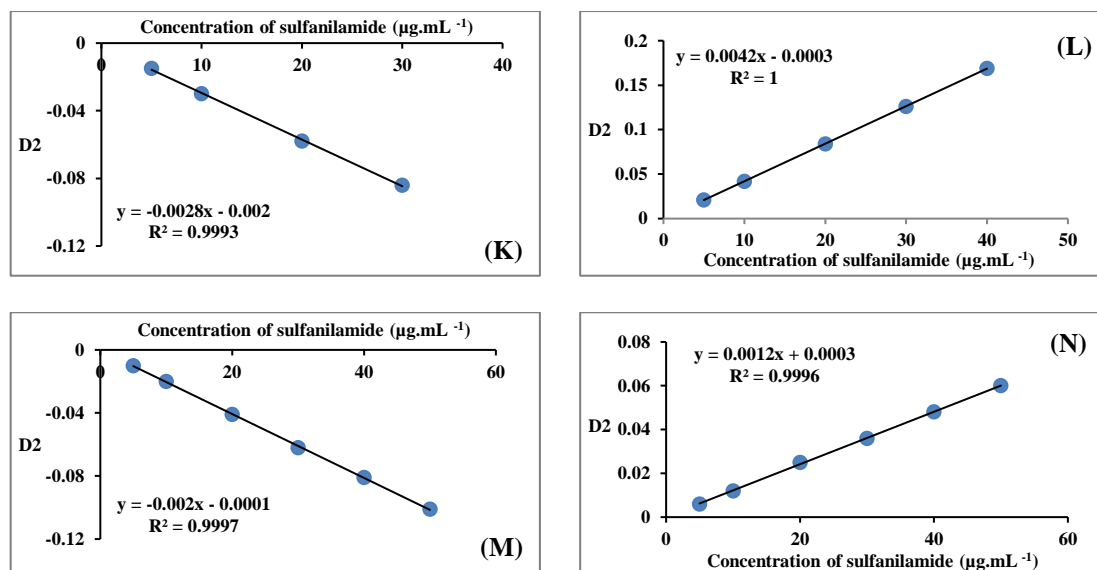


**Figure 4-105:** Calibration curves obtained via second derivative spectra of sulfanilamide for peak area at the interval (K) 210 nm to 224 nm, (L) 224 nm to 245.84 nm, (M) 245.84 nm to 271.28 nm and (N) 271.28 nm to 330 nm.

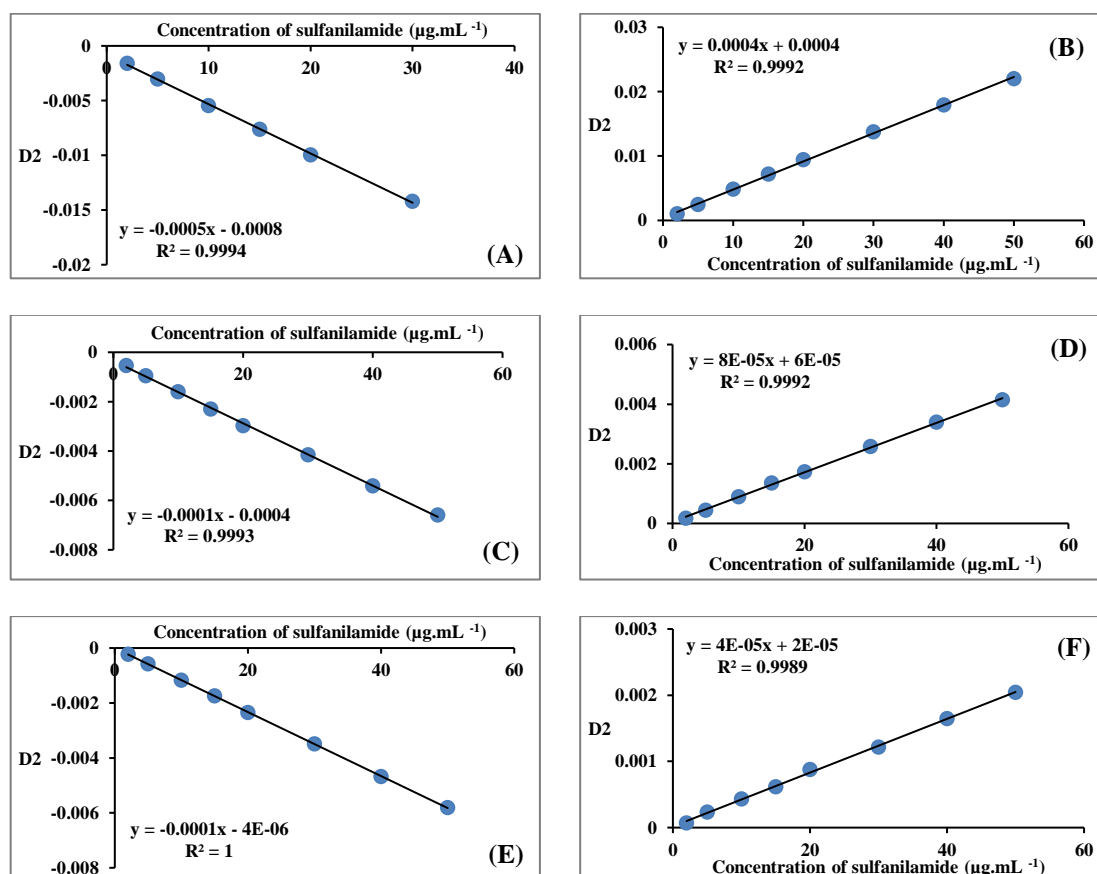


**Figure 4-106:** Calibration curves obtained via second derivative spectra of sulfanilamide ( $2\text{-}50 \mu\text{g.mL}^{-1}$ ) in the presence of ( $2 \mu\text{g.mL}^{-1}$ ) sulfamethoxazole, for peak-to-baseline at (A) 218 nm, (B) 231 nm, (C) 260 nm, (D) 278 nm, (E) height at zero cross at 254 nm and (F) height at zero cross at 281 nm.

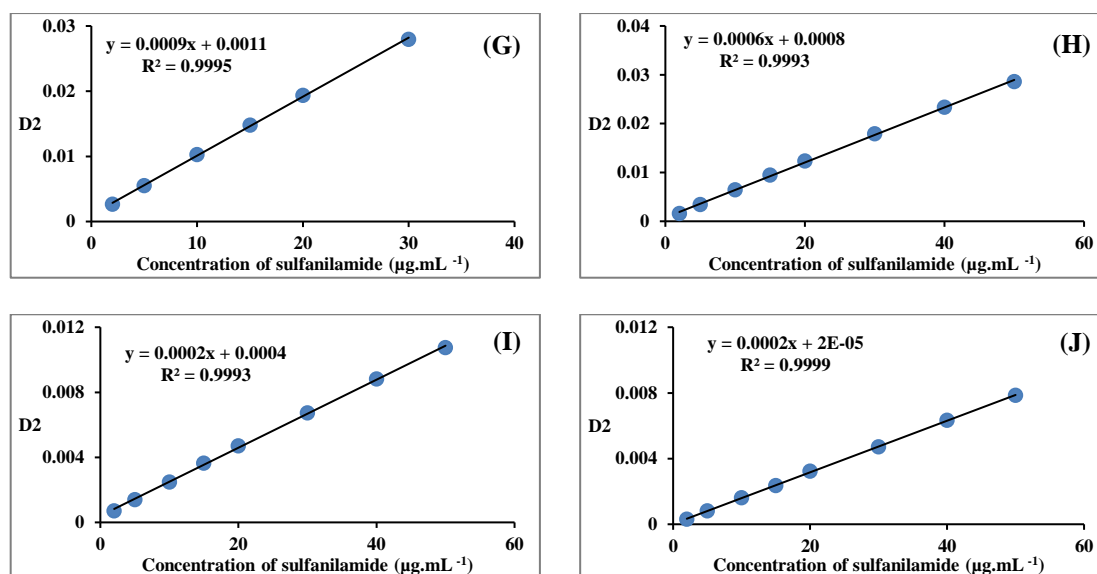


**Figure 4-107:** Calibration curves obtained via second derivative spectra of sulfanilamide (2-50 µg.mL<sup>-1</sup>) in the presence of (2 µg.mL<sup>-1</sup>) sulfamethoxazole, for peak to peak (G) 218-231 nm, (H) 231-260 nm, (I) 260-278 nm and (J) height to height at zero cross 254-281 nm.

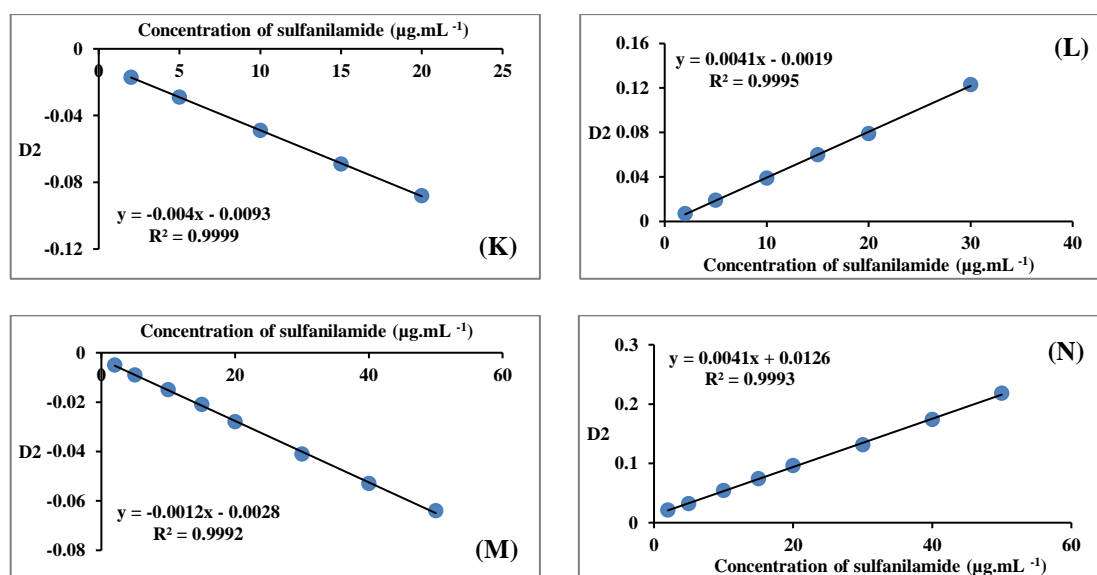


**Figure 4-108:** Calibration curves obtained via second derivative spectra of sulfanilamide (2-50 µg.mL<sup>-1</sup>) in the presence of (2 µg.mL<sup>-1</sup>) sulfamethoxazole, for peak area at the interval (K) 210 nm to 224 nm, (L) 224 nm to 245.84 nm, (M) 245.84 nm to 271.28 nm and (N) 271.28 nm to 330 nm.

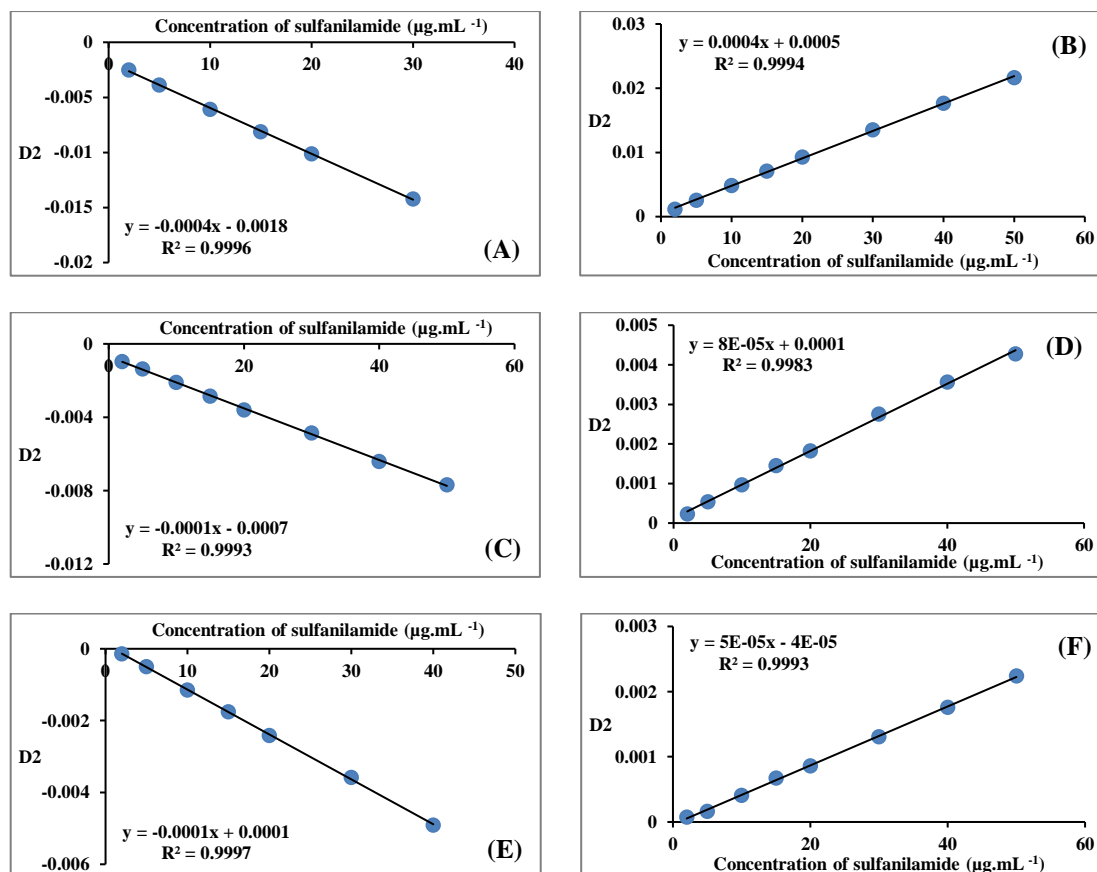


**Figure 4-109:** Calibration curves obtained via second derivative spectra of sulfanilamide ( $2\text{-}50 \mu\text{g.mL}^{-1}$ ) in the presence of ( $5 \mu\text{g.mL}^{-1}$ ) sulfamethoxazole, for peak-to-baseline at (A) 218 nm, (B) 231 nm, (C) 260 nm, (D) 278 nm, (E) height at zero cross at 254 nm and (F) height at zero cross at 281 nm.

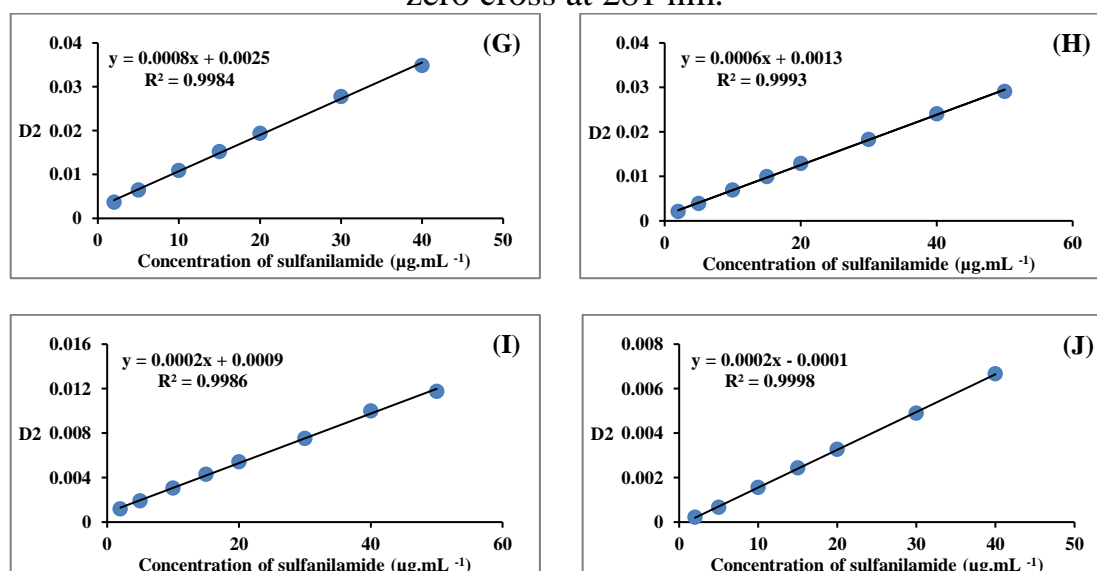


**Figure 4-110:** Calibration curves obtained via second derivative spectra of sulfanilamide ( $2\text{-}50 \mu\text{g.mL}^{-1}$ ) in the presence of ( $5 \mu\text{g.mL}^{-1}$ ) sulfamethoxazole, for peak to peak (G) 218-231 nm, (H) 231-260 nm, (I) 260-278 nm and (J) height to height at zero cross 254-281 nm.

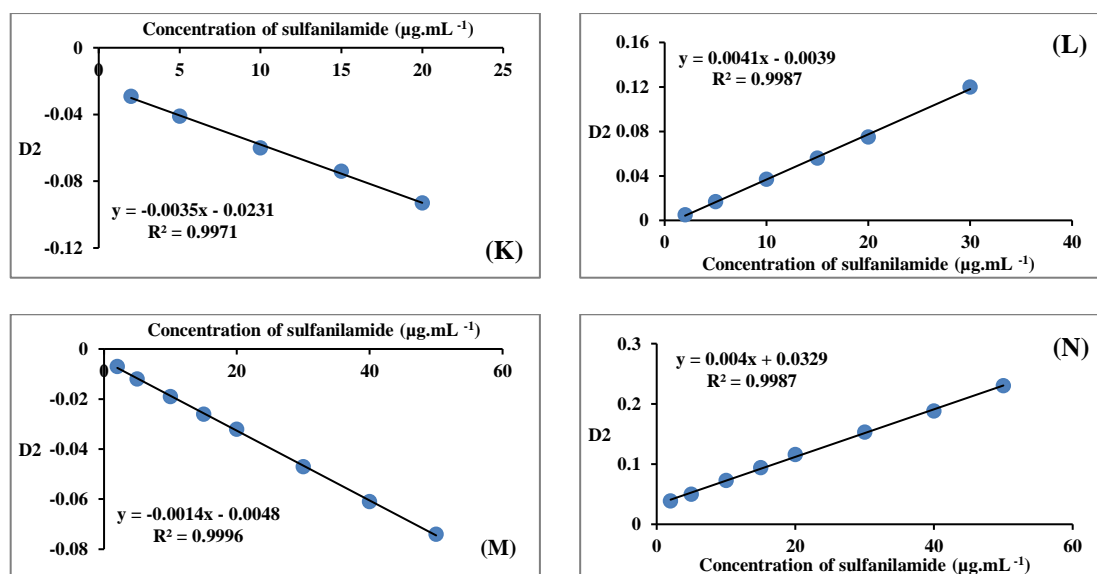


**Figure 4-111:** Calibration curves obtained via second derivative spectra of sulfanilamide ( $2\text{-}50\ \mu\text{g.mL}^{-1}$ ) in the presence of ( $5\ \mu\text{g.mL}^{-1}$ ) sulfamethoxazole, for peak area at the interval (K) 210 nm to 224 nm, (L) 224 nm to 245.84 nm, (M) 245.84 nm to 271.28 nm and (N) 271.28 nm to 330 nm.

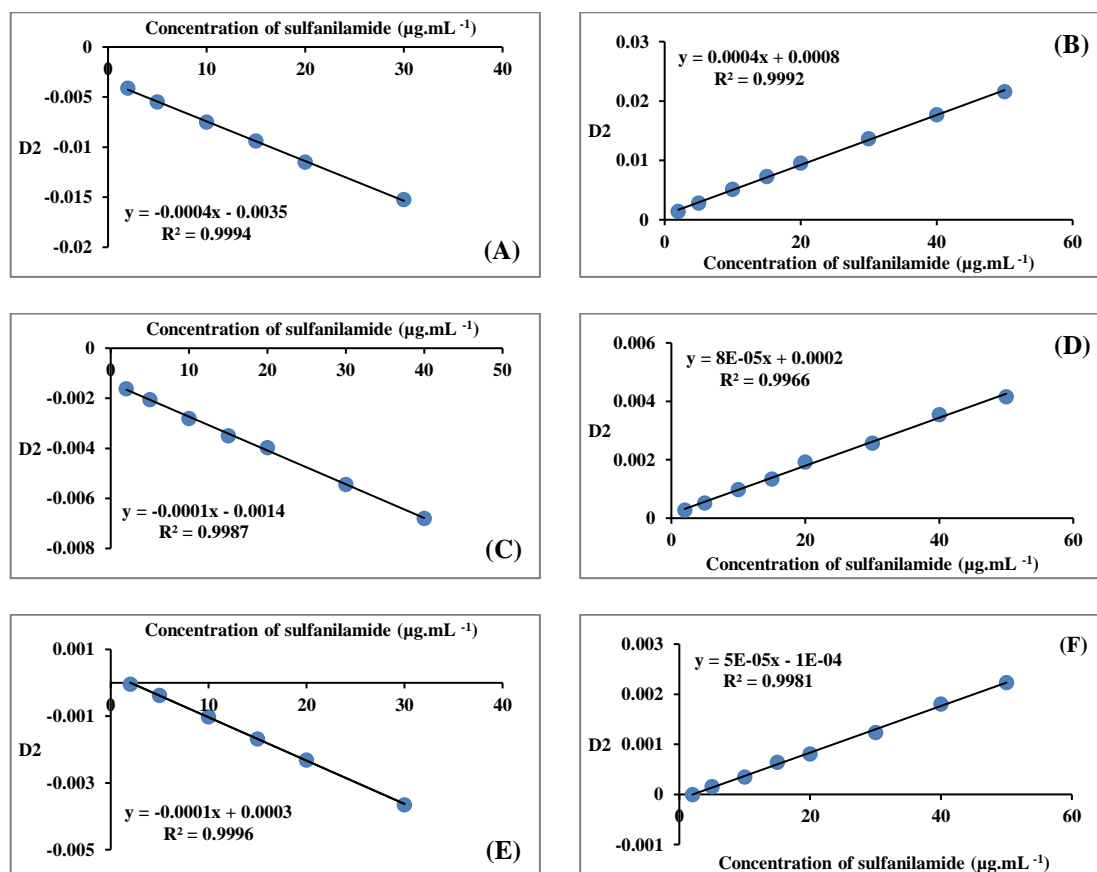


**Figure 4-112:** Calibration curves obtained via second derivative spectra of sulfanilamide ( $2\text{-}50\ \mu\text{g.mL}^{-1}$ ) in the presence of ( $10\ \mu\text{g.mL}^{-1}$ ) sulfamethoxazole, for peak-to-baseline at (A) 218 nm, (B) 231 nm, (C) 260 nm, (D) 278 nm, (E) height at zero cross at 254 nm and (F) height at zero cross at 281 nm.

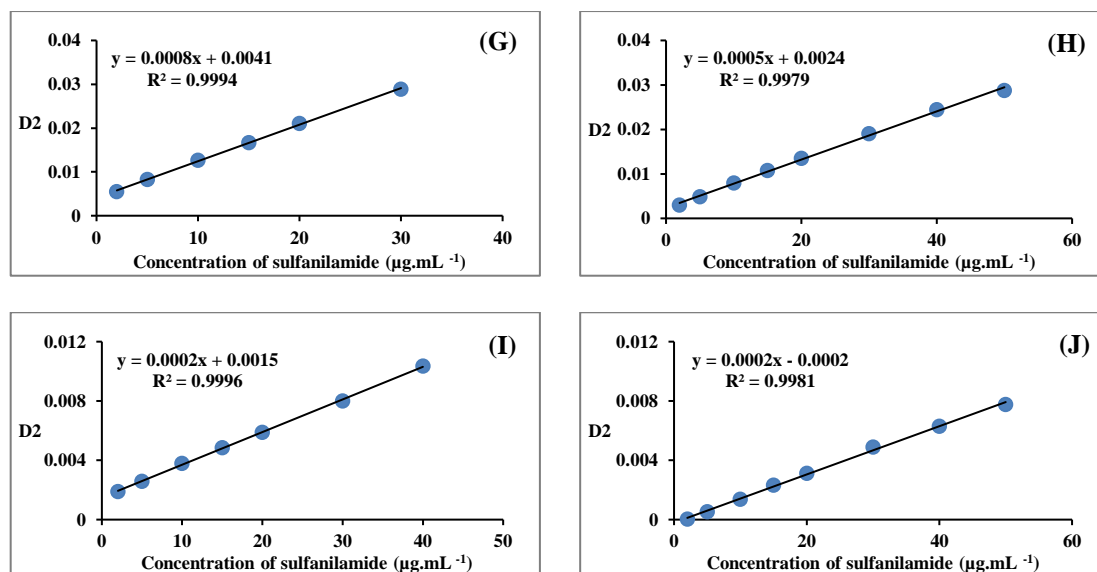


**Figure 4-113:** Calibration curves obtained via second derivative spectra of sulfanilamide ( $2\text{-}50 \mu\text{g.mL}^{-1}$ ) in the presence of ( $10 \mu\text{g.mL}^{-1}$ ) sulfamethoxazole, for peak to peak (G) 218-231 nm, (H) 231-260 nm, (I) 260-278 nm and (J) height to height at zero cross 254-281 nm.

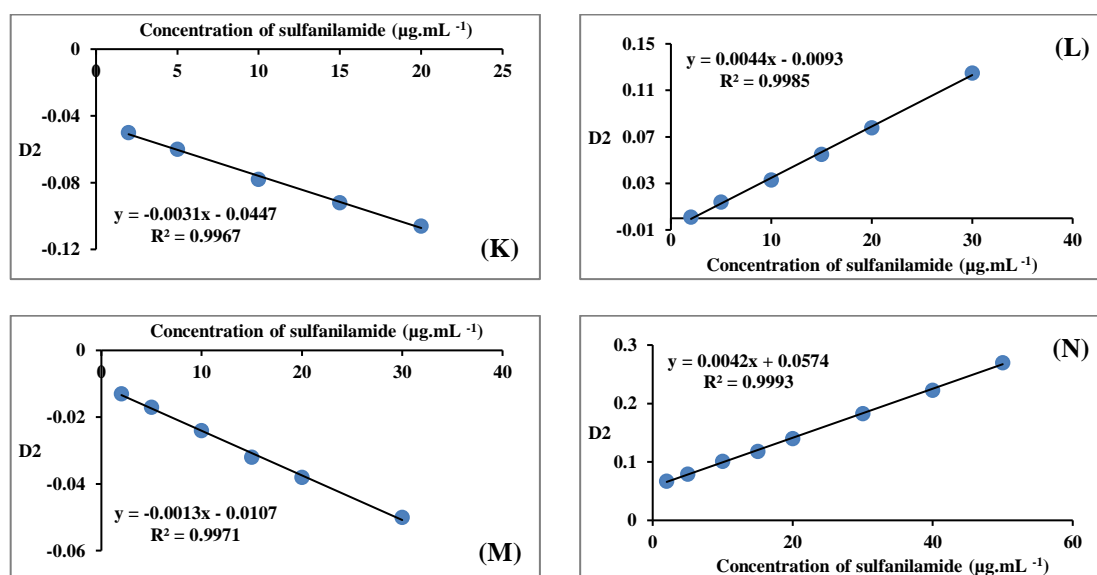


**Figure 4-114:** Calibration curves obtained via second derivative spectra of sulfanilamide ( $2\text{-}50 \mu\text{g.mL}^{-1}$ ) in the presence of ( $10 \mu\text{g.mL}^{-1}$ ) sulfamethoxazole, for peak area at the interval (K) 210 nm to 224 nm, (L) 224 nm to 245.84 nm, (M) 245.84 nm to 271.28 nm and (N) 271.28 nm to 330 nm.

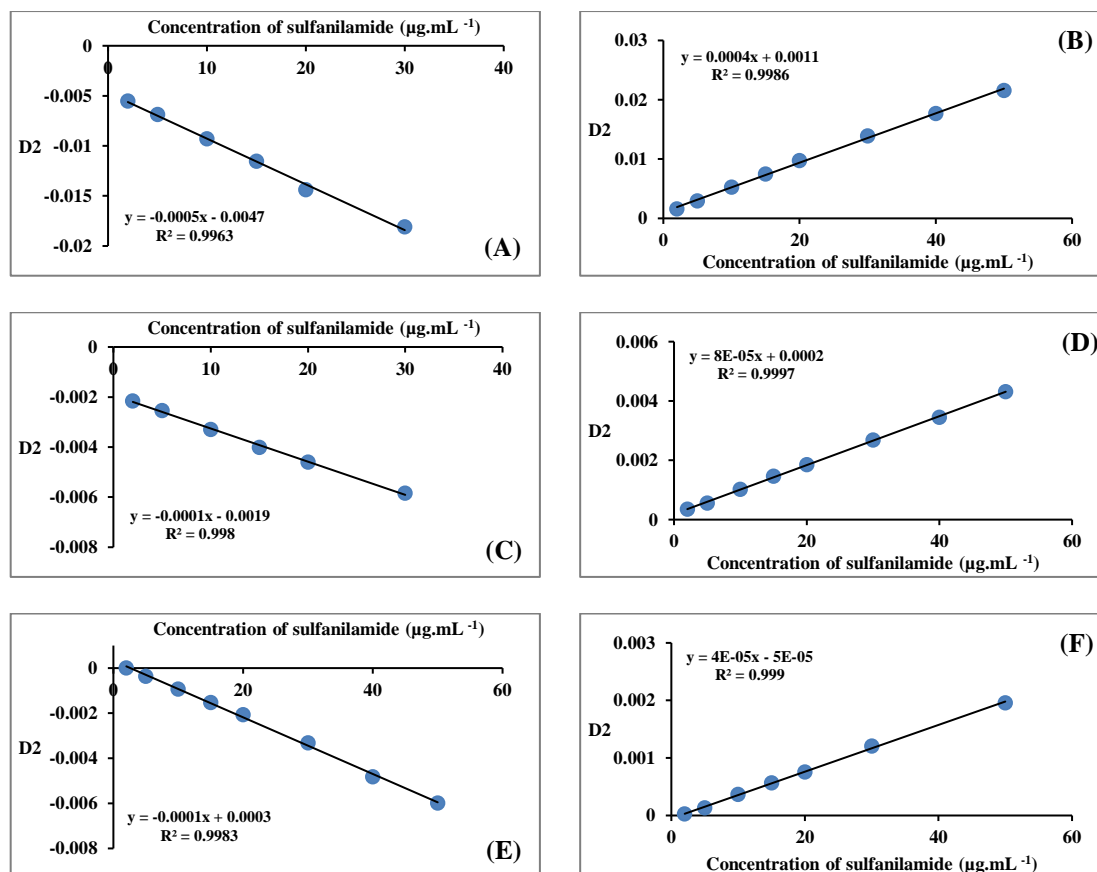


**Figure 4-115:** Calibration curves obtained via second derivative spectra of sulfanilamide ( $2\text{-}50 \mu\text{g.mL}^{-1}$ ) in the presence of ( $15 \mu\text{g.mL}^{-1}$ ) sulfamethoxazole, for peak-to-baseline at (A) 218 nm, (B) 231 nm, (C) 260 nm, (D) 278 nm, (E) height at zero cross at 254 nm and (F) height at zero cross at 281 nm.

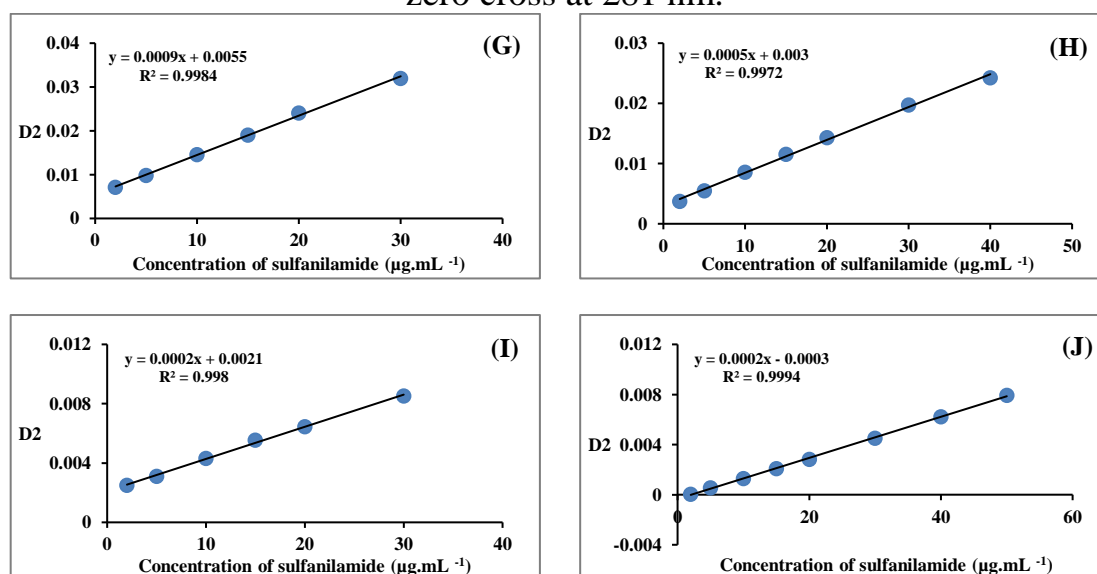


**Figure 4-116:** Calibration curves obtained via second derivative spectra of sulfanilamide ( $2\text{-}50 \mu\text{g.mL}^{-1}$ ) in the presence of ( $15 \mu\text{g.mL}^{-1}$ ) sulfamethoxazole, for peak to peak (G) 218-231 nm, (H) 231-260 nm, (I) 260-278 nm and (J) height to height at zero cross 254-281 nm.

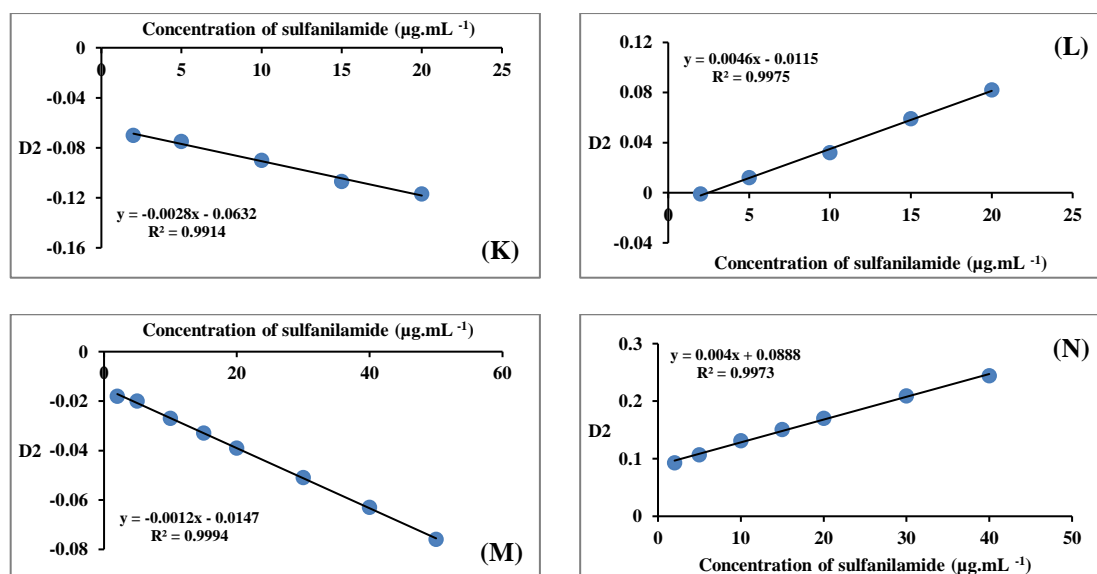


**Figure 4-117:** Calibration curves obtained via second derivative spectra of sulfanilamide ( $2\text{-}50\ \mu\text{g.mL}^{-1}$ ) in the presence of ( $15\ \mu\text{g.mL}^{-1}$ ) sulfamethoxazole, for peak area at the interval (K)  $210\ \text{nm}$  to  $224\ \text{nm}$ , (L)  $224\ \text{nm}$  to  $245.84\ \text{nm}$ , (M)  $245.84\ \text{nm}$  to  $271.28\ \text{nm}$  and (N)  $271.28\ \text{nm}$  to  $330\ \text{nm}$ .

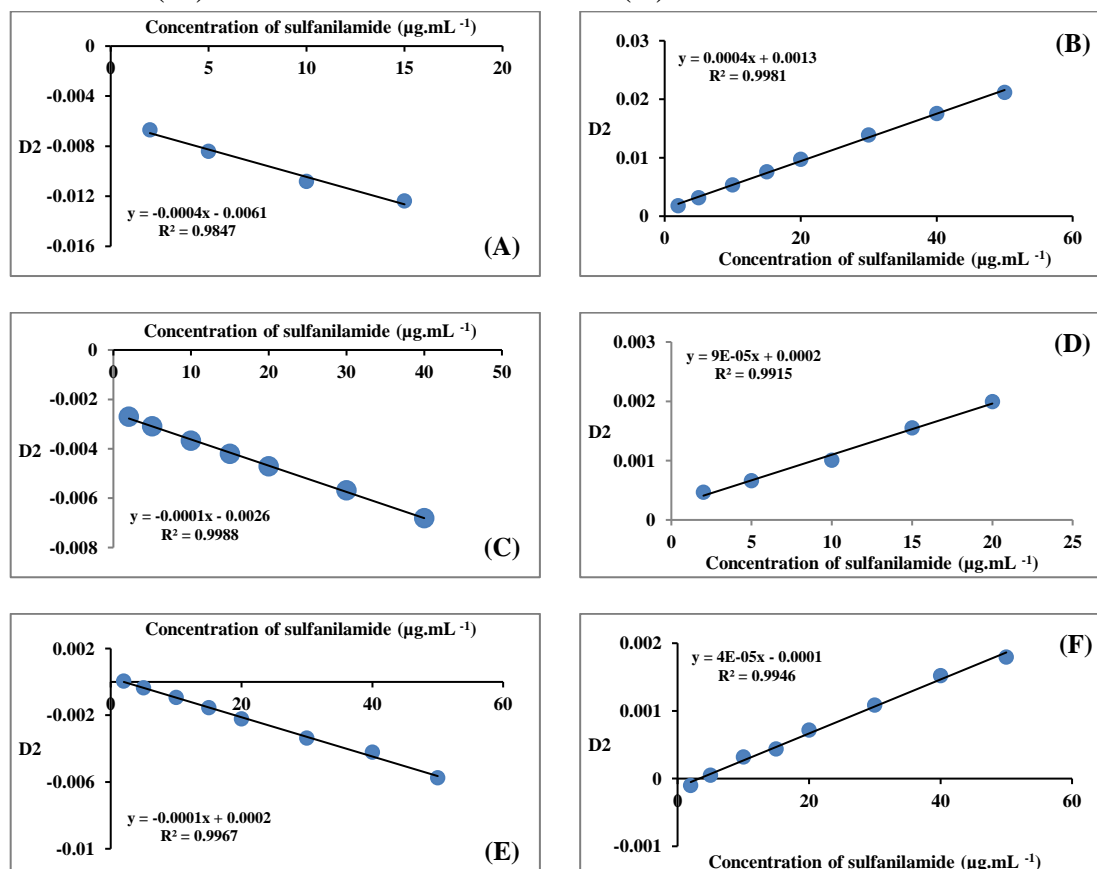


**Figure 4-118:** Calibration curves obtained via second derivative spectra of sulfanilamide ( $2\text{-}50\ \mu\text{g.mL}^{-1}$ ) in the presence of ( $20\ \mu\text{g.mL}^{-1}$ ) sulfamethoxazole, for peak-to-baseline at (A)  $218\ \text{nm}$ , (B)  $231\ \text{nm}$ , (C)  $260\ \text{nm}$ , (D)  $278\ \text{nm}$ , (E) height at zero cross at  $254\ \text{nm}$  and (F) height at zero cross at  $281\ \text{nm}$ .

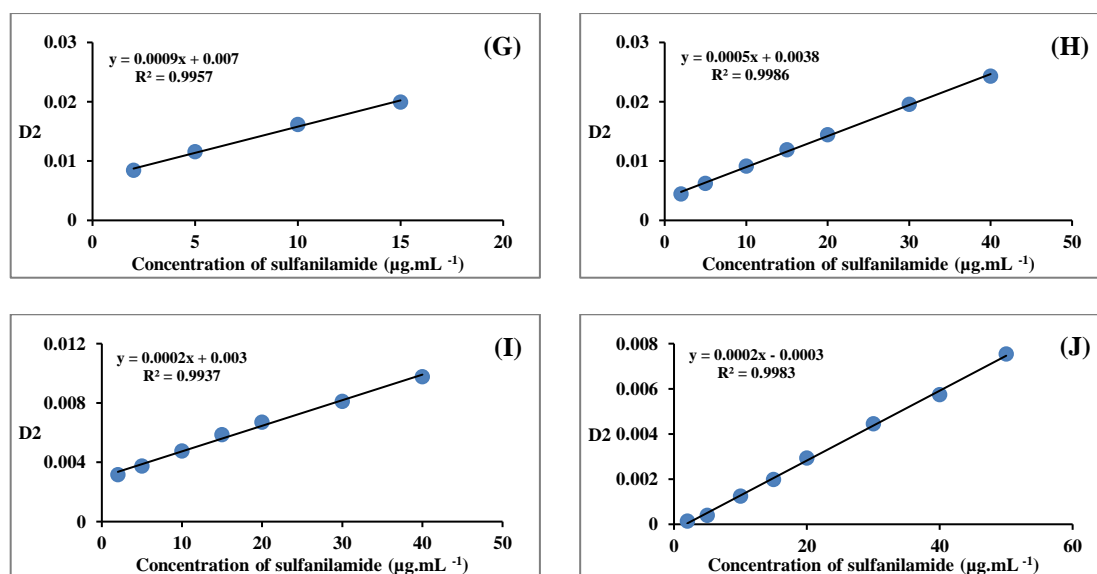


**Figure 4-119:** Calibration curves obtained via second derivative spectra of sulfanilamide ( $2\text{-}50 \mu\text{g.mL}^{-1}$ ) in the presence of ( $20 \mu\text{g.mL}^{-1}$ ) sulfamethoxazole, for peak to peak (G) 218-231 nm, (H) 231-260 nm, (I) 260-278 nm and (J) height to height at zero cross 254-281 nm.

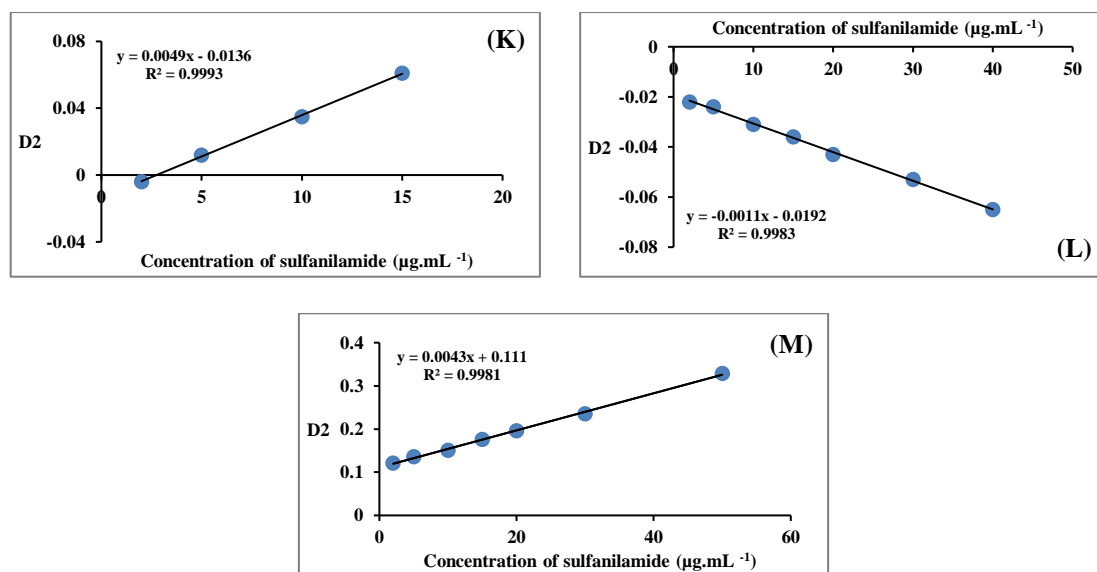


**Figure 4-120:** Calibration curves obtained via second derivative spectra of sulfanilamide ( $2\text{-}50 \mu\text{g.mL}^{-1}$ ) in the presence of ( $20 \mu\text{g.mL}^{-1}$ ) sulfamethoxazole, for peak area at the interval (K) 224 nm to 245.84 nm, (M) 245.84 nm to 271.28 nm and (N) 271.28 nm to 330 nm.



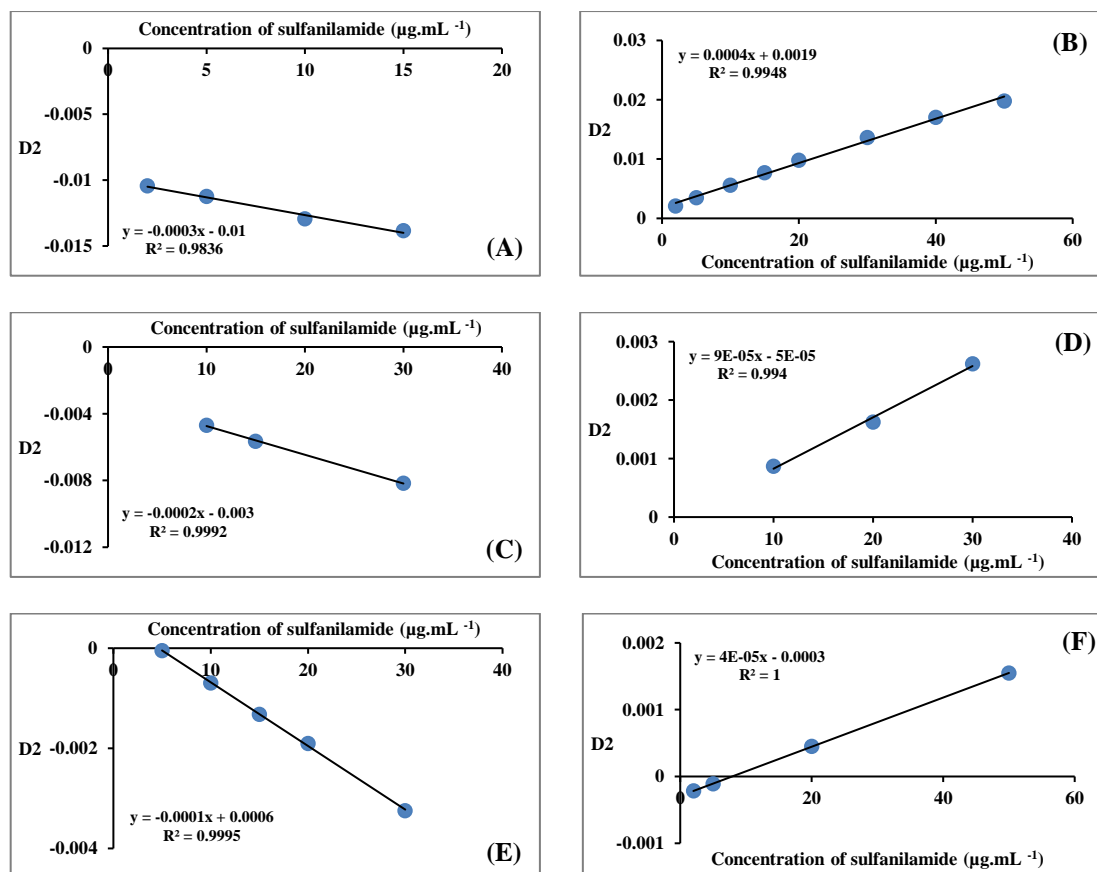


**Figure 4-121:** Calibration curves obtained via second derivative spectra of sulfanilamide ( $2\text{-}50 \mu\text{g.mL}^{-1}$ ) in the presence of ( $30 \mu\text{g.mL}^{-1}$ ) sulfamethoxazole, for peak-to-baseline at (A) 218 nm, (B) 231 nm, (C) 260 nm, (D) 278 nm, (E) height at zero cross at 254 nm and (F) height at zero cross at 281 nm.

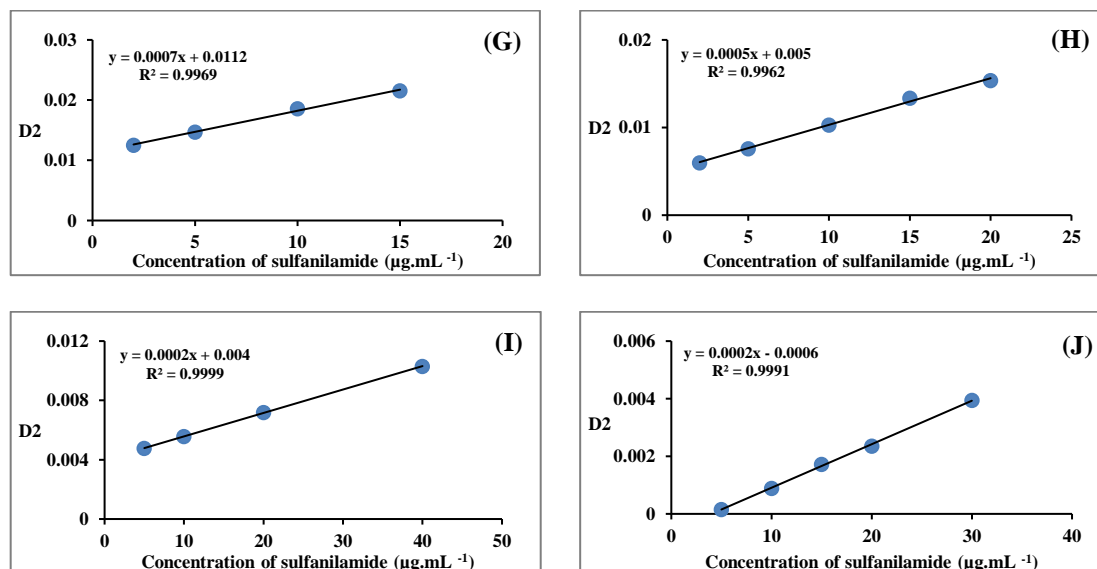


**Figure 4-122:** Calibration curves obtained via second derivative spectra of sulfanilamide ( $2\text{-}50 \mu\text{g.mL}^{-1}$ ) in the presence of ( $30 \mu\text{g.mL}^{-1}$ ) sulfamethoxazole, for peak to peak (G) 218-231 nm, (H) 231-260 nm, (I) 260-278 nm and (J) height to height at zero cross 254-281 nm.

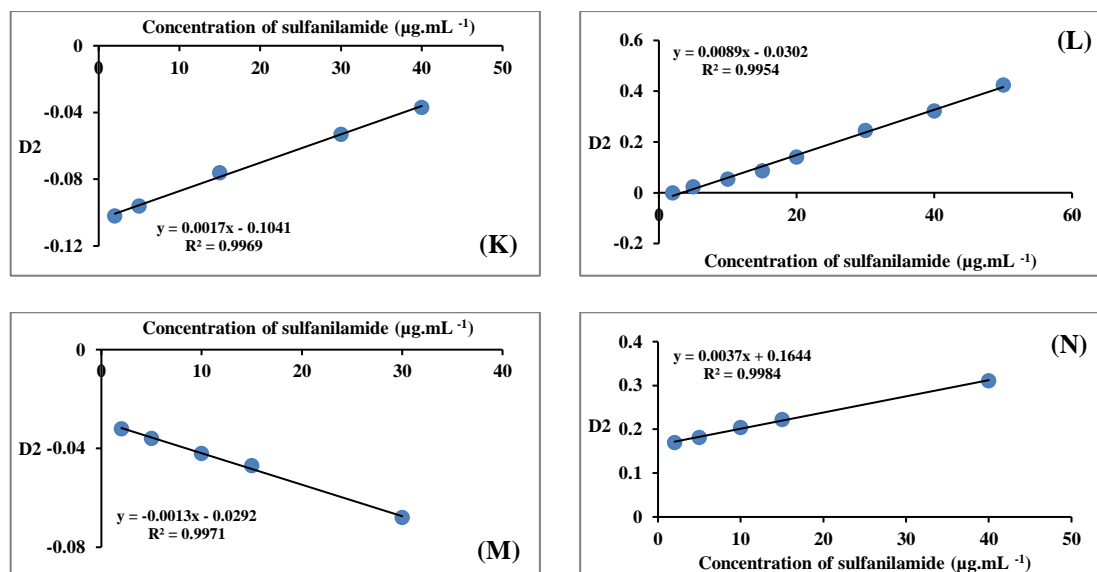


**Figure 4-123:** Calibration curves obtained via second derivative spectra of sulfanilamide ( $2\text{-}50\ \mu\text{g.mL}^{-1}$ ) in the presence of ( $30\ \mu\text{g.mL}^{-1}$ ) sulfamethoxazole, for peak area at the interval (K) 224 nm to 245.84 nm, (M) 245.84 nm to 271.28 nm and (N) 271.28 nm to 330 nm.

Summarize all the results for sulfanilamide analysis by using first and second derivative technique in table 4-3.

**Table 4-3:** Statistical analysis for the determination of sulfanilamide using first and second derivative spectrophotometric technique.

<i>Order of derivative</i>	<i>Mode of calculation</i>	$\lambda$ (nm)	<i>Regression equation</i>	<i>R</i>	<i>Slope</i>
<b>First</b>	Peak to base line	224	$Y = -0.0028x - 0.0036$	0.9986	-0.0028
	Peak to base line	246	$Y = 0.001x + 0.0002$	0.9999	0.001
	Peak to base line	271	$Y = -0.001x - 0.003$	0.9999	-0.001
	Zero cross	241.95	$Y = 0.0009x + 0.0001$	0.9999	0.0009
	Zero cross	267.04	$Y = -0.0009x - 0.0002$	0.9999	-0.0009
	Peak to peak	224-246	$Y = 0.0038x + 0.0039$	0.9992	0.0038
	Peak to peak	246-271	$Y = 0.002x + 0.0005$	0.9999	0.002
	Height to height at zero cross	241.95-267.04	$Y = 0.0018x + 0.0004$	0.9999	0.0018
	Peak area	235.62-258.72	$Y = 0.0148x + 0.0049$	0.9998	0.0148
	Peak area	258.72-331	$Y = -0.0232x - 0.0078$	0.9998	-0.0232
<b>Second</b>	Peak to base line	218	$Y = -0.0003x - 0.0002$	0.9995	-0.0003
	Peak to base line	231	$Y = 0.0004x + 0.0002$	0.9998	0.0004
	Peak to base line	260	$Y = -0.0001x - 5E-05$	0.9998	-0.0001
	Peak to base line	278	$Y = 8E-05x - 3E-05$	0.9998	$8 \times 10^{-5}$
	Zero cross	254	$Y = -0.001x + 2E-05$	0.9999	-0.001
	Zero cross	281	$Y = 5E-05x + 1E-05$	0.9999	$5 \times 10^{-5}$
	Peak to peak	218-231	$Y = 0.0007x + 0.0004$	0.9997	0.0007
	Peak to peak	231-260	$Y = 0.0005x + 0.0003$	0.9998	0.0005
	Peak to peak	260-278	$Y = 0.0002x + 9E-05$	0.9998	0.0002
	Height to height at zero cross	254-281	$Y = 0.0002x + 3E-05$	0.9999	0.0002
	Peak area	210-224	$Y = -0.0028x - 0.002$	0.9996	-0.0028
	Peak area	224-245.84	$Y = 0.0042x - 0.0003$	1.0000	0.0042
	Peak area	245.84-271.28	$Y = -0.002x - 0.0001$	0.9998	-0.002
	Peak area	271.28-330	$Y = 0.0012x + 0.0003$	0.9997	0.0012

#### 4-1-4-5 Accuracy and precision

The accuracies of the proposed methods were confirmed by carrying out three replicate analyses of two different amounts of each of the studied drug (within Beer's law). The different techniques of measurements (i.e. peak-to-baseline, peak-to-peak and area under the peak) were employed to deal with the recorded spectra. Tables 4-4 and 4-5 show the values of relative error percentage which indicate reasonable accuracies. The precision was determined in each case by calculating the percentage relative standard deviation (CV %) for the determinations at each of the studied concentration level.

**Table 4-4:** Results of accuracy and precision for the determination of sulfamethoxazole by derivative technique.

Drug	Order of derivative	Mode of analysis	$\lambda$ (nm)	Drug conc. ( $\mu\text{g.mL}^{-1}$ )		RE %	CV %
				Taken	*Found		
SMZ	First	Peak to baseline	254	5	4.966	-0.68	0.403
				20	19.843	-0.78	0.090
		Peak to baseline	287	5	4.975	-0.50	0.301
				20	19.964	-0.18	0.105
		Peak to peak	254-287	5	5.037	0.74	0.215
				20	20.060	0.30	0.051
	Peak area	241.95-267.04	5	5.004	0.08	0.267	
			20	20.010	0.05	0.093	
	Peak area	267.04-330	5	5.015	0.30	0.315	
			20	20.15	0.75	0.105	
	Second	Peak to baseline	239.5	5	5.024	0.48	0.115
				20	20.055	0.51	0.025
		Peak to baseline	301	5	5.028	0.56	0.101
				20	20.150	0.75	0.213
		Peak to peak	239.5-267.75	5	5.045	0.90	0.315
				20	20.168	0.84	0.235
	Peak area	254.12-281	5	4.980	-0.40	0.370	
			20	20.122	0.61	0.220	
Peak area	286.86-329.5	5	5.018	0.36	0.385		
		20	19.885	-0.57	0.225		

\*Average of three determinations.

**Table 4-5:** Results of accuracy and precision for the determination of sulfanilamide by derivative technique.

Drug	Order of derivative	Mode of analysis	$\lambda$ (nm)	Drug conc. ( $\mu\text{g.mL}^{-1}$ )		RE %	CV %
				Taken	*Found		
SNA	First	Peak to baseline	224.00	5	4.977	-0.46	0.321
				20	19.928	-0.36	0.125
		Peak to baseline	246.00	5	4.973	-0.54	0.537
				20	19.955	-0.22	0.084
		Peak to baseline	271.00	5	5.023	0.46	0.240
				20	20.054	0.27	0.324
		Peak to peak	224.00-246.00	5	4.991	-0.18	0.255
				20	19.892	-0.54	0.368
		Peak to peak	246.00-271.00	5	5.033	0.66	0.236
				20	20.063	0.31	0.129
		Peak area	235.62-258.72	5	4.995	-0.10	0.289
				20	19.982	-0.09	0.099
	Peak area	258.72-331	5	4.975	-0.50	0.295	
			20	19.953	-0.23	0.119	
	Second	Peak to baseline	231.00	5	4.962	-0.76	0.256
				20	19.825	-0.87	0.163
		Peak to baseline	260.00	5	5.040	0.80	0.346
				20	20.115	0.57	0.032
		Peak to baseline	278.00	5	4.959	-0.82	0.115
				20	19.858	-0.71	0.105
		Peak to peak	231.00-260.00	5	5.006	0.12	0.367
				20	20.064	0.32	0.198
		Peak to peak	260.00-278.00	5	5.044	0.88	0.284
				20	20.162	0.81	0.148
Peak area		224.00-245.84	5	5.004	0.08	0.312	
			20	20.012	0.06	0.165	
Peak area	245.84-271.28	5	4.987	-0.26	0.415		
		20	19.953	-0.23	0.217		

\*Average of three determinations.

#### 4-1-4-6 Interferences Study

Derivative spectrophotometry has main advantage, that the presence of a more number of maxima and minima wavelengths gives an opportunity to select a particular wavelength for the determination of active compounds without the interference from other compounds or formulation excipients.

To check the interference from excipients may be used in the dosage forms, percentage recovery was calculated. This study was performed by the addition of known amounts of excipients to mixture solutions of two examined drugs. First and second derivative techniques are used at the selected wavelength for the concentrations of drugs measurement. High recovery showed that no interferences were found using first and second derivative mode for the determination of sulfamethoxazole and sulfanilamide in their mixture even in the presence of the excipients added, these results are listed in Table 4-6.

**Table 4-6:** Percent recovery for mixtures of sulfamethoxazole and sulfanilamide in the presence of 500  $\mu\text{g.mL}^{-1}$  of excipients.

Excipients	Mixture of 5 $\mu\text{g.mL}^{-1}$ of SMZ with 5 $\mu\text{g.mL}^{-1}$ of SNA		Mixture of 15 $\mu\text{g.mL}^{-1}$ of SNA with 5 $\mu\text{g.mL}^{-1}$ of SMZ	
	Conc. found of SMZ ( $\mu\text{g.mL}^{-1}$ )	Recovery %	Conc. found of SNA ( $\mu\text{g.mL}^{-1}$ )	Recovery %
Vanillin	5.074	101.48	15.090	100.60
Glucose	4.980	99.60	14.978	99.85
Lactose	4.967	99.34	14.954	99.69
Starch	5.082	101.64	15.000	100.00
Sucrose	4.965	99.30	15.072	100.48

\* Average of three determinations.

\* D1 and D2 for sulfamethoxazole peak to baseline at 287 nm and 239.5 nm respectively.

\* D1 and D2 for sulfanilamide peak to baseline at 246 nm and 260 nm respectively.

## **4-2 Simultaneous spectrophotometric determination of binary mixture via partial least squares method**

### **4-2-1 Introduction**

Utilization of traditional UV–Vis spectrophotometric techniques for simultaneous determination of two non-interacting species heavily overlapping responses in their binary mixture is difficult without preliminary separation. Multivariate treatment of the overlapping spectral calibration data can offers resolution for such complex system without prior separation steps required for classical spectrophotometric methods<sup>(153)</sup>.

Recently, chemometrics, which rely on the use of a group of mathematical models, statistical principles, and other logic-based methods in the field of chemistry, have gained a great importance in the field dealing with multicomponent analysis those using the especially partial least squares (PLS) multivariate calibration methods<sup>(154-155)</sup>.

In the field of analytical chemistry, various chemometric techniques could be used to extract useful quantitative information by bypassing the difficult mathematics and by focusing on data, and by arguing practicalities rather than dwelling on theory. Application of chemometrics in the field of analytical chemistry evolved rapidly due to availability of powerful, inexpensive personal computers that implement commercial chemometrics softwares<sup>(156)</sup>.

### **4-2-2 Spectrophotometric simultaneous determination of sulfamethoxazole and sulfanilamide by partial least squares**

Chemometrics, as mathematical models, was first developed in 1971 to define the statistical principles, and other logic-based methods in the field of chemistry and, in particular, the field of analytical chemistry to design or select optimal measurement procedures and experiments and to provide maximum chemical information by analyzing chemical data. These models have been rapidly progressed with the evolution of computerized digital analytical instruments which enable obtaining huge amounts of data<sup>(157)</sup>.

Partial least squares regression method (PLS), in recent years has gained more importance in spectrophotometric analyses of mixtures since the method provides accurate description for samples that suffer from various degrees of spectral overlapping<sup>(155,158)</sup>.

### 4-2-3 Experimental

#### 4-2-3-1 Instrumentation

UV-Visible double beam spectrophotometer Cecil CE 7200 & Shimadzu 1800 with 1 cm quartz cuvettes, DELL Windows 8 laptop.

#### 4-2-3-2 Chemicals

All chemicals used in this investigation are described in section 2-2-2.

#### 4-2-3-3 Pharmaceutical compounds

Table 2-4, section 2-2-2, illustrates the used pharmaceutical compounds and their manufactures.

#### 4-2-3-4 Standard drugs solution

The procedures used for the preparation of the standard pharmaceutical solutions, which are used throughout the investigation, are given in section 2-2-4.

#### 4-2-3-5 General recommended procedures

##### 1- Assay procedure for determination sulfamethoxazole or sulfanilamide

Aliquots, of sulfamethoxazole standard solution containing (20.0-500.0  $\mu\text{g}$ ) or sulfanilamide standard solution containing (20.0-500.0  $\mu\text{g}$ ), were transferred into a series of 10 mL volumetric flask and diluted with 0.02 M HCl. The spectrum for each solution was recorded against a reagent blank. The amount of drug was computed from the standard calibration graph.

##### 2- Assay procedure for determination each drug in the presence of the other

Aliquots, of sulfamethoxazole standard solution containing (20.0-500.0)  $\mu\text{g}$  (or sulfanilamide standard solution containing 20.0-500.0  $\mu\text{g}$ ), were transferred into a series of 10 mL volumetric flask containing aliquots of 2.0-50  $\mu\text{g}$  of Sulfanilamide solution (or aliquots of 20.0-500.0  $\mu\text{g}$  of sulfamethoxazole solution); the mixture was then diluted with 0.02 M HCl. The spectrum for each solution was recorded against a reagent blank.



## 4-2-4 Results and discussion

### 4-2-4-1 Absorption spectra

Figure 4-124 shows the spectra of SMZ and SNA in the 190-350 nm wavelength range recorded with 1 nm sampling interval, 1.0 nm slit width, and medium scan speed. The two spectra show serious overlap, therefore, direct UV-spectrophotometric measurements the cited drugs for simultaneously determination in their binary mixture is not possible.

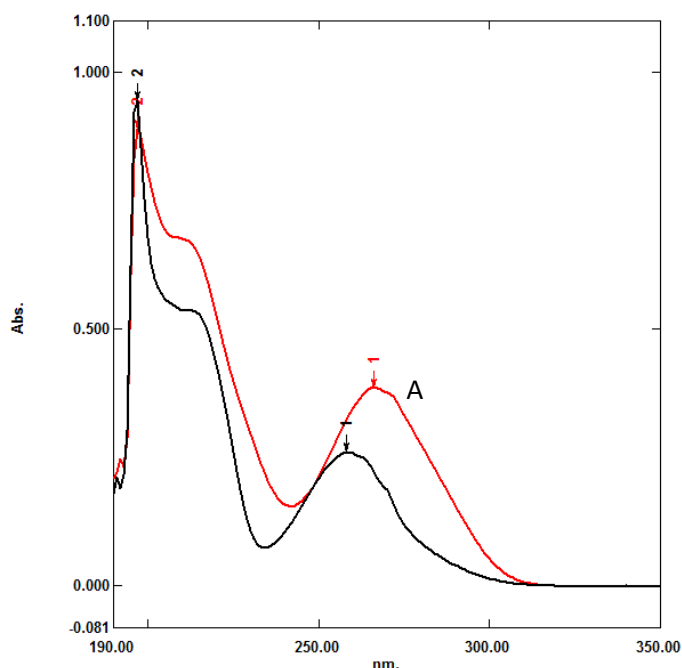


**Figure 4-124:** Normal mode spectrum of (A)  $10 \mu\text{g}\cdot\text{mL}^{-1}$  of sulfamethoxazole and (B)  $10 \mu\text{g}\cdot\text{mL}^{-1}$  sulfanilamide against their blanks.

The application of PLS, which tends to use the full spectrum, provides a more accurate description of the model, more accurate interpretations and expands the applicability of spectrophotometric methods for simultaneous multi-component analysis<sup>(159)</sup> in the near-infrared<sup>(160)</sup> and UV spectra regions<sup>(161)</sup>. Moreover, quantitative spectral information's could be extracted via PLS more powerfully than those methods based on making a single measurement at a specific wavelength or wavenumber, respectively. Measurement at only one wavelength, such as the direct spectrophotometric method, because the simultaneous inclusion of multiple spectral intensities can greatly improve the precision and applicability of the quantitative spectral analysis of mixtures<sup>(162)</sup>. To carryout multivariate, PLS analysis of sulfamethoxazole and

Sulfanilamide in their mixture, it is necessary to prepare calibration matrix that provides the best predictions.

#### 4-2-4-2 Individual calibration

Calibration curves of SMZ and SNA in the range of 2-50  $\mu\text{g.mL}^{-1}$  were constructed as absorbance versus drugs concentrations at 266 nm and 258 nm respectively and statistically evaluated by linear regression (Figures 4-125 and 4-126).

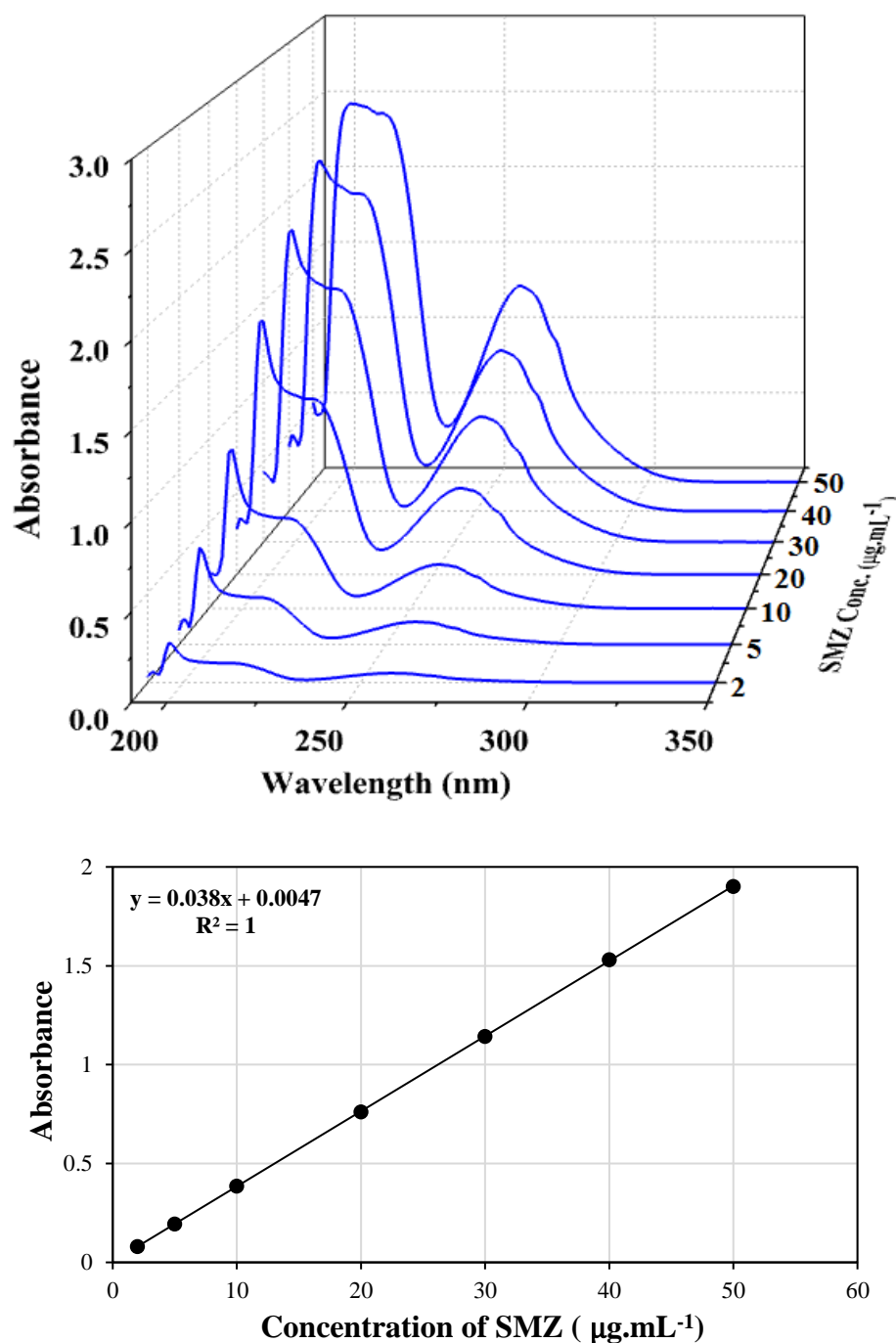
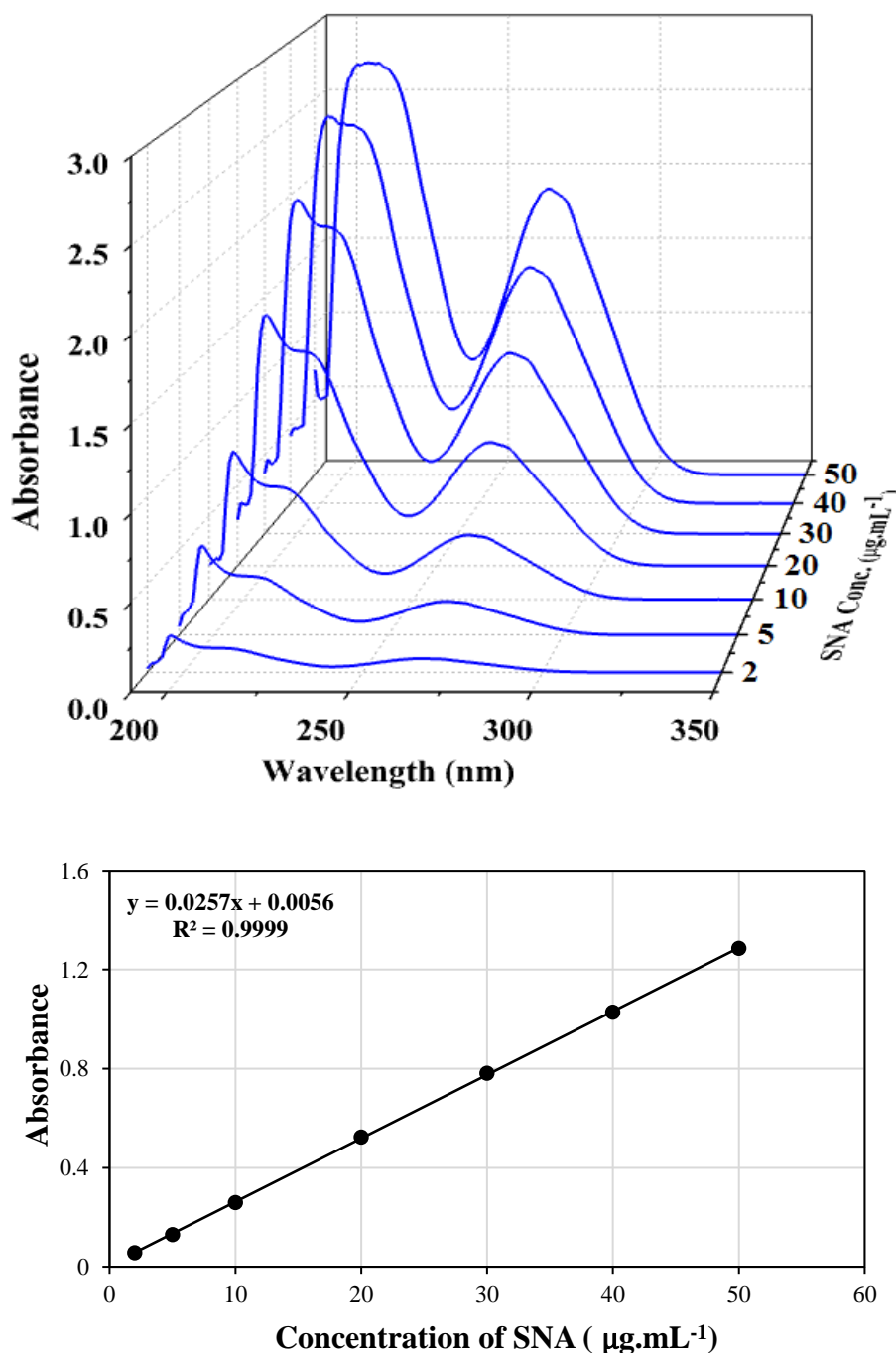


Figure 4-125: Calibration curve of sulfamethoxazole constructed at 266 nm.



**Figure 4-126:** Calibration curve of Sulfanilamide constructed at 258 nm.

#### 4-2-4-3 Multivariate methods

Partial least squares regression is a regression technique, which try to find fundamental linear multivariate model relation between two matrices (X and Y) i.e. between the response and independent variables.

The methodology to factor building offers the description of studied data using minimum number of adjustable parameters to obtain maximum precision and stability of regression model. On the other hand, a decrease

of the productivity of the model may result as additional factors are included in the model due to representation of both the true pattern of relation between descriptors and activity and the random noise and individual features of the training set, although such increase rises the accuracy of description<sup>(163)</sup>.

The training set (i.e. data set containing careful spectrophotometric UV-measurements on a set of known samples) in this work is included in matrices, which are organized into pairs i.e. each absorbance matrix is paired with its corresponding concentration matrix. These data are used to derive the calibration, based on the known samples spectra, to predict the concentrations of unknown samples on one condition that it must be representative, in all ways, of the unknown samples on which the analysis will be used. In practical terms, this means that training sets should:

1. Contain all expected components,
2. Span the concentration ranges of interest,
3. Span the conditions of interest,
4. Contain mutually independent samples.

On the other hand, there are three rules to guide the selection of the number of calibration samples, which are included in a training set.

**Rule of three;** which is the minimum number of samples required for calibration, it simply 3 times the number of samples as there are components.

**Rule of five;** i.e. using 5 times the number of samples, it allows to use enough samples to reasonably represent all possible combinations of concentrations values for not more than a 3-component system.

**Rule of ten;** when 10 times the number of samples as there is components is used, a solid calibration for typical applications is usually could be obtained<sup>(164)</sup>.

The calibration matrix was constructed using the digitalized absorption spectra data (for the region between 190 and 350 nm with medium scan speed) for different solutions of SMZ and SNA mixtures design as the calibration set to fulfill the non-correlated concentration matrix (Table 4-7).

Sixty five prepared SMZ and SNA mixtures were carefully inspected to select twenty mixtures as training set relying on the rule of ten i.e. (from seventy prepared mixtures basing upon linearity ranges of 2.0-50  $\mu\text{g.mL}^{-1}$  for both drugs) by random design as the calibration set so that to fulfill the non-correlated concentration matrix (Table 4-7).

**Table 4-7:** Composition of the training set for applying PLS-2 and PLS-1 methods.

<i>No. of calibration sample</i>	<i>sulfamethoxazole (<math>\mu\text{g.mL}^{-1}</math>)</i>	<i>sulfanilamide (<math>\mu\text{g.mL}^{-1}</math>)</i>
1	50	2
2	50	20
3	50	10
4	40	5
5	40	30
6	30	10
7	30	30
8	30	50
9	20	5
10	20	20
11	20	40
12	15	20
13	15	40
14	10	5
15	10	20
16	10	50
17	5	5
18	5	40
19	2	2
20	2	30

The spectra of all of the selected SMZ and SNA mixtures were recorded in the range of 190 – 350 nm with 0.5 nm sampling interval, 1.0 nm slit width, and medium scan speed and stored as digitalized data in Microsoft Excel file. One hundred and eighty one experimental points per spectrum (range of 220 – 310 nm) were then arranged as row absorbance matrix paired with their corresponding concentration matrix and used to buildup PLS regression model using OriginPro version 9.1.0, 2013.

To select the optimal number of factors included in the regression model, the OriginPro software compute the prediction error sum of squares ( $\text{PRESS} = \sum(y_i - \hat{y}_i)^2$ ) for cross-validated models as an indicator for adequacy of models (the smallest model with fewest numbers of factors) <sup>(165)</sup>. The used cross validation model was to eliminate only one sample at a

time and then PLS2 calibrate the remaining 19 standard spectra, by using this calibration; the concentration of the sample left out was predicted. This process was repeated 20 times (Figure 4-127)

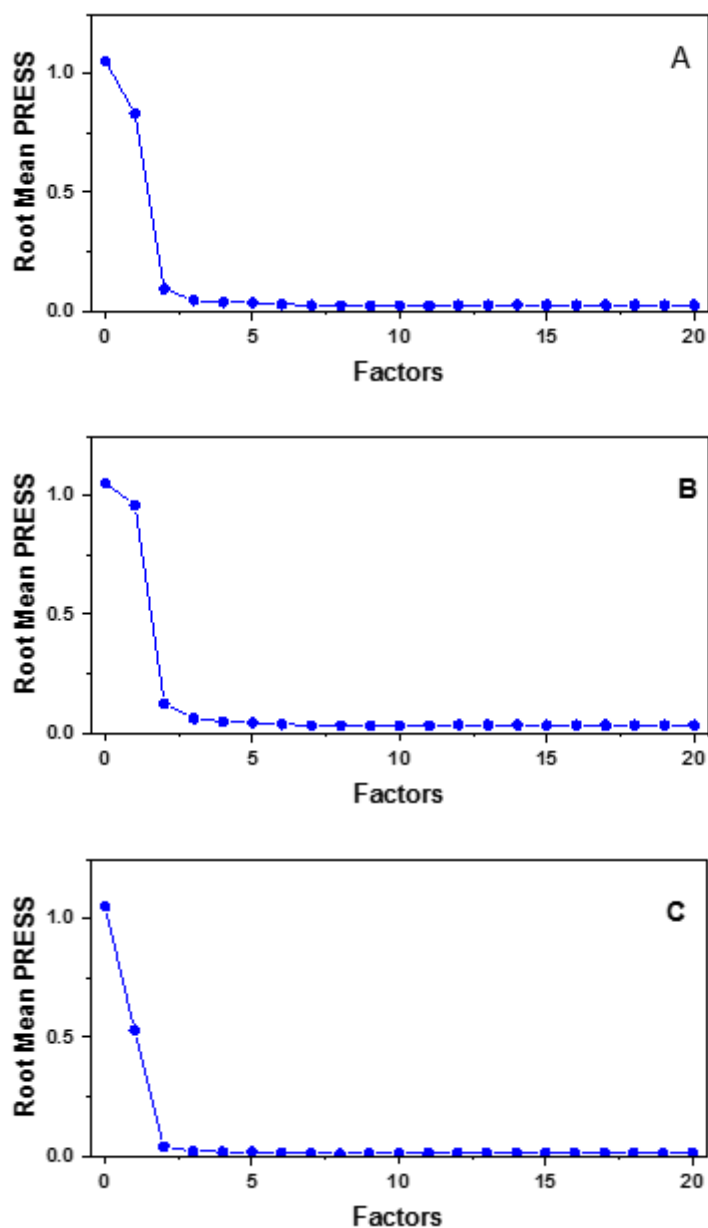


**Figure 4-127:** Plot of PRESS against the number of factors for SMZ and SNA mixture: (A) PLS-2 model, (B) PLS-1 model for SMZ and (C) PLS-1 model for SNA.

The prediction error of each a single component in the mixture contain N samples and total prediction error of M sample mixtures were calculated as the standard error (**R.S.E %**) of the prediction concentration <sup>(166)</sup>. (Tables 4-8 and 4-9 for PLS-1 and PLS-2 models respectively).

**Table 4-8:** Composition of training set, their predictions by PLS-1 model.

Composition ( $\mu\text{g.mL}^{-1}$ )		Prediction ( $\mu\text{g.mL}^{-1}$ )		Recovery %	
sulfamethoxazole	Sulfanilamide	Sulfamethoxazole	Sulfanilamide	Sulfamethoxazole	Sulfanilamide
50	2	50.00354	2.01917	100.0071	100.9585
50	20	50.0017	19.97593	100.0034	99.8797
50	10	49.97867	9.97431	99.9573	99.7431
40	5	40.01712	5.0071	100.0428	100.1420
40	30	40.01067	30.05939	100.0267	100.1980
30	10	30.00781	9.82198	100.0260	98.2198
30	30	30.0018	30.12627	100.0060	100.4209
30	50	29.98959	49.98136	99.9653	99.9627
20	5	19.98184	4.98294	99.9092	99.6588
20	20	19.92689	20.06724	99.6345	100.3362
20	40	20.05567	39.9563	100.2784	99.8908
15	20	14.98964	20.03859	99.9309	100.1930
15	40	14.98415	39.90593	99.8943	99.7648
10	5	10.05291	4.96514	100.5291	99.3028
10	20	10.06655	20.23195	100.6655	101.1598
10	50	9.97662	50.01592	99.7662	100.0318
5	5	4.97043	5.04168	99.4086	100.8336
5	40	5.0071	39.8859	100.1420	99.7148
2	2	1.98472	1.93039	99.2360	96.5195
2	30	1.99259	30.01252	99.6295	100.0417
Mean recovery				99.9700	99.7762
* R.S.E.(%) single				0.1115	0.3277
▪R.S.E.(%) total				0.0390	

$$* \text{R.S.E. (\%)} \text{ single} = \sqrt{\sum_{i=1}^N (\hat{y}_i - y_i)^2 / \sum_{i=1}^N (y_i)^2} \times 100,$$

$$\text{▪R.S.E. (\%)} \text{ total} = \sqrt{\sum_{j=1}^M \sum_{i=1}^N (\hat{y}_{ji} - y_{ji})^2 / \sum_{j=1}^M \sum_{i=1}^N (y_{ji})^2} \times 100$$

**Table 4-9:** Composition of training set, their predictions by PLS-2 model.

Composition ( $\mu\text{g.mL}^{-1}$ )		Prediction ( $\mu\text{g.mL}^{-1}$ )		Recovery %	
sulfamethoxazole	Sulfanilamide	Sulfamethoxazole	Sulfanilamide	Sulfamethoxazole	Sulfanilamide
50	2	49.90909	1.98726	99.8182	99.3630
50	20	50.01211	19.97388	100.0242	99.8694
50	10	50.04560	10.02278	100.0912	100.2278
40	5	40.02742	5.03386	100.0686	100.6772
40	30	39.96078	30.02167	99.9020	100.0722
30	10	30.04728	9.80844	100.1576	98.0844
30	30	29.98976	30.08250	99.9659	100.2750
30	50	30.03156	50.01057	100.1052	100.0211
20	5	20.01781	5.01438	100.0891	100.2876
20	20	19.92058	20.07075	99.6029	100.3538
20	40	20.00762	39.96174	100.0381	99.9044
15	20	15.05684	20.05544	100.3789	100.2772
15	40	14.92847	39.87278	99.5231	99.6820
10	5	10.10150	4.95221	101.0150	99.0442
10	20	10.07240	20.24119	100.7240	101.2060
10	50	10.00530	50.01915	100.0530	100.0383
5	5	4.92306	5.02453	98.4612	100.4906
5	40	5.00852	39.90731	100.1704	99.7683
2	2	1.94714	1.92345	97.3570	96.1725
2	30	1.98716	30.01610	99.3580	100.0537
Mean recovery				99.8452	99.7934
*R.S.E.(%) single				0.1901	0.3315
▪R.S.E.(%) total				0.0425	

$$* \text{R.S.E. (\%)} \text{ single} = \sqrt{\frac{\sum_{i=1}^N (\hat{y}_i - y_i)^2}{\sum_{i=1}^N (y_i)^2}} \times 100,$$

$$\text{▪R.S.E. (\%)} \text{ total} = \sqrt{\frac{\sum_{j=1}^M \sum_{i=1}^N (\hat{y}_{ji} - y_{ji})^2}{\sum_{j=1}^M \sum_{i=1}^N (y_{ji})^2}} \times 100$$

The results show excellent values for single and total relative standard error of both models. The mean squares ( $\text{MSE} = \frac{\sum (y_i - \hat{y}_i)^2}{N}$ ), the root mean squares error ( $\text{RMSE} = \sqrt{\frac{\sum (y_i - \hat{y}_i)^2}{N}}$ ), which is an indication of the average error in the analysis, for each component, was determined for the calibration ( $\text{RMSEC}$ ), where  $y_i$  and  $\hat{y}_i$  are the known and predicted



analyte concentrations, respectively, and N is the number of mixtures in the data set <sup>(159)</sup>. Moreover, mean standard deviation of all the calibrated mixture solutions and coefficient of determination ( $r^2$ ) between the used and calculated concentration in the mixture are given in Table 4-10. Figure 4-128, represents the plots of the predicted values obtained via PLS-1 and PLS-2 model, show high agreements in the results.

**Table 4-10:** Goodness of fit statistics for training set analyses.

Parameter	PLS-1		PLS-2	
	Variable SMZ	Variable SNA	Variable SMZ	Variable SNA
Observations	20.000			
Sum of	20.000			
$r^2$	1.000	1.000	1.000	1.000
Std. deviation	$3.18 \times 10^{-2}$	$8.74 \times 10^{-2}$	$5.41 \times 10^{-2}$	$8.85 \times 10^{-2}$
MSE	$9.59 \times 10^{-4}$	$7.26 \times 10^{-3}$	$2.78 \times 10^{-3}$	$7.43 \times 10^{-3}$
RMSEC	$3.10 \times 10^{-2}$	$8.52 \times 10^{-2}$	$5.28 \times 10^{-2}$	$8.85 \times 10^{-2}$

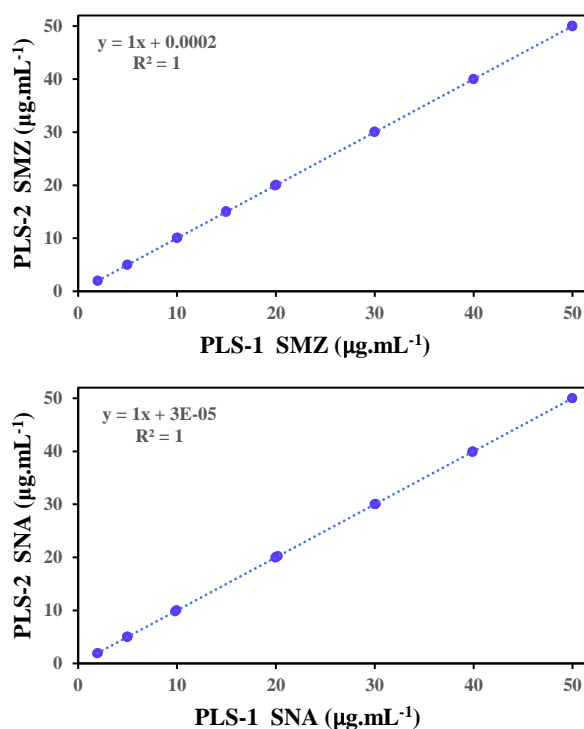


**Figure 4-128:** Plot of predicted concentrations of training sulfamethoxazole and sulfanilamide sets obtained by PLS-1 against those obtained by PLS-2 model.

#### 4-2-4-4 Accuracy and precision

The accuracy and precision of the proposed PLS-1 and PLS-2 regression models for simultaneous prediction of the concentrations of SMZ and SNA in training set was confirmed by performing replicate analyses for two different levels of concentration of sought drugs by calculating the average relative error percentage and the relative standard deviation (Table 4-11). The results indicated excellent accuracy and precision of the method at each concentration level.

**Table 4-11:** Evaluation of accuracy and precision of the proposed method.

	<i>Taken</i> ( $\mu\text{g.mL}^{-1}$ )		<i>Found</i> ( $\mu\text{g.mL}^{-1}$ )				<i>Mean</i>	<i>RE%</i>	<i>RSD%</i>
<b>SMZ</b>	10	PLS-1	10.05291	10.06655	9.97662	--	10.0320	0.3203	0.4831
		PLS-2	10.1015	10.0724	10.0053	--	10.0597	0.5973	0.4904
	50	PLS-1	50.00354	50.0017	49.97867	--	49.9946	-0.0107	0.0277
		PLS-2	49.90909	50.01211	50.0456	--	49.9889	-0.0221	0.1423
<b>SNA</b>	5	PLS-1	5.0071	4.98294	4.96514	5.04168	4.9992	-0.0157	0.8012
		PLS-2	5.03386	5.01438	4.95221	5.02453	5.0062	0.1249	0.7821
	40	PLS-1	39.9563	39.90593	39.8859	--	39.9160	-0.2099	0.0909
		PLS-2	39.96174	39.87278	39.90731	--	39.9139	-0.2151	0.1124

#### 4-2-4-5 Application of the method

Calibration PLS-1 and PLS-2 models were applied for simultaneous determination of SMZ and SNA in twenty synthetic sample mixtures set. Results are shown in Tables 4-12 and 4-13, while other statistical parameters are given in Table 4-14.

**Table 4-12:** Composition of synthetic mixture samples, their predictions by PLS-1 model and statistical parameters for the system.

Composition ( $\mu\text{g.mL}^{-1}$ )		Prediction ( $\mu\text{g.mL}^{-1}$ )		Recovery %	
Sulfamethoxazole	Sulfanilamide	Sulfamethoxazole	Sulfanilamide	Sulfamethoxazole	Sulfanilamide
50	10	49.97867	9.97431	99.9573	99.7431
50	15	50.23726	15.18886	100.4745	101.2591
50	30	50.79031	29.50902	101.5806	98.3634
40	2	40.03695	1.99813	100.0924	99.9065
40	20	39.93310	20.58013	99.8328	102.9007
40	10	40.02046	10.17278	100.0512	101.7278
30	15	30.02374	15.10622	100.0791	100.7081
30	20	30.08871	20.11420	100.2957	100.5710
30	2	29.85440	1.74846	99.5147	87.4230
20	10	20.21143	9.98364	101.0572	99.8364
20	30	20.01822	30.11446	100.0911	100.3815
20	50	19.93882	50.25453	99.6941	100.5091
15	50	14.96115	50.78764	99.7410	101.5753
15	15	15.10628	15.09654	100.7085	100.6436
15	30	14.98913	30.18767	99.9275	100.6256
10	10	10.05978	10.10215	100.5978	101.0215
2	5	1.99824	5.04347	99.9120	100.8694
5	2	5.05893	1.95885	101.1786	97.9425
2	10	1.99303	10.20009	99.6515	102.0009
2	50	1.94806	49.76384	97.4030	99.5277
Mean recovery				100.2336	99.8239
*R.S.E.(%) single				0.6809	1.2545
▫R.S.E.(%) total				0.0851	

$$* \text{R.S.E. (\%)} \text{ single} = \sqrt{\sum_{i=1}^N (\hat{y}_i - y_i)^2 / \sum_{i=1}^N (y_i)^2} \times 100,$$

$$\text{▫R.S.E. (\%)} \text{ total} = \sqrt{\sum_{j=1}^M \sum_{i=1}^N (\hat{y}_{ji} - y_{ji})^2 / \sum_{j=1}^M \sum_{i=1}^N (y_{ji})^2} \times 100$$

**Table 4-13:** Composition of synthetic mixture samples, their predictions by PLS-2 model and statistical parameters for the system.

<b>Composition (<math>\mu\text{g.mL}^{-1}</math>)</b>		<b>Prediction (<math>\mu\text{g.mL}^{-1}</math>)</b>		<b>Recovery %</b>	
<i>Sulfamethoxazole</i>	<i>Sulfanilamide</i>	<i>Sulfamethoxazole</i>	<i>Sulfanilamide</i>	<i>Sulfamethoxazole</i>	<i>Sulfanilamide</i>
50	10	50.04560	10.02278	100.0912	100.2278
50	15	50.14987	15.21792	100.2997	101.4528
50	30	50.65188	29.60079	101.3038	98.6693
40	2	40.02374	2.01084	100.0594	100.5420
40	20	39.79815	20.56166	99.4954	102.8083
40	10	39.94859	10.18277	99.8715	101.8277
30	15	30.06190	15.09884	100.2063	100.6589
30	20	30.10065	20.09508	100.3355	100.4754
30	2	29.95391	1.74928	99.8464	87.4640
20	10	20.18865	10.00990	100.9433	100.0990
20	30	19.97165	30.12414	99.8583	100.4138
20	50	19.88975	50.24047	99.4488	100.4809
15	50	14.99205	50.79572	99.9470	101.5914
15	15	15.12676	15.09785	100.8451	100.6523
15	30	14.95891	30.17518	99.7261	100.5839
10	10	10.05591	10.08888	100.5591	100.8888
2	5	1.94462	5.03833	97.2310	100.7666
5	2	4.99948	1.94788	99.9896	97.3940
2	10	1.92138	10.18360	96.0690	101.8360
2	50	1.95357	49.74717	97.6785	99.4943
Mean recovery				99.8452	99.9164
*R.S.E.(%) single				0.5891	1.2137
▫R.S.E.(%) total				0.0821	

$$* \text{R.S.E. (\%)} \text{ single} = \sqrt{\sum_{i=1}^N (\hat{y}_i - y_i)^2 / \sum_{i=1}^N (y_i)^2} \times 100,$$

$$\text{▫R.S.E. (\%)} \text{ total} = \sqrt{\sum_{j=1}^M \sum_{i=1}^N (\hat{y}_{ji} - y_{ji})^2 / \sum_{j=1}^M \sum_{i=1}^N (y_{ji})^2} \times 100$$

**Table 4-14:** Goodness of fit statistics for synthetic samples set analyses.

Parameter	PLS-1		PLS-2	
	Variable SMZ	Variable SNA	Variable SMZ	Variable SNA
Observations	20.000			
Sum of	20.000			
$r^2$	0.9999	0.9997	0.9999	0.9998
Std. deviation	$2.04 \times 10^{-1}$	$2.89 \times 10^{-1}$	$1.76 \times 10^{-1}$	$2.80 \times 10^{-1}$
MSE	$3.94 \times 10^{-2}$	$7.92 \times 10^{-2}$	$2.95 \times 10^{-2}$	$7.47 \times 10^{-2}$
RMSEC	$1.99 \times 10^{-1}$	$2.81 \times 10^{-1}$	$1.72 \times 10^{-1}$	$2.73 \times 10^{-1}$

Figures 4-129 and 4-130 show plots of the predicted concentrations of synthetic SMZ and SNA mixture samples obtained with constructed PLS-1 and PLS-2 models against their true concentrations.

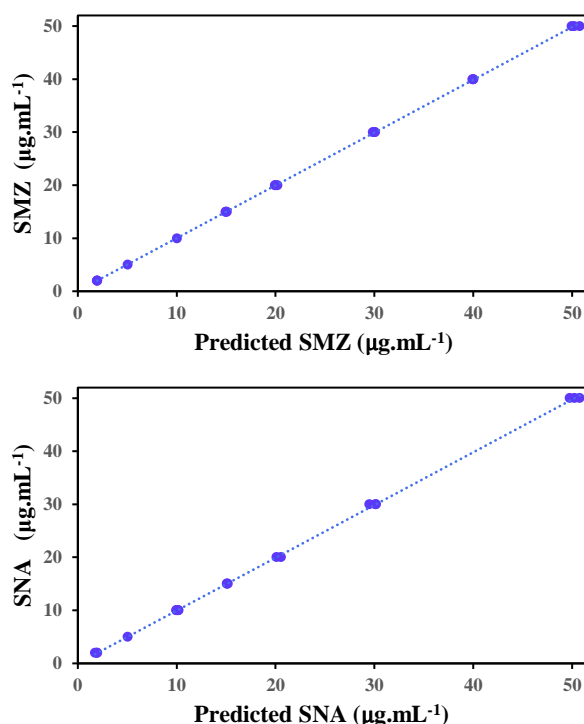


**Figure 4-129:** Plots of predicted sulfamethoxazole and sulfanilamide concentrations in synthetic mixture samples obtained by PLS-1 against their true concentrations.

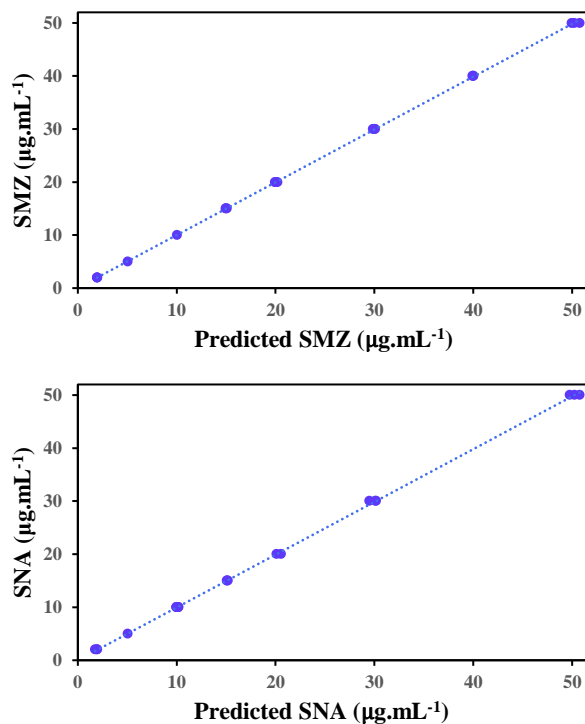


**Figure 4-130:** Plots of predicted sulfamethoxazole and sulfanilamide concentrations in synthetic mixture samples obtained by PLS-2 against their true concentrations.

The concentration residuals were plotted against the actual concentrations of the prepared mixtures (Figures 4-131- 4-132) for SMZ and SNA in all samples appear to be randomly distributed around zero.

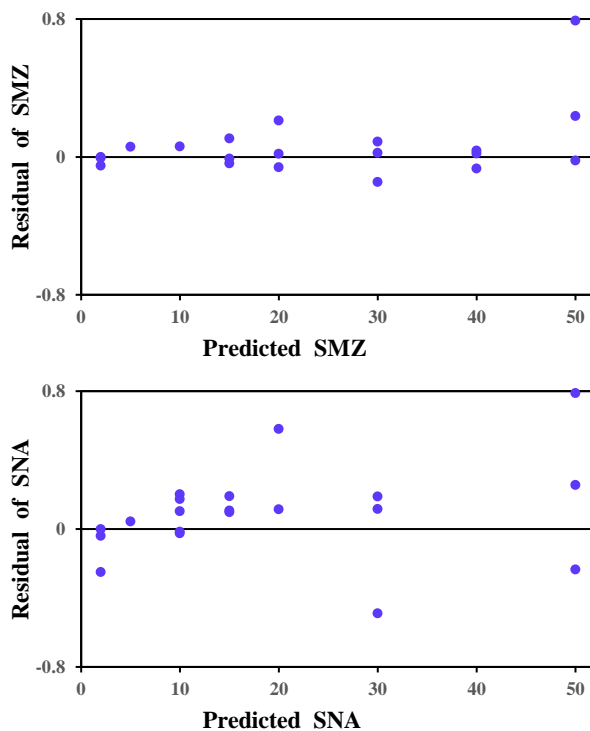


**Figure 4-131:** Plots of residuals of SMZ and SNA against their actual concentrations in the synthetic mixture samples, by PLS-1 model.

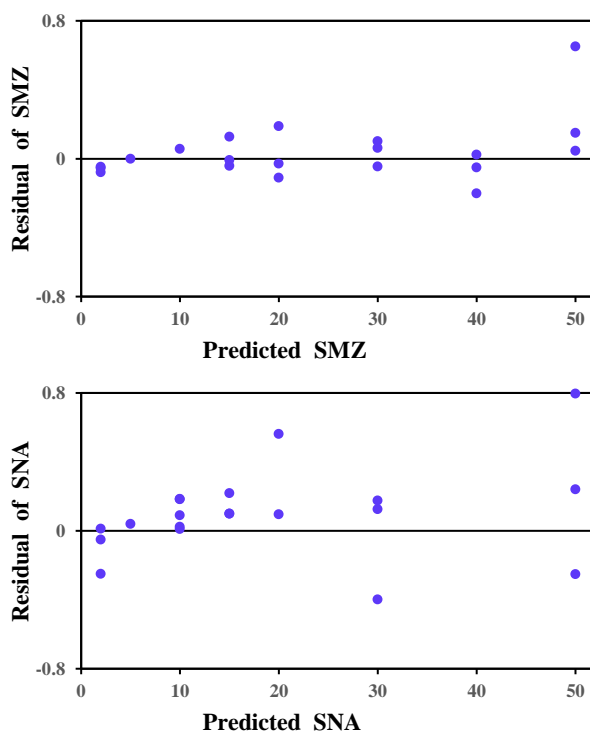


**Figure 4-132:** Plots of residuals of SMZ and SNA against their actual concentrations in the synthetic mixture samples, by PLS-2 model.

The precision and the accuracy of the obtained results of SMZ and SNA in replicate samples of their synthetic mixtures was tested by calculating the relative standard deviation percent and the average relative error percent when PLS-1 and PLS-2 models are used for this purpose. Results in Table 4-15 indicate good accuracy and precision.

**Table 4-15:** Evaluation of accuracy and precision of the proposed method.

	<i>Taken</i> ( $\mu\text{g.mL}^{-1}$ )		<i>Found</i> ( $\mu\text{g.mL}^{-1}$ )			<i>Mean</i>	<i>RE</i> %	<i>RSD%</i>
<b>SMZ</b>	2	PLS-1	1.99824	1.99303	1.94806	1.9798	-1.0112	1.3936
		PLS-2	1.9446	1.9214	1.9536	1.9399	-3.0072	0.8565
	30	PLS-1	30.02374	30.0887	29.8544	29.9890	-0.0368	0.4034
		PLS-2	30.0619	30.1007	29.9539	30.0388	0.1294	0.2532
	50	PLS-1	49.97867	50.2373	50.7904	50.3354	0.6708	0.8237
		PLS-2	50.0456	50.1499	50.6519	50.2825	0.5649	0.6447
<b>SNA</b>	2	PLS-1	1.9589	1.9981	1.7485	1.9018	-4.9093	7.0592
		PLS-2	1.9479	2.0108	1.7493	1.9027	-4.8667	7.1750
	30	PLS-1	29.5090	30.1145	30.1877	29.9371	-0.2098	1.2442
		PLS-2	30.1241	30.1752	29.6008	29.9667	-0.1110	1.0609
	50	PLS-1	50.2545	50.7876	49.7638	50.2687	0.5373	1.0186
		PLS-2	50.2405	50.7957	49.7472	50.2611	0.5222	1.0437

### 4-3 Conclusion

Both reported methods are rapid, simple, economical, and sensitive. They can be used in routine analysis of SMZ and SNA in their pure forms without prior separation or treatment.

The analysis of SMZ and SAN in synthetic samples was performed via PLS models. The results obtained were compared statistically by variance ratio F-test with the proposed derivative technique. The experimental F-values did not exceed the theoretical ones at 95% confidence level, indicating the absence of any significant difference between the compared methods (Tables 4-16 – 4-17).



**Table 4-16:** F-Test Two-Sample (Derivative and PLS) for Variances for the analysis of SMZ.

	<i>Derivative</i>	<i>PLS</i>
Mean	12.52495	12.42054
Variance	59.46600	49.78681
Observations	20.00000	20.00000
Df	19.00000	19.00000
F	1.19441	
P(F<=f) one-tail	0.35127	
F Critical one-tail	2.16825	

**Table 4-17:** F-Test Two-Sample (Derivative and PLS) for Variances for the analysis of SNA.

	<i>Derivative</i>	<i>PLS</i>
Mean	12.47765	11.01813
Variance	58.97609	38.02828
Observations	20.00000	20.00000
Df	19.00000	19.00000
F	1.55085	
P(F<=f) one-tail	0.17357	
F Critical one-tail	2.16825	

#### 4-4 Recommendations and future works

- 1- According to this study other drugs can be analysis using these methods.
- 2- Applying derivative spectrophotometry and partial least squares methods for determination the above drugs in visible region i.e. using above chromogenic reagents.
- 3- Investigation of the possibility of application of the recommended procedures in the analysis of ternary mixtures of drugs.
- 4- Investigation of the possibility of using artificial neural network for simultaneous determination of binary and ternary mixtures of studied drugs in addition to other drugs.
- 5- Application of the proposed methods for the determination of sulfamethoxazole and sulfanilamide in serum.

## References

1. Greenlief "UV-VIS Absorption Spectroscopy" CH 4200, (2004), 1-5.
2. F. X. Schmid "Biological Macromolecules: UV-visible Spectrophotometry" ENCYCLOPEDIA OF LIFE SCIENCES, (2001), 1-4.
3. S. Kumar "Spectroscopy of Organic Compounds" Organic Chemistry, (2006), 1-26.
4. D. A. Skooge and D. M. West, Principles of instrumental Analysis, 2<sup>nd</sup> edition, Saunders Ctiege/Holt, Rinchart and Winston, USA, (1980).
5. H. Hamid "Ultraviolet and Visible Spectrophotometry "PHARMA-CEUTICAL ANALYSIS, (2007), 1-27.
6. S. Sekkin and C. Kum "Antibacterial Drugs in Fish Farms Application and Its Effects" In Tech Europe, (2011), 217-251.
7. T. Saga and K. Yamaguchi "History of Antimicrobial Agents and Resistant Bacteria "JMAJ, 52(2), (2009), 103–108.
8. A.N. Boa "Antibacterial and Antifungal Drugs" MODULE, 1-59.
9. "Sulfa Antibiotics-Synthesis of Sulfanilamide" [www.chem.wisc.edu/...pdfs/A00.Sulfanilamide/expt/pdf](http://www.chem.wisc.edu/...pdfs/A00.Sulfanilamide/expt/pdf), 1-10.
10. E. Matthew and M. D. Levison "Pharmacodynamics of antimicrobial Drugs" Infect Dis Clin N Am, 18, (2004), 451–465.
11. U. Tekur "Antimicrobial Agents: Antibacterial Drugs" PHARMACOLOGY, (2007), 1-38.
12. R. C. Atkins and F. A. Carey, Organic chemistry, 3<sup>rd</sup> edition, McGraw-Hill higher education, New York, (2002), 286-290.
13. "Sulfonamides" [www. Drugs.com](http://www.Drugs.com), (2013).
14. Martindale, The Extra Pharmacopoeia, 30<sup>th</sup> ed., Reynolds, J.E.F., ed., Pharmaceutical Press (London, England: 1993), 154, 209.
15. M. Votava and O. Kroftová, Antimicrobial Agents, 1-126.
16. "Sulfonamide (medicine)" [www.wikipedia](http://www.wikipedia), the free encyclopedia, (2013).
17. Mérieux, "Antibiotic Classification and Modes of Action" Vitek 2 technology, (2008), 1-95.
18. Linrong, Artificial Synthetic Antimicrobial Drugs, 1-41.
19. "Antimicrobial Drugs" <http://smymission./lamission./edu.>, (2010), 1-39.
20. G. P. Wormser, "Co-Trimoxazole (Trimethoprim -Sulfamethoxazole): An Updated Review of Its Antibacterial Activity and Clinical Efficacy" Drugs, 24(6), (1982), 459-518.

21. M. R. Sohrabi, M. Fathabadi and A. H. Nouri, "Simultaneous Spectrophotometric determination of sulfamethoxazole and Trimethoprim in pharmaceutical preparations by using multivariate Calibration methods" *Journal of Applied Chemical Researches*, 3(12), (2010), 47-52.
22. E. Dinça, Y. Kadioğlub, F. Demirkayab and D. Baleanuc, "Continuous Wavelet Transforms for Simultaneous Spectral Determination of Trimethoprim and Sulfamethoxazole in Tablets" *J. Iran. Chem. Soc.*, 8(1), (2011), 90-99.
23. "SULFAMETHOXAZOLE " monographs./iarc./fr/ENG/Monographs ...mono79-15.p..., 1-18.
24. "Sulfamethoxazole" *EUROPEAN PHARMACOPOEIA 5.0*, (2005), 2511, 2512.
25. Michael Kent *Advanced Biology*, Oxford University Press, 2000, p. 46.
26. Paul Gelmo "Über Sulfamide der p-Amidobenzolsulfonsäure, " *Journal für Praktische Chemie*, (May 14, 1908) 77: 369-382.
27. Deutsches Reich Patentschrift number for sulfanilamide was awarded to Heinrich Hörlein of the Bayer Corporation. May 18, 1909, P 226, 239
28. G. Domagk, "Ein Beitrag zur Chemotherapie der bakteriellen Infektionen", *Deutsche Medizinische Wochenschrift*, 61, Feb. 15, 1935, p. 250.
29. J. et T. Tréfouël, F. Nitti and D. Bovet, "Activité du p-aminophénylsulfamide sur l'infection streptococcique expérimentale de la Souris et du lapin", *C. R. Soc. Biol.*, 120, Nov. 23, 1935, p. 756.
30. **(French)** Daniel Bovet, "Les étapes de la découverte de la sulfamidochrysoïdine dans les laboratoires de recherché de la firme Bayer à Wuppertal-Elberfeld (1927-1932)", in *Une chimie qui guérit : Histoire de la découverte des sulfamides*, Coll. "Médecine et Société", Payot, Paris, 1988, p. 307
31. S. Louis, "Sulfanilamide" *Sigma-Aldrich, Inc.*, (2013).
32. "Sulfanilamide" *www.wikipedia, the free encyclopedia*, (2009).
33. Company: *Sigma-Aldrich Chemie GmbH*, "Sulfanila mide" *sigma-aldrich.com*, (2013).
34. G. Nagamalleswari D. Phaneendra, A. E. Prabakar, P. V. Suresh and N. Ramarao, "New Colorimetric Method Development and Validation of Sulfacetamide in Bulk and Formulation by Different Analytical

- Reagents" International Journal of Advances in Pharmaceutical Analysis, 3, (2013), 30-36.
35. M. H. Givianrad and M. Mohagheghian, "Net Analyte Signal Standard Additions Method for Simultaneous Determination of Sulfamethoxazole and Trimethoprim in Pharmaceutical Formulations and Biological Fluids" E-Journal of Chemistry, 9(2), (2012), 680-692.
  36. K. Upadhyay, A. Asthana and N. Tiwari, "Solid Phase Extractive Spectrophotometric Determination of Some Sulfa Drugs" Asian J. Pharm. Clin. Res. 5, (2012), 222-226.
  37. P. Nagaraja, A. K. Shrestha, A. Shivakumar and A. K. Gowda, "Use of N,N-diethyl-*p*-phenylenediamine sulphate for the spectrophotometric determination of some phenolic and amine drugs" Acta Pharm., 60, (2010), 217–227.
  38. R. S. Abdulsatar, "Spectrophotometric determination of sulfacetamide sodium and sulfamethoxazol in pharmaceutical preparations by oxidative coupling with pyrocatechol" J. Kirkuk Univ. Scient. Stud., 4, (2009), 33.
  39. G. V. Raja, C. B. Sekaran, D. W. Teja, B. Madhuri and B. Jayasree, "Simple Spectrophotometric Methods for the Determination of Sulfamethaxazole in Pharmaceuticals Using Folinicicalteau and Orcinol as Reagents" E-Journal of Chemistry, 6(2), (2009), 357-360.
  40. P. Nagaraja, S. D. Naik, A. K. Shrestha and A. Shivakumar, "A sensitive spectrophotometric method for the determination of sulfonamides in pharmaceutical preparations" Acta Pharm., 57, (2007), 333–342.
  41. Reza Hajian, Esmat Mousavi, Nafiseh Shams "Net analyte signal standard addition method for simultaneous determination of sulphadiazine and trimethoprim in bovine milk and veterinary medicines" Food Chemistry, 138(2-3), (2013),745-749.
  42. .A. Punta Cordero, F. J. Barragán de la Rosa, A. Guiraum "Spectrophotometric determination of sulfanilic acid and sulfonamides in pharmaceutical samples with potassium 1,2-naphthoquinone-4-sulfonate" Canadian Journal of Chemistry., 67(10),(2011),1599-1605.
  43. Betageri, Virupaxappa S.; Kulkarni, Raviraj M.; Shivaprasad, K. H.; Shivshankar, Latha M. "Kinetic spectrophotometric determination of Sulfa drugs in Pharmaceutical formulations", Der Pharma Chemica, 3(2), 2011, 227-235.

44. M.H. Givianrad, (Givianrad, Mohammad Hadi); Saber-Tehrani, M (Saber-Tehrani, Mohammad); Zarin, S (Zarin, Saber) “Genetic algorithm-based wavelength selection in multicomponent spectrophotometric determinations by partial least square regression: application to a sulfamethoxazole and trimethoprim mixture in bovine milk” JOURNAL OF THE SRBIAN CHEMICAL SOCIETY, 78(4), (2013), 555-564.
45. M.H Givianrad, (Givianrad, M. H.); Saber-Tehrani, M (Saber-Tehrani, M.); Aberoomand-Azar, P (Aberoomand-Azar, P.); Mohagheghian, M (Mohagheghian, M.) “H-point standard additions method for simultaneous determination of sulfamethoxazole and trimethoprim in pharmaceutical formulations and biological fluids with simultaneous addition of two analytes” SPECTROCHIMICA ACTA PART A-MOLECULAR AND BIOMOLECULAR SPECTROSCOPY, 78(3), (2011), 1196-1200.
46. Wang, MH (Wang, Mi-Hung); Chang, HW (Chang, Heng-Wei); Wang, SP (Wang, Shu-Ping) “Analysis of Sulfonamides by Liquid Chromatography Mass Spectrometry and Capillary Electrophoresis Combining with Voltage-Assisted Liquid-Phase Microextraction” JOURNAL OF THE CHINESE CHEMICAL SOCIETY, 60(12), (2013), 1479-1483.
47. Herrera-Herrera, AV (Herrera-Herrera, Antonio V.); Hernandez-Borges, J (Hernandez-Borges, Javier); Afonso, MM (Afonso, Maria M.); Palenzuela, JA (Antonio Palenzuela, J.); Rodriguez-Delgado, MA (Angel Rodriguez-Delgado, Miguel) “Comparison between magnetic and nonmagnetic multi-walled carbon nanotubes-dispersive solid-phase extraction combined with ultra-high performance liquid chromatography for the determination of sulfonamide antibiotics in water samples” TALANTA, 116, (2013), 695-703.
48. Mahmoud, WMM (Mahmoud, Waleed M. M; Khaleel, NDH (Khaleel, Nareman D. H.); Hadad, GM (Hadad, Ghada M.); Abdel-Salam, RA (Abdel-Salam, Randa A.); Haiss, A (Haiss, Annette)[ 1 ] ; Kummerer, K (Kummerer, Klaus) “Simultaneous Determination of 11 Sulfonamides by HPLC-UV and Application for Fast Screening of Their Aerobic Elimination and Biodegradation in a Simple Test” CLEAN-SOIL AIR WATER, 41(9), (2013), 907-916.

49. Pamreddy, A (Pamreddy, Annapurna); Hidalgo, M (Hidalgo, Manuela); Havel, J (Havel, Josef); Salvado, V (Salvado, Victoria) "Determination of antibiotics (tetracyclines and sulfonamides) in biosolids by pressurized liquid extraction and liquid chromatography-tandem mass spectrometry" JOURNAL OF CHROMATOGRAPHY A , 1298, (2013), 68-75.
50. Asadi, S (Asadi, Sorayya); Gharbani, P (Gharbani, Parvin) "simultaneous Determination of Sulfamethoxazole and Phthalazine by HPLC and Multivariate Calibration Methods" IRANIAN JOURNAL OF CHEMISTRY & CHEMICAL ENGINEERING-INTERNATIONAL ENGLISH EDITION, 32(2), (2013), 1-8.
51. Li, YF (Li, Yanfang); Han, J (Han, Juan); Yan, YS (Yan, Yongsheng); Chen, B (Chen, Bo); Zhang, GC (Zhang, Guocai); Liu, Y (Liu, Yu); Sheng, CZ (Sheng, Chengzhuo) "Simultaneous extraction and determination of sulfadiazine and sulfamethoxazole in water samples and aquaculture products using [Bmim]BF<sub>4</sub>/(NH<sub>4</sub>)<sub>3</sub>C<sub>6</sub>H<sub>5</sub>O<sub>7</sub> aqueous two-phase system coupled with HPLC" JOURNAL OF THE IRANIAN CHEMICAL SOCIETY, 10(2), (2013), 339-346.
52. Han, J (Han, Juan); Wang, Y (Wang, Yun); Liu, Y (Liu, Yan); Li, YF (Li, Yanfang); Lu, Y (Lu, Yang); Yan, YS (Yan, Yongsheng); Ni, L (Ni, Liang), "Ionic liquid-salt aqueous two-phase extraction based on salting-out coupled with high-performance liquid chromatography for the determination of sulfonamides in water and food" ANALYTICAL AND BIOANALYTICAL CHEMISTRY , 405(4), (2013), 1245-1255.
53. Pietron, WJ (Pietron, Wojciech Jerzy); Cybulski, W (Cybulski, Wojciech); Krasucka, D (Krasucka, Dorota); Mitura, A (Mitura, Agata); Kos, K (Kos, Katarzyna); Antczak, M (Antczak, Maja) "Determination of five sulfonamides in medicated feedingstuffs by liquid chromatography with ultraviolet detection" BULLETIN OF THE VETERINARY INSTITUTE IN PULAWY, 57(4), (2013), 545-552.
54. A.V. Herrera-Herrera, J. Hernández-Borges, T. M. Borges-Miquel and M. Á. Rodríguez-Delgado, "Dispersive liquid-liquid micro extraction combined with ultra-high performance liquid chromatography for the simultaneous determination of 25 sulfonamide and quinolone antibiotics in water samples" J. Pharma. Biomed. Anal., 75, (2013), 130-137.

55. H. Shaaban and T. Go´recki, "Optimization and validation of a fast Ultrahigh-pressure liquid chromatographic method for simultaneous determination of selected sulphonamides in water samples using a fully porous sub-2  $\mu\text{m}$  column at elevated temperature" *J. Sep. Sci.*, 35, (2011), 216–224.
56. R. Liu, P. He, Z. Li, and R. Li, "Simultaneous Determination of Sixteen Sulfonamides in Animal Feeds by UHPLC–MS–MS" *Journal of Chromatographic Science*, 49, (2011), 640-646.
57. Director, Laboratory Quality Assurance Division, "Determination and Confirmation of Sulfonamides" United States Department of Agriculture Food Safety and Inspection Service, Office of Public Health Science, (2009), 1-38.
58. R. Injac, N. Kočevar and B. Štrukelj, "Optimized Method for Determination of Amoxicillin, Ampicillin, Sulfamethoxazole, and Sulfacetamide in Animal Feed by Micellar Electrokinetic Capillary Chromatography and Comparison with High-Performance Liquid Chromatography" *Croat. Chem. Acta*, 82 (3), (2009), 685–694.
59. S. P. Ozkorucuklu, Y. Sahinb and G. Alsancaka, "Determination of Sulfamethoxazole in Pharmaceutical Formulations by Flow Injection System/HPLC with Potentiometric Detection using Polypyrrole Electrode" *J. Braz. Chem. Soc.*, 22(11), (2011), 2171-2177.
60. Y. J. Azeez, "Flow- Injection Spectrophotometric Determination of some Sulpha Drugs via Oxidative Coupling with 4-Amino-N, N-diethyl aniline. Application to Various Samples" *Journal of Zankoy Sulaimani*, 12(1), (2009), 67-76.
61. M. C. Icardo, J. V. G. Mateo, M. F. Lozano and J. M. Calatayud, "Enhanced flow-injection–chemiluminometric determination of sulfonamides by on-line photochemical reaction " *Analytica Chimica Acta*, 499, (2003), 57–69.
62. M. L. F. Córdova, P. O. Barrales, G. R. Torné and A. M. Díaz, "A flow injection sensor for simultaneous determination of sulfamethoxazole and trimethoprim by using Sephadex SP C-25 for continuous on-line separation and solid phase UV transduction" *Journal of Pharmaceutical and Biomedical Analysis*, 31, (2003), 669–677.

63. da Silva, IS (da Silva, Iranaldo Santos); Vidal, DTR (Rajh Vidal, Denis Tadeu); do Lago, CL (do Lago, Claudimir Lucio); Angnes, L (Angnes, Lucio), "Fast simultaneous determination of trimethoprim and sulfamethoxazole by capillary zone electrophoresis with capacitively coupled contactless conductivity detection" JOURNAL OF SEPARATION SCIENCE, 36(8), (2013), 1405-1409.
64. Sun, HW (Sun, Hanwen); Qi, HJ (Qi, Haijing); Li, H (Li, Hui), "Development of Capillary Electrophoretic Method Combined with Accelerated Solvent Extraction for Simultaneous Determination of Residual Sulfonamides and Their Acetylated Metabolites in Aquatic Products" FOOD ANALYTICAL METHODS, 6(4), (2013), 1049-1055.
65. Chen, FY (Chen, Fang-Yuan); Li, P (Li, Peng); Wang, YH (Wang, Yan-Hong); Lian, HZ (Lian, Hong-Zhen), "Separation and Determination of Sulfonamides by Microchip Electrophoresis with Laser-Induced Fluorescence" ASIAN JOURNAL OF CHEMISTRY, 25(12), (2013), 6685-6689.
66. L. Yuqin, C. Yingjie, J. Baoxiu, W. Hao, L. Caihong and Q. Yongxiu, "Capillary electrophoresis with field-amplified sample stacking for rapid and sensitive determination of sulfadiazine and sulfamethoxazole" Die Pharmazie - An International Journal of Pharmaceutical Sciences, 67(9), (2012), 768-773.
67. I. Wen, J. Li, W. Zhang and L. Chen, "Dispersive liquid-liquid micro extraction coupled with capillary electrophoresis for simultaneous determination of sulfonamides with the aid of experimental design" ELECTROPHORESIS, 32, (2011), 2131-2138.
68. L. Yu-qin, Z. Su-yan, C. Ying-jie, Q. Yong-xiu, Z. Xiao-ming and C. Ming-liang, "Determination of Sulfadiazine and Sulfamethoxazole in Pharmaceutical Preparation by Capillary Electrophoresis with Field-enhanced Stacking" Journal of Instrumental Analysis, 6, (2007).
69. D. Teshima, K. Otsubo, K. Makino, Y. Itoh and R. Oishi "Simultaneous determination of sulfamethoxazole and trimethoprim in human plasma by capillary zone electrophoresis" Biomedical Chromatography, 18, (2004), 51-54.



70. Elsaid, FAG (Elsaid, Fathi A. G.); Hamza, S (Hamza, Salem); Rizk, N (Rizk, Nashwa); Matter, HAB (Matter, Hamdy A. B.); Amerah, EAS (Amerah, Elsayda A. S.), "Ni<sup>2+</sup> Selective Membrane Sensors Based on Sulfamethoxazole Diazonium Resorcinol in Poly (Vinyl Chloride) (PVC) Matrix" ARABIAN JOURNAL FOR SCIENCE AND ENGINEERING, 38(7), (2013), 1681-1689.
71. L. S. Andrade, R. C. Rocha-Filho, Q. B. Cass and O. Fatibello-Filho, "Simultaneous Differential Pulse Voltammetric Determination of Sulfamethoxazole and Trimethoprim on a Boron-Doped Diamond Electrode" *Electro analysis*, 21, (2009), 1475–1480.
72. C. D. Souza, O. C. Braga, I. C. Vieira and A. Spinelli, "Electroanalytical determination of sulfadiazine and sulfamethoxazole in pharmaceuticals using a boron-doped diamond electrode" *Sensors and Actuators B: Chemical*, 135, (2008), 66–73.
73. M. M. A. K. Nazer, T. K. Shabeer and P. Riyazuddin, "Indirect Potentiometric Titration of Sulfamethoxazole in the Presence of Trimethoprim in Co-trimazole Tablets Using Copper Based Mercury Film Electrode" *Chem. Pharm. Bull.*, 49(3), (2001), 278—281.
74. S. S. Hassan and M. H. Eldesouki, "Potentiometric and atomic absorption spectrometric determination of sulfonamides in pharmaceutical preparations" *Journal - Association of Official Analytical Chemists*, 64(5), (1981), 1158-1163.
75. C. S. C. Beveridge and R. S. Schechter, "Optimization Theory and Practice" McGraw-Hill, New York, (1970).
76. Harvey, D., "Modern Analytical Chemistry", McGraw-Hill Higher Education, Boston, (2000).
77. J.A. M. Pulgarín, A. A. Molina and M.T. A. Pardo, "The use of modified simplex method to optimize the room temperature phosphorescence variables in the determination of an antihypertensive drug" *Talanta*, 57, (2002), 795–805.
78. S. Al-Najafi, "Flow Injection Analysis and HPLC studies" M. Sc. Thesis, University of Wales, (1984).
79. S. Gorji and M. Bahram, "Experimental design for the study and optimization of the effect of different surfactants on the

- spectrophotometric determination of sulfide based on phenothiazine dye production" *Anal. Methods*, 2, (2010), 948–953.
80. C. Lewis, *Linear Programming: Theory and Applications*, (2008), 3.
  81. A. E. Fonner, J. R. Buck and G. S. Banker, "Mathematical optimization techniques in drug product design and process analysis" *J. Pharm Sci.*, 65(11), (1970), 1587-1596.
  82. Murray, J. *X-STAT Menu*, (1992).
  83. "simplex method definition algorithm" [www. Dictionary.com](http://www.Dictionary.com), (2013).
  84. F. H. Walters, L. R. J. R. Parker, S. L. Morgan and S. N. Deming, *Sequential Simplex Optimization*, CRC Press LLC, 2000 Corporate Blvd., N.W., Boca Raton, Florida 33431, Electronic Reprint, (1999).
  85. J. A. Nelder and R. Mead, "A Simplex Method for Function Minimization", *Comput. J.*, 7, (1965), 308.
  86. F. Suliman and E. Osman, "Chemometric Optimization and Kinetic Developments in Flow Injection Analysis" Thesis of Ph. D. in Chemistry, College of Graduate studies University of Petroleum and minerals, K. S. A., (2006), 33, 34.
  87. [http://www.history.mcs.st.andrews.ac.uk/Extras/Fisher\\_Statistical\\_Methods.html](http://www.history.mcs.st.andrews.ac.uk/Extras/Fisher_Statistical_Methods.html).
  88. Z. R. Lazic, *Design of Experiments in Chemical Engineering*, (2004) WILEY-VCH Verlag GmbH & Co. KGaA, Weinheim, USA, 157,158.
  89. R. E. Kirk, *Experimental Design: Procedures for the Behavioral Sciences*, 3rd Edition, Pacific Grove, CA: Brooks/Cole, (1995).
  90. P. G. Mathews, M. Malnar and Bailey, *Design of Experiments*, (1999-2012), 2.
  91. R. H. Myers, *Response Surface Methodology*, Allyn and Bacon Boston, (1971).
  92. "Engineering Statistics Handbook", NIST/SEMATECH e-Handbook of Statistical Methods, <http://www.itl.nist.gov/div898/handbook/>, date.
  93. <http://www.iue.tuwien.ac.at/phd/plasun/node32.html>.
  94. D. C. Montgomery, *Design and analysis of Experiments*, 5th edition, John Wiley & sons, New York, (2007).
  95. M. Palaniyappan, V. Vijayagopal, R. Viswanathan and T. Viruthagiri, "Statistical Optimization of Substrate, Carbon and Nitrogen Source by Response Surface Methodology for Pectinase Production Using

- Aspergillus fumigatus MTCC 870 in Submerged Fermentation" African Journal of Biotechnology, 8 (22), (2009), 6355-6363.
96. S. Narongchai, B. Putipong and P. Bandhita, " Central Composite Design in Optimization of the Factors of Automatic Flux Cored Arc Welding for Steel ST37" Proceeding of the 2nd IMT-GT Regional Conference on Mathematics, Statistics and Applications Universiti Sains Malaysia, Penang, (2006), 13-15.
  97. J. Mc Murry, organic chemistry, 6<sup>th</sup> edition, THOMSON BROOKS/COLE, International Student Edition, New York, (2004), 917-921.
  98. R. C. Atkins; F. A. Carey, Organic Chemistry, 5<sup>th</sup> edition, Mc Graw Hill, Higher Education, New York, (2006).
  99. H. P. Stanley, Organic Chemistry, 2<sup>nd</sup> edition (1981), 633.
  100. The Merck Index, 7th edition, Merck & Co, Rahway, New Jersey, USA, 1960.
  101. Suzuki, T.; Kajii, Y.; Shibuya, K.; Obi, K., Photocyclization of diphenylamine studied by time-resolved thermal lensing. Heat of reaction, energetics, and reactivity of intermediates, **Bull. Chem. Soc. Jpn.**, 1992, 65, 1084-1088.
  102. K. A. Connors, Reaction Mechanisms in Organic Analytical Chemistry, John Wiley & Sons: New York, (1973).
  103. S. A. Aderibigbe, O. A. Adegoke and O. S. Idowu " A New Colorimetric Method for The Determination of Nifedipine Tablets by Derivatization Using 4-Carboxyl-2,6-Dinitrobenzene Diazonium Ion" International Journal of Industrial Chemistry, 3(5), (2012), 1-8.
  104. A. Bali and P. Gaur "A Novel Method for Spectrophotometric Determination of Pregabalin in Pure Form and in Capsules" Chemistry Central Journal, 5(59), (2011), 2-7.
  105. S. S. Rjendran, Ch. Deepthi, N. Santhi, C. S. Kandasamy, R. V. Narayanan "Colorimetric Method of Ziprasidone in Bulk and in Pharmaceutical Dosage Forms" Research Journal of Pharmaceutical, Biological and Chemical Sciences, 2, (2011) 294-298.
  106. A. B. Babu, G. Ramu, CH. M. Krishna, S. B. Reddy, and C. Rambabu "Spectrophotometric Determination of Lamivudine in Pure and Tablet Forms" E-Journal of Chemistry, 9(2), (2012), 569-575.

107. O. A. Adegoke and O. E. Umoh "A New Approach to The Spectrophotometric Determination of Metronidazole and Tinidazole Using p-Dimethyl Amino Benzaldehyde" *Acta Pharm.*, 59, (2009), 407-419.
108. M. V. Krishna and D. G. Sankar "New Diazo Coupling Reactions for Visible Spectrophotometric Determination of Alfuzosin in Pharmaceutical Preparations" *E-Journal of Chemistry*, 4(4), (2007), 496-501.
109. K. N. Prashanth, K Basavaiah, M. S. Raghu "Rapid and Sensitive Spectrophotometric Measurement of Non- Specific Beta Blocker Propranolol Hydrochloride Using Three Sulphonphthalein Dyes in Pure Form, Pharmaceuticals and Human Urine" *Chemical Sciences Journal*, 2012, (2012), 1-14.
110. Bala S. Chandra, S. S. Bhogela, M. Shaik, C. S. Vadlamudi, M. Chappa and N. S. Maddirala "Simple and Sensitive Spectrophotometric Methods for the Analysis of Mesalamine in Bulk and Tablet Dosage Forms" *Quim. Nova*, 34(6), (2011), 1068-1073.
111. R. I. Vogel, *A Text Book of Macro and Semi Micro Qualitative Inorganic Analysis*, 4<sup>th</sup> edition, (1954), Longmans, Green and Co, London.
112. Tomás P-Ruiz; Carmen, M-Lozano; Virginia, T; Antonio Sanz and Elisa, S, "Flow-injection extraction-spectrophotometric method for the determination of ranitidine in pharmaceutical preparations", *Journal of Pharmaceutical and Biomedical Analysis*, 26(4), November, (2001), p 609-615.
113. M. Boniger, 1894, 27, 23.
114. Sastry, C.S.P., Prasad, T.N.V. and Rao, E.V., *Indian J. Pharm. Sci.*, 49, 95, 1987.
115. G. M. Loudon, *Organic Chemistry*, 4th edition, Oxford University press, Inc, New York, (2002), 874-87.
116. R. C. Atkins; F. A. Carey, *Organic chemistry*, 3rd edition, McGraw-Hill higher education, New York, (2002), 286-290.
117. Ibrahim A. Darwish, Heba H. Abdine, Sawsan M. Amer, Lama I. Al-Rayes, *International Journal of Analytical Chemistry*, **2009**; Article ID 237601, 8 pages, doi:10.1155/2009/237601
118. L. Xu, H. Wang, Y. Xiao, *Spectrochimica Acta Part A*, **2004**, 60, 3007–3012.
119. Acidity values from M. S. Silberberg *Chemistry*, 5th edition, McGraw-Hill, 2009.

120. A. F. Wells, 'Structural Inorganic Chemistry, 5th ed., Oxford University Press, Oxford, UK, 1984.
121. N. N. Greenwood, A. Earnshaw, Chemistry of the Elements, 2nd ed., Butterworth-Heinemann, Oxford, UK, 1997.
122. CH. A. Kumar, T. A. Kumar, B. M. Gurupadayya, S. N. Sloka and M. B. R. Reddy "Novel spectrophotometric determination of Valacyclovir and Cefotaxime using 1, 2-naphthaquinone-4-sulfonic acid sodium in bulk and pharmaceutical dosage form" Archives of Applied Science Research, 2 (4), (2010), 278-287.
123. K. Srikanth, K. A. Emmanuel "Spectrophotometric Determination of Reboxetine through Condensation and Diazo-Coupling Reactions" E-Journal of Chemistry, 8(1), (2011), 281-287.
124. P. S. Sarsambi, D. Gowrisankar, k. Anupama "Condensation Reactions for The Estimation of Entacapone in Bulk Drug and Its pharmaceutical Formulations" An International Journal of Pharmaceutical Sciences, 2, (2011), 40-47.
125. C. J. G. Babu, G. V. Kumar "Validated Spectrophotometric Estimation of Famciclovir in Tablet Dosage Form" International Journal of Chem Tech Research, 1(4), (2009), 1368-1371.
126. S. V. Rao, M. Srinivasarao, G. Ramu and C. Rambabu "UV Visible spectrophotometric determination of bortezomib in its bulk and formulation dosage forms" Der Pharmacia Lettre, 4(3), (2012), 720-727.
127. P. S. Sarsambi, D. Gowrisankar, A. Sonawane, Abdul Faheem "Visible Spectrophotometric Determination of Ganciclovir by Condensation and Oxidative Coupling Reactions" International Journal of ChemTech Research, 2(1), (2010), 282-285.
128. C. M. Jamakhandi, C. Javali, J. I. Disouza, U. S. Chougule H, A. K. Mullani "Spectrophotometric Determination of Lisinopril Dosage Form by Condensation Reaction" International Journal of Pharmacy and Pharmaceutical Sciences, 3, (2011), 185-187.
129. P. Lavudu, A. P. Rani, C. B. Sekaran, K. S. Kumar, A. Ramesh "Determination of Pramipexole Dihydrochloride in Tablet Dosage Forms by Visible Spectrophotometric Method Using Acetyl Acetone-Formaldehyde Reagent" Chemical Sciences Journal, 2012, (2012), 1-10.

130. A. Douglas Skoog, Holler F. James; Crouch Stanley R. "Principles of instrumental Analysis", 6th Edition, Thomsan. Brooks/Cole.p, Publisher, david Harris, p 336-338, 371-374, (2007).
131. Al-saidi, Khaleda Hamid "Quantitative determination of some antibiotic drugs of penicillin and cephalosporin groups through a new selective electrodes and derivative spectrophotometry", A thesis Submitted to the College of Science Al-mustansiria University. PP.20, 111, (2006).
132. Sigurds Skujins; Varian A G, "Applications of UV-Visible Derivative Spectrophotometry", A review of areas of application and the basic principles of the derivative technique, Part I,33, April (1986).
133. [http://terpconnect.umd.edu/~toh/SPECTRUM/Resolution Enhancement.html](http://terpconnect.umd.edu/~toh/SPECTRUM/Resolution%20Enhancement.html).
134. El-oSayed, A., A. Y. and El- Salem, N., A., Recent Development of Derivative Spectrophotometry and their Analytical Applications", J. of Analytical Science V. 21, PP 595-64, (2005).
135. Ojeda, C.B.; Rojas, F.S.andPavon, J.M. "Recent developments in derivative ultraviolet/visible absorption spectrophotometry", J., Talanta. Sep; 42(9): PP, 1195-1214, (1995).
136. El-Sayed, Youssef A., Y. and. Khalil, M. M.H, "Simultaneous first-derivative spectrophotometric determination of iron(III) and molybdenum(VI) in cobalt-chromium and nickel-chromium alloys", Talanta, Volume 43, Issue 4, April, PP, 583-588,( 1996).
137. Robert Lipka; Marta Sobczak; Stanis aw Ku, S.; Awomir Oszwadowski and MaciejJarosz "Determination of fluoride impurities in Leuprolide. Comparison of analytical methods", J. of Micro- chemical vol: 65, 1, PP. 51-58, (2002).
138. Popović. G.V.; Pfenndt, L.B. and Moskovljević, V.M "Derivative spectrophotometric method for determination of acidity constants of single step acid-base equilibria", J. of Talanta, 55(2) page: 363-370, (2001).
139. Zafer, D.; Hasan, B. and Nilgün, G.Göge,"Quantitative determination of ambroxol in tablets by derivative UV spectrophotometric method and HPLC", Journal of Pharmaceutical and Biomedical Analysis, 31(5), P 867-872, (2003).

140. Baltazar de Castro; Paula Gameiro; José, L. F. C. Lima; Carla Matos and Salette Reis a Fast and reliable “spectroscopic method for the determination of membrane-water partition coefficients of organic compounds”, *J. of Lipids*, 36(1), PP. 89-96, (2001).
141. Merás, I. Durán ; Mansilla, A. Espinosa ; López, F. Salinas “Comparison of UV derivative-spectrophotometry and partial least-squares(PLS-1) calibration for determination of methotrexate and leucovorin in biological fluids”, *J. of Analytical and Bioanalytical Chemistry*, 373, Numbers 4-5 , PP. 251-258, (2002).
142. Jerzy D.; Dorota, Na.; and Piotr M. “Reversed-phase high-performance liquid chromatography on-line with the second and fourth derivative ultraviolet spectroscopy as a tool for identification of milk proteins”, *J. of Analytica Chimica Acta*, 449 (1-2), PP. 243-252, (2001).
143. Sarmad B., Dikran and Mohammed, J.M., Hussan, “First and second Derivative Spectrophotometry for individual and simultaneous determination of Amoxicillin and Cephalexin”, *national J. of Chemistry*, Volume 34, PP, 260-269, (2009).
144. El- Zeany, B.A.; Moustafa, A. A. and Farid, N.F. “Determination of imipramine in presence of iminodibenzyl and inpharmaceutical dosage form”, *Journal of Pharmaceutical and Biomedical Analysis*, 33, Number 4, 24 November , pp. 775-782, (2003).
145. Ouanes, S., Kallel, M.; Trabelsi, H.; Safta, F. and Bouzouita, K. “Zero-crossing derivative spectrophotometry for the determination of haloperidol in presence of parabens”, *J. of Pharmaceutical and Biomedical Analysis*, Volume 17, Issue 3, July, PP. 361-364, (1998).
146. Vladi Olga Consigliere; Nelson Rafael Matta Vals and João Fernandes Magalhães “First-Derivative Spectrophotometric Determination of Pyroxidine Hydrochloride in Pharmaceutical preparation”, *Analytical Letters*, Volume 34, Issue 11 , pp. 1875 – 1888,(2001).
147. Murillo, J. A.; Lemus, J. M and García, L. F. “Resolution of binary mixtures of cephalothin and clavulanic acid by using first derivative spectrophotometry”, *Volume 349, Numbers 10-11*, pp. 761-767, (1994).
148. Dogan H. N.; Duran, A. “Simultaneous spectrophotometric determination of aspirin, acetaminophen and ascorbic acid in pharmaceutical formulation”, *J. of Pharmazie*, V.53, (110), PP. 781-784, (1998).

149. Erk, Nevin, "Simultaneous determination of dorzolamide HCl and timolol maleate in eye drops by two different spectroscopic methods", *Journal of Pharmaceutical and Biomedical Analysis*, V. 28(2), PP. 391-397, (2002).
150. Dinc, Erdal; Onur, Feyyaz "Application of derivative and ratio spectra derivative spectrophotometry for the determination of pseudoephedrine hydrochloride and acrivastine in capsules", *J. of Analytical Letters*, V. 30 (6), PP. 1179-1191, (1997).
151. Mahmure, Ü. ÖzgürGüzin Alpdoğan and Bürge Aşçi, "A Rapid Spectrophotometric Method to Resolve Ternary Mixtures of Propyphenazone, Caffeine, and Acetaminophen in Tablets", *J. of Monatshefte für Chemie*, Volume 133, Number 2, PP. 219-223, (2002).
152. Meyers, R. A. (Chief Editor), "Encyclopedia of Analytical Chemistry Applications, Theory and Instrumentation", John Wiley and Sons, Inc., 1764, (Copyright © 1999-2010).
153. Khoshay and M.R., Abdollahi H., Ghaffari A., Shariatpanahi M., Farzanegan H. "Simultaneous Spectrophotometric determination of paracetamol, phenylephrine and chlorpheniramine in pharmaceuticals using chemometric approaches", *DARU*, Vol. 18, No. 3, (2010).
154. Sarlak N., Anizadeh M., "Simultaneous kinetic spectrophotometric determination of sulfide and sulfite ions by using an optode and the partial least squares (PLS) regression", *Sensors and Actuators B* 160, 644-649, (2011).
155. Jahan B., Ghasemi E. Z., "Simultaneous spectrophotometric determination of trace amounts of uranium, thorium, and zirconium using the partial least squares method after their preconcentration by benzoin oxime modified Amberlite XAD-2000 resin", *Talanta*, 80, 1191-1197, (2010).
156. RITZ M., VACULÍKOVÁ L., PLEVOVÁ E., MATÝSEK D. and MALIŠ J., "Determination of Chlorite, Muscovite, Albite and Quartz in Claystones and Clay Shales by Infrared Spectroscopy and Partial Least-Squares Regression", *Acta Geodyn. Geomater.*, Vol. 9, No. 4 (168), 511-520, (2012).
157. KRAMER R., "Chemometric Techniques for Quantitative Analysis", Marcel Dekker, Inc., New York, Basel, USA, (1998).



158. Gemperline P., Practical Guide to Chemometrics 2<sup>nd</sup> ed., Taylor & Francis Group, LLC, 2006.
159. Afkhami A. and Sarlak N., "Simultaneous Determination of Salicylamide and Paracetamol by Spectrophotometric H-Point Standard Addition Method and Partial Least Squares Regression", *Acta Chim. Slov.*, 52, 98–103, (2005).
160. David M. H. and Edward V. T., Partial Least-Squares Methods for Spectral Analyses. 1. Relation to Other Quantitative Calibration Methods and the Extraction of Qualitative Information, *Anal. Chem.* 60, 1202-1208, (1988).
161. Lee K. R., Zuber G., Katrincic L., "Chemometrics approach to the determination of polymorphism of a drug compound by infrared spectroscopy", *Drug Dev Ind Pharm.*; 26(2):135-47, (2000).
162. Khoshayand M. R., Abdollahi H., Ghaffari A., Shariatpanahi M., Farzanegan H., "Simultaneous spectrophotometric determination of paracetamol, phenylephrine and chlorpheniramine in pharmaceuticals using chemometric approaches", *DARU Vol.* 18, No. 3, (2010).
163. Qadir H. A., "Simultaneous Spectrophotometric Determination of Binary and Ternary Mixtures using Derivative and Some Chemometrics Techniques", Ph. D. Thesis, College of Education-Salahaddin University, May 2013.
164. Höskuldsson A., PLS regression methods, *J. Chemometrics.*, 2(3) 211-228, 1988.
165. Kramer R., "Chemometric Techniques for Quantitative Analysis", Marcel Dekker, Inc., New York, USA, 1998.
166. Aguerassif N., Benamor M., Kachbi M. and Draa M. T. "Simultaneous determination of Fe(III) and Al(III) by first-derivative spectrophotometry and partial least-squares (PLS-2) method – Application to post-haemodialysis fluids", *Journal of Trace Elements in Medicine and Biology*, 22, 175–182, (2008).
167. Afkhami A. and Sarlak N. "Simultaneous Determination of Salicylamide and Paracetamol by Spectrophotometric H-Point Standard Addition Method and Partial Least Squares Regression", *Acta Chim. Slov.*, 52, 98–103, (2005).

## الخلاصة

السلفاميثوكسازول والسلفانيل أمايد احدى أعضاء عائلة السلفون أمايد المضادة للبكتيريا. استخدمت اربعة طرائق طيفية مختلفة في هذه الدراسة لتقدير هذين الدوائين في المستحضرات الصيدلانية ونماذجهما المصنعة وفي الشكل النقي ؛ وكانت هذه الطرائق سريعة ،بسيطة، حساسة، دقيقة، وغير مكلفة. فقد أظهرت نتائج الدراسة ما يأتي:

**الطريقة الأولى:** تعتمد على تفاعل العقارين مع نترتيت الصوديوم وحامض الهيدروكلوريك لأزوتتهما تبع ذلك اجراء تفاعل ازدواج مع داي فينيل أمين في وسط حامضي لتكوين صبغة الأزو ذات اللون الأزرق التي تظهر أعظم امتصاص ( $\lambda_{max}$ ) عند 530 نانومتر لمعقد السلفاميثوكسازول و531 نانومتر لمعقد السلفانيل أمايد ضد محلول الخلب ومن ثم تم تقدير تركيز العقارين طيفياً. وقد تم تعيين الظروف الفضلى التي تؤثر على التفاعل والعوامل التحليلية الأخرى. وبالإضافة الى الطريقة الكلاسيكية بنمط المتغير الواحد طبقت طريقة السمبلكس المحورة لتعيين الظروف الفضلى للمتغيرات التي تؤثر على التفاعل اللوني قيد الدراسة. أظهرت النتائج أن الخصائص البصرية لمنحنيات المعايرة والبيانات الأحصائية التي تم الحصول عليها عند اختيار الظروف المثالية كانت أفضل لطريقة السمبلكس المحورة بالمقارنة بالطريقة الكلاسيكية لكلا العقارين.

تم تطبيق قانون بير على مدى من التراكيز يتراوح بين ( $0.5-12.0 \mu\text{g.mL}^{-1}$ ) و ( $0.5-12.0 \mu\text{g.mL}^{-1}$ ) لكلا العقارين السلفاميثوكسازول والسلفانيل أمايد على التوالي مع قيمة معامل الامتصاص المولي مساوية لـ  $4.9617 \times 10^4 \text{ L.mol}^{-1}.\text{cm}^{-1}$  للسلفاميثوكسازول و  $5.9185 \times 10^4 \text{ L.mol}^{-1}.\text{cm}^{-1}$  للسلفانيل أمايد وكان حد الكشف يساوي  $0.036 \mu\text{g.mL}^{-1}$  و  $0.016 \mu\text{g.mL}^{-1}$  لكلا المعقدين على التوالي باستخدام طريقة السمبلكس. أظهرت الدراسة عدم وجود أي تأثير للمتداخلات المتعارف على وجودها في المستحضرات الصيدلانية في تقدير الدوائين، لذلك طبقت الطريقة بنجاح في تقدير السلفاميثوكسازول والسلفانيل أمايد في المستحضرات الصيدلانية وفي نماذجهما المصنعة.

**الطريقة الثانية:** تعتمد على تفاعل التكتيف لتكوين المعقدات بتفاعل العقارين مع كاشف صوديوم 2,1-نفثاكوينون-4-سولفونيت، حيث أظهرت المعقدات المتكونة أعظم امتصاص عند الطول الموجي 460 نانومتر للسلفاميثوكسازول، و 455 نانومتر للسلفانيل أمايد، ضد محلول الخلب. وقد تمت دراسة العوامل التي تؤثر في إتمام التفاعل بعناية للحصول على الظروف الفضلى وذلك باتباع نمط المتغير الواحد وبالاعتماد على طريقة تصميم التجربة (DOE) والنتائج التي تم الحصول عليها تحت الظروف المثالية بواسطة طريقة تصميم التجربة كانت أفضل من حيث الخصائص البصرية لمنحنيات المعايرة والبيانات الأحصائية بالمقارنة مع الطريقة الكلاسيكية لكلا العقارين.

أظهرت النتائج مطاوعة لقانون لامبرت بير؛ ولمدى من التراكيز  $(5.0-50) \mu\text{g.mL}^{-1}$  لمعد السلفاميثوكسازول و  $(5.0-30) \mu\text{g.mL}^{-1}$  لمعد ألسفانيل أميد وبحد كشف  $0.359 \mu\text{g.mL}^{-1}$  لمعد السلفاميثوكسازول و  $0.536 \mu\text{g.mL}^{-1}$  لمعد ألسفانيل أميد وبأمتصاصية مولارية  $7.0918 \times 10^4 \text{ L.mol}^{-1}.\text{cm}^{-1}$  للسلفاميثوكسازول و  $7.0774 \times 10^4 \text{ L.mol}^{-1}.\text{cm}^{-1}$  للسفانيل أميد باستخدام طريقة تصميم التجربة.

أخيراً" أظهرت الدراسة عدم وجود أي تأثير للمتداخلات المتعارف على وجودها في المستحضرات الصيدلانية في تقدير الدوائين. طبقت الطريقة بنجاح في تقدير السلفاميثوكسازول والسفانيل أميد في المستحضرات الصيدلانية وفي نماذجها المصنعة.

**الطريقة الثالثة:** المشتقة الطيفية تعتمد على المشتقة الأولى والثانية لطيف امتصاص عقاري السلفاميثوكسازول والسفانيل أميد (في المنطقة ما فوق البنفسجية) لتقديرهما أنيا في مزيج لهما، من أجل التخلص من الخطأ الناتج في قيم الامتصاص بسبب وجود الدوائين معا أو بسبب وجود المتداخلات.

لقد وجد أنه بالأمكان تقدير السلفاميثوكسازول ولمدى من التراكيز  $(2-50) \mu\text{g.mL}^{-1}$ ؛ في مزيج يحتوي على  $(2-30) \mu\text{g.mL}^{-1}$ ، من عقار ألسفانيل أميد كمتداخل. ألتائج ألتى حصلنا عليها في قياسات المشتقة الأولى تشير ألى أنه عند أالحفاظ على تركيز ثابت لعقار ألسفانيل أميد مع تراكيز مختلفة من السلفاميثوكسازول وجد أن قيم القمم المقاسة عند (peak to baseline) 223، 254، 287 نانومتر و (peak to peak height) بين 223-254 نانومتر، 254-287 نانومتر و (height at zero cross) عند 235.62، 258.72 نانومتر. (height to height at zero Cross) بين 235.62-258.72 نانومتر وقياسات المساحة تحت ألقمة (area under peak) بين 241.95-267.04 نانومتر، 267.04-330 نانومتر. تتناسب مع تركيز السلفاميثوكسازول، لذلك أستخدمت في تقديره.

بينما في المشتقة الثانية أستخدمت الأطوال الموجية عند 239.5 نانومتر، 263.5 نانومتر، 267.75 نانومتر، 301 نانومتر، 215 نانومتر (peak to baseline)، والأطوال الموجية عند 271.28 نانومتر، 245.86 نانومتر (height to baseline at zero cross) والأطوال الموجية بين 239.5-264.25 نانومتر، 239.5-267.75 نانومتر، 271.28-301 نانومتر، 215-239.5 نانومتر، (peak to peak)، والأطوال الموجية بين 245.86-271.28 نانومتر تمثل (height to height at zero cross)، بالإضافة ألى الأطوال الموجية عند 245.86-271.28 نانومتر، 286.95-329.5 نانومتر، 221.75-254.12 نانومتر تمثل قياسات المساحة تحت ألقمة (Area under peak) تتناسب مع تركيز السلفاميثوكسازول، لذلك أستخدمت في تقديره.

يتم تقدير السفانيل أميد ولمدى من التراكيز  $(2-50) \mu\text{g.mL}^{-1}$ ؛ في مزيج يحتوي على  $(2-50) \mu\text{g.mL}^{-1}$  من السلفاميثوكسازول كمتداخل. وجد أن قيم القمم المقاسة عند 224 نانومتر، 246 نانومتر، 271 نانومتر (peak to baseline)، وعند 67.04، 241.95 نانومتر

(height at zero cross) وعند 246-224 نانومتر، 271-246 نانومتر (peak to peak) 271-241.95 نانومتر (height to height at zero cross) ، 235.62-258.72 نانومتر (area under peak) استخدمت لتقدير السلفانيل أمايد باستخدام المشتقة الأولى. من ناحية أخرى، استخدمت الأطوال الموجية عند 218 نانومتر، 231 نانومتر، 260 نانومتر، 278 نانومتر (peak to baseline) والأطوال الموجية عند 281-254 نانومتر، تمثل (height at two zero cross) والأطوال الموجية بين 218-231 نانومتر، 260-231 نانومتر ، 278-260 نانومتر (peak to peak)، والأطوال الموجية عند 254,281 نانومتر، (height to height at zero cross)، والأطوال الموجية بين 210-224 نانومتر، 245.84-224 نانومتر، 330-271.28 نانومتر (area under peak) لتقدير السلفانيل أمايد باستخدام المشتقة الثانية.

أظهرت النتائج غياب التداخل الذي تسببه المتداخلات في تقدير الدوائين عند استخدام هذه الطريقة، لذلك فمن الممكن تطبيق الطريقة بنجاح في تقدير هذين العقارين في المستحضرات الصيدلانية وفي نماذجهما المصنعة.

*الطريقة الرابعة:* طريقة المربعات الجزئية الصغرى، طبقت الطريقة طيفياً لتقدير السلفاميثوكسازول و السلفانيل أمايد أنياً" في مزيج منهما. في هذه الدراسة، حضرت مجموعة التدريب بالاعتماد على قاعدة العشرة، بمعنى آخر تم اختيار عشرين مزيج ثنائي (من ضمن خمس وستون) مزيج تم تحضيرها بالاعتماد على مدى الخطية للسلفاميثوكسازول  $2-50 \mu\text{g.mL}^{-1}$  و السلفانيل أمايد  $2-50 \mu\text{g.mL}^{-1}$  بتصميم عشوائي.

تم الحصول على مصفوفة المعايرة بعمل مسح لطيف الأمتصاص للمحاليل العشرين المختارة من مزيج السلفاميثوكسازول و السلفانيل أمايد وبمدى 190-350 نانومتر وبفاصل 1 نانومتر وعرض الشق 0.5 نانومتر مع مسح بسرعة متوسطة.

تم استخدام برنامج Originpro version 9.1.0, 2013 لبناء طراز أنحدار المربعات الجزئية الصغرى 1 و2 ومن خلالها تم التنبؤ بتركيز العقارين. أثبتت نتائج النسبة المئوية للانحراف المعياري النسبي (RSD%) (0.8012-0.0277) والنسبة المئوية للخطأ النسبي (RE%) (-0.2151-0.5973) دقة وضبط ممتازة لطريقة PLS للتنبؤ بتركيز SMZ و SNA أنياً". طبقت الطريقة بنجاح في تقدير العقارين أنياً" في مزيج مصنع منهما.



بِسْمِ اللّٰهِ الرَّحْمٰنِ الرَّحِیْمِ  
قَالُوا سُبْحٰنَكَ لَا عِلْمَ لَنَا  
اِلَّا مَا عَلَّمْتَنَا اِنَّكَ اَنْتَ  
الْعَلِیْمُ الْحَكِیْمُ

سورة البقرة الآية 32





جمهورية العراق  
وزارة التعليم العالي والبحث العلمي  
جامعة بغداد  
كلية التربية للعلوم الصرفة-ابن الهيثم

# طرائق تحليلية جديدة لتحليل الأدوية دراسة مقارنة

رسالة مقدمة الى

كلية التربية للعلوم الصرفة ابن الهيثم - جامعة بغداد

كجزء من متطلبات نيل درجة الدكتوراه فلسفة في علوم الكيمياء

من قبل

حسام سليم خلف

بكالوريوس علوم كيمياء 1993

ماجستير علوم كيمياء 2006

بإشراف

الأستاذ الدكتور عبدالمحسن عبدالحميد الحيدري

الأستاذ الدكتور علاء كريم محمد

الأستاذ الدكتور سرمد بهجت ديكران

2014